MARITIME BATTERY SAFETY JOINT DEVELOPMENT PROJECT

Technical Reference for Li-ion Battery Explosion Risk and Fire Suppression

Partner Group

Report No.: 2019-1025, Rev. 4
Document No.: 1144K9G7-12
Date: 2019-11-01

Project name:	Maritime Battery Safety Joint Development project	DNV GL AS Maritime Environment Advisory
Report title:	Technical Reference for Li-ion Battery Explosion Risk and Fire Suppression	Veritasveien 1 1363 Høvik Norway
Customer:	Partner Group	Tel: +47 67 57 99 00

Customer contact:

Date of issue:	2019-11-01
Project No.:	PP180028
Organisation unit:	Environment Advisory
Report No.:	2019-1025, Rev. 4
Document No.:	1144K9G7-12

Applicable contract(s) governing the provision of this Report:

Objective: This report is intended for persons assessing energy storage installations, from a design, engineering or regulatory perspective, to better evaluate risks and solutions with regard to lithium-ion battery fire, off-gassing and explosion.
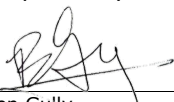
Prepared by:	Verified by:	Approved by:
Ben Gully Senior Engineer	Narve Mjøs Director Maritime Battery Services	Terje Sverud Head of Section
Henrik Helgesen Senior Consultant	Asmund Huser Senior Principal Specialist	
John Erik Skogtvedt Consultant	Nathaniel Frithiof Senior Consultant	
Dimitrios Kostopoulos Consultant	Gerd Petra Haugom Principal Consultant	

DNV GL Distribution:

☒ OPEN. Unrestricted distribution, internal and external.

☐ INTERNAL use only. Internal DNV GL document.

☐ CONFIDENTIAL. Distribution within DNV GL according to applicable contract.*

☐ SECRET. Authorized access only.

Keywords:

Fire, Suppression, Battery, Safety, Ventilation, CFD analyses, Lithium-Ion, Off-gas, explosion, Quantitative Risk Assessment, Qualitative Risk Assessment, Thermal Runaway, Toxicity, Temperature Class, Gas Group

Rev. No.	Date	Reason for Issue	Prepared by	Verified by	Approved by
1	2019-04-29	First JDP Committee Draft Review	Ben Gully	Gerd Petra Haugom	Terje Sverud
2	2019-09-06	Second JDP Committee Draft Review	Henrik Helgesen	Nathaniel Frithiof	Terje Sverud
3	2019-09-30	Third JDP Committee Draft Review	Henrik Helgesen	Nathaniel Frithiof	Terje Sverud
4	2019-11-01	Final Report	Henrik Helgesen	Nathaniel Frithiof	Terje Sverud

Table of contents

The following report presents the findings from a joint development project incorporating expert input and perspective from the following key industry organizations and authorities:

1 EXECUTIVE SUMMARY

This report is intended to enable persons assessing energy storage installations, whether from a design, engineering or regulatory perspective, to better evaluate risks, capabilities and solutions with regard to safety. The focus and context are on installations in the maritime environment although most findings will apply similarly to other applications and industries.

Like any energy source, lithium-ion batteries pose significant hazards with regard to fire and safety risk. Systems and tools are available which are fully capable of handling these risks, but it is necessary to better understand both these risks as well as the tools available so that they may be appropriately selected and implemented. It is important that the protection systems match the failure modes and consequences of a particular battery system.

Thus, the primary objective of this report is to provide information which enables:

1. The regulative authorities to write clearer and more prescriptive rules and guidelines.

2. An easier and more thorough approval process.

3. Engineers to better understand the risks and ensure that effective protection systems and barriers are implemented.

Two key areas were prioritized to provide information.

The first key focus was quantifying off-gas content and explosion risks. Different test setups can give different results and it was needed both to normalize these inputs and provide characterization of gas contents and quantity that can be used for consistent evaluation of explosion risks. Testing was performed at both the cell and multi-cell level, for different chemistries and form factors, and under different failure modes. Cell and rack/module testing results were used as input to calibrate Computational Fluid Dynamics (CFD) models which were then used to evaluate a wider range of configurations. These results provide reference and guidance on the amount of ventilation and the effectiveness. In general, the magnitude of potential consequence depends heavily on the number and size of the battery cells expected to be involved in an incident, and guidance is provided such that this can be assessed for a given system and used as input for evaluating explosion consequences.

The second primary objective was evaluation of the capabilities of various fire suppression and extinguishing media with respect to lithium-ion battery fires. Each of the systems available has different strengths and weaknesses, and thus different systems may be more effective or necessary depending on the key risks posed by a particular battery arrangement or installation. In general, fire suppression is more effective when detected and deployed early and if it can be released into the module. Key factors to evaluate as far as requirements are short term cooling, long term cooling, and gas absorption.

In addition, a Quantitative Risk Assessment (QRA) has been performed to present a framework quantifying the risks involved to an acceptance criterion. Frequencies of failures has been calculated with and without common safeguards to highlight the importance of the protection systems. Finally, a comparison of the probability of a conventional engine room fire has been made.

This report consists first of a summary of all main findings in Section A, followed by a Section B containing a detailed account of those findings from the standpoint of test setup, analysis methodologies, key assumptions and more.

Project work was initiated and managed by DNV GL, as a Joint Development Project; a collaborative effort from many essential partners representing the entire maritime battery value chain. Funding was

contributed by all members and by the Research Council of Norway, and all members provided input to approaches and technical objectives as well as review and assessment of results.

1.1 Main conclusions

This section summarizes the main conclusions for the safety aspects of Li-ion batteries investigated. Note that the conclusions are based on tests performed at Li-ion batteries containing liquid electrolyte with Nickel Manganese Cobalt Oxide (NMC) and Lithium Iron Phosphate (LFP) cathode chemistries. These batteries are the most common for maritime applications at the publication time of this report. Battery technology is in rapid development, and new advancements might influence the presented results.

Limited tests were also performed, and the conclusions are only drawn where clear patterns between the different test results could be found. Calculations and evaluations are also made with conservative assumptions, compensating for the lack of parallel tests.

1.1.1 Fire suppression systems

Tested fire suppression systems provide different benefits, with unique strengths and drawbacks, providing no 'silver bullet' solution. The different properties are presented in a comparison table.

Direct injection of foam shows the best heat mitigating performance compared with all tested methods. This method had the highest potential for module-to-module fire mitigation, especially when designed for sufficient capacity to flood the modules/racks over longer time periods. In cases where alternative ship integration concepts are to be evaluated - such as a battery installed without a dedicated battery room - this may be a particularly attractive approach to evaluate the equal level of safety. The gas temperature and gas absorption are not evaluated.

High pressure water mist protection provides good heat mitigation at module level in addition to providing full battery space protection from external fires. It also has good gas absorption and gas temperature reduction capabilities.

NOVEC extinguish the battery fire flames, but performs poorer regards to heat mitigation, gas temperature reduction and gas absorption compared to water mist. Room ventilation needs to be closed for this suppression method to be functional. This can increase the toxic and explosive battery gas concentration in the room until ventilation can start again.

Sprinklers do not extinguish the visible flames but records similar heat mitigation capabilities at module level as high-pressure water mist. Since water can displace the gas into pockets with high concentrations, the explosion risk is considered to become more severe with sprinklers.

Each battery installation will have to assess necessary barriers in consultation with the battery manufacturer to identify the application most suited for that project. Due to limited amount of available suppression media onboard a vessel, the actual volumes and release rates needs to be calculated and are dependent on the battery system.

A methodology for comparative tests between different battery fire suppression systems available in the maritime market is proposed. Both heat and gas mitigation performance are evaluated.

1.1.2 Heat and gas generation

The cell level and module level tests presented in this report provided evidence that visual combustion produced more heat, but less gas compared to tests without visual combustion. Tradeoffs in the risk evaluation needs to be done between extensive heat generation vs extensive explosive and toxic gas generation.

The NMC cell which released significantly more volume was the one test that did not induce visible combustion external to the cell. It seems that the gas production is halved when there is visible combustion. However, further tests are needed to quantify the exact number.

The amount of oxygen released is not sufficient to affect combustibility external to the cell. It is considered more likely that O2 is released internal to the cell and play a very central role in the onset of thermal runaway. This will also result in more aggressive heat development and increased CO or CO2 production.

It is also seen that limiting the oxygen supply will suppress the battery fire, but not be sufficient to cool down the battery. In these cases, the off-gassing is increased compared to fires where oxygen is fueled to the fire.

It is seen that modules with IP4X produces less heat and more gas compared to modules of IP2X. This is due to the limitation of oxygen in the IP4X modules.

1.1.3 Toxicity

If the room is to be entered after an event, all the identified toxic gases needs to be considered. The gasses identified in this project are carbon monoxide, nitrogen dioxide, hydrogen chloride, hydrogen fluoride, hydrogen cyanide, benzene, toluene.

Very small gas concentrations will make the atmosphere toxic, and the gas will dilute fast. Hence the sensor detecting the toxic gases can be placed in the normal breathing zone for people, 1-1.8 meters from the floor.

Personal Protection Equipment should be used when re-entering the battery space after a battery fire, also after deployment of fire suppression material.

The properties of a battery fire can be compared to burning plastics.

When weighting the Immediately Dangerous to Life or Health (IDLH) values with the released gas amounts, CO, NO2 and HCL will first reach its IDLH values.

1.1.4 Off-gas detection

Gas release profile - CO is the main component present for the longest period of time and is considered especially important for early stage detection.

Off-gas in the early stages of thermal runaway events will be colder than off-gas release in the later stages. The early off-gas can therefore become heavier than the air, collecting at floor level. It should therefore be considered if gas-detection related to room explosion risks should be applied at both levels, close to the floor and close to the ceiling.

Tests conducted in this project indicate that solely relying on Lower Explosion Limit sensor(s) and cell voltage levels to detect early stages of a thermal runway event is insufficient.

Both the Li-ion Tamer sensor® and smoke detector, when placed close to or inside the affected module, proved the most reliable means of pre-thermal runaway warning. The early detection of thermal runaway has also proven that a cell can be disconnected, effectively stopping the overheating process.

1.1.5 Ventilation

In order to realize the most potential of a forced extraction duct, a high extraction point in the room has proven to be the key factor. This ensures that the required air changes per hour stays low while still providing the necessary dilution of explosive gases in the space.

The explosion pressure limit is set to 0.5 barg. Above this pressure the bulkheads will be damaged. With a ventilation rate of 6 ACH it should be sufficient to avoid such pressure if 350 liters of battery gas released in the room is considered as a worst case. This corresponds to a cell or module of 115-175Ah. If cells of total 250Ah is failing, this requires 10 ACH, while failing 500Ah requires 22 ACH in a room of 25m3 of free space. The ventilation can be turned on demand based at early off-gas detection with sensors close to or inside the modules.

If batteries of 4000 Ah is failing, it will not be sufficient with 100 ACH to avoid an explosion magnitude of 0.5 barg.

A ventilation formula for a battery room is proposed. The formula calculates the air changes per hour (ACH) with the size of the failed batteries, the design bulkhead pressure, the room volume and the vent distance from the ceiling as input variables.

1.1.6 Temperature class and gas group

The key requirements when designing explosion proof equipment are temperature class and gas group.

Based at the tests performed, the temperature class for battery off-gas explosion proof equipment is recommended to be T2 according to the IEC 60079 standard.

The gas group is identified as Group IIC according to the IEC 60079-20-1 standard.

1.1.7 Thermal runaway identification

Based at the tests performed, significant difference was observed between the Nickel Manganese Cadmium (NMC) and Lithium Iron Phosphate (LFP) cells. The LFP cylindrical cells were much harder to force into thermal runaway compared to the NMC pouch cells.

For the NMC pouch cells, a temperature increase rate above 10 °C/sec together with a max temperature above 450°C seems to be sufficient to identify the onset point for a thermal runaway with visual combustion.

For the LFP cells, a temperature increase of 4 °C/sec seems to be sufficient to identify the onset point for the thermal runaway. The chance of achieving this increase with increased state of charge, and it might be necessary to charge the LFP battery cells beyond 100% SOC to provoke visual combustion.

1.1.8 Quantitative Risk Assessment

Key findings based on a Quantitative Risk Assessment (QRA) for the battery system, are that fire propagation protection and the Current Interruptive Device are two of the most important safeguards to be installed in the battery system.

When comparing the battery fire risks with data registered in the HIS Fairplay database for fires in a diesel engine room, it seems that the likelihood of a battery fire is lower compared to a diesel fire. However, engine room fires registered in the HIS Fairplay database include fires of many different magnitudes not necessarily correlating to the fire scenario established in battery system QRA. This means that better data would be necessary to fully evaluate if a battery system is safer than a conventional combustion engine.

1.1.9 Battery system design

The required ventilation rate and the amount of fire suppression material depends on the number and the size of the battery cells involved in the fire. If the complete battery system catches fire, the suppression and ventilation will not be able to mitigate the fire and explosion risks. It is of most importance to design a battery system with fire propagation protection and Current Interruptive Devices

to limit the fire to one part of the battery system, and to install a well-tested Battery Management System capable of preventing several modules being overcharged at the same time.

SECTION A: MAIN REPORT

A discussion and summary of findings from the project, aimed as useful reference for assessment of the primary factors with regard to lithium-ion battery safety. This is based on the test results presented in detail in Section B.

2 INTRODUCTION

The main safety concern when installing a lithium-ion battery system is that the battery will start to burn and the development of explosive and toxic gasses. When a battery is heated up, it can start an internal exothermic reaction called thermal runaway. Figure 2-1 summarizes the causes and consequences of thermal runaway. It often starts from an abuse mechanism that causes the internal temperature to rise such that the electrolyte is gasified, released and ignited. This fire might then ignite the electrodes, thus producing high temperature fires involving both liquids and gases. These fires are hard to extinguish and to cool down.
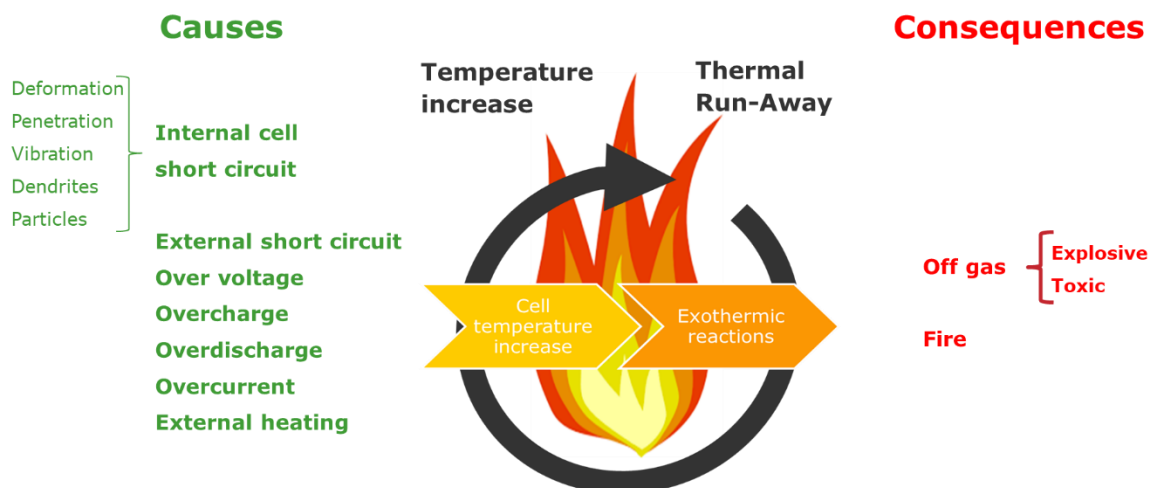
Figure 2-1: Causes and consequences of a thermal runaway in a battery system.

This report is intended to enable persons assessing energy storage installations, whether from a design, engineering or regulatory perspective, to better evaluate risks, capabilities and solutions regarding safety. The focus and context are on installations in the maritime environment although the vast majority of findings apply similarly to other applications and industries. The focus has been to give guidance regards the mitigating safeguards, addressing the battery fire and off-gassing.

2.1 Background

Lithium-ion batteries are a disruptive technology that has already significantly altered almost every industry sector, including maritime. They are a crucial, if not the central, component in the next generation of power systems and green or renewable technologies; a fact that is most immediately apparent in transportation and maritime. However, this utilization and deployment must be built upon a basis of safety.

Batteries are a complex technology comprising of many interrelated scientific phenomena – and this holds true for their fundamental internal operation, their application and usage in power systems, and absolutely regarding safety. Rules and requirements have evolved to cover the full spectrum of risk, but the complexity of safety aspects mean that additional learning and understanding provide an opportunity for both improving the total level of safety as well as the efficiency of the approval process. More public knowledge on key threats and technical aspects means more consistent and focused engineering solutions. Better understanding of the total risk picture means more consistent and effective regulations and requirements. Thus, the focus of this Joint Development Project (JDP) was to bring together members of the entire value chain to identify these key issues as a team. Testing and analysis would

then be performed to provide technical input for results that would then be discussed and reviewed as a team in order to provide recommendations that had been reviewed from all perspectives.

There are many different battery system designs or engineering approaches that may focus on mitigating certain challenges. In addition, there are many different tools that may be used for mitigating certain risks. Understanding the risks of a given battery design is the key and ensuring sufficient systems are in place to produce an acceptable level of risk. This document seeks to provide information that can be used as reference in assessing these risks.

3 BATTERY OFFGAS CONTENTS AND DETECTION

The off-gases in a lithium-ion battery is known to be flammable as well as toxic. This presents an explosion risk in enclosed spaces. Accurate understanding of the constituents of this gas is difficult as it depends on many variables. Often the test procedure can involve practices for measurement that may not be relevant for use as input to an evaluation of explosion potential.

3.1 Off-gas contents

Table 3-1 shows the off-gas quantities that were found in the cell level testing conducted in this project. Tests are conducted in a steel chamber with air flow through, and gas measured by FTIR; setup details can be found in Section B 13.1. Cells are charged to specific SOC values as indicated in the table and then heated using radiant and band heaters, except in the cases indicated as OC (overcharge), in which case a constant current of 50A is applied until failure.

NMC cells tested were a pouch type while both LFP cells were cylindrical. Notably, the NMC cell which released significantly more volume was the one test that did not induce visible combustion external to the cell – such that nominally the other NMC tests thus indicate how much gas may be consumed when there is combustion. This is an important phenomenon that is revisited in the module testing, Section A 7 and Section B 14.2.

Table 3-1 – Off-gas values as measured in project testing - from different chemistries, heating at different SOC, overcharge (OC) and external short circuit (SC) when possible

Value	NMC, 63Ah					LFP1, 2.5Ah				LFP2, 1.5Ah		
SOC	50	75	100	OC	SC	50	75	100	OC	50	75	100
CO_2	19,6	25,7	40,3	38,8	65,9	44,3	20,2	63,4	20,9	22,5	23,0	35,1
CO	29,2	38,1	11,4	34,4	19	7,6	15,9	15,1	26,1	12,0	13,9	11,3
NO_2	-	-	-	-	-	4,9	9,7	5,9	1,3	4,8	5,6	4,9
CH_4 (methane)	12,6	9,4	19,4	12,5	2,7	4,3	5,6	3,0	3,7	5,9	5,9	5,6
C_2H_6 (ethane)	10,6	10,5	11,7	4,8	7,6	15,6	23,0	7,7	15,4	21,0	23,1	20,0
C_2H_4 (ethylene)	10,5	4,4	9,6	4,9	1,6	7,3	11,4	1,9	13,7	12,0	8,8	5,8
C_3H_8 (propane)	-	-	-	-	-	3,9	5,8	0,6	4,2	5,8	3,7	4,5
HCL	9,7	0,8	1,9	0,2	0,2	1,1	0,8	0,2	0,3	2,1	1,9	1,0
HF	0,7	0,3	0,3	0,1	0,1	1,6	1,6	0,4	0,1	1,9	3,7	3,6

HCN	0,0	0,0	0,0	0,0	0,0	0,1	0,1	0,0	0,1	0,4	0,7	0,6
C6H6 (benzene)	4,1	5,2	1,1	4,3	1,9	0,0	0,7	0,0	13,6	0,6	0,0	0,3
C7H8 (toluene)	2,0	4,1	0,3	0,5	0,9	0,0	0,0	0,2	0,0	0,1	0,5	0,7
C2H6O (ethanol)	0,3	0,7	2,9	0,1	0,0	3,7	0,4	0,5	0,0	7,0	4,6	4,0
CH4O (methanol)	0,7	0,8	1,1	0,5	0,2	5,6	4,7	0,9	0,4	3,9	4,6	2,5
Volume [L]	527	182	233	245	180	9,4	8,4	27	19,1	5,5	6,1	6,5
Average ambient temperature during Thermal Runaway [C]	131	166	201	221	57	102	99	81	28	91	82	99
Volume normalized to 25C ambient temperature [L]	388	124	146	148	161	7,5	6,7	23,1	18,9	4,5	5,1	5,2
L/Ah normalized to 25C ambient temperature	6,2	2,0	2,3	2,3	2,6	3,0	2,7	9,2	7,6	3,0	3,4	3,5

Notably, hydrogen, H2 is missing from the table above. In all cases the H2 sensor was saturated at a value of 1%. This saturation happens almost immediately upon the onset of thermal runaway, with only a few cases showing trace amount of hydrogen released just beforehand. H2 is an important component to consider in safety and explosion considerations. Thus, a literature review was conducted to determine the best way to incorporate the hydrogen gas content. Most literature sources do not report the full spectrum of gasses shown in Table 3-1; but, when tested under similar conditions, literature is quite consistent in reporting values between 5% to 30%. As a worst-case example, the values of CO2, CO, CH4, & C2H6 are normalized for a 30% H2 concentration, and shown all together in Table 3-2.

Table 3-2 – Calculated off-gas contents incorporating assumed hydrogen content of 30%

Value	LGC NMC, 63Ah					LFP1, 2.5Ah				LFP2, 1.5Ah		
Case	50	75	100	OC	SC	50	75	100	OC	50	75	100
CO2	16	20	30	28	48	40	20	49	18	22	21	31
CO	25	30	9	25	13	7	14	12	23	12	13	10

Gas species												
CH4	11	8	15	9	2	3	5	2	3	6	5	5
C2H6	9	8	9	4	6	14	21	6	13	21	21	18
C2H4	9	4	7	4	1	6	10	1	12	12	8	5
H2 estimated	30	30	30	30	30	30	30	30	30	27	30	30
Average ambient temperature [C]	*131*	*166*	*201*	*221*	*57*	*102*	*99*	*81*	*28*	*91*	*82*	*99*
Volume normalized to 25C ambient temperature [L]	*458*	*193*	*193*	*199*	*223*	*10*	*7*	*30*	*21*	*5*	*5*	*6*
L/Ah	*7*	*3*	*3*	*3*	*4*	*3*	*4*	*12*	*9*	*3*	*4*	*4*

Batteries with layered metal oxide cathodes (i.e. NMC) theoretically release oxygen as the cathode is combusted. During testing, it is not uncommon to observe that lithium-ion battery fires will consume all available oxygen and/or push out oxygen, such that at some point in the event, off-gassing of an NMC cell could be occurring in an oxygen deprived space. More specifically, in these cases O_2 levels do not seem to rise or to come back, as would be expected based on this O_2 release phenomenon. Thus, it is suggested that the amount of O_2 released is not of sufficient volume to affect combustion or combustibility external to the cell. It is considered more likely that O_2 is released internal to the cell and may play a very central role in the onset of thermal runaway and the temperature of the fire.

3.2 Gas contents pre-thermal runaway

NMC overheat 50% SOC and the overcharge tests were used to provide an indication of the average content and concentrations of the gasses released before the onset of thermal runaway, shown in Table 3-3.

Table 3-3 - Composition of off-gas released from cell before full thermal runaway

Gas species	Composition in overheating 50% SOC case (%)	Composition in overcharging case (%)
CO	32.1	47.9
Ethane	24.1	13.1
Methane	16.1	7.2
Benzene	11.3	24.0

Gas species	Composition in overheating 50% SOC case (%)	Composition in overcharging case (%)
Ethylene	9.6	4.8
Toluene	5.5	3.0
HCl	0.7	-
Methanol	0.6	-

Notably – hydrogen is not seen. This held true for the vast majority of cases, where hydrogen was not seen until the onset of thermal runaway, though due to anecdotal experience the hydrogen is often consumed rapidly. In only one or two cases was hydrogen seen before the onset of thermal runaway – and then only in small amounts, ramping up in the seconds before thermal runaway occurred.

3.3 Gas release profile

Figure 3-1, Figure 3-2 and Figure 3-3 show the off-gas release from all measured battery gases for overheating NMC at 50%, overcharging NMC and overheating NMC at 100% respectively.

It is seen that for overheating at 50% and overcharging, CO is the most continuously present gas and thus provides a good indication of the full spectrum of gas profiles that may be expected. The CO concentration presented in Figure 3-4 provides a reference for the shape of off-gas release from cells. For the 100% SOC case, a similar profile can be found by monitoring CO2, as shown in Figure 3-3.

In all three cases, it is shown that the full release generally occurs in less than 150 seconds. In addition, initial gas release quantities of 5,000 to 10,000 ppm are relatively small, particularly in comparison to the peak values seen. The rapid increase in gas release directly corresponds to the thermal runaway event as characterized in Chapter 9.
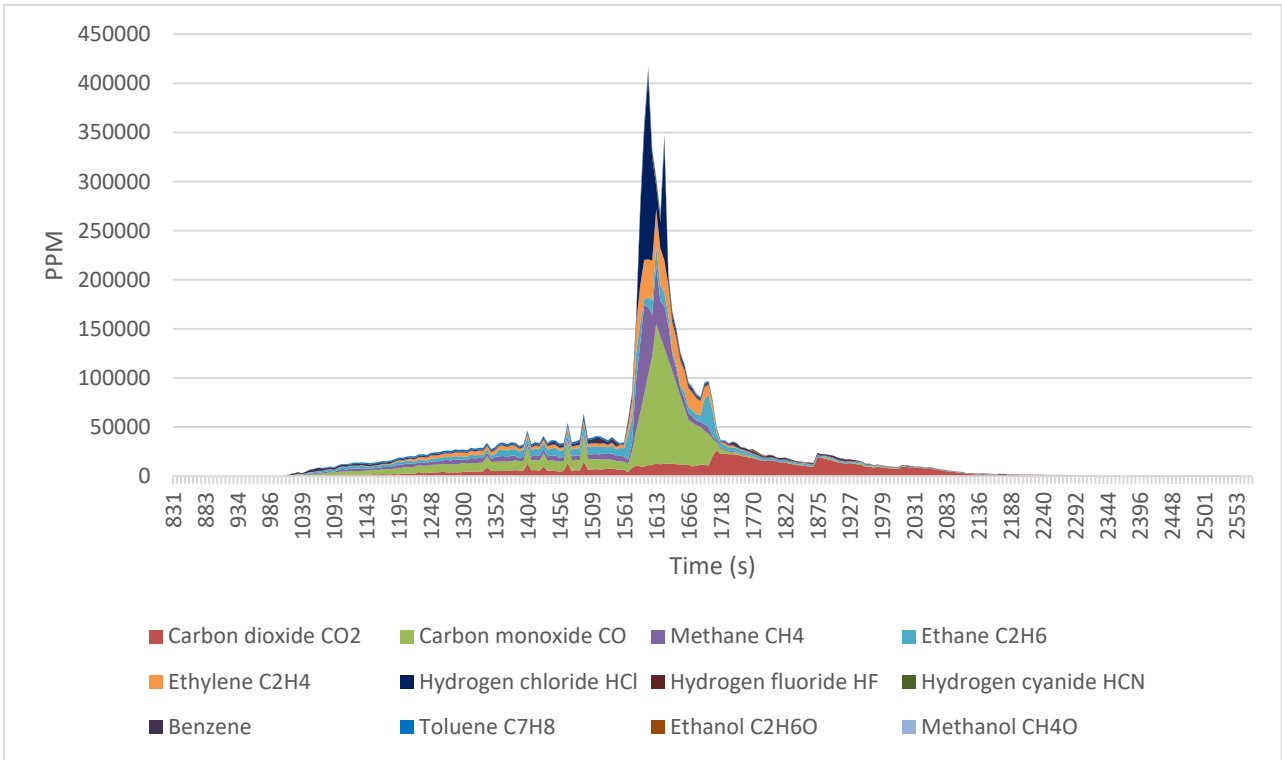
Figure 3-1: Gas release profile for an overheated NMC pouch cell with 50% SOC
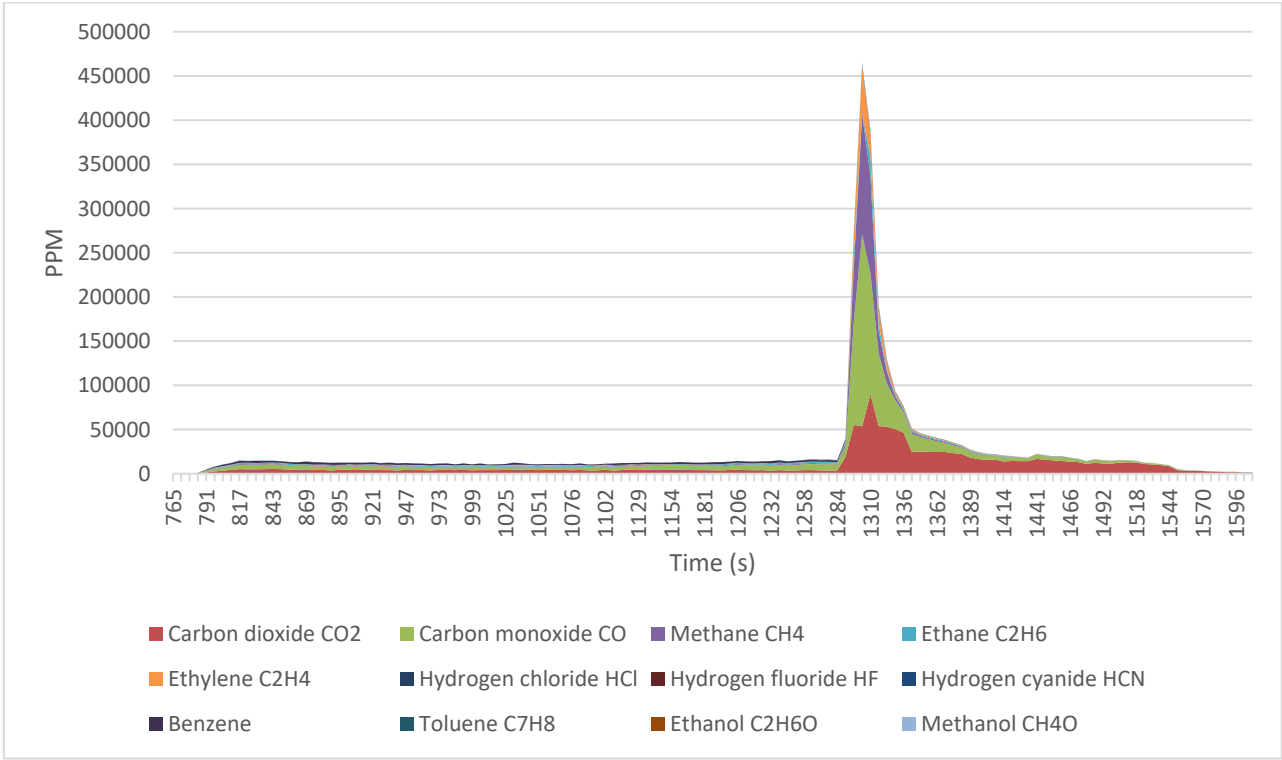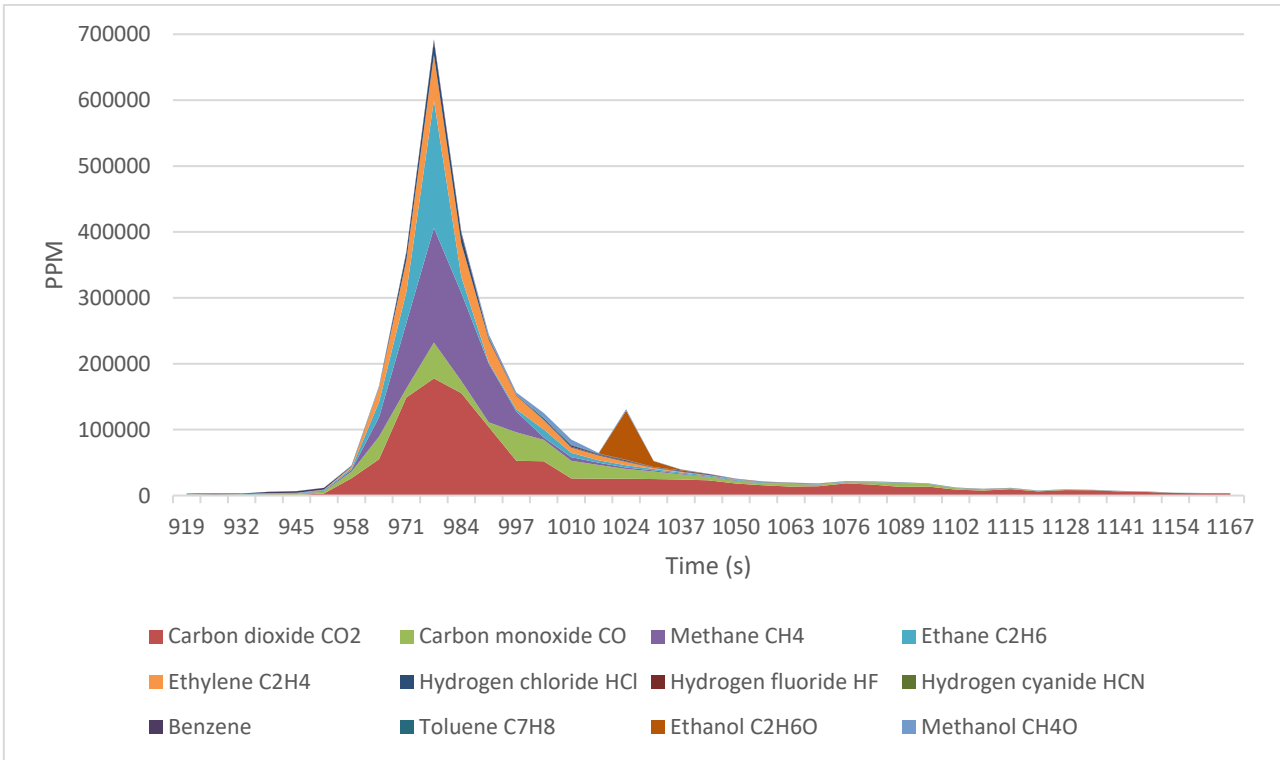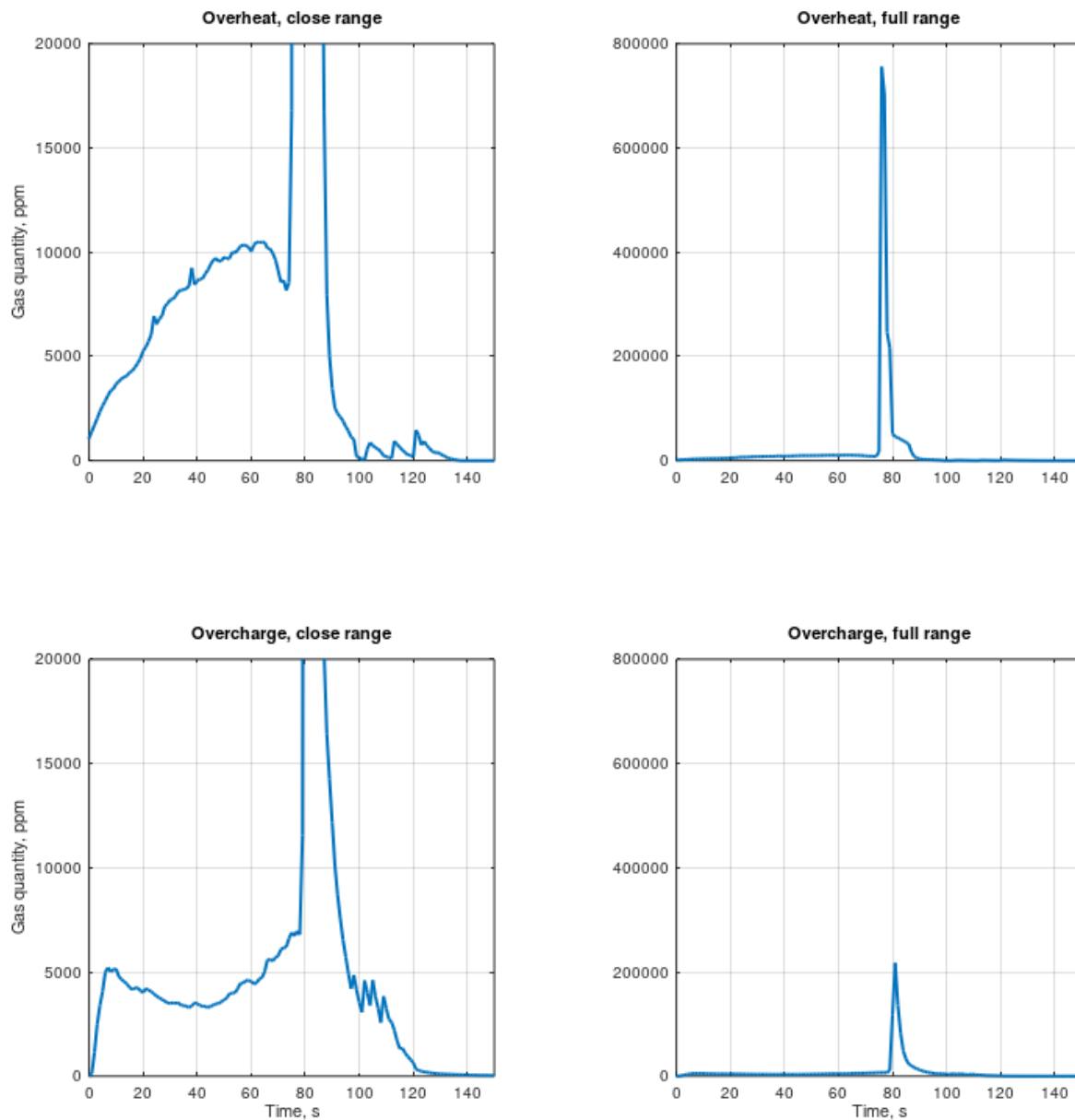

Figure 3-2: Gas release profile of an overcharged NMC pouch cell

Figure 3-3: Gas release profile of an overheated NMC pouch cell 100% SOC

Figure 3-4 – Off-gas release profiles represented by CO for two different failure modes

3.4 Off-gas detection

3.4.1 Single cell gas detection tests

Tests were monitored with thermocouples, a Lower Explosion Limit (LEL) sensor, an off-gas specific sensor called the Li-ion Tamer® developed by Nexceris and cell voltage. From the tests conducted, average values about the rates of detection and indication are provided below. Note, voltage as indicated here is when there is a loss of voltage across the terminals, in cases of overcharging clearly there is earlier indication that voltage is out of spec. LEL indication as reported here is the first time a measurement is indicated – in the vast majority of cases the LEL reading goes from zero to saturated. In addition, in many cases the LEL sensor would display erroneous values and required multiple

recalibrations to become functional again if at all. By comparison the Nexceris sensor showed high sensitivity and more stable behavior. However, it should also be mentioned that with regard to standard installations, these devices would not be expected to undergo repeated exposure to high temperature and concentrations as was done in repeated thermal testing.

With regard to functionality as indication mechanisms, a summary in Table 3-4 is provided. Times are presented relative to thermal runaway as was indicated by temperature sensors on the cell. It can be seen that LEL sensors and voltage do not provide a mechanism for early warning. In comparison, the Li-ion Tamer® sensor indicates only seconds after off-gassing occurs. In addition, testing was performed where a cell was being overcharged and charging stopped when off-gas was released as indicated by the Li-ion tamer®. The cell temperatures ceased to increase, and off-gassing started to decline until the cell was considered stable. Thus, demonstrating it is feasible to 'pull back' a cell after it has begun off-gassing but before thermal runaway occurs. Meaning early detection, coupled with correct system shutdown measures is an important safety barrier.

Table 3-4 - Average responses from different sensors and indication mechanisms tested in cell level tests

	Off-gas Release	Li-ion Tamer® sensor	Thermal Runaway	Cell Voltage	LEL Sensor
Time of occurrence relative to thermal runaway, average, seconds	-381	-371	0	+7	+28

3.4.2   Module scale gas detection tests

Off-gas detection was also evaluated similarly as a part of the full-scale testing with complete, enclosed modules in the representative battery room. The Li-ion® Tamer sensor was evaluated together with a smoke detector. Sensors were placed on the module above the device under test for this measurement, thus nominally giving a 'best case' capability evaluation.

The key properties of the tests are shown in Table 14-4.

Table 3-5: Key properties of gas detectors for module level tests

Test ID	IP Rating of box	Combustion	Visual external Combustion	Time difference between Li-ion Tamer® and Smoke detector	Max temperature inside the test box before detection
1	44	Yes	No	22 sec	16℃
3	20	Yes	Yes	9 sec	290℃
7	44	Yes	No	21 sec	173℃
9	20	Yes	Yes	44 sec	440℃

Both the smoke detector and Li-ion Tamer® can detect the gas for cases with and without external combustion. The Li-ion Tamer® detects the gas first in all tests, 10-45 seconds faster than the smoke detector. However, it seems the gas is not always detected before the cells has entered thermal runaway. Compared with the cell level tests, where the sensors were placed in the same enclosure as the battery cells, the gas is detected much later when the sensors are placed outside the modules.

It can be concluded that both the smoke sensor and Li-ion Tamer® gas sensor are capable of detecting the battery gas. The placement of the sensor is a key factor for early detection, and the sensor should be placed as near the battery as possible, ideally within the module enclosure.

3.5 Main Conclusions

Main Conclusions
1. The NMC cell which released significantly more volume was the one test that did not induce visible combustion external to the cell. It seems that the gas production is halved when there is visible combustion. However, further tests are needed to quantify the exact number. 2. The amount of oxygen released is not sufficient to affect combustibility external to the cell. It is considered more likely that O2 is released internal to the cell and play a very central role in the onset of thermal runaway. This will also result in more aggressive heat development and increased CO or CO2 production. 3. Carbon Monoxide is the main component present for the longest period and is considered especially important for early stage detection. 4. Off-gas in the early stages of thermal runaway events will be colder than off-gas release in the later stages. The early off-gas can therefore become heavier than the air, collecting at floor level. It should therefore be considered if gas-detection related to room explosion risks should be applied at both levels, close to the floor and close to the ceiling. 5. Solely relying on Lower Explosion Limit sensor(s) and cell voltage levels to detect early stages of a thermal runway event is insufficient. 6. Both the Li-ion Tamer® sensor and smoke detector, when placed close to or inside the affected module, proves the reliable means of pre-thermal runaway warning.

4 TEMPERATURE CLASS AND GAS GROUP

A key motivation for identification of off-gas contents was to provide greater clarity on requirements for EX (explosion proof) equipment to be used in the battery room and ventilation fan(s) installed. The requirements for such identification are temperature class and gas group, which are functions of the gas itself. These characterizations are outlined in IEC 60079. Note that the battery cells themselves can never be EX proof, but equipment installed where high gas concentrations are expected, such as the extraction fan of the battery system or battery room can pose a high threat.

4.1 Temperature class

Figure 4-1 shows the different Temperature Class categories and indicates the dependency on ignition temperature for determination. The requirement states that the surface temperature may not reach the ignition temperature of any of the gasses and thus, it is considered that the lowest autoignition value of any of the gasses expected to exist shall be used. The autoignition temperatures of the gas constituents detected in this project testing are indicated in Table 4-1. As shown, the lowest value is found to be 365°C for ethanol. Thus, the temperature class for battery off-gas EX equipment consideration is recommended to be T2.

Temperature class required by the area classification	Ignition temperature of gas or vapour in °C	Allowable temperature classes of equipment
T1	> 450	T1 – T6
T2	> 300	T2 – T6
T3	> 200	T3 – T6
T4	> 135	T4 – T6
T5	> 100	T5 – T6
T6	> 85	T6

Figure 4-1 - Temperature Class requirements based on gas autoignition temperature as defined in IEC 60079 (Table 4)

Table 4-1 - Autoignition temperatures of key gasses found in lithium-ion battery off-gas

Value	Autoignition Temperature (°C)
Ethylene Carbonate	465
CO2	-
CO	609
NO2	-
H2	536
CH4 (methane)	580
C2H6 (ethane)	515
C2H4 (ethylene)	450
C3H8 (propane)	455
HCL	-
HF	-
HCN	538
C6H6 (benzene)	560
C7H8 (toluene)	530
C2H6O (ethanol)	365
CH4O (methanol)	470

4.2 Gas group

The specific gas group is classified according to their maximum experimental safe gaps (MESG), as defined in IEC 60079-20-1. The groups for equipment for explosive gas atmospheres are:

1. Group I: equipment for mines susceptible to firedamp.

2. Group II: equipment for places with an explosive gas atmosphere other than mines susceptible to firedamp.

    a. Group IIA: MESG ≥ 0,9 mm.

    b. Group IIB: 0,5 mm < MESG < 0,9 mm.

    c. Group IIC: MESG ≤ 0,5 mm.

For mixtures of gasses, the process for identifying the gas group is based on Le Chatelier's mixing rule according to the standard. This equation is shown below.

$$MESG_{mix} = \frac{1}{\sum \left(\frac{X_i}{MESG_i} \right)}$$

According to the standard, the calculated MESG value will be higher than the actual value for the mixed gas when CO is greater than 5%.

For calculating combined MESG, the case of NMC at 50% was used as a worst case since it had the lowest proportion of CO2. The values presented Table 3-2 is used in the calculation, since it assumes 30% of hydrogen.

For actual calculation, CO2 was omitted, and the combined amount was calculated as a percentage of remaining gasses. Some gasses are not considered in the assessment, but their omission results only a small deviation towards a more conservative result as the main constituents of CO and H2 contain the lowest MESG values of the gasses present in large quantities.

Using Le Chatelier's mixing rule the MESG value is found to be 0.5. Since the concentration of CO is 30%, far beyond 5%, the actual MESG value is expected to be lower.

This places lithium-ion battery off-gas within Gas Group IIC according to standard IEC 60079-20-1.

Table 4-2: MESG values of identified battery gases, and the MESG value of the combined battery gas.

Value	MESG	Normalized gas concentration when CO2 is omitted
Ethylene Carbonate	NA	-
CO2	NA	-
CO	0.84	30
NO2	NA	-
H2	0.29	36
CH4 (methane)	1.12	13
C2H6 (ethane)	0.91	11
C2H4 (ethylene)	0.65	11
C3H8 (propane)	0.92	-
HCL	NA	-
HF	NA	-
HCN	0.80	-
C6H6 (benzene)	0.99	-
C7H8 (toluene)	NA	-
C2H6O (ethanol)	0.89	-
CH4O (methanol)	0.92	-
COMBINED	**0.5**	**100**

4.3 Main Conclusions

Main Conclusions
1. The temperature class for battery off-gas explosion proof equipment is recommended to be T2 according to the IEC 60079 standard.
2. The gas group is identified as Group IIC according to the IEC 60079-20-1 standard.

5 TOXICITY

For the most part, lithium-ion batteries are not more significantly toxic than a comparable plastics fire; but there absolutely is the potential for low concentrations of more harmful gasses to be produced, which can depend on the cell being used (particularly the electrolyte formulation; Polyvinylidene Fluoride in particular can directly affect HF levels) /3/. Thus, the primary recommendation is that, following a lithium-ion battery fire, there should be no re-entry without sufficient Personal Protective Equipment. For general guidance on quantities of the more toxic substances that should be expected to be present, see Table 5-1.

Table 5-1 - Volumes of primary gasses of concern with regard to toxicity

Gas	Max % observed from cell level	L of specific gas per Ah (assuming 2.6 total L/Ah)	Immediately dangerous to life or health (IDLH) [ppm]	Relative Vapor density (air = 1)
CO	38.1%	0.9906 L/Ah	1200	0.97
NO2	9.7%	0.2522 L/Ah	20	2.62
HCL	9.7%	0.2522 L/Ah	50	1.3
HF	3.7%	0.0962 L/Ah	30	0.92
HCN	0.7%	0.0182 L/Ah	50	0.94
C6H6 (benzene)	13.6%	0.3536 L/Ah	500	2.7
C7H8 (toluene)	4.1%	0.1066 L/Ah	500	3.1

The relative vapor density is also included in the table to give an indication if the gas will accumulate close to the floor or the ceiling. However, according to /17/, these gases tend to diffuse and mix quickly. Even if the gas starts out stratified, it cannot stay stratified for a long time in a small, confined space. Very small concentrations of gas in the ppm range will make the atmosphere toxic. The placement of a toxic gas detector is then of less importance compared to a LEL sensor, which is in a range of vol%. Explosive gas can be more stratified, and it is important to measure at various levels before entering a confined space. Hence, it can be concluded, that the gas sensor measuring the toxicity level should be placed in the normal operating zone for people, 1-1.8m from the floor /19/,/20/.

Depending on gas compositions released from the various tests performed, the gas types that first reached IDLH limits were CO, HCL and NO2; based on the following formula:

$$IDLH_{Normalized} = \frac{IDLH_i}{x_i}$$

where x_i is the gas concentration of the specific toxic gas.

5.1 Main Conclusions

Main Conclusions

1. Very small gas concentrations will make the atmosphere toxic, and the gas will dilute fast. Hence the sensor detecting the toxic gases can be placed in the normal breathing zone for people, 1-1.8 meters from the floor.

2. Personal Protection Equipment should be used when re-entering the battery space after a battery fire, also after deployment of fire suppression material.

3. If the room is to be entered after an event, all the identified toxic gases needs to be considered. The gasses are carbon monoxide, nitrogen dioxide, hydrogen chloride, hydrogen fluoride, hydrogen cyanide, benzene and toluene.

4. The properties of a battery fire can be compared to burning plastics.

5. When weighting the Immediately Dangerous to Life or Health (IDLH) values with the released gas amounts, CO, NO2 and HCL will first reach its IDLH values.

6 OFF-GAS VENTILATION AND EXPLOSION RISKS

As discussed in the previous subsection, battery off-gas constitute both an explosive and a toxic hazard. In order to avoid high concentrations collecting in the battery space a well-designed ventilation system is required. Different philosophies to diffuse such gases are employed in the market today. The two main principles being either; containing the battery modules and off-gas in gas-tight enclosures leading directly to a safe area on open deck, without passing the battery room first. The other option being; open battery racks where off-gas release first into the room before being diffused by a forced exhaust system of sufficient air changes per hours (ACH). The following tests were conducted in order to further understand the effects of room scale ventilation systems and the impact of such on observed and measured gas clouds during thermal runaway events.

6.1 Module scale tests

Module scale tests were performed (further detail in Section B, 14 and 15) which were used to evaluate the evolution of battery off-gas from a module configuration representative of batteries configured in a rack. This test setup was used to evaluate effects of various enclosures, cell types, ventilation rates, as well as fire suppression materials.

Comparing the effects of different enclosures, it was found that more open systems have a greater possibility of providing oxygen to the fire and this will tend to result in a higher chance of prolonged combustion with higher temperatures. In addition, the primary source for ignition of gasses is the failing battery cell itself, so more open modules also increase the chance of external combustion of gasses.

To measure the amount of gases in the battery room, a LEL sensor is used. This sensor records the LEL% as shown in the formula below.

$$LEL\% = \frac{Gas\ Consentration\ in\ Room\ [vol\%]}{LEL\ for\ Gas\ [vol\%]}$$

When the gasses produced from a lithium-ion battery are combusted, rather than accumulating, the explosion risk goes down substantially. This is represented in the significantly lower maximum LEL% value as seen in the IP2X case of Table 6-1. Limiting the oxygen to the fire will reduce the module heat, while the off-gassing and hence the explosion risk increases. This also indicate that if the ventilation is closed, the heat will eventually go down when the oxygen is consumed, while the off-gassing will increase. This is an important finding when evaluating the explosion risk of the room.

Experimental LEL% measurement results from the case that did not ignite were used to match CFD results and this way the amounts of gas produced from the tests was indicated, see also Chapter 14.

Table 6-1 – Effect of module enclosure on gas and heat produced

Cells	Enclosure	External Combustion	Max measured LEL%	Time to max measured LEL% (s)	Max Internal Temp Module above	Max External Temp Module above
NMC Pouch	IP44	No	69%	120	29	92
NMC Pouch	IP20	Yes	26%	500	152	252

Table 6-2 – More open modules have a higher incidence of combustion

Module Enclosure	IP4X	IP2X	Open Lid
Percentage of Tests with External Combustion	0	60%	80%

NOTE: the IP2X test indicated also consisted of a NOVEC release approximately 30 seconds after the identification of the fire.

Figure 6-1 – 30 seconds after thermal runaway for a IP4X module (top) compared to a IP2X module (bottom) shows how much combustion consumes and removes gas.

6.2 Guidance to needed ventilation

Two CFD models and different gas release scenarios are used to analyze further ventilation rates and different rooms to provide guidance on how ventilation can be expected to reduce explosive atmospheres. Simulations were also run for different gas release volumes which represent failure of different sized modules. The main results are shown in Figure 6-3 and Table 6-3.

6.2.1 Determine the gas volume released

Assessment of the needed ventilation rates requires knowledge of how many liters of gas that are expected to be released from a cell and how many cells and modules will be involved in the event. In this way the total volume of gas to be released is found and used for an assessment. The total volume of gas released is hence used as the decisive design parameter for the ventilation system.

For instance, the event under consideration may be several cells, or a full module or potentially a full string. Tests of the battery cell or module are needed to determine the amount of gas produced. This can then be used to give an indication of the total amount of gas that is produced for the worst case scenario considered. The total gas production volume tends to be proportional to the Ah size of the battery that is involved in the off-gas scenario. If one module is 1000 Ah, and the amount of gas produced from one cell is 2 l/Ah, then the total amount of gas from the module becomes 2000 L. The amount of gas produced as a function of battery size and type is considered further in Chapter 3.

6.2.2 Propagation rate

Propagation rate is the next crucial factor as shown by preliminary CFD analyses performed in Chapter 15.1. This scenario can in general be quantified by a release profile that first rises to a certain value, then continues with a more constant value as long as the propagation goes on from cell to cell, before it either escalates to another module, or dies out. Fast propagation between cells significantly increases the rate of gas accumulation in the room. Based on experience from all members of the JDP team it was considered reasonable to assume that cells will propagate, starting from a single cell with a significant amount of thermal mass and cooling capability, at a rate of 2 additional cells every 60 seconds. For a typical event as observed in the module experiment, the amount of gas rises quickly to a stable value (within 10-20 seconds is applied) and continues until it starts decaying after 100 to 250 seconds (or more, depending on the number of cells in the module), see also Section B 15.2. The event will further decay until it dies out unless it also propagates to another module.

If more than one module is involved in the dimensioning scenario, then the release rate is assumed to increase further instead of decaying when it is escalating to the next module. Then the release rate will get a new step up and continue with a higher total rate as long as both modules are releasing gas. The time to escalation to another module will vary, and 3 minutes is applied in the CFD analysis. This is assumed to be a possible, but quick escalation time. Hence, it is assessed to be on the conservative side. A plot and further discussion of how the release scenarios are quantified is given in Section B 15.3.

The CFD analysis that is performed finds the maximum size of a gas cloud inside the room during the off-gassing event. It is assumed that ignition occurs at the point of maximum flammable atmosphere – thus are considered worst case. It is further assumed that the walls can withstand 0.5 barg overpressure without breaking for a typical battery space forming a part of the vessel structure. This explosion pressure occurs during combustion of a stoichiometric gas cloud that is 1/16th of the room volume. The pressure is generated due to expansion of the gas during combustion where it is applied that the expansion causes maximum 8 barg when the room is filled up to 100%, see Section B 15.1.1 and Figure 15-3. This is a finding that is quite constant for different compositions of flammable gases from natural gas to pure hydrogen /4/. Structural strength of maritime walls, bulkheads, decks, ceilings, etc. can vary a lot, and the pressure of 0.5 barg is assumed a typical strength of a bulkhead wall. When new or retrofit

battery rooms are designed, it is important to know the strength of the bulkheads and relate it to the design explosion pressure. Results provided can be used to find needed ventilation rates for different design pressures. For example, if a stronger bulkhead than 0.5 barg is designed, then the needed ventilation rates can be reduced compared to the rates in Table 6-3.

The CFD assessments are based on two rooms with a free volume of 15 and 25 m^3, respectively. Results are considered applicable to other room volumes through the use of ACH for ventilation rates but for cases significantly departing from this setup (i.e. crowded, oddly shaped, very large, or very small rooms) it is recommended to perform an analysis for the specific case. Note, increased room volume will also reduce the overpressure caused by expansion and thus reduce the magnitude of the structural impact.

Results from the simulations are summarized in Figure 6-3 and Table 6-3. The results show that a relatively high ventilation rate is needed when 500Ah battery is failing; 22 and 70 ACH is needed for the large and the small room, respectively.

A higher ventilation rate is needed for the small room partly because in this room the air extraction duct is located 80 cm down from the ceiling (to the centerline of the duct). In the large room, this extraction duct is located 40 cm down from the ceiling. If the air extraction ducts are located higher up, the needed ventilation rate is reduced. If the room has extraction in the ceiling, then the calculated cloud size is reduced further. From the initial simulation results presented in Figure 15-9 and Figure 15-10 in Section B 15.1, the cloud size at 10 ACH and 30 ACH can be reduced by approximately 20% and 60% respectively. If it is assumed that this trend is general, the results from the large room can be reduced further as shown in Figure 6-2 and Figure 6-3. This is an indication of the benefit from designing ventilation suction from the ceiling.

For the largest release rate, no ventilation rate is found that would reduce the cloud to an acceptable size. It is simulated a ventilation rate up to 100 ACH, and this was found not to be sufficient.

For releases that are smaller than 1000 l, the needed ventilation rate will decrease further, however, the ventilation rate should not be zero. At zero ventilation, gas can accumulate even with a small release rate. By interpolating the test results between 120 liters and 500 liters, the typical ventilation requirement of 6 ACH is assessed to be sufficient for 350 liters of gas. This corresponds to a battery of 115-175 Ah, depending if 2 l/Ah or 3 l/Ah is assumed.
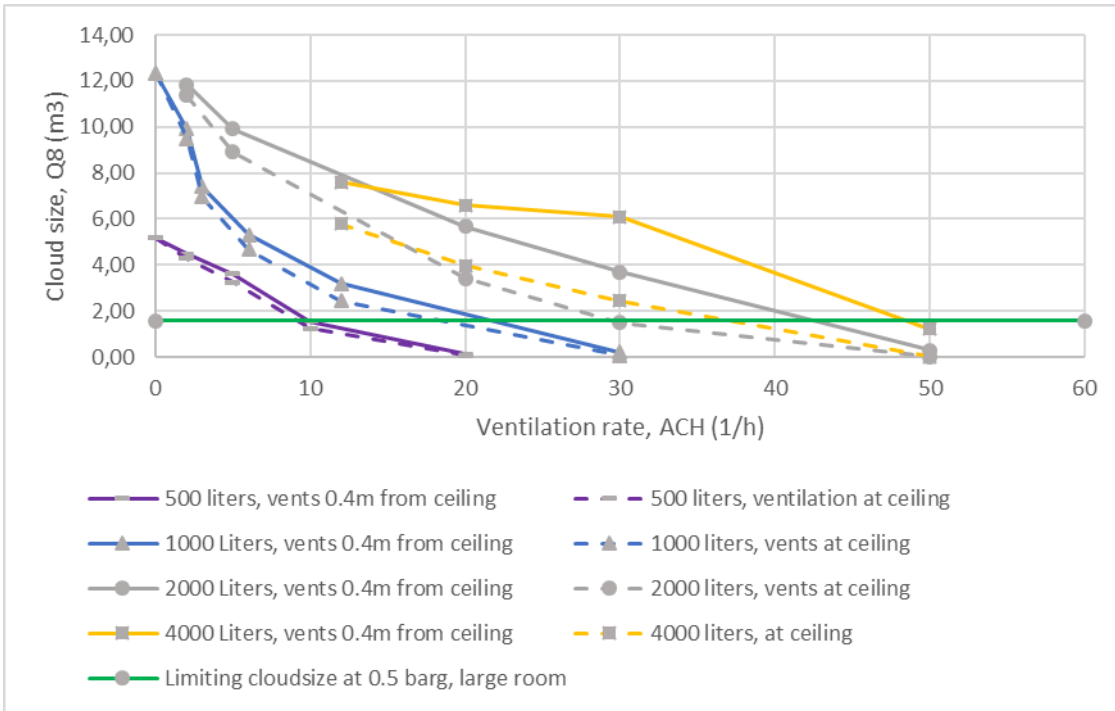
Figure 6-2 – Effect of ventilation located at ceiling for large room at 25m3.
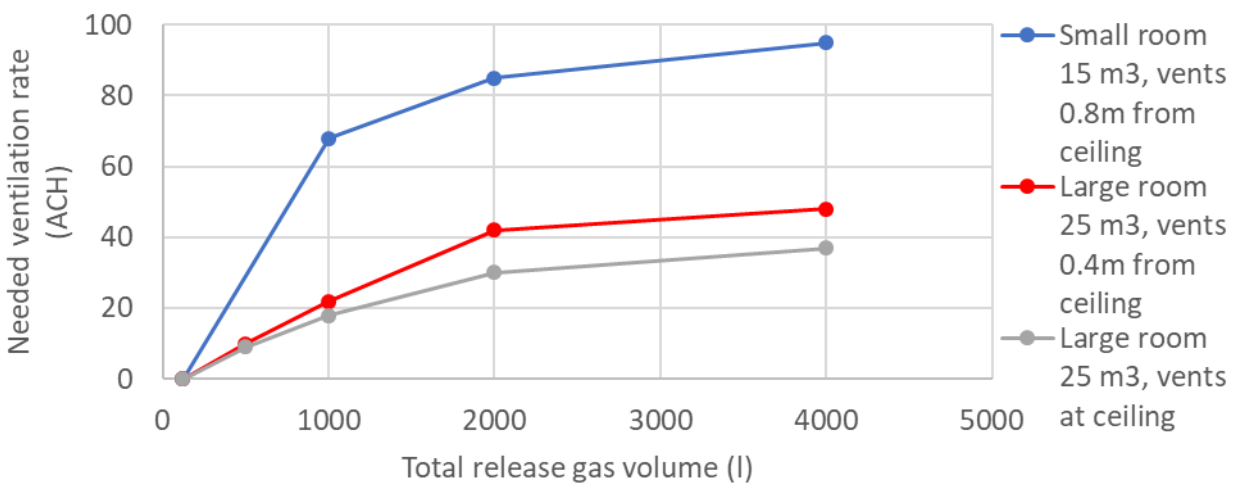
Figure 6-3   Needed ventilation rates as a function of the total volume of gas released from the battery. Note that the biggest contribution is the vent distance from the ceiling, and not the size of the room.

Table 6-3 – Needed ventilation rates (ACH) from CFD analysis based on gas volumes produced and types of room. The battery size in Ah is shown assuming a gas production rate of 2 L/Ah. This gas production rate may change between different cells.

Battery size releasing* (Ah)	60	250	500	1 000	2 000	4 000
Total gas released (l)	120	500	1 000	2 000	4 000	8 000
Small room 15 m3 ventilation, vents 0.8m from ceiling (ACH)			68	85	95	NA (>100)
Large room 25 m3 ventilation, vents 0.4m from ceiling (ACH)	0	10	22	42	48	NA (>100)
Large room 25 m3 ventilation, vents at ceiling (ACH)	0	9	18	30	37	NA (>100)

 * Assuming gas production is 2 l/Ah.

It is critical to take into account fire suppression with regard to ventilation requirements. Some fire suppression systems operate based on principles that require shutting down ventilation in order for them to be effective – particularly gas-based systems, such as CO_2 or Novec 1230.

6.3 Derivation of ventilation formula based at CFD results

Based at the CFD results, a formula for the ventilation for a typical battery room is here presented. This formula should only be for the assumptions listed in Section B 15.3.1. More specifically,

- Free volume from 10-30m^3.

- Leaking gas volume less than 4 000 liters.

- The extraction duct should be located less than 0.8 meter from the ceiling.

- If the extraction duct is at the bottom only, the formula is not valid.

If the room volume, release profile, ventilation arrangement and the shape of the room is severely different, a separate CFD analysis should be carried out.

The derivation is solely based at inspecting the curves from the CFD results, and a suitable function taken into account max $Q8_T$ size, the amount of battery gas released, the vent distance from ceiling and the room volume. The required air changes per hour (ACH) can be expressed as shown in the equation below,

$$ACH = A\frac{(1+Bh)}{v}e^{c\frac{(Q8_T+D)}{g}}$$

where $Q8_T$ (m3) is the critical stoichiometric gas cloud size, h (m) is the vent distance from the ceiling, g (liter) is the total liters of gas from the batteries and v is the room volume.

The variables $Q8_T$ and g can be replaced such that the function considers the design pressure p and the size of the failed batteries Q instead. The relationship between design pressure p, room volume v and threshold cloud size $Q8_T$ are $Q8_T = p\,v/8$, as discussed in Section 15.3.3. The total battery gas released can be expressed as $g = r\,Q$, where r is the gas released per ampere hour and Q is the size of the failed batteries in ampere hours. To account for CFD model uncertainties and simplifications made in the curve fitting process, a safety factor S should also be included.

Hence, the ventilation rate can be expressed as:

$$ACH = SA \frac{(1 + Bh)}{v} e^{\frac{C}{8} \frac{(vp+8D)}{rQ}}$$

where p (barg) is the design pressure of the bulkhead, h (m) is the vent distance from the ceiling, Q (Ah) is the size of the failed batteries and v (m3) is the room volume. The parameter r is in this chapter assumed to be 2 l/Ah, which is an established rule of thumb. However, the single cell CFD results in this project indicates that this number can be increased up to 3 l/Ah for cases where no external combustion is observed. Cases with no combustion may happen although it is more likely that the gas ignites early without explosion. Since cases with combustion are observed and possible, it is advised that this scenario is accounted for. A proposed value of S = 1.1 gives a margin of 10%.

The values for the parameters are listed in Table 6-4. The values for A, B, C and D are found by using curve fitting. Adjusting the parameters to find an optimal fit for the CFD results at 0.5-1.0 barg design pressure has been prioritized. Also, the room with free volume of 25m3 has been given priority over the small room of 15 m3. Finally, the release of 500 liters, 1 000 liters and 2 000 liters have been prioritized over the 4 000 liters case.

Table 6-4: Ventilation formula parameters

Parameter	Value
A *)	1282.7
B *)	0.498
C *)	-311.8
D *)	1.579
r **)	2-3 l/Ah
S **)	1.1

*) Parameter found by *curve_fit* in Python

**) Parameter chosen by rule of thumb, and can be changed by the user

The CFD simulation plots for the large room with vents 0.4m from the ceiling are plotted together with the proposed function in Figure 6-4. The ventilation rates with a design pressure of 0.5 barg is shown in Figure 6-5.

Table 6-5 provides example values with r = 2 l/Ah and S = 1.1.

Table 6-5: Example values for the formula presented.

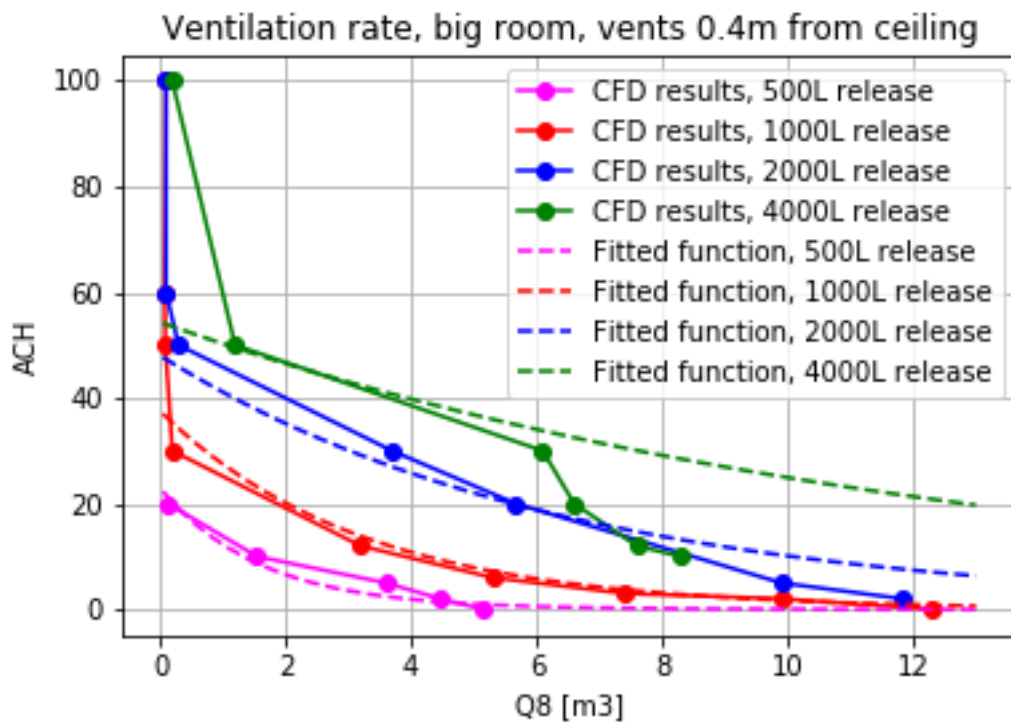| Battery size releasing with 2 l/Ah	60	250	500	1 000	2 000
Small room 15 m3 ventilation, vents 0.8m from ceiling (ACH)	0	27	60	89	108
Large room 25 m3 ventilation, vents 0.4m from ceiling (ACH)	0	10	25	41	53
Large room 25 m3 ventilation, vents at ceiling (ACH)	0	8	21	35	44

Figure 6-4: Ventilation rates for the big room with vents 0.4 m from the ceiling. Both the CFD simulations and the corresponding fitted function is plotted. *S* = 1.0.
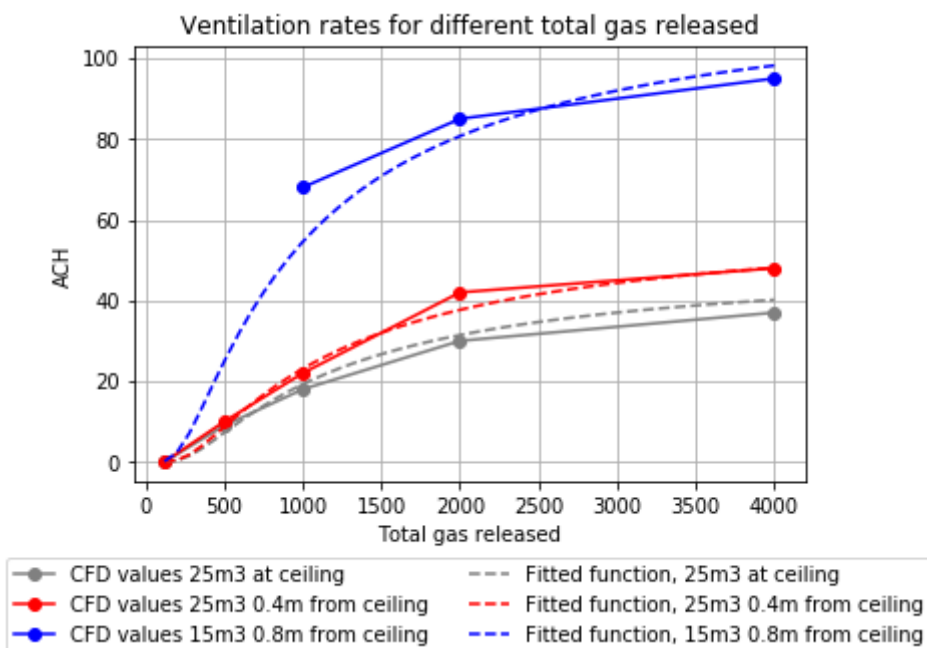

Figure 6-5: Ventilation rates for different gas releases with a design pressure of 0.5 barg. CFD results and the corresponding fitting function is shown. *S* = 1.0.

6.4 Main Conclusions

Main Conclusions
1. More open modules have greater possibility of providing oxygen to the fire and this will tend to result in a higher chance of prolonged combustion with higher temperatures and increase the chance of external combustion of gasses. 2. When the gasses produced from a lithium-ion battery are combusted, rather than accumulating, the explosion risk goes down substantially. 3. Limiting the oxygen to the fire will reduce the chance of prolonged combustion with lower temperatures. However, the off-gassing and hence the explosion risk increases. 4. The CFD results for two battery rooms with free volume of 15 and 25 m^3, show that a relatively high ventilation rate is needed even for the smallest gas release rate. 22 and 70 ACH is needed for the large and the small room, respectively. The ventilation can be turned on demand based at early off-gas detection with sensors close to or inside the modules. 5. The further the extraction duct is located down from the ceiling; the higher ventilation rate is needed. 6. The typical ventilation requirement of 6 ACH is assessed sufficient for "small" gas releases of 350 liters, which corresponds to a battery of 115-175 Ah. 7. If batteries of 4 000 Ah is failing, it will not be sufficient with 100 ACH to avoid an explosion magnitude of 0.5 barg. 8. A ventilation formula for a battery room is proposed. The formula calculates the air changes per hour (ACH) with the size of the failed batteries, the design bulkhead pressure, the room volume and the vent distance from the ceiling as input variables.

7 FIRE SUPPRESSION SYSTEMS

7.1 Li-ion fire hazards

The core of a lithium-ion battery fire – the cell itself – is typically not accessible and extremely difficult to extinguish, having elements of multiple types of fire (metallic, chemical, etc.) as well as being exothermic and potentially producing its own oxygen. However, a single cell fire is typically not of significant concern with regard to safety or survival of the ship. The prime concern is that a battery is made up of tens of thousands of cells, and this fire will tend to propagate to additional cells – thus increasing the heat load and increasing the likelihood that it will propagate further, to a worst case of having involved the entire battery system. Thus, extinguishing the fire at the single cell level is not the focus of fire suppression systems. The key role of fire suppression systems is to absorb heat and reduce the degree of propagation, or the number of batteries which will be involved in the fire.

Based on this arrangement, several principles become evident. First, detection and early release of suppression medium greatly increase its effectiveness. The more a fire has propagated, the more heat is being produced and the more difficult it is to put out. It is recommended that fire suppression, detection and release systems still are fully functional after a single failure in any other subsystem, such as the BMS. With regard to all of these issues and integration complexity, it is imperative that the battery manufacturer is involved and provide recommendations to necessary safety barriers. Each battery system is different, and each installation is potentially unique. However, a standardized comparative test method has been proposed in Section 7.5, to evaluate the performance of the fire suppression systems.

A fire external to the battery itself presents a significant danger. The battery system normally has no way of protecting itself in such an event, and an external fire is likely to heat up multiple cells and modules simultaneously. A designated battery room thus provides significant protection from such an event – particularly with the requirements for no fire-risk objects to be installed in the room and with fire rated boundaries. Should the passive barrier fail, a fixed total-flooding fire suppression system constitute an important secondary barrier.

7.2 Means for suppression

It is considered a credible failure mode that more than one module can catch fire – nominally occurring at a full string level, due to BMS failure, a contactor failure or welding, power converter failure, or ground isolation fault.

The fire suppression system shall be able to swiftly extinguish a fire in the space of origin, and in order to fulfill the functional requirements as stipulated in SOLAS Chapter II-2 Regulation 2.2, the following objectives should be met in particular:

- Preventing module-to-module propagation

- Multiple battery module fire suppression

The functional requirements above must be evaluated considering the particular battery system being considered – for instance: whether active fire suppression is used to prevent module-to-module propagation or whether different suppression media will be able to access and remove heat from the neighboring battery modules. A key metric used to evaluate effectiveness was the external and internal temperature of neighboring modules as the device under test went through failure – the fire suppression system role is considered primarily to manage the heat transferred to these neighboring modules. The different functional requirements, combined with the testing conducted, point to several key attributes of

different fire suppression media necessitating consideration. In general, the different fire suppression systems all excel in different areas and there is no identified 'silver bullet' solution. The fire suppression media or systems evaluated were:

- Sprinklers: Offer a common method for fire extinguishment that is in line with lithium-ion expected requirements – large amounts of volume can be supplied to provide for maximal heat absorption.

- Hi-Fog: Is a high-pressure water mist system that produce a fine mist which increases surface area for heat absorption. A typical water mist system would have capacity for a minimum of 30 min freshwater release, followed by back-up access to seawater from the vessel fire main providing cooling properties over time. However, the time duration of the discharge can be increased based upon required protection time limits defended in the design phase of the system.

- NOVEC 1230: Is an equivalent gas-based fire suppression system. The primary function of NOVEC is to put out flames by physically cooling below the ignition temperature of what is burning and chemically inhibiting the fuel source. The agent does not deplete oxygen levels in the room, where fire itself is the only actually consuming oxygen. Sealing of the space is key for ensuring adequate concentrations of NOVEC 1230.

- Direct injection of water: For the purpose of combating heat generation, direct injection of water is considered as the most efficient alternative. In the stationary industry today, this method is generally included as a last resort back-up since the affected module(s) will be considered lost after deployment. This method is not recommended to be used in practice for high voltage applications, due to the risk of short circuit and hydrogen production. The test setup included a fire hose connection with direct access to the interior of the battery module under testing.

- FIFI4Marine CAFS: Is a foam-based system, that can be installed to deploy directly in to the battery modules, their surroundings in the racks or in the room. The concept evaluated in this report is only direct injection into the modules. The FIFI4Marine CAFS system is designed to re-deploy several times during an incident as the foam will degrade over time as it participates in combating the battery fire.

7.3 Test results

All the tested systems where able to extinguish visible flames, except for the sprinklers. Not enough water was able to get in between the modules, such that flames was observed even during deployment of the water drops. Water mist, NOVEC 1230 and the direct injected foam from FIFI4Marine was able to extinguish the flames.

The cooling capabilities of the sprinkler and the water mist system were found to be very similar. Both resulted in maximum temperatures external on neighboring modules of just above 600°C, though these persisted longer in the case of sprinklers; but both reduced all external temperatures to lower than 200°C within 100 seconds (systems deployed 30 seconds after thermal runaway initiates) and temperatures continued to decline after the initial 100 seconds. In addition, video as well as anecdotal evidence from several project participants indicates that sprinkler system had a difficult time suppressing flames and, in some instances, appeared to increase the intensity of the fire. By comparison, NOVEC 1230 reduced temperatures quickly – within 30 seconds – to under 250°C, but these temperatures remained stable for 1000+ seconds. Considering such a long-time scale, neighboring module external temperatures when using sprinklers or water mist can be expected to reduce to less than 30°C or 60°C, respectively.

Suppression systems' capability to affect off-gas concentrations in the battery space was also measured. Indication of gas concentrations was taken primarily from LEL% measurements. The values presented in Table 7-1 represent the percentage of a given LEL% limit. These measurements were taken in the center of the room. Hence, the values do not correspond to a stoichiometric mixture that would be assumed to exist in the whole space. The measurements are nonetheless representative of the relative capability of the different systems to affect the amount of explosive hazard existing in the space. The LEL% was not recorded for the sprinkler test. Based upon experience and other tests performed by the project participants, it is concluded that the sprinklers are not capable of reducing the gas concentration. It can actually be argued that it increases the explosion risk, since the water displaces the gas into pockets with higher concentrations.

Table 7-1 – Effect of fire suppression system medium on LEL

Fire Suppression System Used	Maximum LEL% recorded (%)
None	69 %
Hi-Fog	10 %
NOVEC 1230	26%

The effect of injecting fire suppression media directly into a battery module was also evaluated for comparison. Direct injection of water is not expected or recommended to be used in practice in high voltage systems due to the risk of short circuit and hydrogen production. However, the method is presented as a reference point for the best flame extinction and heat absorption capabilities, that can be expected by a fire suppression system. The direct water injection test also provides a valuable reference point for evaluating the capabilities of the FIFI4MARINE CAFS (foam) system which is designed and engineered to be injected directly into the module. Another key differentiating factor is that the foam-based system is likely to require a significantly reduced volume of water compared to pure water-based injection. Additionally, the foam-based system is deployed using de-ionized water to limit conductivity and corrosive effects.

Due to limited amount of suppression media available onboard the vessel it should be considered how much suppression media that should be used, how many modules that should be sprayed and how many releases the system should be able to produce. This applies for all the tested suppression systems.

Both the foam-based and the water-based systems reduced the main battery fire temperatures to under 80°C within 600 seconds. This represents a significant improvement over what can be achieved with fire suppression media applied outside of the module – where the main battery fire temperature was unaffected and quite stable at around 900°C. External temperatures on neighboring modules are also significantly reduced from the use of direct water injection – reducing to below 20°C within 150 seconds after release. The direct injection foam-based system had recorded temperatures below 50°C within 700 seconds, while the total-flooding water mist system achieved temperatures that were just above 60°C after 700 seconds. Although some of the results may be similar, ultimately it is difficult to compare the capabilities between direct injection and external suppression systems since the reason behind the results were so different in each case. In general, it can be considered that direct injection of fire suppression media is much more effective compared to external application. In cases where the approach to safety may be different – such as a battery installed without a dedicated battery room – this may be a particularly attractive approach to evaluate.

7.4 Performance comparison

Fire extinguishing systems can be designed to combat fires based on different principles, by limiting oxygen supply, reacting chemically with the fire or by removing heat. It is therefore not self-evident that a given fire-suppression media will act as efficiently with a lithium-ion battery fire involving many types of fires as described in Section 7.1.

A summary of the test results is shown in Table 7-2 and aim to summarize the results achieved during a full module thermal runaway event. Parameters are split into those considered primary in combating a lithium-ion fire and those considered as secondary safety barriers during such an event.

To deliver on the primary function – mitigating heat transfer to neighboring modules – our results show that some suppression systems with low or non-existent long-term heat absorption properties will require a passive barrier to propagation or additional coolants to achieve the necessary safety level.

Due to the prevalent risk of a lithium-ion battery reigniting – which can happen several hours or days after an event – it is recommended that the fire suppression system is engineered for multiple releases if no other mitigating measures can be made. Actual volumes and release rates need to depend on the battery system as well as the suppression media being used.

Table 7-2: Fire suppression systems' capability matrix

	Primary objective			Secondary objective		Suppression method properties	
	Flame extinction	Long Term Heat Absorption	Short Term Heat Absorption	Reduce Gas Temp in room	Gas Absorption in room	Can be Used with Ventilation	Suppression method
Sprinkler	▨	▨	▨	▨		YES	Total-flooding
Hi-Fog	▨	▨	▨	▨	▨	YES	Total-flooding
NOVEC 1230	▨		▨	▨		NO	Total-flooding
FIFI4Marine	▨	▨	▨	Not evaluated	Not evaluated	YES	Direct injection
Direct Water injection *)	▨	▨	▨	Not evaluated	Not evaluated	YES	Direct injection

*) Not expected or recommended to be used in practice for high voltage applications, due to the risks of short circuit and hydrogen production. The method is presented as a flame extinction and heat absorption capability reference.

▨ High capability	▨ Low capability
▨ Medium capability	☐ No or very low capability

7.5 Defining a test program for fire suppression

In waiting of internationally recognized maritime test programs for lithium-ion fire suppression systems this project aimed to develop a methodology for comparative tests between different fire suppression systems available in the maritime market. When dealing with lithium-ion battery fires the identified primary threat that a suppression system should be tested for is that of a full module going into a thermal runaway event with combustion. Thereby the single module fire scenario is designed to capture the main threat based on risk and consequence to a battery system.

This subsection aims to highlight key considerations made and to summarize learnings from tests conducted in order to establish a base for future tests and standardization work.

7.5.1 The test setup

To establish a common baseline, it is important to consider what the key parameters are for normalizing the tests. The following parameters are considered the most important for comparative results in further studies.

- Test room volume – 19.25 m^3 (20ft container): Chosen to be representative of a smaller scale battery space in addition to limiting the amount of installed equipment and/or batteries needed in the space. A limited space is crucial in order to asses risks related to off-gas concentrations and ambient temperatures, as a bigger test hall would not be representative of maritime installations typically characterized by volume and weight constraints.

- Battery chemistry – NMC pouch cells: These cells should be used as they represent the highest fire risk, being more susceptible to thermal runaway and obtaining the highest temperatures when combusted. The NMC cells are also the most commonly used cell in the maritime industry.

- Module size – 1.3 kWh: The energy contained in such a module is on the lower scale compared to more sophisticated modules found in the market. The relative effectiveness of suppression systems is nonetheless achieved by keeping the module to a constant energy capacity.

- Module casing – IP2X mild steel enclosure of 0.5 mm thickness: The low IP rating is chosen to more easily establish a full module fire as the free access to oxygen is necessary for combustion.

- Battery rack configuration: Modules were fitted in 3 columns distributed in 6 rows. The live module placed in the bottom 3rd row, second column. This configuration was chosen to represent a typical rack setup and providing enough neighboring thermal mass to effectively simulate a module-to-module heat transfer during the single module fire scenario.

- Temperature measurements: Thermocouples should be placed on the live module, along the faces of the neighboring modules, in addition to internal module thermocouples. Additionally, each neighboring dummy module should be fitted with internal thermal mass to represent missing battery cells. Figure 7-1 show an example of a thermocouple placement in the test setup.

- Concentration of flammable gas measurements: Even if explosion risk is not considered as a primary function for a fire suppression system it is still identified as a secondary function or additional benefit. It is recommended that tests include gas measurements at different heights due to possible stratification effects of temperature gradients in the test hall.

- Fire suppression installation: Nozzle configurations and fire-extinguishing system installation should always follow the maker's specifications and installation requirements. For a NOVEC 1230 system it should be noted that different battery electrolytes could require higher than normal

design concentrations of the extinguishing media and the maker should always be consulted prior to installation for a given battery system.

- Ventilation: During the tests the ventilation system was closed for comparison. When conducting system specific tests, it is recommended that the test hall ventilation is designed to run as intended during a thermal runaway event based on the characteristics of that system.

- Initiating thermal runaway: This should be achieved by installing resistive heat elements in-between the installed battery cells, providing thermal stress until the point of thermal runaway is initiated. Alternatively, comparable behavior can be achieved by overcharging the cells.

- State of Charge (SOC): 100% SOC should be chosen to provide the most consistent combustion results.

- Fire suppression release: The fire suppression systems should be all employed after a 30 seconds time delay. This time delay is considered as the worst case between sensor activation and the automatic system release.

- Re-ignition: While not the focus in the comparative tests presented in this report, temperature and gas measurements should continue after an initial extinguishing operation has been carried out. As the DUT internal temperatures remain largely unaffected during an initial release of a fixed fire-extinguishing system it is important to monitor the systems for re-ignition or further temperature spikes.

These parameters where chosen to provide a comparative result for a bare-bones battery system, completely lacking safety measures other than the fire suppression systems. A commercial battery system, approved for marine use, would necessitate additional barriers such as passive propagation protection. Conclusions of absolute nature with regards to effectiveness of a given fire suppression system should only be done after system specific tests at this point.
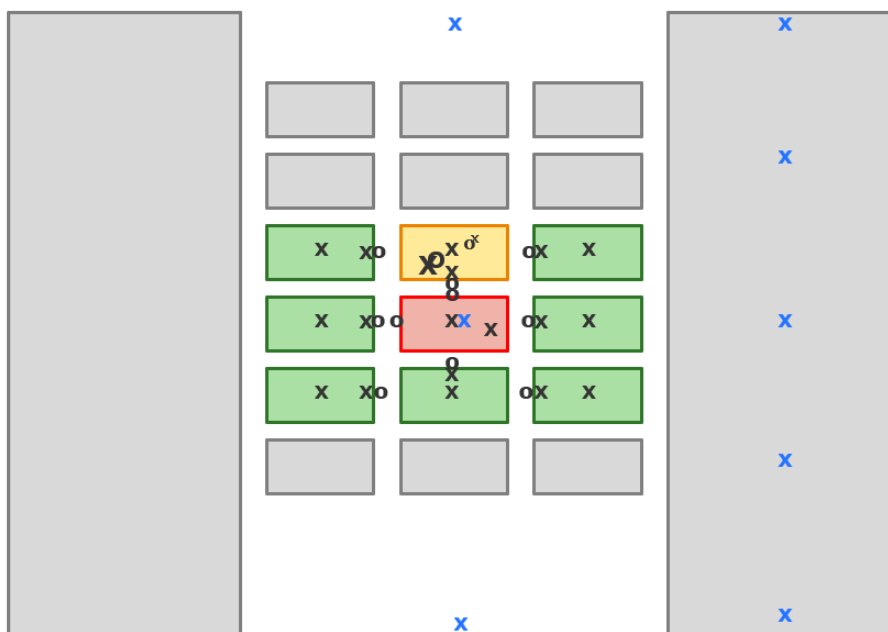
Figure 7-1 – Placement of thermocouples for all module testing – black 'x' internal to modules, black 'o' external to modules, blue 'x' indicating ambient room thermal gradient temperatures.

7.5.2 Total flooding versus direct injection tests

For fire-extinguishing systems that are to be installed to combat any fire in the battery space, applicable IMO test standards for such systems are considered a pre-requisite for lithium-ion battery fire application. For a water mist system (Hi-Fog) this would refer to IMO MSC.1/Circ.1165 as amended, or for the equivalent gas-based systems (NOVEC 1230) this would refer to IMO MSC.1/Circ.848 as amended. The IMO standards referred to are established to primarily combat petroleum fires, while the tests performed in this report are made to assess effectiveness for a lithium-ion battery fire in particular.

For direct injection systems, designed to primarily protect against battery fires, a test as carried out in this report is crucial in order to assess effectiveness in accordance with identified functional requirements unique for lithium-ion battery fires. For external hazards, these systems would typically require the installation of a complementary room protection. From the tests presented in this report the FIFI4Marine CAFS had the highest potential for module-to-module fire mitigation, especially when designed for sufficient capacity to flood the modules/racks over longer time periods.

7.6 Main Conclusions

Main Conclusions
1. Tested fire suppression systems provide different benefits, with unique strengths and drawbacks, providing no 'silver bullet' solution. The different properties are presented in Table 7-2. 2. Direct injection of foam shows the best heat mitigating performance compared with all tested methods. This method had the highest potential for module-to-module fire mitigation, especially when designed with capacity to flood the modules/racks over longer time periods. In cases where alternative ship integration concepts are to be evaluated – such as a battery installed without a dedicated battery room – this may be a particularly attractive approach to evaluate the equal level of safety. The gas temperature and gas absorption are not evaluated. 3. High pressure water mist protection provides good heat mitigation at module level in addition to providing full battery space protection from external fires. It also shows good gas absorption and gas temperature reduction capabilities. 4. NOVEC 1230 extinguish the battery fire flames, but performs poorer with regards to heat mitigation, gas temperature reduction and gas absorption compared to water mist. Room ventilation needs to be closed for this suppression method to be functional. This can increase the toxic and explosive battery gas concentration in the room until ventilation can start again. 5. Sprinklers do not extinguish the visible flames but records similar heat mitigation capabilities at module level as high-pressure water mist. Since water can displace the gas into pockets with high concentrations, the explosion risk is considered to become more severe with sprinklers. 6. Each battery installation will have to assess necessary barriers in consultation with the battery manufacturer to identify the application most suited for that project. Due to limited amount of available suppression media onboard a vessel, the actual volumes and release rates needs to be calculated and are dependent on the battery system. 7. A methodology for comparative tests between different battery fire suppression systems available in the maritime market is proposed. Both heat and gas mitigation performance are evaluated.

8 RISK COMPARISON & ACCEPTANCE CRITERIA

8.1 Risk evaluation

Since no statistics of maritime battery fires are available, an approach to Quantitative Risk Assessment (QRA) of a battery thermal failure has been developed. Quantifying the risk through an analysis like this can be used to determine how the system compares to acceptance criteria. The risk model is shown in Figure 8-1. Various threats and safety barriers have been identified for a battery system. The frequency of occurrence of these threats and failures in the barriers are to statistics found in Center for Chemical Process Safety (CCPS) /1/ and Institute of Electrical and Electronics Engineers, Inc. (IEEE) /2/. Details of the threats and barriers considered in the QRA is outlined in the detailed report in Section B 17.
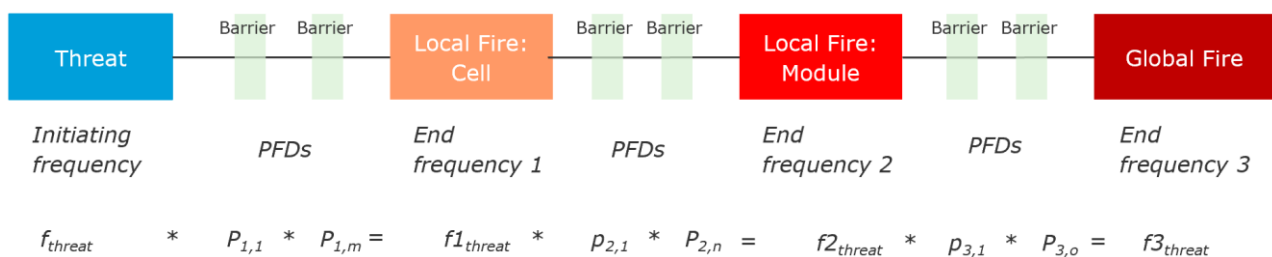
Figure 8-1 – Scheme for calculating frequencies for the different consequence categories caused by a threat

The frequency for each failure event is summarized and presented in Table 8-1.

Table 8-1 Fire frequencies for generic battery system

Consequence Category	Total frequency (per year)
Local Fire: Cell	3.8E-04
Local Fire: Module	1.4E-04
Global Fire	1.3E-07

Although the results may be uncertain in terms of absolute values, the analysis can be used to highlight the importance of different barriers, and the relative effect of not having them in place. To illustrate this, the risk resulting from the following system variations is studied:

- No barrier against cell propagation

- Less effective BMS

- Without independent shutdown

- Without CID

- As a (unrealistic) extreme case, removing all of the above.

It is seen that the fire propagation protection and the Current Interruptive Device is two of the most important safeguards to be installed in the battery system.

A comparison with an engine room fire probability has also been made. For the engine room fire, a ballpark frequency is calculated by using the engine room fires registered in the global HIS Fairplay database for the period 1998-2017.

Table 8-2: Calculated frequency of a fire in a battery room vs reported frequency of a fire in the engine room in the HIS Fairplay database

System	Total frequency of a fire (per year)
Battery System	5.2E-4
Engine Room	6.8E-4

Based at the numbers presented, it seems that the likelihood of a battery fire is lower compared to a diesel fire. However, engine room fires as registered in the HIS Fairplay database include fires of many different magnitudes not necessarily correlating to the Global fire scenario established in battery system QRA. This means that better data would be necessary to fully evaluate if a battery system is safer than a conventional combustion engine.

8.2 Main Conclusions

Main Conclusions
1. A model for Quantitative Risk Assessment for a battery system has been proposed.   2. Fire propagation protection and the Current Interruptive Device is two of the most important safeguards to be installed in the battery system.   3. More and better data would be necessary to fully evaluate if a battery system is safer than a conventional combustion engine.

Table 8-3: Fire frequencies for systems without barriers compared to base case with all barriers present

Consequence Category		Local Fire: Cell	Local Fire: Module	Global Fire
Base case: system with all barriers		3.8E-04	1.4E-04	1.2E-07
Without cell propagation design	Frequency	3.8E-04	4.8E-04	3.5E-07
	Relative to base case	**0 %**	**248 %**	**177 %**
Less effective BMS	Frequency	5.2E-04	1.5E-04	1.4E-07
	Relative to base case	**37 %**	**10 %**	**11 %**
Without independent shutdown	Frequency	9.3E-04	1.9E-04	1.4E-07
	Relative to base case	**143 %**	**40 %**	**11 %**
Without Current Interruptive Devise	Frequency	2.9E-03	3.9E-04	2.6E-07
	Relative to base case	**664 %**	**183 %**	**105 %**
Extreme case: Without any of the above	Frequency	2.2E-02	2.3E-02	1.7E-05
	Relative to base case	**5785 %**	**16197 %**	**13562 %**

9 THERMAL RUNAWAY TEMPERATURE PROFILES

Accurate characterization of 'thermal runaway' is important from the standpoint of understanding when it has occurred. Typically, thermal runaway infers the point at which the battery is 'self-heating' in an exothermic reaction. However, this still does not give distinct guidance for an observer to be able to identify if a cell has been successfully put into thermal runaway to for example initiate a given propagation test.

The literature /9/ define the thermal runaway into three main steps, as the temperature increases:

1. The solid-electrolyte interface (SEI) decomposes in an exothermic reaction. Can occur at 90 °C with a temperature increase of 0.00167 °C/sec.

2. An exothermic reaction between the intercalated Li-ions and the electrolyte starts. Can occur at 130 °C with a temperature increase of 0.4°C/sec

3. An exothermic reaction between the positive material and the electrolyte takes place. Can occur at temperatures above 200°C with a temperature increase of 1.7-17.0 °C/sec

The aim is to identify the worst case scenario, when the cell has reached stage 3, which is when the cell releases the largest amount of heat.

Thus, data is presented from tests conducted in this project to show different cases and what may be expected. Results are based on surface temperature measurements of the cell. In the cases of external heat application, this heat would be affecting the temperature indicated by the thermocouple. The intention here is to provide reference such that it can be better understood if a given phenomenon shown should be considered as thermal runaway.

9.1 Heat release profile results

9.1.1 NMC pouch cells

Figure 9-1, Figure 9-3, Figure 9-5, Figure 9-7 and Figure 9-9 provide visual indication of what the temperature profile looks like as a cell goes into thermal runaway. Figure 9-2, Figure 9-4, Figure 9-6, Figure 9-8 and Figure 9-10 show the temperature raise profiles for all NMC tests. In almost all cases, there is a point at which heating of the cell accelerates, characterized by a point that does visually appear as an inflexion point relative to the rate of temperature increase. However, detailed inspection shows that these points still only increase at a rate of less than 1 degree Celsius per second. Following this, it is common to see a point where the temperature will dip down – this coincides with a preliminary gas release. However, we see that this is still clearly not 'thermal runaway'. The primary points of focus are the sharp spikes in temperature, where we see close to 25°C per second temperature rise, or several hundred in the overcharge case shown here. This will define the onset of the thermal runaway. Table 9-1 provides a summary of key data points to use for comparison.

In addition, as shown in Figure 9-9 and included in Table 9-1; the thermal result of an external short circuit is found to be very mild compared to an actual thermal runaway event. This can be misleading as external short circuit does produce a sharp increase in temperature, but the actual rate as well as particularly the highest temperature reached are significantly lower than in other cases.

**Table 9-1 – Characteristics for identification of thermal runaway NMC pouch cells**

	Max Temp (°C)	Max Temp increase rate (°C/second)	Temperature at onset (approximate)
Overheat at 50% SOC	417	29.27	250
Overheat at 75% SOC	481	24.36	200
Overheat at 100% SOC	475	66.07	173
Overcharge	602	229	80
Ext Short Circuit	177	13.6	30
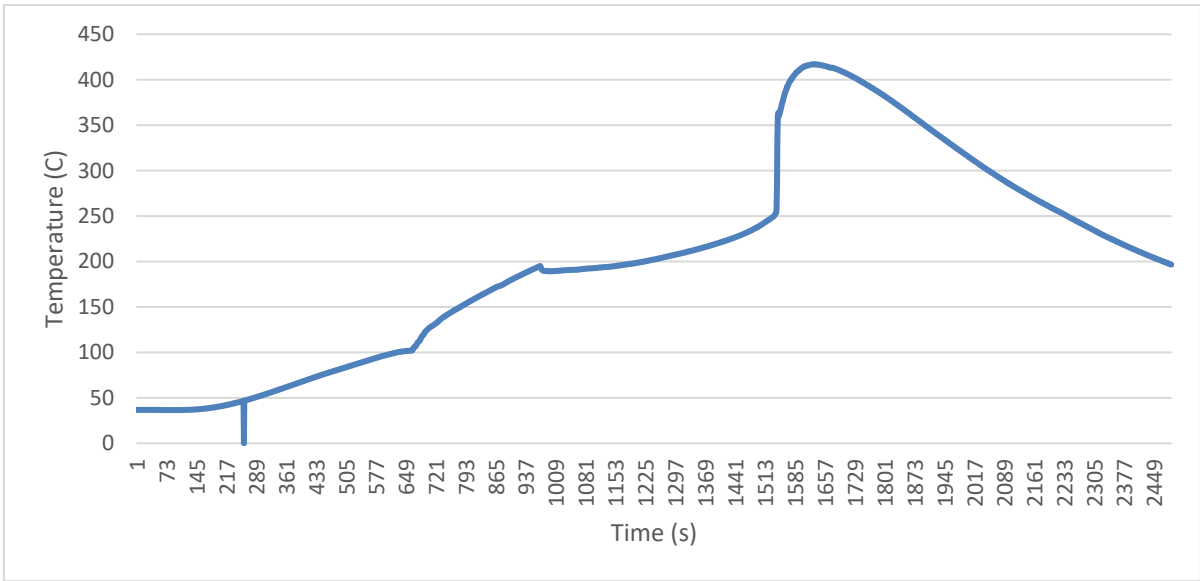
Figure 9-1 – Battery surface temperature for overheating a cell at 50% SOC distinguishes thermal runaway from other points of rising temperature
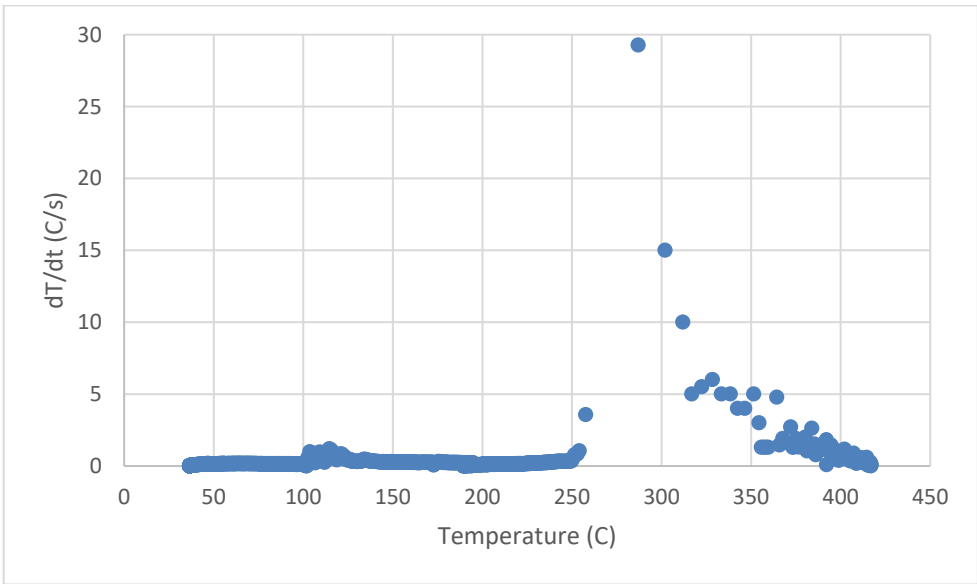
Figure 9-2: Temperature rate curve for test JDP2, NMC 50% SOC overheat
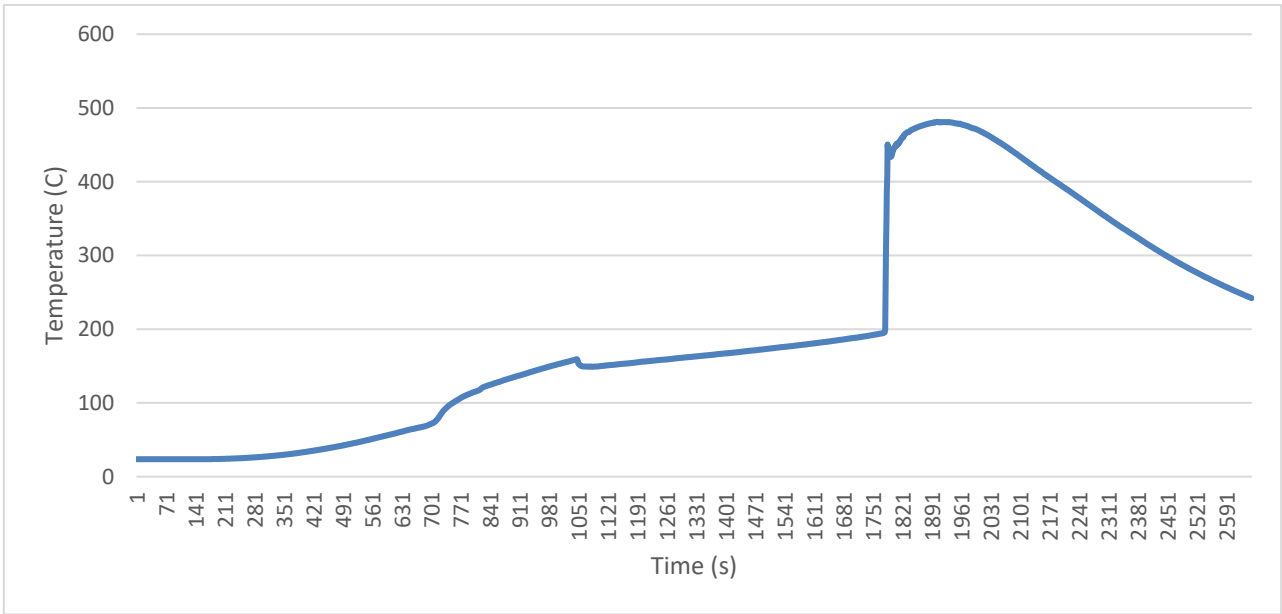
Figure 9-3 – Battery surface temperature for overheating a cell at 75% SOC distinguishes thermal runaway from other points of rising temperature
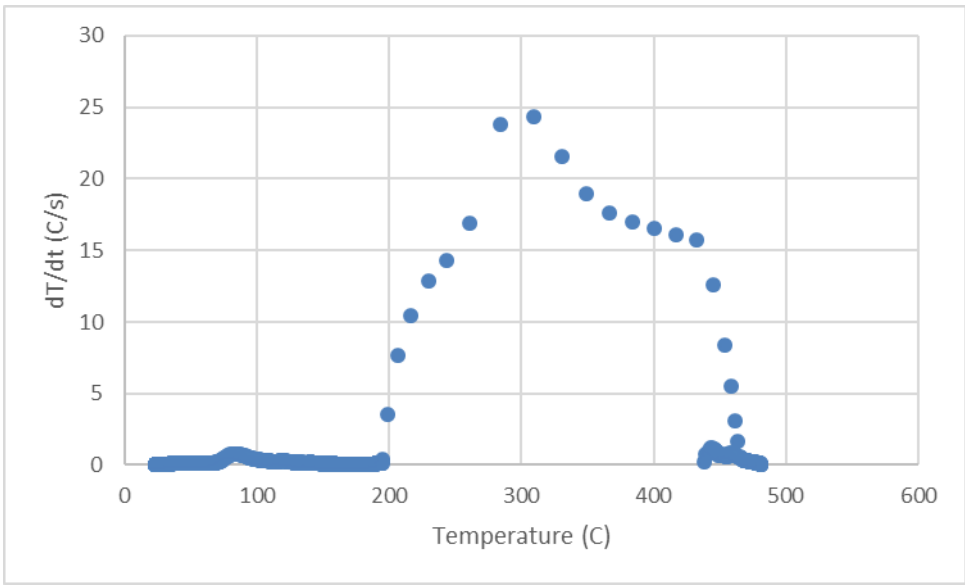
Figure 9-4: Temperature rate curve for test JDP5, NMC 75% SOC overheat
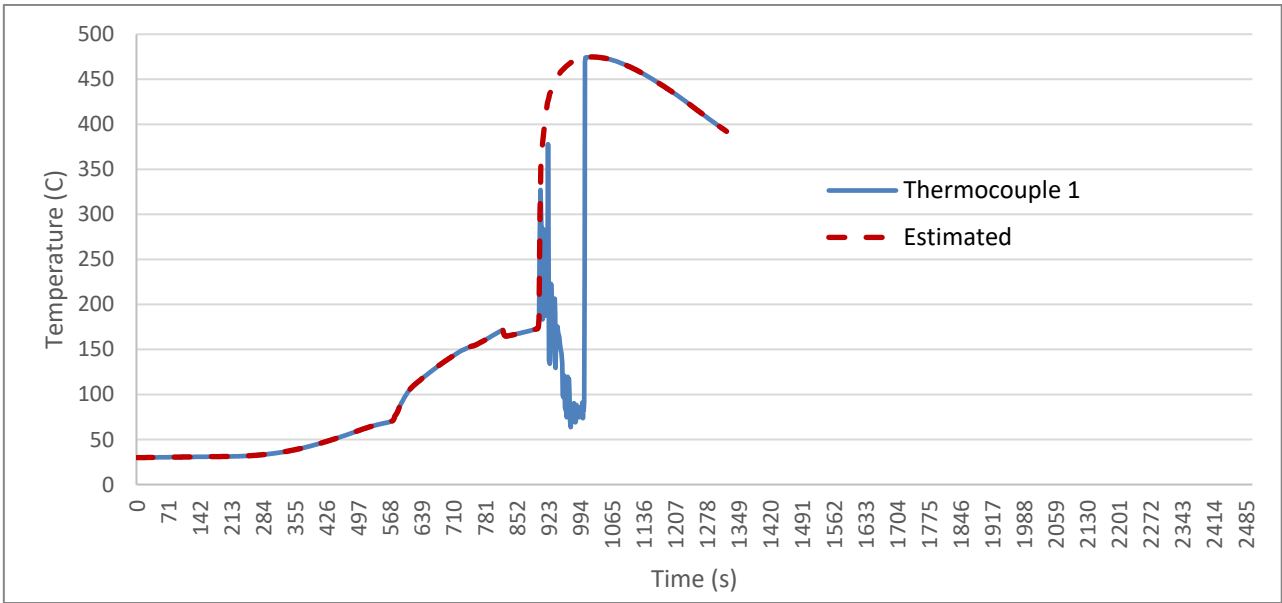
Figure 9-5 – Battery surface temperature for overheating a cell at 100% SOC distinguishes thermal runaway from other points of rising temperature
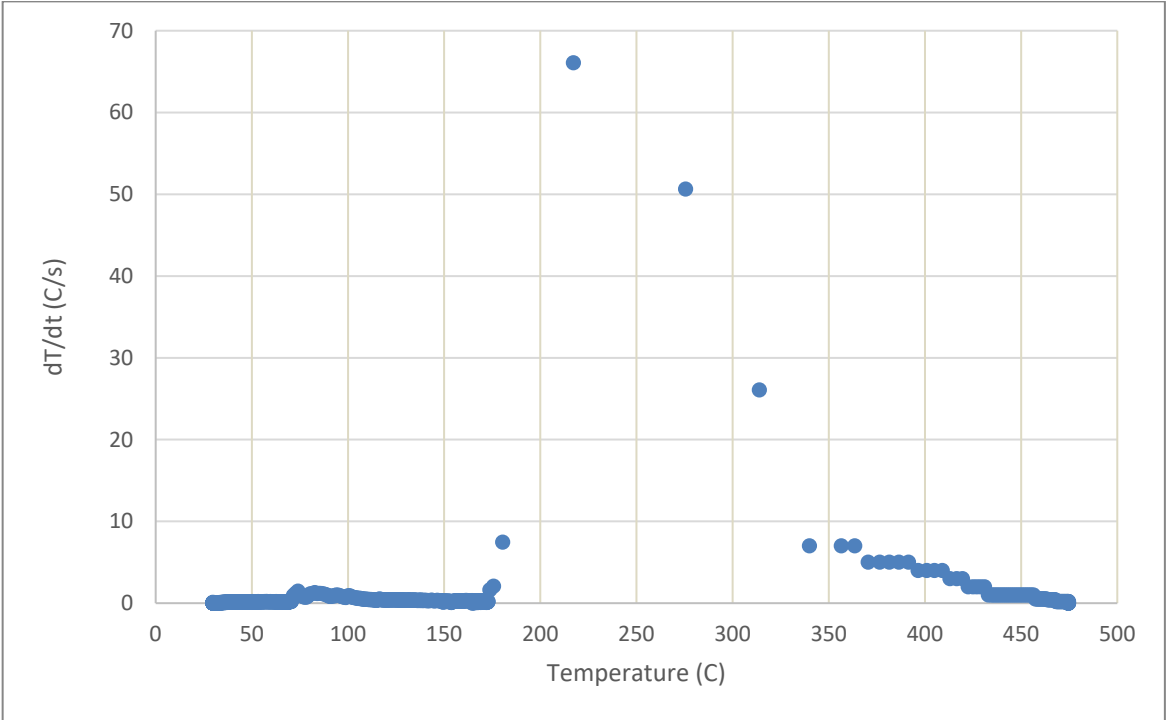
Figure 9-6: Temperature rate curve for test JDP1, NMC 100% SOC overheat
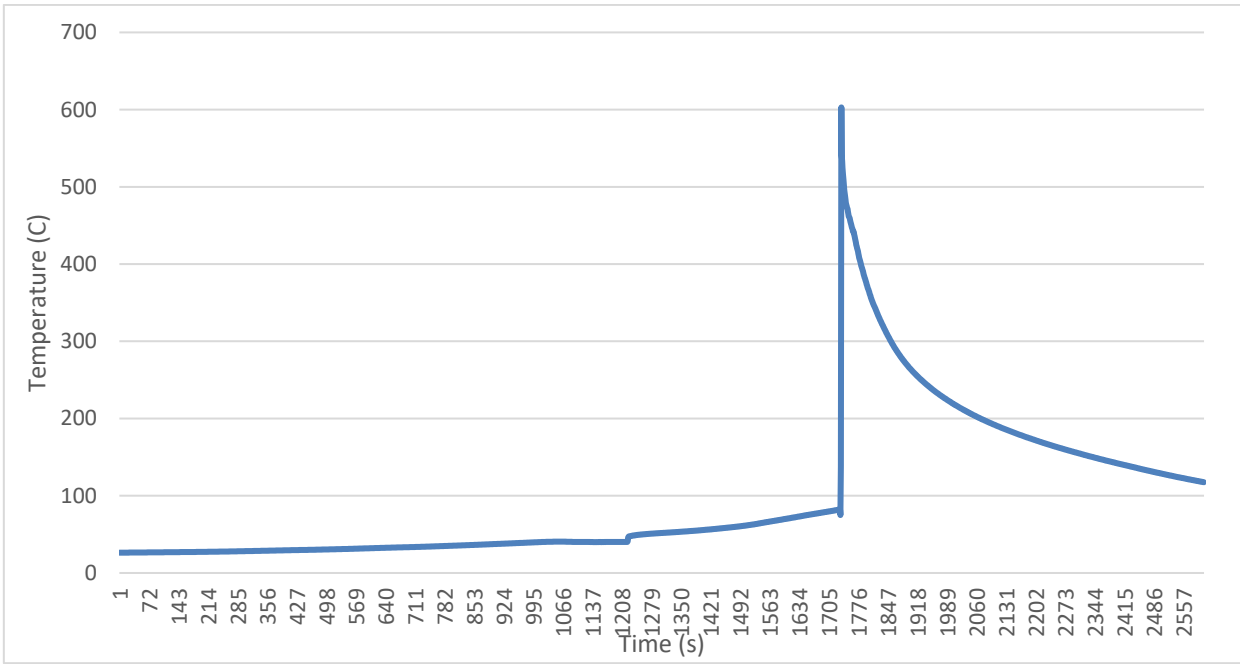
Figure 9-7 – Battery surface temperature for overcharging distinguishes thermal runaway from other points of rising temperature
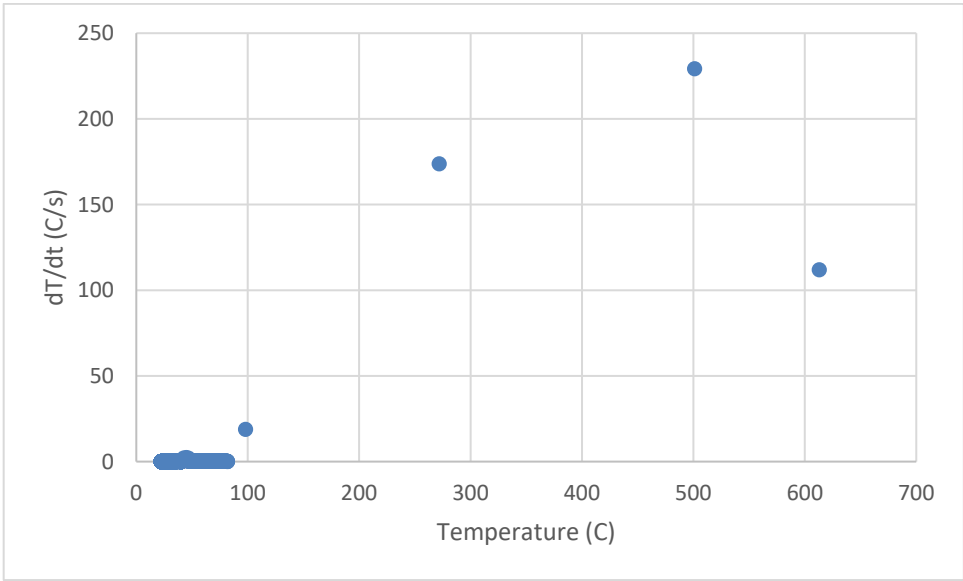
Figure 9-8: Temperature rate curve for test JDP3, NMC Overcharge
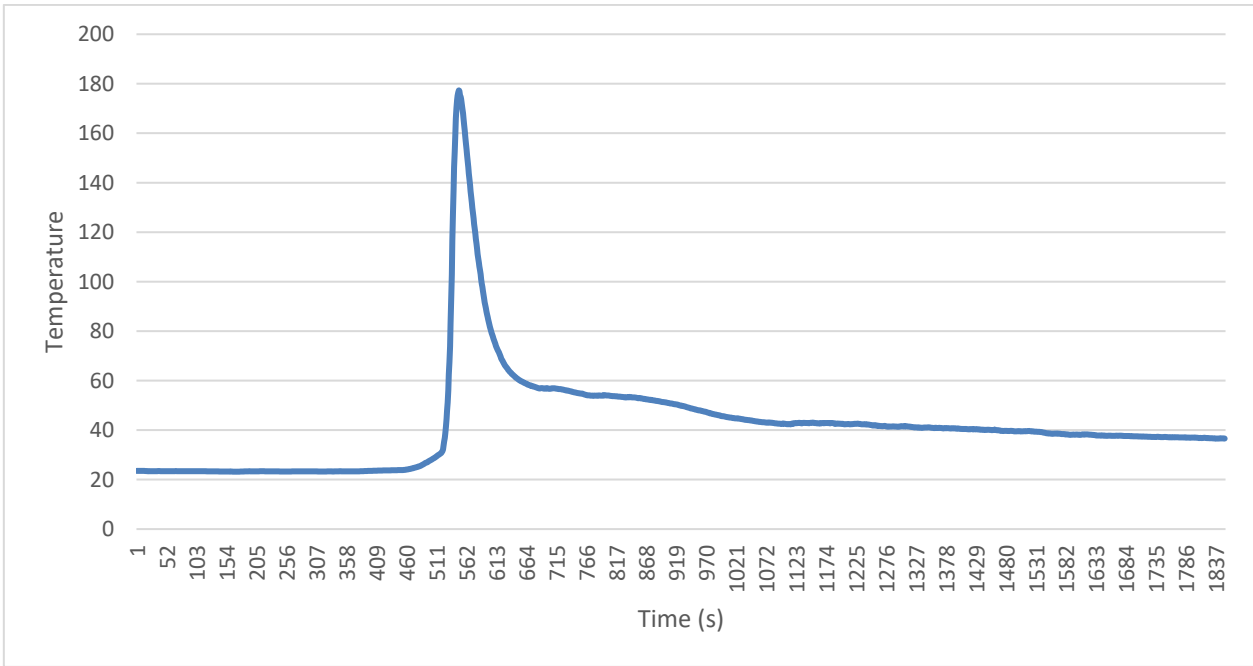
Figure 9-9 – The thermal result of an external short circuit can provide a fast temperature rise, but the rate and maximum value are not similar to other cases or considered to have entered thermal runaway
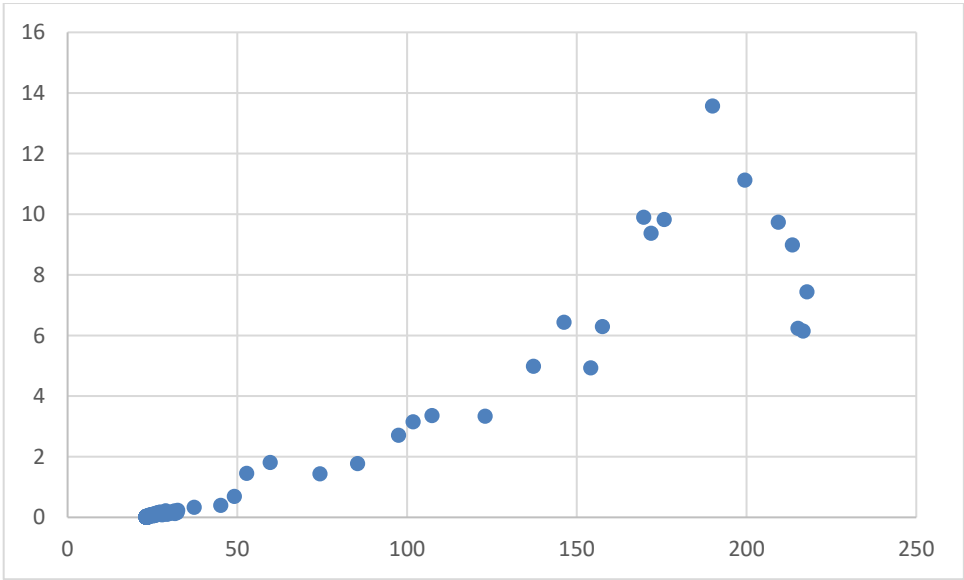
Figure 9-10: Temperature rate curve for test JDP7, NMC external short circuit

9.1.2 LFP cylindrical cells

Two sizes of LFP cylindrical cells where tested, one 26650 type of 2.5 Ah and one 18650 type of 1.5 Ah. The battery surface temperatures for all the tests are shown in Figure 9-11, Figure 9-12, Figure 9-13, Figure 9-15, Figure 9-17, Figure 9-19 and Figure 9-21. The heat raise curves are shown in Figure 9-14, Figure 9-16, Figure 9-18, Figure 9-20 and Figure 9-22. As seen from the figures and from the key data provided in Table 9-2, the temperature characteristics for these cells differs a lot from the NMC pouch cells in terms of max temperature and temperature rise.

For the 2.5 Ah type, the point of thermal runaway cannot be identified based at the surface temperature, since it has a steady growth when exposed for external heat. No visual combustion was observed, and the temperature increase rate is also very low compared to the NMC pouch cell. From the temperature plots it seems that no of the cells reached stage 3 in the thermal runaway process.

The onset of the thermal runaway was easier to identify for the 1.5 Ah cells. In Figure 9-17 and Figure 9-19 a dip in the temperature rise can be seen when the cell starts to vent, followed by an increase in the temperature rise when the thermal runaway is started. Note however that the temperature increase at that point is very low in all cases compared to the NMC pouch cells. Since the data was corrupted at the time the cell went into thermal runaway in the 100% SOC test case, a temperature estimation has been done based on two measurements at the cell surface, as shown in Figure 9-21. This is consistent with the results presented by Golubkov /8/. It is also debatable whether the 18650 cells with 75% SOC reached step 3. It seems that the 18650 cell with 50% and 100% SOC reached the step 3 with a max temperature increase of 3.37°C/sec and 5.06°C/sec respectively.

**Table 9-2 – Characteristics for identification of thermal runaway LFP cylindrical cells**

Cell type / size	Failure mode	Max Temp (°C)	Max Temp increase rate (°C/second)	Temperature at onset (approximate)
26650 / 2.5 Ah	Overheat at 50% SOC	243	0.57	Not able to identify based at temperature
	Overheat at 75% SOC	201	0.60	Not able to identify based at temperature
	Overheat at 100% SOC	170	0.14	Not able to identify based at temperature
	Overcharge	162	0.93	75
18650 / 1.5 Ah	Overheat at 50% SOC	330	3.37	233
	Overheat at 75% SOC	298	0.60	210
	Overheat at 100% SOC	383 (estimated)	5.06	225
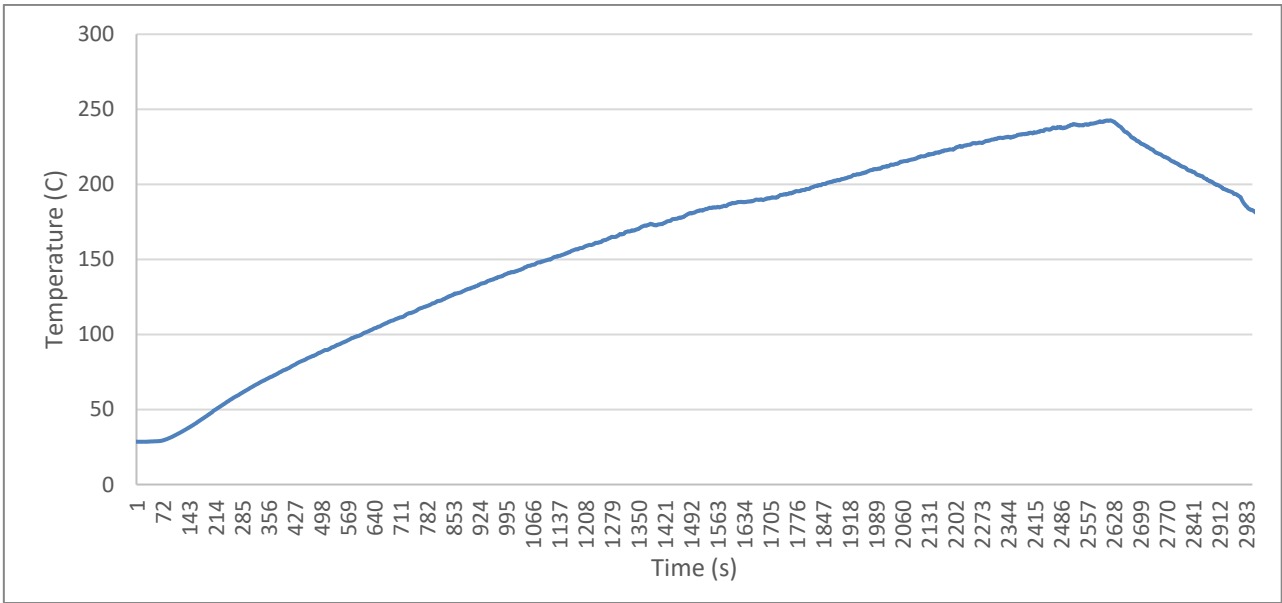
Figure 9-11: Battery surface temperature for 2.5 LFP 50% SOC with overheat
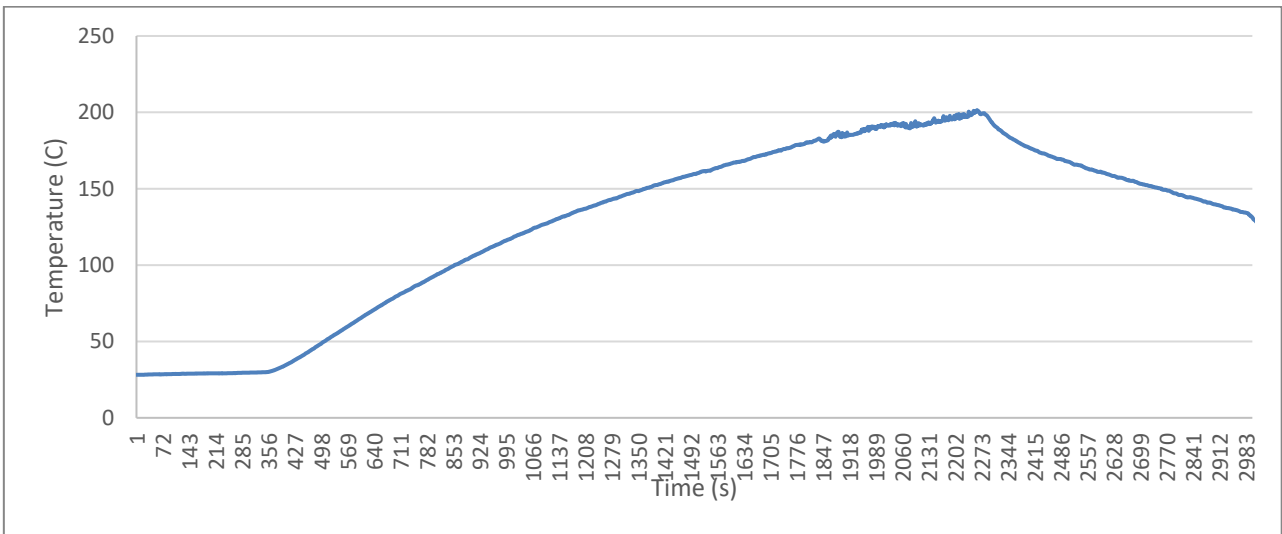
Figure 9-12: Battery surface temperature for 2.5 LFP 75% SOC with overheat
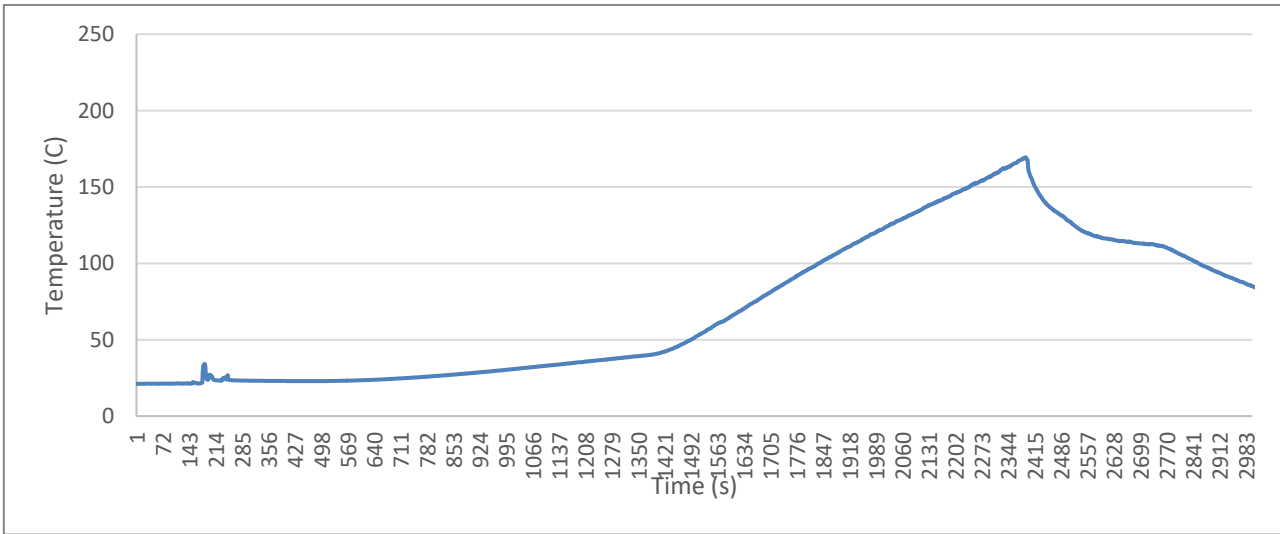
Figure 9-13: Battery surface temperature for 2.5 LFP 100% SOC with overheat
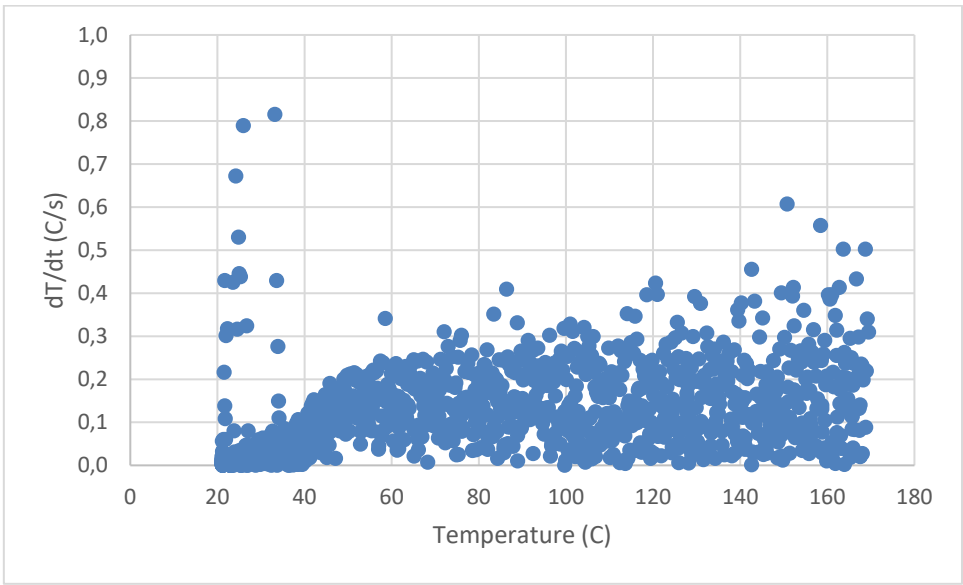
Figure 9-14: Temperature rate curve for test A3, LFP 2.5 26650 100% SOC overheat
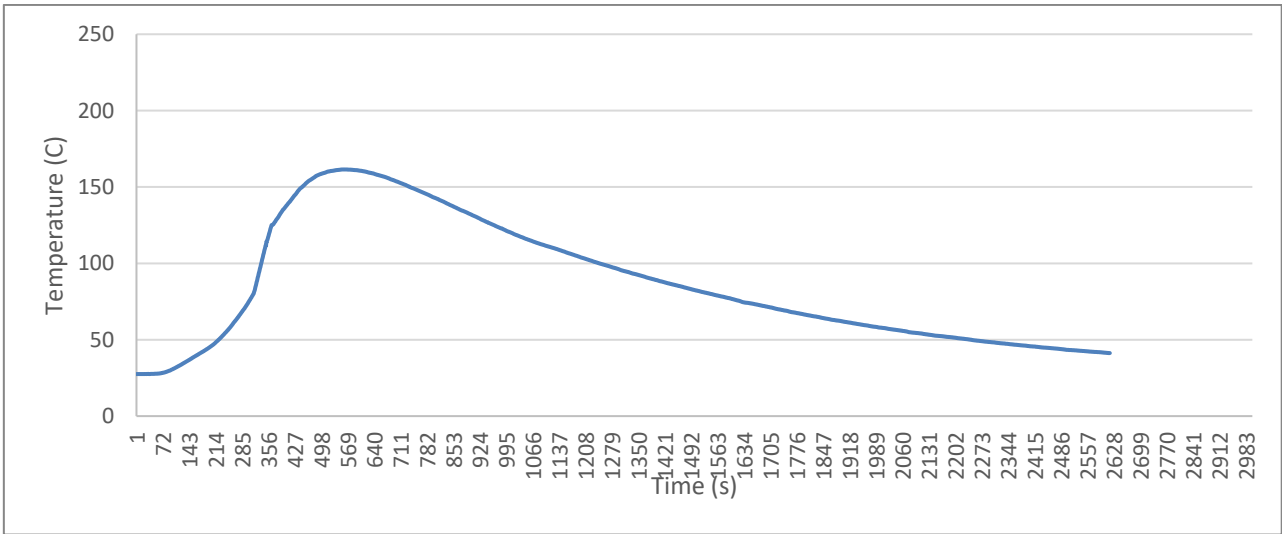
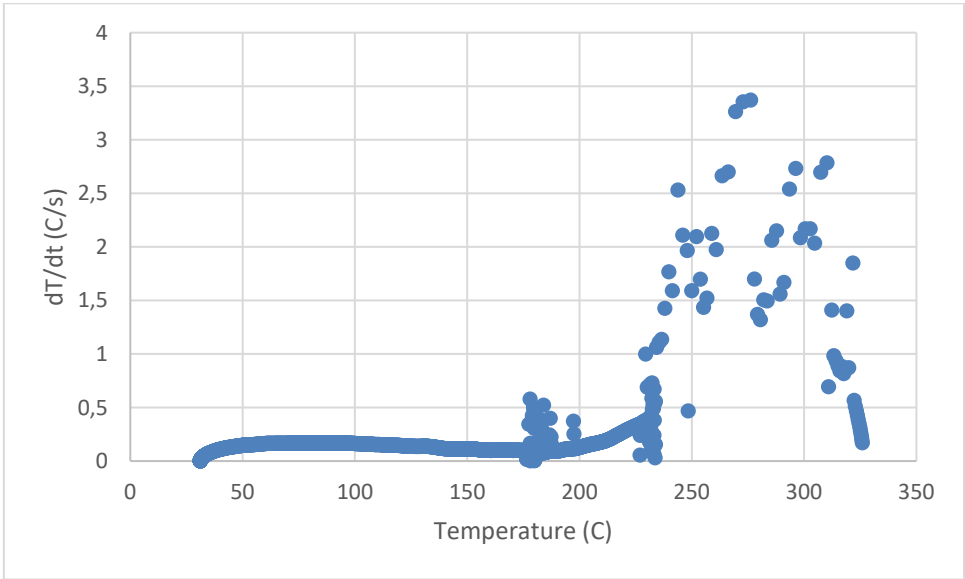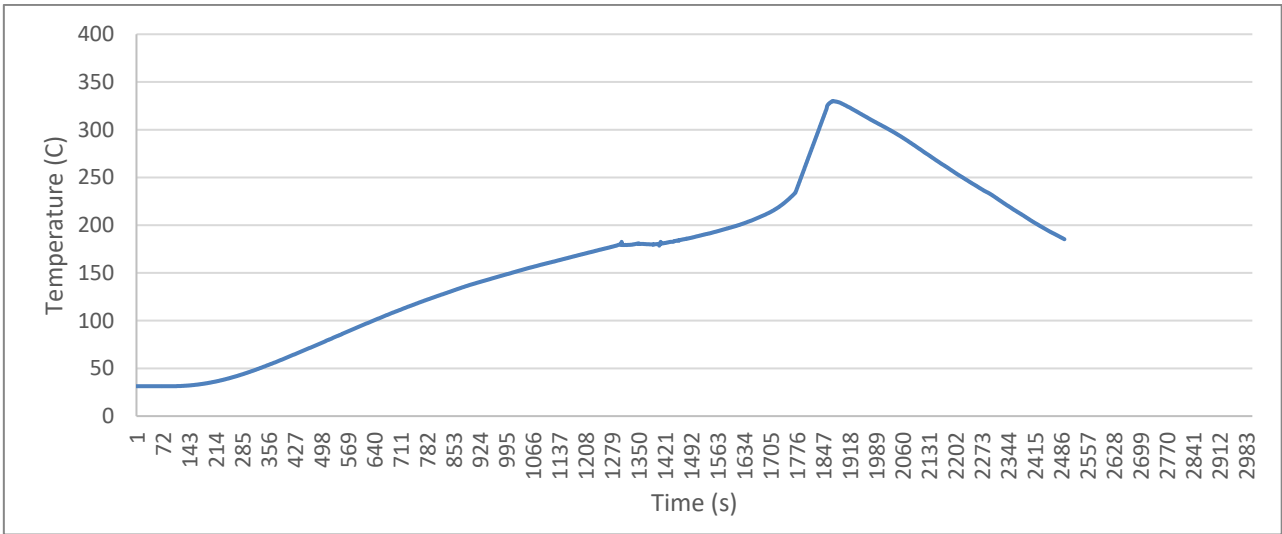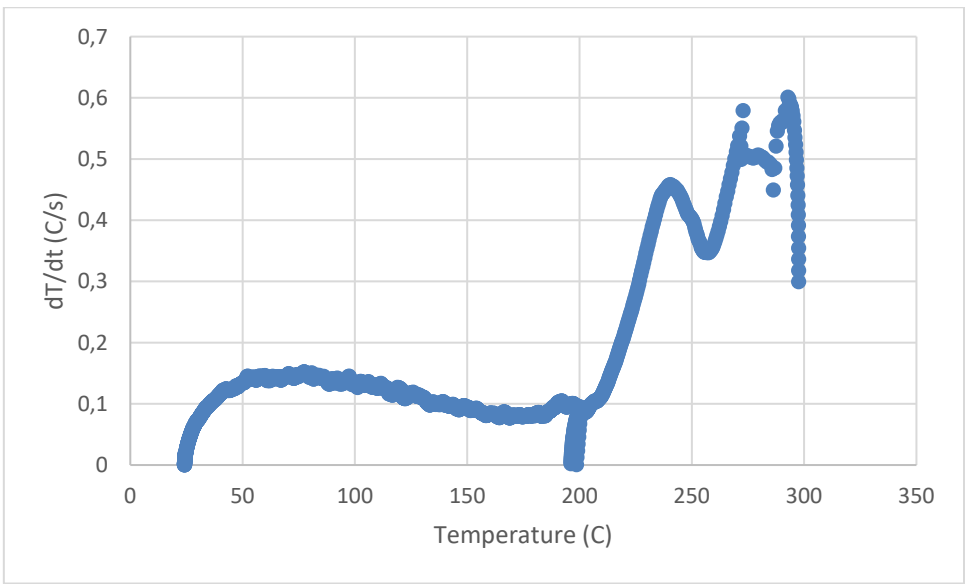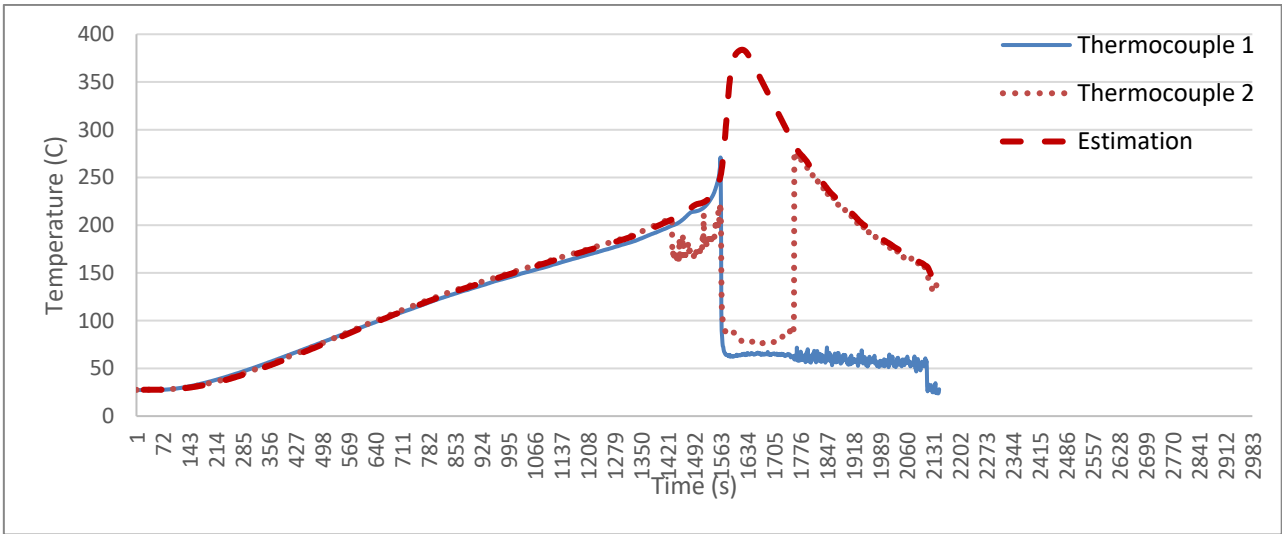**Figure 9-15: Battery surface temperature for 2.5 LFP 100% SOC with overcharge**
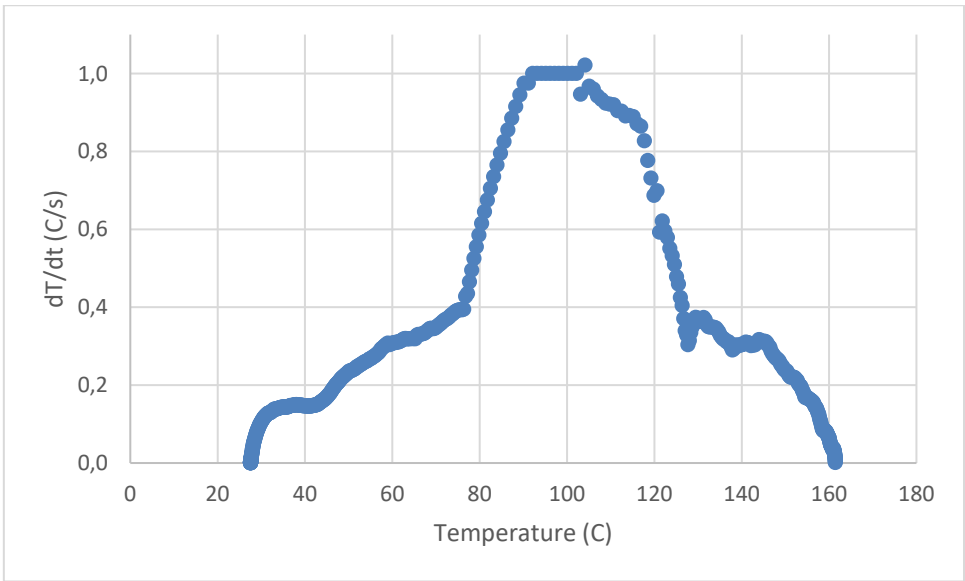
Figure 9-16: Temperature rate curve for test A4, LFP 2.5Ah 26650 overcharge
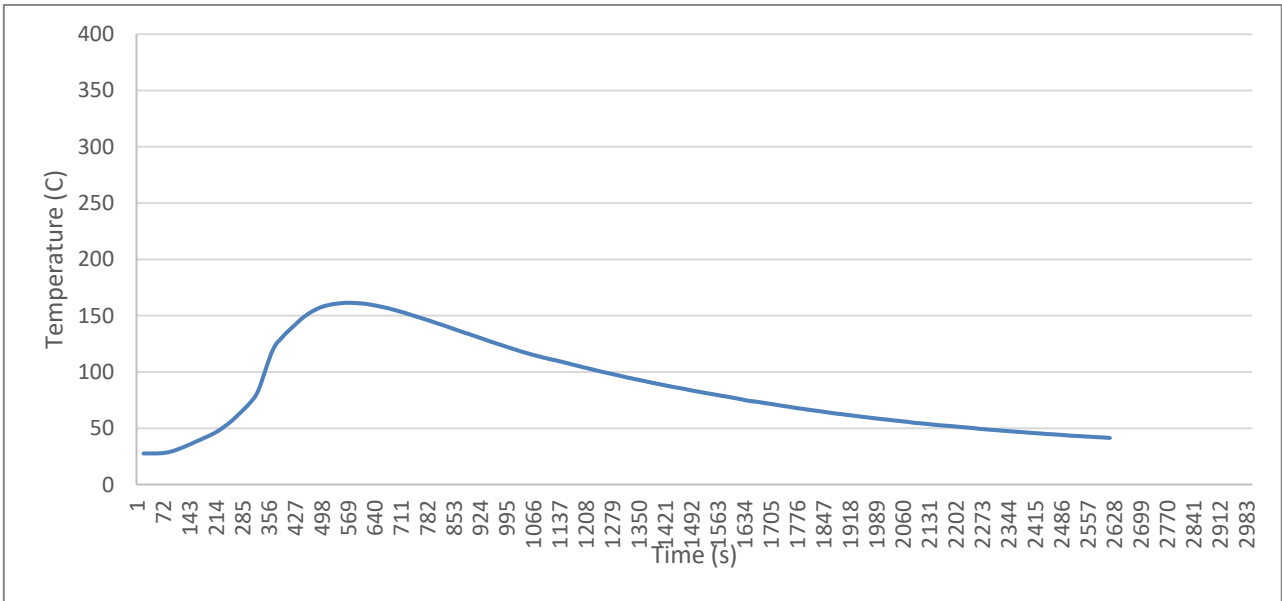
Figure 9-17: Battery surface temperature for 1.5 LFP 50% SOC with overheat

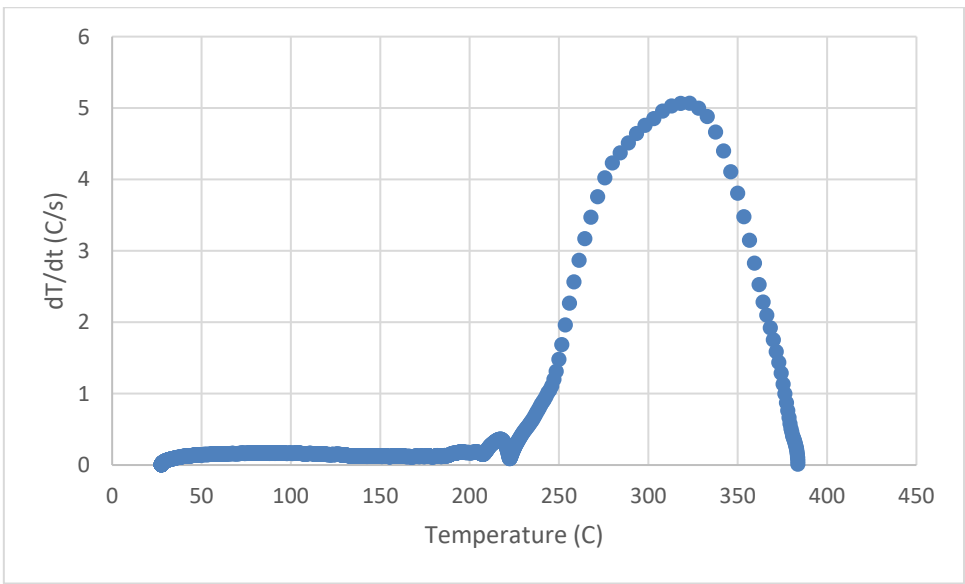**Figure 9-18: Temperature rate curve for test B1, LFP 1.5Ah 18650 50% SOC overheat**

Figure 9-19: Battery surface temperature for 1.5 LFP 75% SOC with overheat

Figure 9-20: Temperature rate curve for test B2, LFP 1.5Ah 18650 75% SOC overheat

**Figure 9-21: Battery surface temperature for 1.5 LFP 100% SOC with overheat**

Figure 9-22: Estimated temperature rate curve for test B1, LFP 1.5Ah 18650 100% SOC overheat

## 9.2 Literature review of thermal runaway heat release profiles

The temperature rates for NMC and LFP cells reported in the literature is discussed below. The results in presented by Golubkov /8/, shown in Figure 9-23, are quite consistent with the test results in this report. The results by Lei /9/, shown in Figure 9-24, indicates that stage 3 in the thermal runaway process was not reached for the LFP 18650 cells with only a max temperature increase of 0.05 °C/sec. Ouyang /7/, shown in Figure 9-25, reports a similar temperature increase rate between the tested 18650 NCM and LFP cells. Note that the LFP cells are charged to 4.2-5.0V when overheated. Normally the nominal voltage is 3.6V at 100% SOC. This can explain the more aggressive behavior of these LFP cells compared to the tests performed in this study and the reported results in the two other reports.
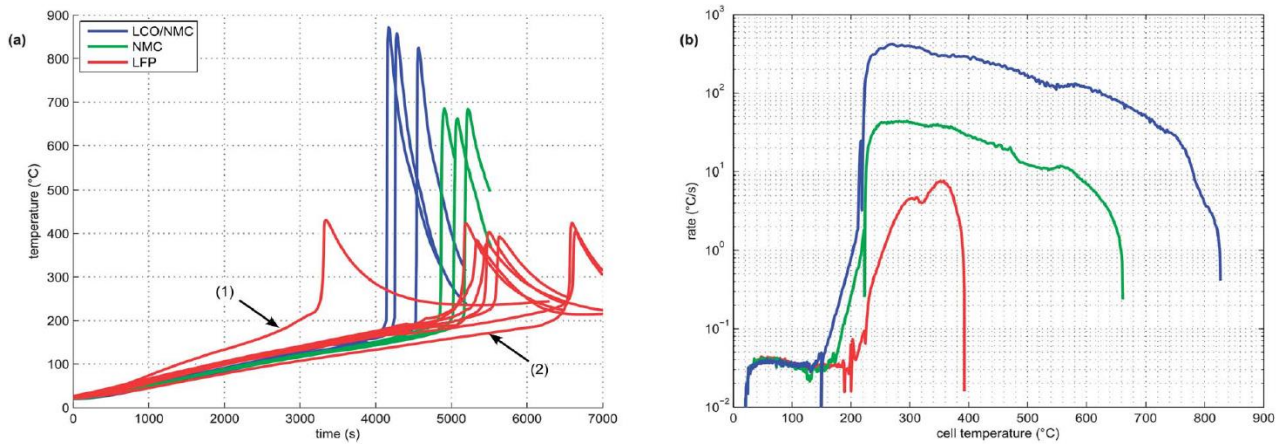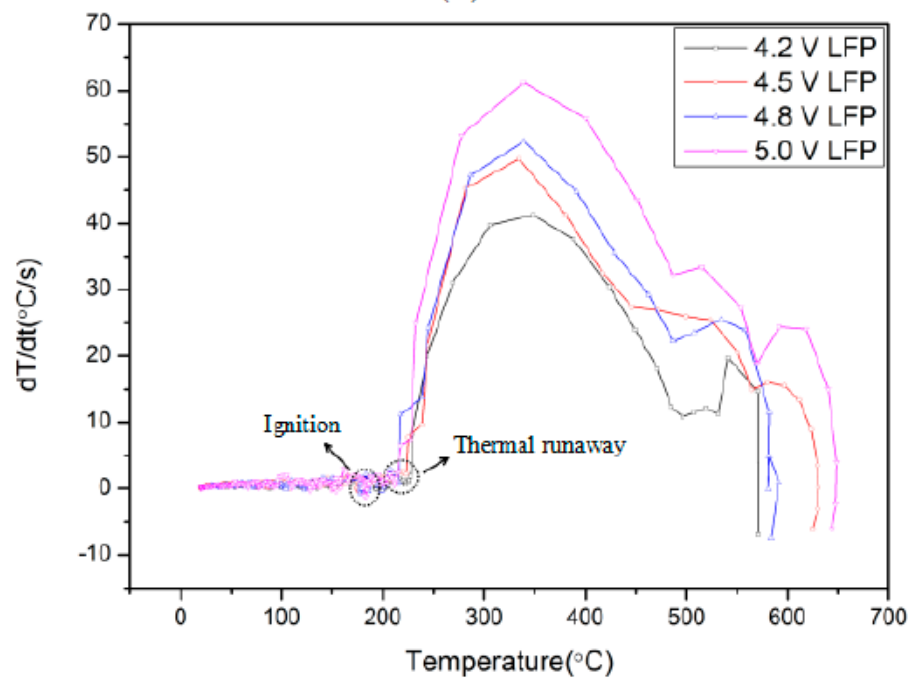
Figure 9-23: (a) Overview of the time–temperature profiles for the cells tested in /8/. (b) Temperature rates from three representative experiments in /8/
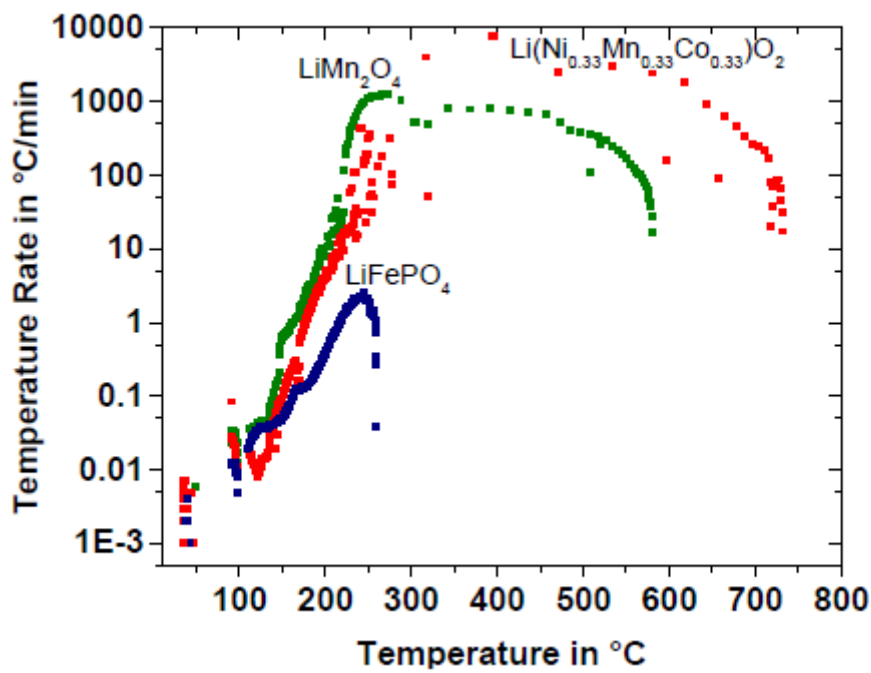
Figure 9-24: Temperature rates for the cells tested in /9/
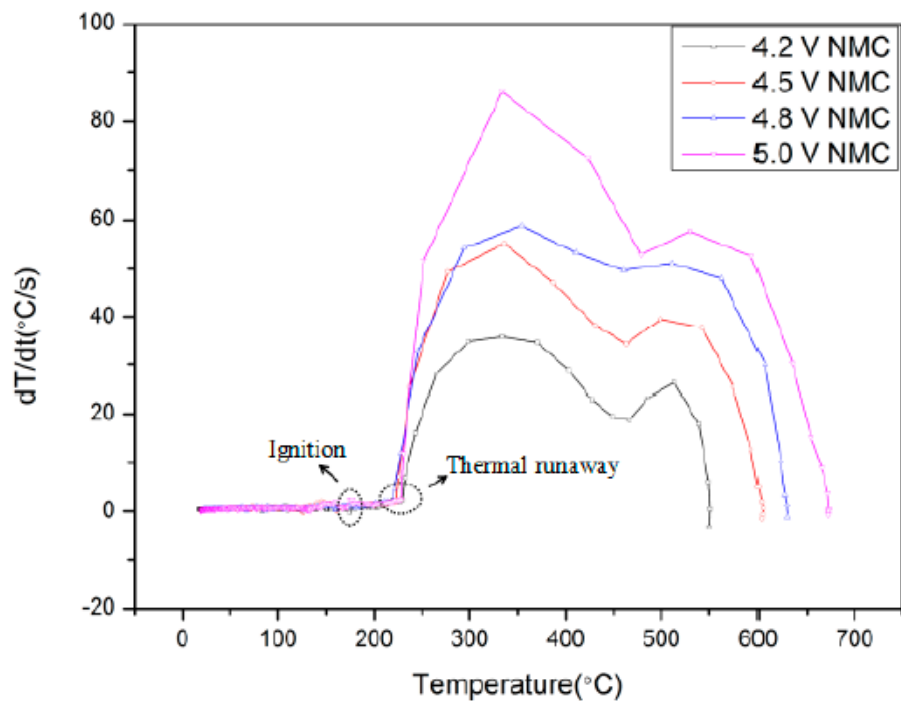
Figure 9-25: Temperature rate curves for the cells tested in /7/.

9.3 Thermal runaway identification discussion

Based at the observed temperature increase rate, the NMC cells all reached step 3 in the thermal runaway process. All tests that had external combustion had a max temperature at 475°C or above, together with a temperature rise of approximately 25°C/ sec. Visual combustion was not observed for 50% overheat and short circuit. In these tests the max temperature observed was 417°C.

Based at the observed test results and the literature review, it seems that none of the 2.5 Ah 26650 went into thermal runaway. The temperature increase rate more or less flat during the test period.

The LFP cells are generally harder to force into thermal runaway compared to the NMC cells. The temperature increase rate is also lower for these cells. Only the 18650 cell with 50% SOC and the 18650 cell with 100% SOC exceeded 1.7°C/sec, which indicates that step 3 in the thermal runaway process has been reached /9/.

From the test results, it seems that the ability to monitor thermal runaway, will vary based on cell packaging. For cylindrical cells, packaging is often more robust, and failures will thus be more delayed and then also more drastically as more temperature and pressure nominally has been built up (for instance a very quick pressure release or pop) after building up, rather than a clear thermal runaway. Further, in cases of fire and distinct thermal runaway, high temperatures are concentrated at the ends where gasses are released, often visually representing specific jet flames.

Based at the temperature increase rate reported in the literature and the tests performed in this study, a temperature increase rate above 10 °C/sec together with a max temperature above 450°C seems to be sufficient to identify the onset point for a thermal runaway with visual combustion for NMC pouch cells. No combustion can be observed at the same temperature increase rates, but with lower maximum temperatures.

For the LFP cells, the increase rate is lower. It should be possible to force these cells into a stage 3 thermal runaway, but this is harder for these cells. Based at the reported literature and the tests performed in this study, a temperature increases of 4 °C/sec seems to be sufficient to identify the onset point for stage 3 of the thermal runaway process for the LFP cells. The chance of achieving this increase with the SOC, and it might be necessary to charge the LFP battery beyond 100% SOC to provoke visual combustion.

9.4 Main Conclusions

Main Conclusions
1. The LFP cells are generally harder to force into thermal runaway compared to the NMC cells. The temperature increase rate is also lower for these cells. 2. For cylindrical cells, packaging is often more robust, and failures will thus be more delayed. Temperature and pressure nominally build up and is followed by a quick pressure release or pop, rather than a clear thermal runaway. High temperatures are concentrated at the ends where gasses are released, often visually representing specific jet flames for cylindrical cells. 3. For NMC pouch cells, a temperature increase rate above 10 °C/sec together with a max temperature above 450°C seems to be sufficient to identify the onset point for a thermal runaway with visual combustion. 4. For the LFP cells, a temperature increases of 4 °C/sec seems to be sufficient to identify the onset point the thermal runaway stage 3. 5. It might be necessary to charge the LFP cells beyond 100% SOC to provoke a thermal runaway with visual combustion.

10 RISKS ACOSIATED WITH WATER BASED FIRE SUPPERSION

10.1 Discussion

When water-based fire suppression system is used – will the water conductivity result in heat generation in neighboring modules and hydrogen gas formation through electrolysis?

Testing of lithium-ion battery modules being submerged in water has not been performed in this project, but was conducted as a part of Consolidated Edison project /3/ and the discussion below stems from those results as well as other test results that have been conducted or observed by the JDP members.

Experiments have included submersion of batteries on fire as well as new battery modules. In cases for batteries on fire, the act of submerging helped significantly to reduce temperatures – and thus reduced the risk of propagation to new/additional cells. In addition, the release of CO that was occurring before submersion continued for over 30 minutes but did not appear to increase in rate. New batteries were visibly damaged and corroded, and temperatures raised from 22 to over 70 °C but there were no signs of any cells venting or exploding.

Thus, it is generally suggested that water will not escalate the failure mode of a battery system. These are results for fully submerged battery modules with voltages in the range of 24-48V.

Cases where water build up in the room, submerging high voltage contactors, breakers or other electrical components at string level, the risks for short circuits and H2 production by electrolysis needs to be evaluated.

To avoid water inside the battery modules when water based total flooding systems are used, battery modules with IP44 is recommended. Most notably, when submerged or extinguished batteries can produce a severely alkaline solution in the water used, climbing to pH 10-11. Other solutions gradually became slightly acidic (pH 6), where the most severely burned batteries produce the most basic solution. This is considered to be the primary risk or consideration with regard to the use of water-based suppression measures.

10.2 Main Conclusions

Main Conclusions
1. Water will not escalate the failure mode of fully submerged battery modules with voltages in the range of 24-48V.
2. Cases where local water build up in the room, submerging high voltage switchgears or components at string level, the risks for short circuits and hydrogen gas production by electrolysis needs to be evaluated.
3. To avoid water inside the battery modules when water based total flooding systems are used, battery modules with IP44 is recommended.
4. The water can become severely alkaline, climbing to pH 10-11. Some solutions gradually became slightly acidic (pH 6), where the most severely burned batteries produce the most basic solution.

SECTION B: DETAILED PROJECT REPORT

This section provides a more detailed account of the entire Battery Safety Joint Development project – including background, initial assessments, safety concepts, methods and test setups used, as well as more specificity on results. These are prepared for completeness and to provide background insight for the discussions in Section A.

11 PROJECT PARTNERS AND OBJECTIVES

11.1 Project partners

Authorities	Ship Owners/Operators
Norwegian Maritime Authority	Scandlines
Danish Maritime Authority	Stena
MARAD	
Power System Vendors	Ship Yard
Kongsberg Maritime	Damen
ABB	
Battery system vendors	Safety Protection Systems
Leclanche	FIFI4Marine
Corvus Energy	Nexceris
Super B	Marioff
Funding and partnership	Research team
Research Council of Norway	DNV GL
	FFI (Norwegian Defense Research Establishment)

11.2 Project objectives

The main objectives of this report include:

- Help align and provide additional reference to uncertain areas within lithium-ion.

- Provide a technical reference to be used in quantitative assessments.

- Provide a technical basis for accurate representation and consideration of major lithium ion battery safety barriers.

- Provide guidance for requirements and qualitative safety assessment.

- Distinguish key areas of safety – that needs attention – from the areas that are not as risky as they seem.

- Provide input on main uncertainties from test data and analysis.

More specifically, the topics presented in this report include:

- A general explanation of the specific safety risks regarding batteries so they can be better understood in context of assessment of safety of a given system in a given application.

- A review of battery cell level test results, which give an indication of off-gas quantities and constituents.

- A review of battery module fire tests to evaluate the effectiveness of different fire suppression media.

- A review of results from CFD analysis adjusted from both the cell level and module tests which give an indication of ventilation effectiveness.

- Provide reference data to use in assessing risk and safety levels for a given system.

- Provide key rules of thumb or design concepts regarding safety requirements.

- Provide a context of safety compared to other systems, and what reasonable acceptance criteria should look like.

12 INTRO TO LITHIUM ION BATTERY SAFETY CONCEPTS

This section provides an explanation of fundamentals of lithium ion battery safety, in the maritime context. The main safety concerns are identified as when a thermal runaway propagate throughout the battery system and the explosion risk of the battery off-gas.

12.1 Thermal Runaway and Propagation

The main concern of a battery system is that the temperature will rise to such level that it will go into thermal runaway. Thermal runaway is the exothermic reaction that occurs when a lithium ion battery starts to burn. The thermal event often starts from an abuse mechanism that causes sufficient internal temperature rise to the electrolyte within a given cell, causing high pressure and often release, and then ignition. This fire then poses significant risk of igniting the electrodes that are contained within the battery cell, thus producing a high temperature fires involving both liquids and gases. These fires are hard to extinguish and to cool down. Additionally, the electrodes may contain oxygen, which is released as it burns. Not all lithium-ion batteries contain oxygen within the electrodes but all lithium-ion batteries on the market today contain electrolyte that can ignite and cause this thermal runaway scenario.

As shown in Figure 12-1 there are several causes leading to a thermal runaway. Note that dendrites and particle formation itself seldom will cause an internal short circuit without some sort of external abuse. It will however make the battery cells more vulnerable for the presented abuse mechanisms /3/.
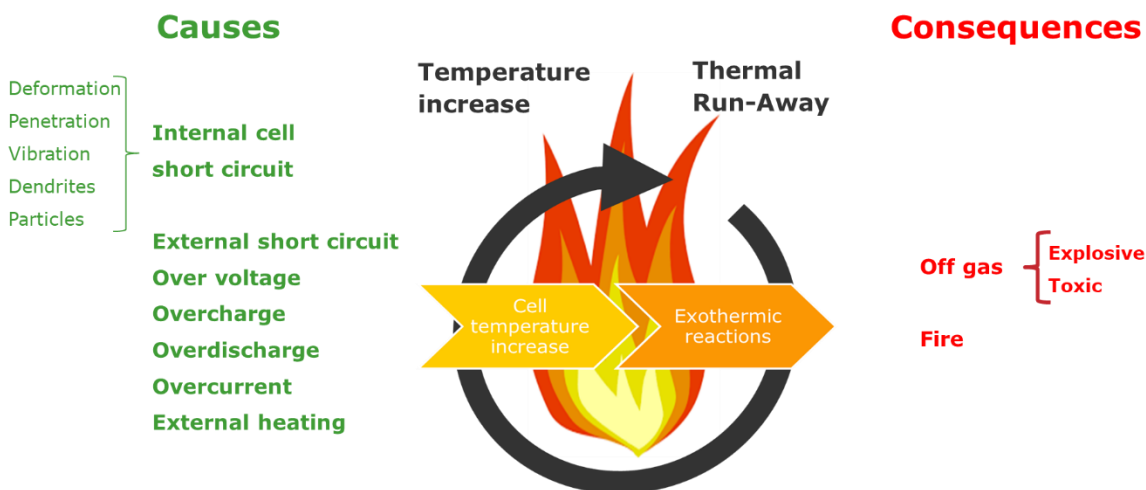
Figure 12-1: Causes and consequences of a thermal runaway in a battery system.

A maritime battery system is typically made up of hundreds or thousands of cells. The failure and total heat release of a single cell is a relatively minor threat. The greater threat comes from that thermal event producing sufficient heat that it propagates to other cells, causing them to go into thermal runaway. As this cascade through the battery, heat produced increases exponentially and the risk is developed of a fire in which the entire battery is involved. Battery modules and systems must be engineered to protect against propagation based on the cell that is used, and these cascading protections are the key feature with regard to system design for safety.

12.2 Explosion and toxicity of off-gas

The electrolyte that is contained within a given cell consists of an organic solvent, typically variants of ethyl carbonates and ethyl acetates. This means that they are flammable, and additionally, this means

the gasses that are produced during a failure scenario are also flammable and can present an explosion risk.

These gasses also typically contain other species which are toxic – such as HCl and HF. For the most part the lithium-ion batteries are not more significantly toxic than a plastics fire. These aspects of battery off-gas thus require consideration with regard to ignition sources and ventilation within both the battery module and battery room.

12.3 Operational safety risks of lithium-ion batteries

The following are the primary ways in which a lithium-ion battery can be misused or abused in such a way that is at high risk of producing a safety event as described in the preceding sections. Many of these risks come from undesired electrical operation, and thus the control system – Battery Management System, BMS – plays a key role with regard to safety, as well as electrical architecture and electrical system protections. These factors are described as they pertain to a cell, but if electrical protections are insufficient, the risk posed by these abuse mechanisms increases exponentially when applied to a full module or even worse, a full rack.

OVERCHARGE

Overcharging a lithium-ion battery represents one of the highest likelihood and highest consequence scenarios that can occur. Overcharging a battery means charging it to a point where its voltage is greater than it is rated to be at. When a battery is overcharged, internal temperature rises and the electrolyte is at significant risk of breaking down into gaseous constituents. Both of these lead to risk of igniting the electrolyte in liquid or gaseous form. Incorrect communication of SOC from the BMS to the converter or the Power Management System, imbalance between cells, or even a short circuit producing an excessive charge current are all scenarios which may pose a risk of overcharge. Voltage limits will vary at the cell level depending on battery chemistry.

OVERDISCHARGE

Similar to overcharge, overdischarge represents a scenario where the battery voltage has dropped below manufacturer recommended limits. This can lead to decomposition of the electrodes within the battery which then poses a risk of short circuiting – and thus of heating electrolyte and causing a fire. Also similar to overcharge, the BMS has a prime role in protecting against overdischarge. Voltage limits will vary at the cell level depending on battery chemistry.

OVERCURRENT

Overcurrent comes from charging or discharging the battery at a power level that is too high. This can cause excessive temperature generation thus leading to electrolyte ignition. In addition, this can lead to incorrect voltage management, and thus accidental overcharging or overdischarging. The converter connected to the battery should be equipped with an overcurrent protection, where the limits are set by the BMS. In severe cases, the excessive current may be of a fault or short circuit type, and thus out of control; thus, passive electrical protections such as fuses and breakers are the key to prevent this failure.

OVERHEATING

Thermal management of a battery system is the key. Excessive temperatures will drive degradation and can also lead to a safety event. If ambient temperature is too high, then the battery may operate in a way that further increases its internal temperature beyond acceptable limits. Acceptable upper temperature limits are often near 45°C.

EXCESSIVE COLD

Operating a battery in temperatures below its rated range will increase internal resistance, decrease efficiency and can also lead to a safety event through lithium plating on the anode or formation of dendrites – thus resulting in an internal short circuit and rapid heating of the electrolyte. Lower temperature thresholds range widely between different cell chemistries, and manufacturer recommendations should be followed closely, but it can be considered generally inadvisable to operate below 10°C.

EXTERNAL SHORT CIRCUIT

An external short circuit is likely a familiar concept and poses the same risk as many other failure modes described in this section. If the battery is rapidly charged or discharged, the electrolyte in a cell may heat to the point of ignition and pose a threat of thermal runaway and/or flammable or toxic off-gas release. As mentioned before, passive electrical protections such as fuses, and breakers are the key to prevent this failure.

MECHANICAL DAMAGE

Mechanical damage may result from external protrusion into the battery room under collision, errant crane operation, or perhaps in the case of explosion or other mistakes. If a cell is mechanically damaged, a risk is posed of the electrodes coming into contact and short circuiting as well as many other electrical components. This short-circuiting thus produces the same failure mode of heating the electrolyte to the point of ignition.

EXTERNAL FIRE

An external fire poses the threat of involving the battery system and thus direct overheating and combustion of all battery materials. An external fire might also heat up the battery space, such that the ambient temperature exceeds the acceptable limit of safe battery operation. Proper fire segregation of the battery rom and a fire extinguishing system that removes the heat from the battery space is then important.

INTERNAL DEFECT

An internal defect represents perhaps the largest threat to a lithium-ion battery system because it is something that cannot be detected by the battery BMS. Most all other failures will result in indications from voltage or temperature sensors that will be detected and accounted for by the BMS. An internal defect may produce an internal short with little to no warning. This is the result of issues or quality control from manufacturing. Although many cell producers maintain a high degree of quality control, the large number of cells required for an installation and the inability to detect, make an internal defect a significant risk and the main reason that off-gas and thermal runaway must be considered and protected against in even the most highly controlled and monitored systems.

12.4 Definitions

Definitions are vital for a common and consistent discussion and assessment of safety. This comprehensive account is contained in Appendix A of this document. This includes the current range of definitions that are found in different reference and standard documents, particularly relating to safety. In addition, this appendix includes key definitions as agreed upon as needed by the JDP team, and as defined by the JDP team.

13 CELL LEVEL TEST RESULTS

This section provides a summary of observations and results from a cam reference data on the concentrations of gasses produced from different cells under different failure modes. CFD models of the test chamber were developed to produce better representation

13.1 Test setup

Three different cell types where tested in DNV GL's Large Battery Destructive Test Chamber, shown in Figure 13-4. NMC pouch cells of 63 Ah, LFP cylindrical 18650 cells of 1.5 Ah and LFP cylindrical 26650 cells of 2.5 Ah where tested. The pouch cells were constrained with steel plates with tow strip heaters of 500 kW each as shown in Figure 13-1. Radiant heaters were also placed in the test chamber of 4 kW.
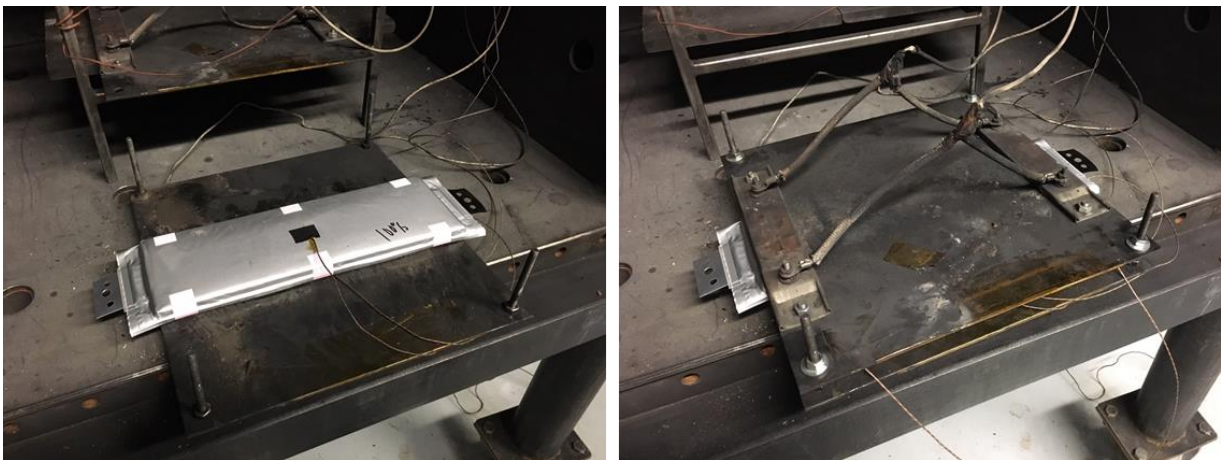
Figure 13-1: Steel plates with heaters where attached to the NMC 63 Ah pouch cells

Figure 13-2: LFP 2.5 Ah cylindrical cell heated up

Figure 13-3: LFP 1.5 Ah cylindrical cell heated up

The test camber is shown in Figure 13-4. The chamber volume is 30" x 30" x 30" (0.762m x 0.762m x 0.762m), which gives a total volume of 0.44 m^3. At the bottom of the chamber, there is eight 1" diameter holes. At the upper part, it is three 1" pipes that are connected together at one pipe of 2", and the finally to a 3" pipe, where an extraction fan is installed. The exhaust fan in the upper part of the exhaust plenum was computer controlled to create a flow rate of 11 L/s.

Opposed to a test environment with inert atmosphere, this test setup will be closer to the environmental conditions battery will be exposed to under real operations.

Figure 13-4 Large Destructive Test Chamber Setup

The gas data was collected by a Gasmet DX4000 Fourier transform infrared spectroscopy (FTIR) gas analyser. This unit sampled the air inside the chamber every seven seconds, set up to monitor off-gases common to batteries undergoing abuse testing based on DNV GL's experience. The gases sampled are shown below:

Water Vapor (H_2O, %)   Carbon Dioxide (CO_2, %)   Carbon Monoxide (CO, ppm)
Nitrogen Monoxide (NO, ppm)   Nitrogen Dioxide (NO_2, ppm)   Sulfur Dioxide (SO_2, ppm)
Methane (CH_4, ppm)   Ethane (ppm)   Ethylene (C_2H_4)
Hydrogen Chloride (HCl, ppm)   Hydrogen Fluoride (HF, ppm)   Hydrogen Cyanide (HCN, ppm)
Benzene (ppm)   Toluene (ppm)   Ethanol (ppm)
Methanol (ppm)   Oxygen (O_2, %)

In line with the FTIR analyzer were MSA Ultima sensors for O_2 (redundant measurement), H_2, and F_2/Cl_2. A final MSA sensor was placed directly off the chamber for flammability measurements. The sensor was of the catalytic bead type and was factory calibrated to non-specific gas for total LEL% measurement. This was deemed suitable as a range of flammable gases were expected and calibration to one may show improper bias. In addition to the LEL% sensor, a battery off-gas specific sensor called Li-ion Tamper®, developed by Nexerius, was also installed.

As noted in the set-up and shown in Figure 13-5, thermocouples were placed around the unit, totaling 14, with eight comprising a thermopile to capture heat release rate around the unit, three thermocouples placed on the cells directly, and three placed in the chamber to measure ambient and inlet and exhaust temperatures. Thermocouples on the cells were placed on the axially along the cell near the top, in the middle and at the bottom for all tests. DNV GL utilized K-type, glass braid thermocouples.

With the exception of the FTIR gas analysis, Gas Analysis all data was collected via a National Instruments data acquisition setup, which controlled the fan and ignitors mounted in the chamber to prevent an explosion.
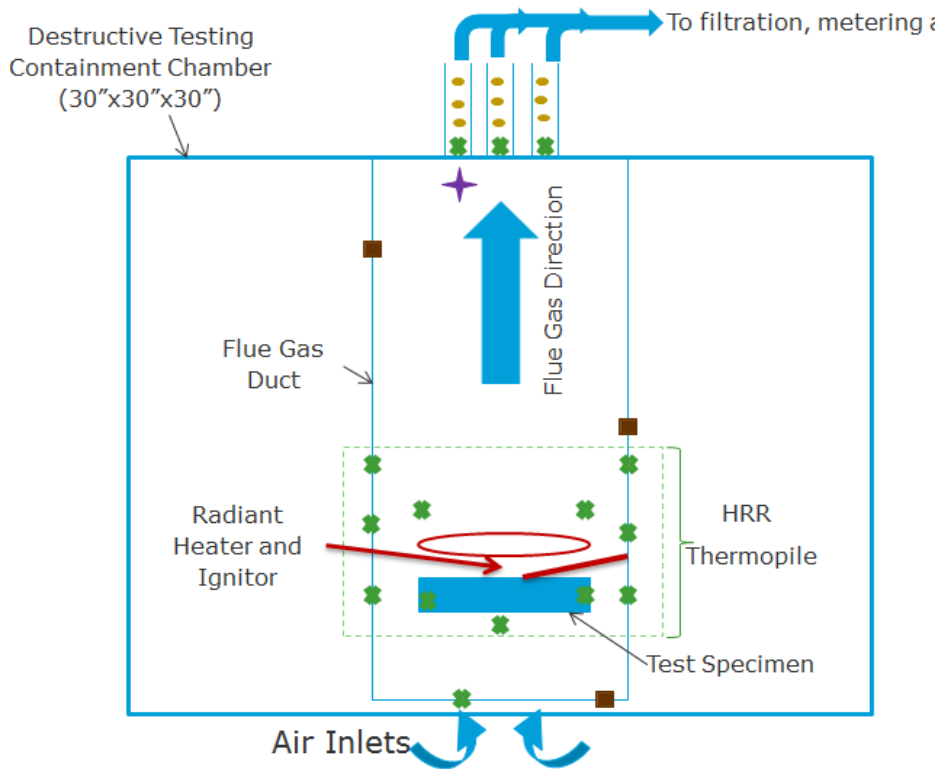
Figure 13-5: Diagram of the abuse chamber used for single cell testing

13.2 Cell Level Test results

The tests shown in Table 13-1 are presented in this section.

Table 13-1: Overview of the cell level tests performed

Test ID	Chemistry	Size (Ah)	Cell type	SOC	Failure mode	Visual Combustion
JDP1	NMC	63	Pouch	100%	Overheat	Yes
JDP2	NMC	63	Pouch	50%	Overheat	No
JDP3	NMC	63	Pouch	100%	Overcharging 50A	Yes
JDP5	NMC	63	Pouch	75%	Overheat	Yes
JDP7	NMC	63	Pouch	100%	Short Circuit between battery terminals	No
A1	LFP	2.5	26650	50%	Overheat	No
A2	LFP	2.5	26650	75%	Overheat	No
A3	LFP	2.5	26650	100%	Overheat	Explosion
A4	LFP	2.5	26650	100%	Overcharge 50A	No
B1	LFP	1.5	18650	50%	Overheat	No

| B2 | LFP | 1.5 | 18650 | 75% | Overheat | No |
| B5 | LFP | 1.5 | 18650 | 100% | Overheat | Explosion |

13.2.1 Gas release profile

Below follows the measured concentration of the different gasses identified. Note that hydrogen is not one of the gases, since the sensor used where saturated at 1%. It can only be used to determine if hydrogen was present, but not quantify the amount.

13.2.1.1 NMC 63 Ah

JDP2 50% SOC overheat

It can be seen from Figure 13-6 that initially the gasses are released at constant rate, followed by heavy off-gassing at thermal runaway. Note however that no 'ignition' was observed, only large amount of gas. A considerable amount of CO and Ethane where observed during the early gas release. At thermal runaway, there is a spike in CO, Methane, Ethylene and HCL. The CO2 only starts to rise after the spike in the gas release. This indicates that total combustion has not been reached. The H2 sensor shows that it steps up during the steady off-gassing, and saturates at thermal runaway. Note also
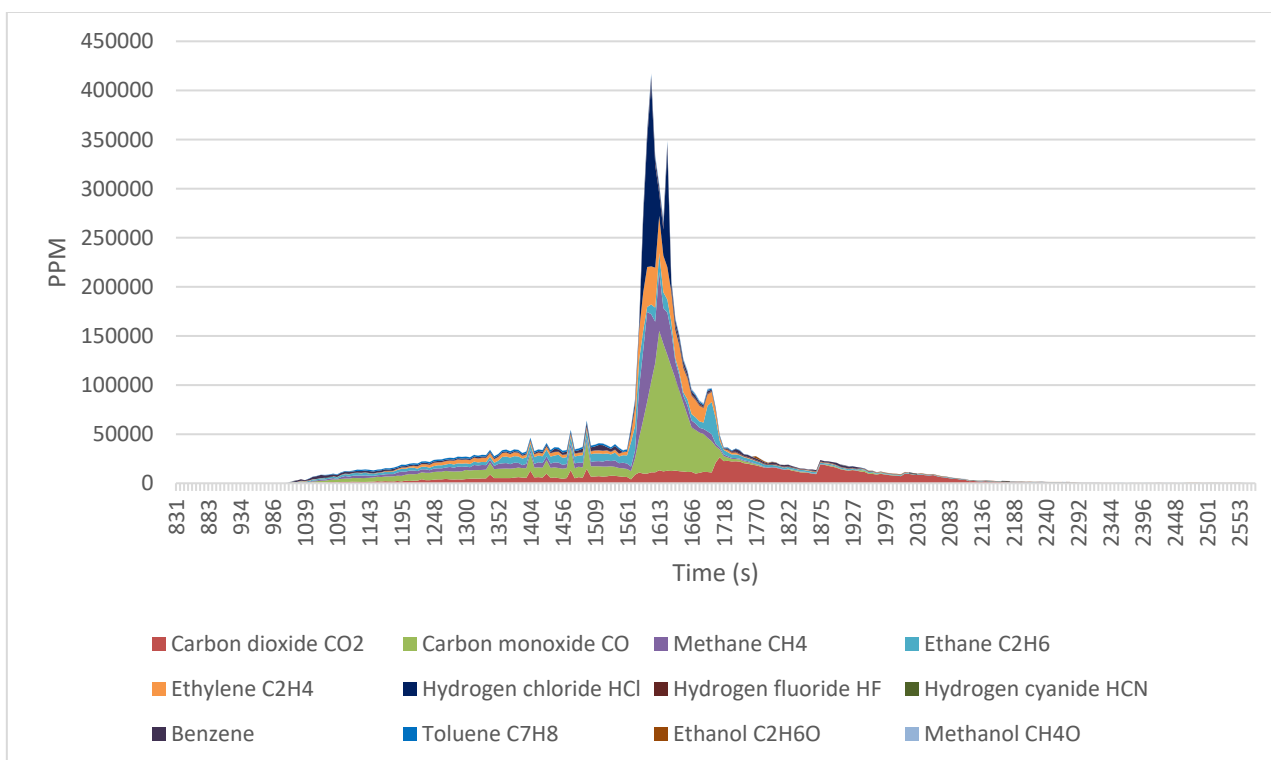
Figure 13-6: Concentration of the measured battery gasses for test JDP2, 63 Ah NMC pouch cells 50% SOC overheat.

Figure 13-7 shows the oxygen level together with the sum of the measured battery gasses. It is seen that the oxygen level drops when the battery starts to vent. This is mainly due to the battery gasses are displaces the oxygen in the chamber.
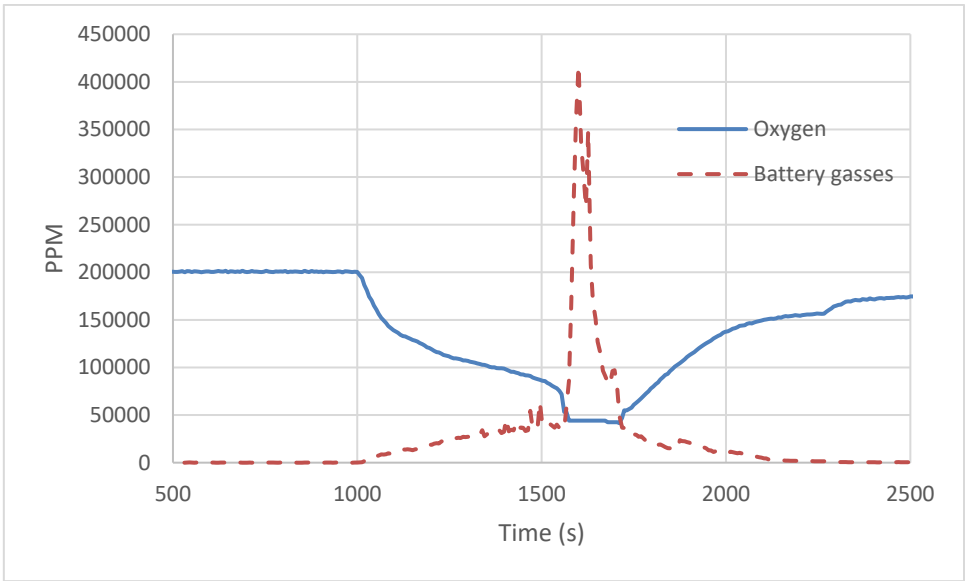
Figure 13-7: Oxygen level and the sum of the measured battery gasses for JDP2, 63 Ah NMC pouch cells 50% SOC overheat.

JDP5 75% SOC overheat

Figure 13-8 show that the battery has a steady initial release mainly of CO, methane and ethane, before it starts to heavy off-gas. At this point the dominant gas is CO2, and a spike in Ethylene is also observed. The large amount of CO2 supports that visible combustion starts at this point. Note also the short spike in Ethanol. The hydrogen starts to ramp at the beginning of the steady off gassing period, and saturates at thermal runaway.
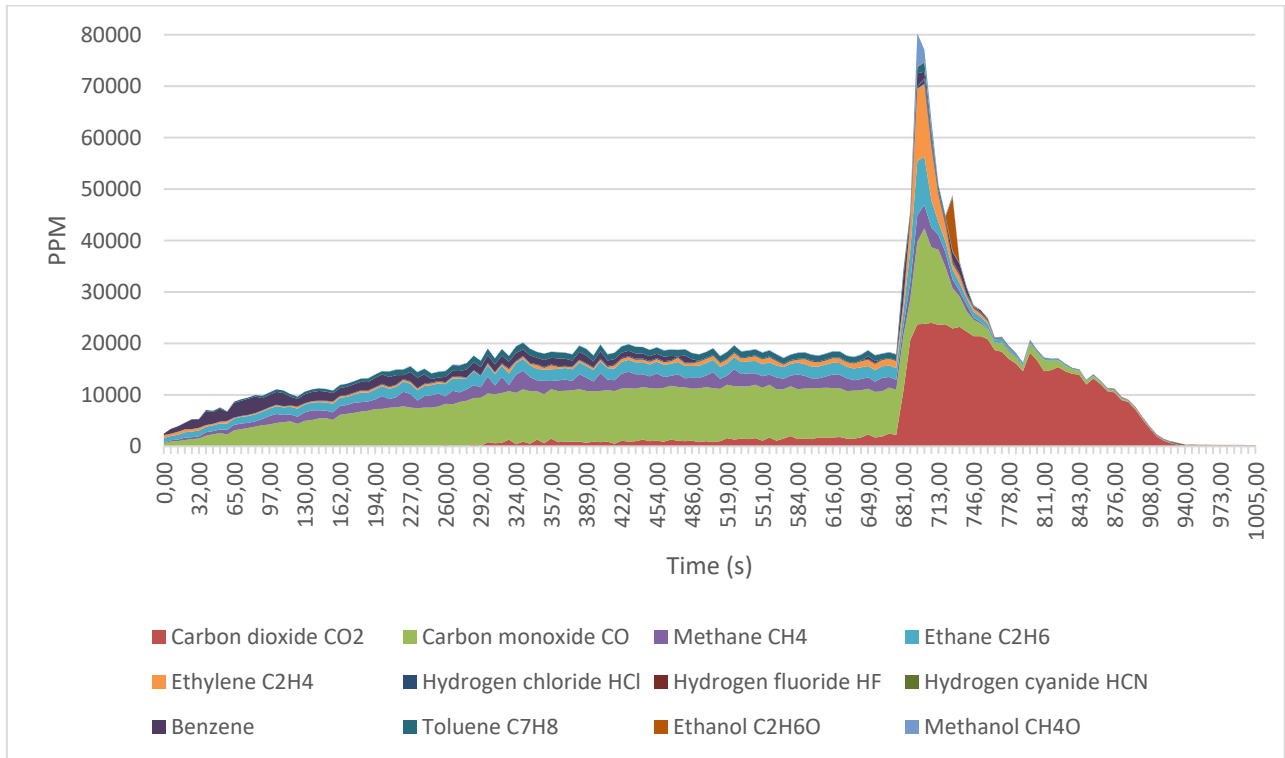
Figure 13-8: Concentration of the measured battery gasses for test JDP5, 63 Ah NMC pouch cells 75% SOC overheat.

JDP1 100% SOC overheat

Opposed to the tests with lower SOC, Figure 13-9, shows a shorter time of initial gas release before the thermal runaway starts with heavy off-gassing. Sparks were observed, which then ignited the gas. The dominant gas is here CO2, which supports the visible combustion. A late bust in ethanol is observed at 1025 sec.
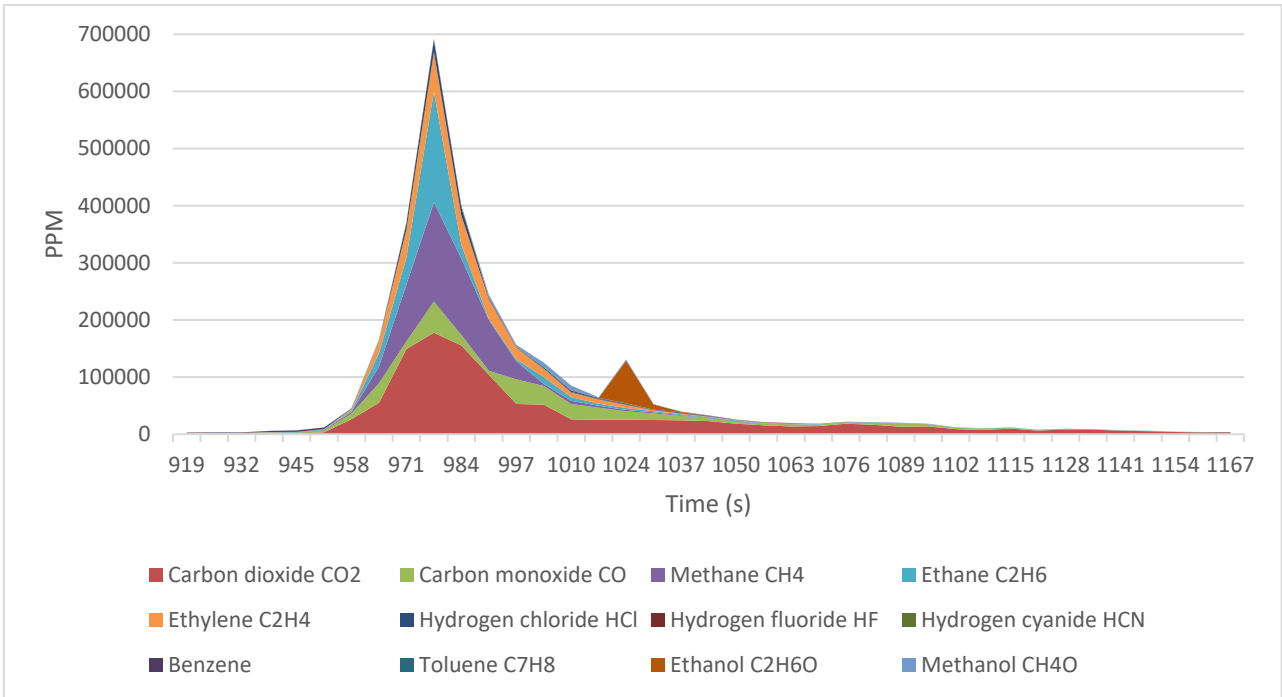
Figure 13-9: Concentration of the measured battery gasses for test JDP1, 63 Ah NMC pouch cells 100% SOC overheat.
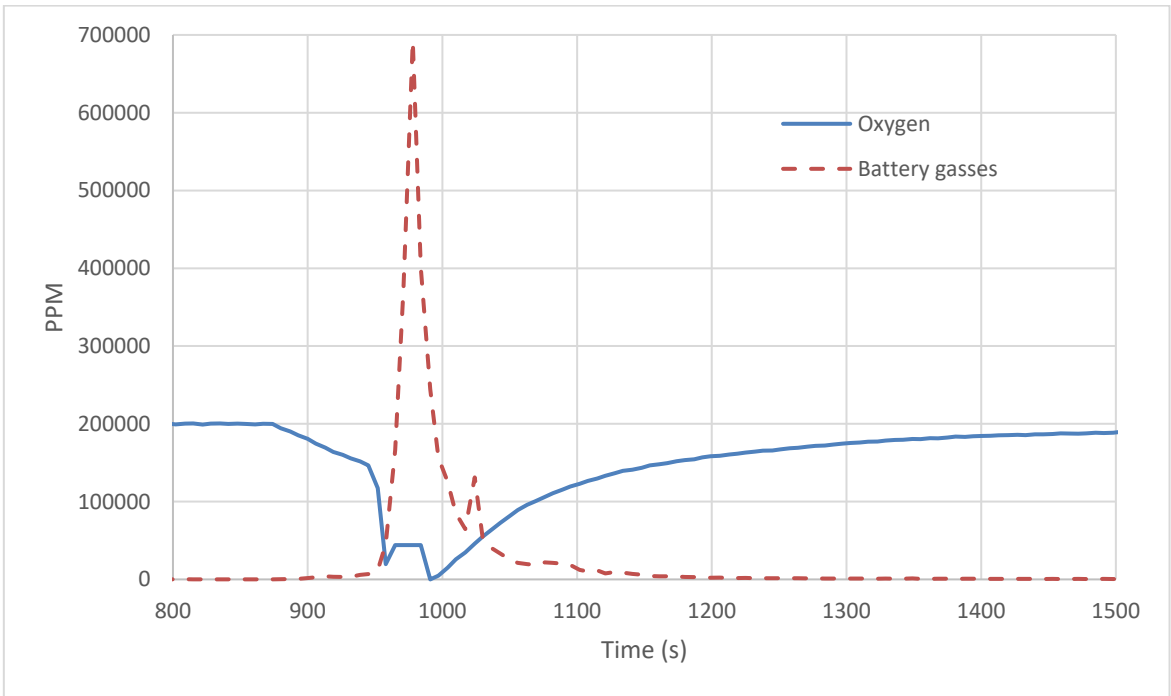

Figure 13-10: Oxygen level and the sum of the measured battery gasses for JDP1, 63 Ah NMC pouch cells 100% SOC overheat.

Figure 13-10 shows the oxygen level together with the sum of the measured battery gasses. The drop in oxygen is explained by both displacement and consumption from the battery fire.

JDP3 100% SOC Overcharge

The release profile shown in Figure 13-11 is similar when the cell was overheated at 100% SOC. It starts with an initial release followed by heavy off-gassing and very quick ignition. The hydrogen sensor saturates at combustion, and drops back down under saturation after 530 seconds.
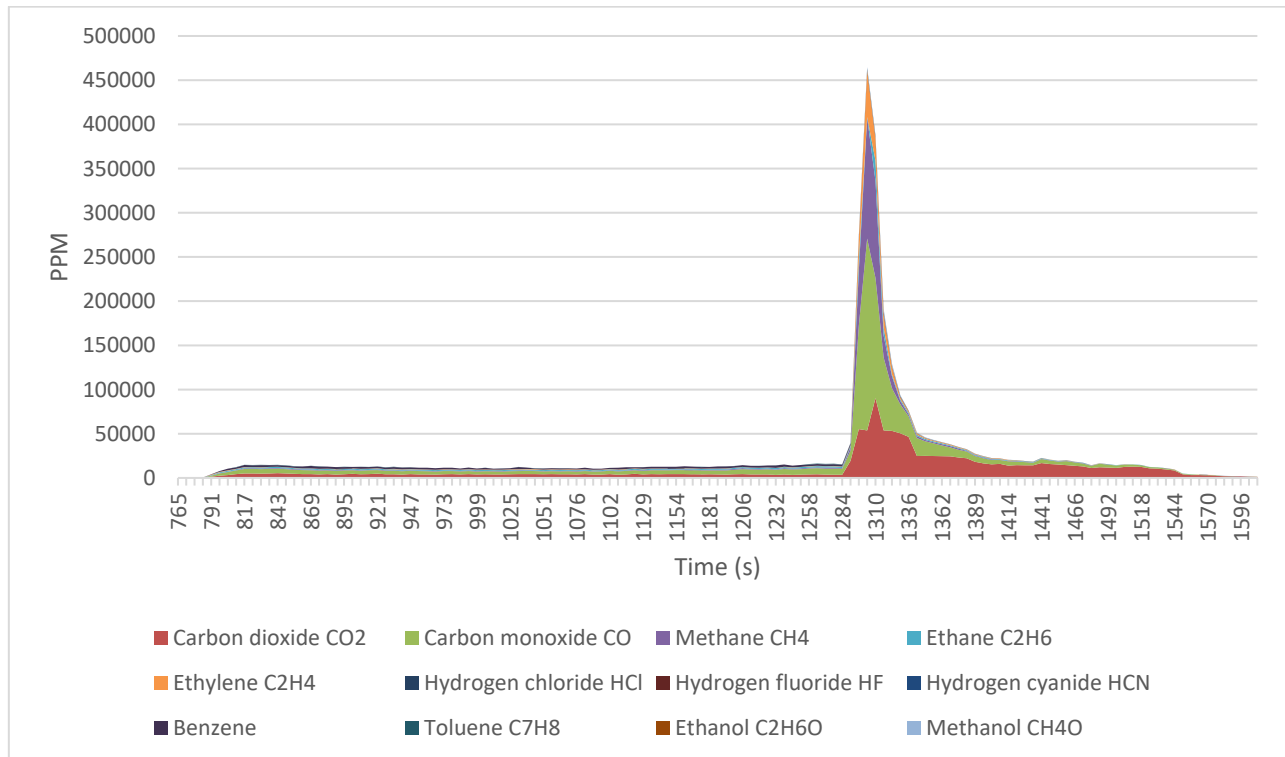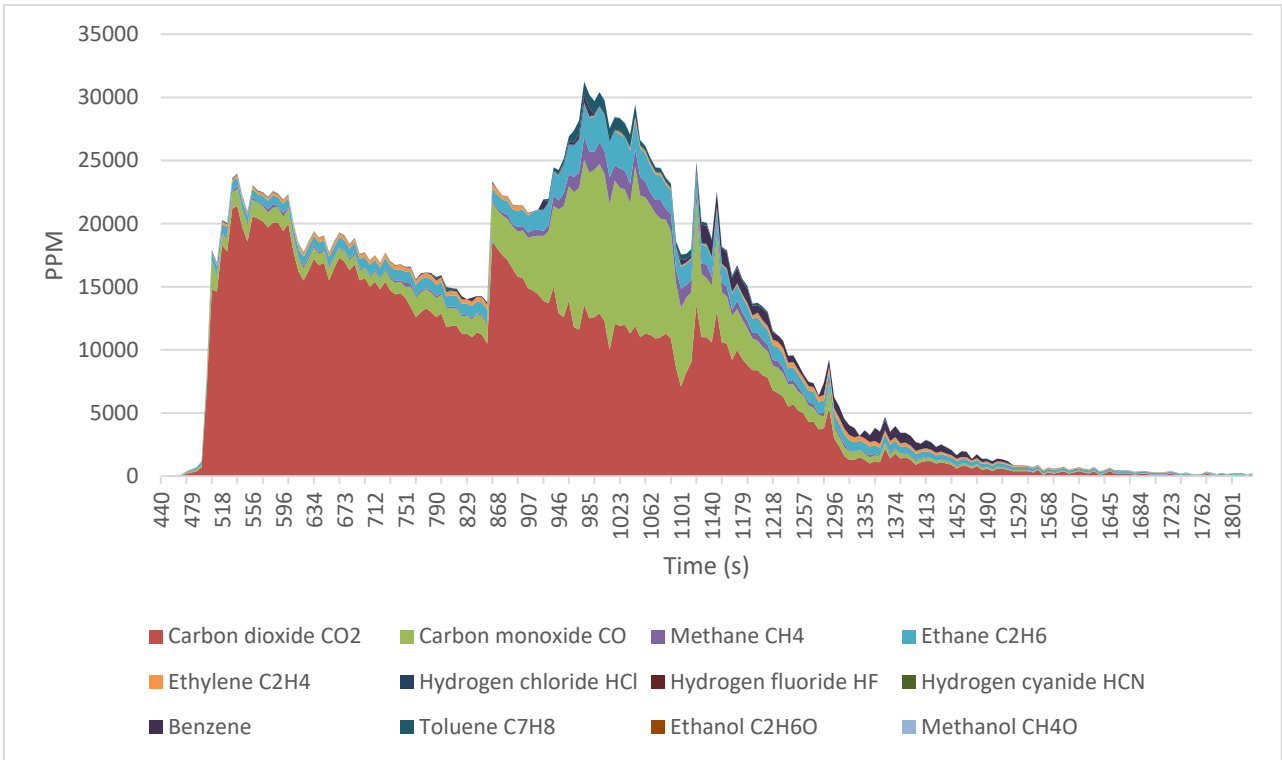

Figure 13-11: Concentration of the measured battery gasses for test JDP3, 63 Ah NMC pouch cells 100% SOC overcharge.
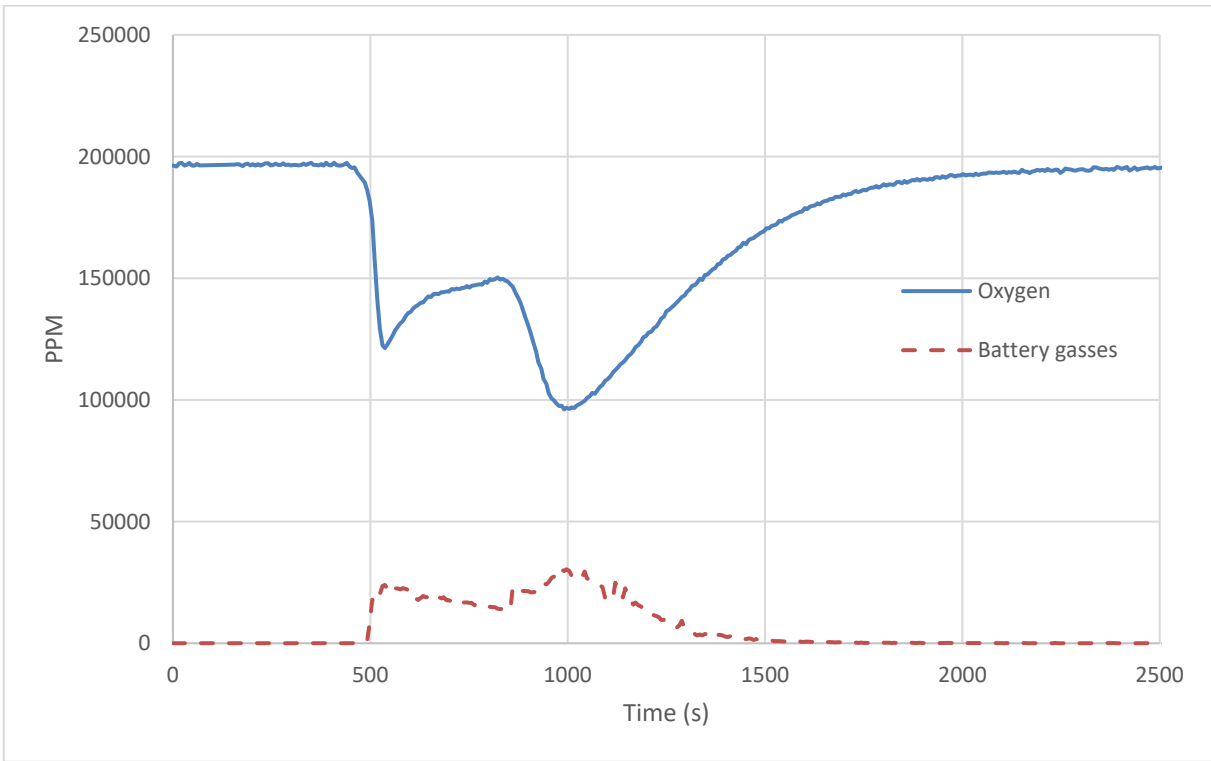
JDP7 100% SOC Short Circuit

Figure 13-12 shows a very low and steady release compared to the other tests, even when the cell is charged at 100%. This indicates that external short circuit is not as severe as external overheat or overcharge.

The oxygen drop shown in Figure 13-13 is considerably lower than for the overcharge at 100% test. However, the amount of oxygen in the room will be lower during a thermal runaway, and not higher, even for this failure mode.

Figure 13-12: Concentration of the measured battery gasses for test JDP7, 63 Ah NMC pouch cells 100% SOC Short Circuit.
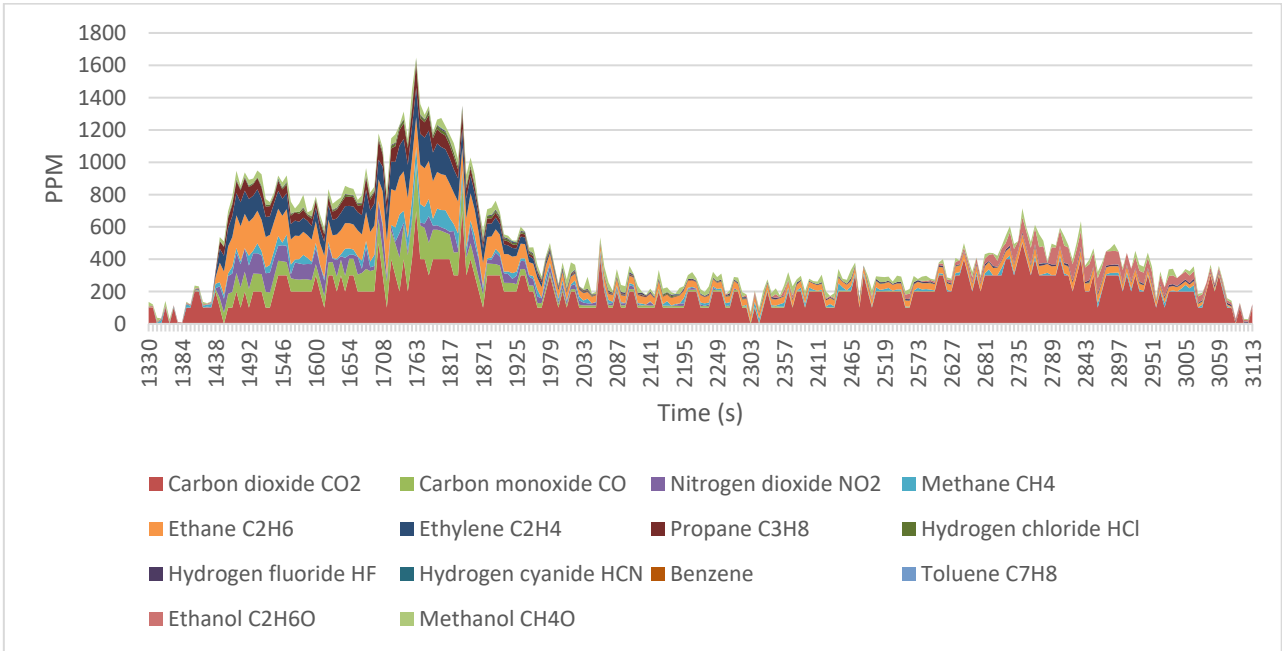

Figure 13-13: Oxygen level and the sum of the measured battery gasses for JDP7, 63 Ah NMC pouch cells 100% SOC Short Circuit.

13.2.1.2 LFP 2.5 Ah

A1 50% SOC Overheat

Figure 13-30 show a steady release of CO2 during the total off gas period, even after the off-gassing has been relaxed. Note that the level of Ethane and NO2 released is also quite high compared to the NMC batteries.

Figure 13-14: Concentration of the measured battery gasses for test A1, 2.5 Ah LFP cylindrical cells 50% SOC overheat.

Figure 13-15 shows the drop in oxygen in the test chamber during the test. The drop is explained both by combustion and displacement.
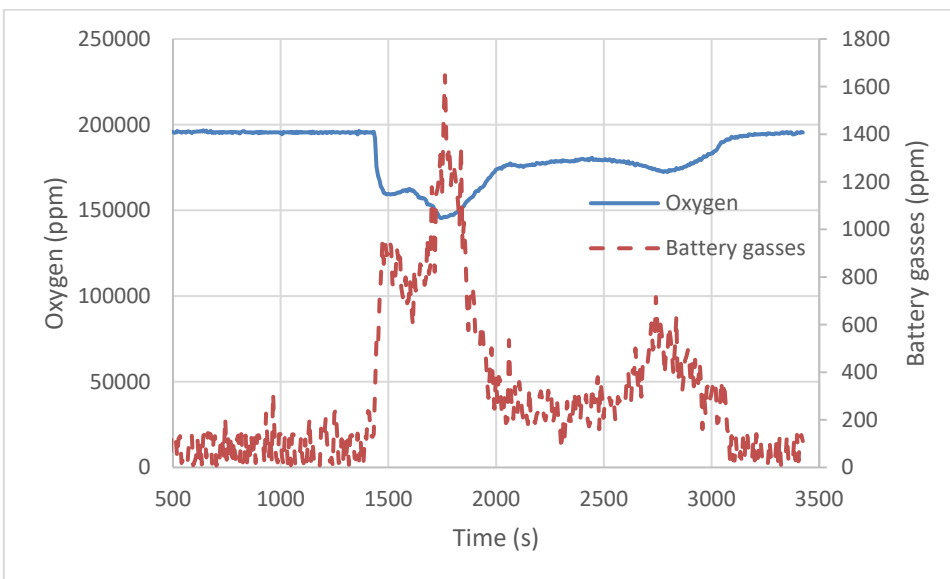
Figure 13-15: Oxygen level and the sum of the measured battery gasses for A1, 2.5 Ah LFP cylindrical cells 50% SOC overheat.

A2 75% SOC Overheat

Figure 13-16 show a low release of CO2 during the total off gas period. It has a high release of CO and Ethane during the off-gas peak.
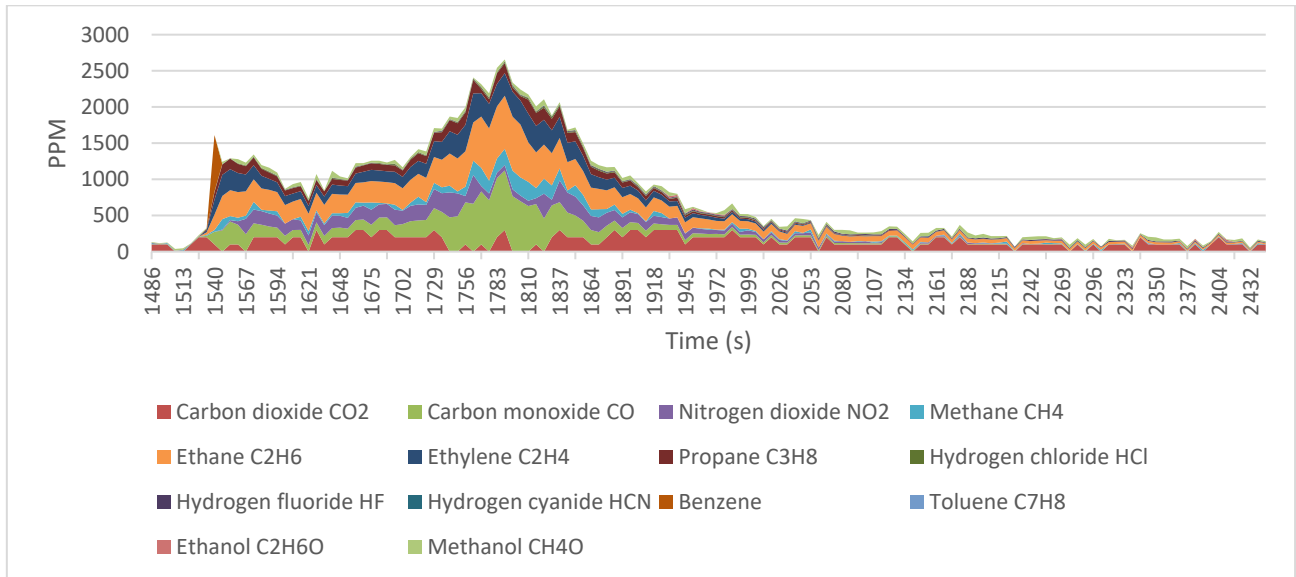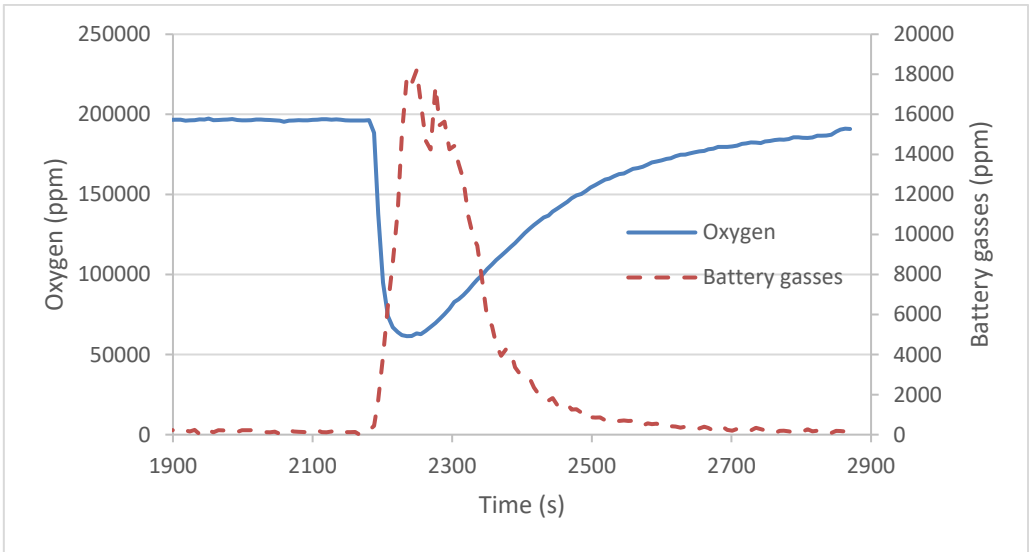

Figure 13-16: Concentration of the measured battery gasses for test A2, 2.5 Ah LFP cylindrical cells 75% SOC overheat.

A3 100% SOC overheat

The amount of gas released shown in Figure 13-17 is considerable higher than for test A1 and A2. The quantity of CO2 and CO is considerable higher, which indicates a high rate of combustion. The oxygen drop shown in Figure 13-18 also supports this.
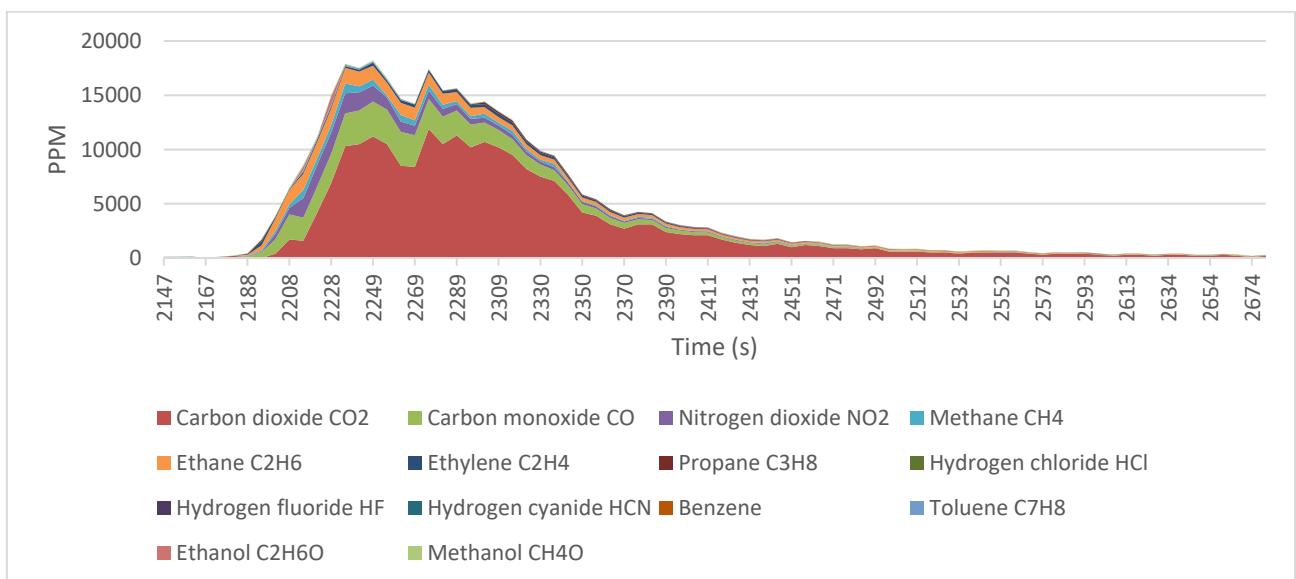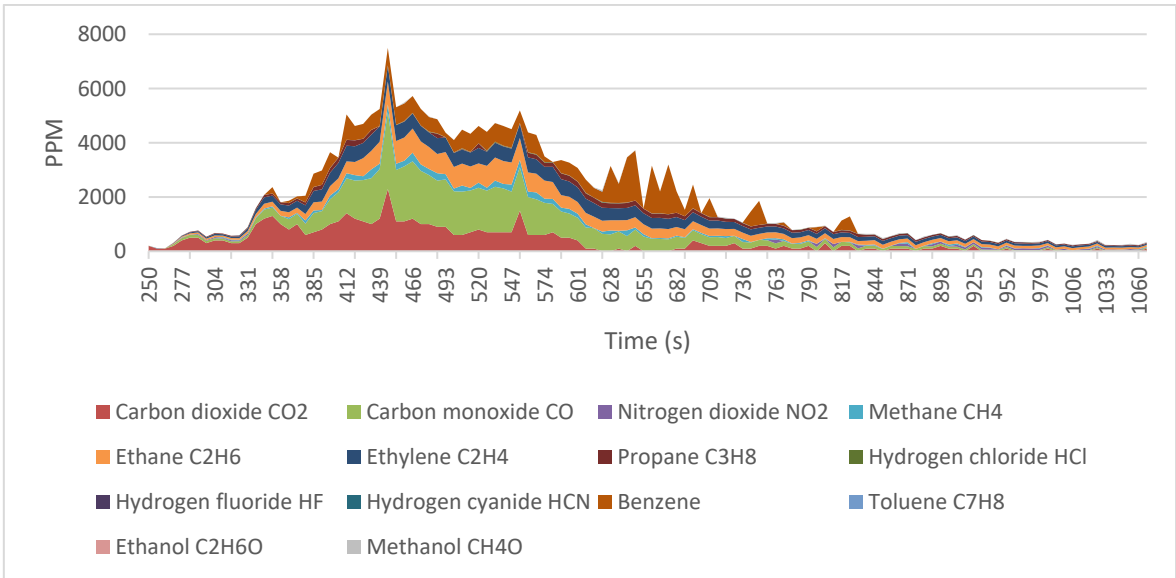

Figure 13-17: Concentration of the measured battery gasses for test A3, 2.5 Ah LFP cylindrical cells 100% SOC overheat.

Figure 13-18: Oxygen level and the sum of the measured battery gasses for A3, 2.5 Ah LFP cylindrical cells 100% SOC overheat.

A4 100% SOC overcharge

The release profile shown in Figure 13-19 indicates a lower level of total combustion compared to overheat at 100% SOC. Note also the large amount of Benzene released.
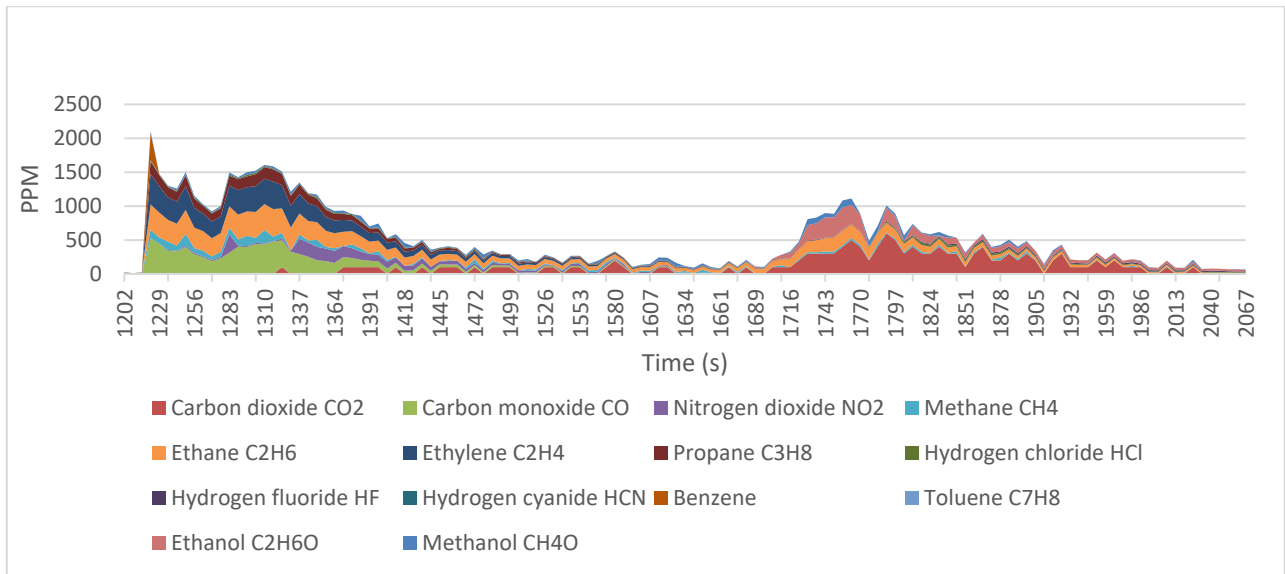

Figure 13-19: Concentration of the measured battery gasses for test A4, 2.5 Ah LFP cylindrical cells 100% SOC overcharge.

13.2.1.3 LFP 1.5 Ah

B1 50% SOC overheat

Figure 13-20 show the gas release for test B1. Note the high amount of ethane compared to CO2 and CO. It is two spikes in the release, the first dominated by CO and ethane, ethylene and propane. The

second release is dominated by CO2, ethane and ethanol. The release profile itself is similar to A1, where the cell also was overheated at 50% SOC.

Figure 13-20: Concentration of the measured battery gasses for test B1, 1.5 Ah LFP cylindrical cells 50% SOC overheat.
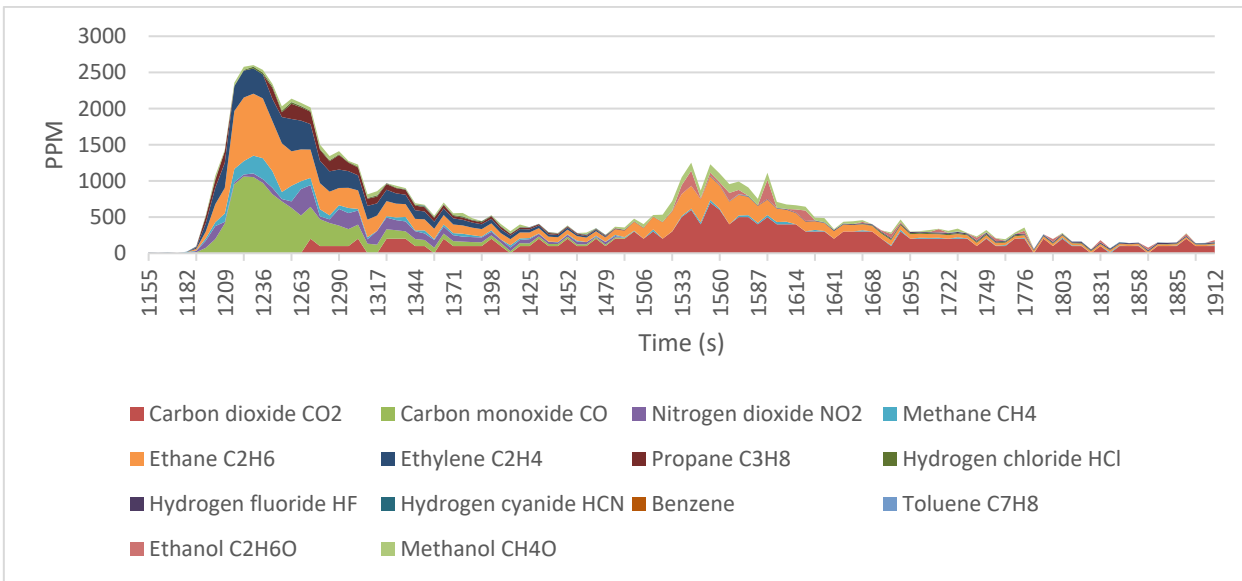
The drop in oxygen shown in Figure 13-21 can be explained both by combustion and displacement.
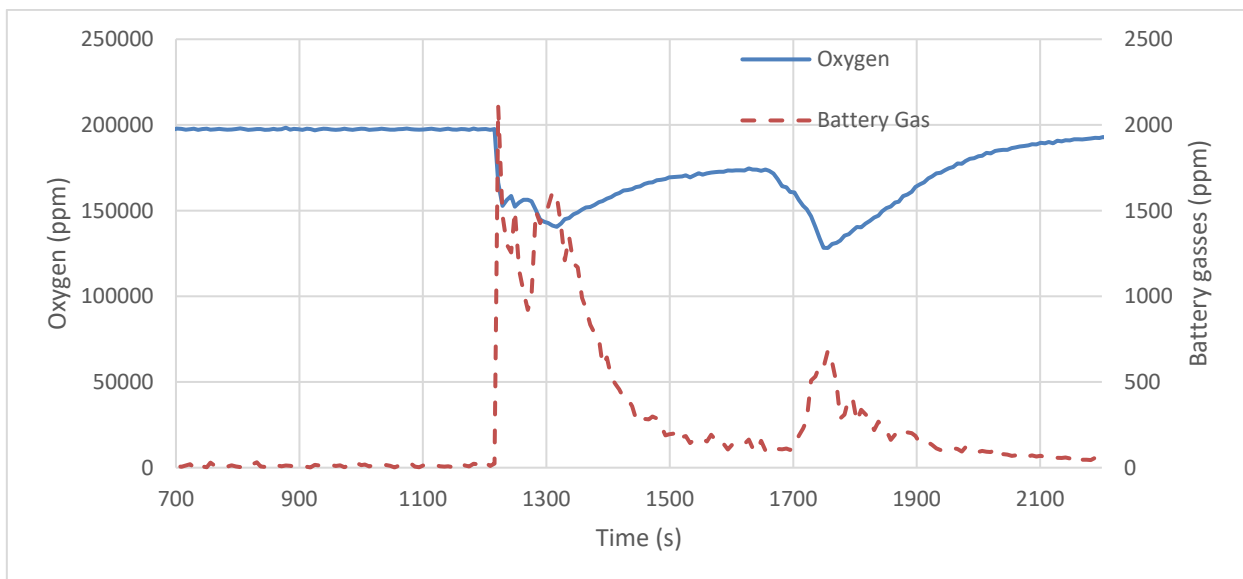
Figure 13-21: Oxygen level and the sum of the measured battery gasses for B1, 1.5 Ah LFP cylindrical cells 50% SOC overheat.

B2 75% SOC Overheat

The release in Figure 13-22 also show two spikes, the first dominated by CO and ethane, while the second is dominated by CO2 and ethane.

Figure 13-22: Concentration of the measured battery gasses for test B2, 1.5 Ah LFP cylindrical cells 75% SOC overheat.

B5 100% SOC overheat

The release profile shown in Figure 13-23 also shows two spikes, the first initiated by CO and the second initiated by CO2. However, the two spikes appear quite close compared to B1 and B2, so the total release appears to be only one spike.

Figure 13-23: Concentration of the measured battery gasses for test B5, 1.5 Ah LFP cylindrical cells 100% SOC overheat.

Figure 13-24 show the drop in oxygen. It is linked with the displacement and the consumption of oxygen in the fire.

Figure 13-24: Oxygen level and the sum of the measured battery gasses for B5, 1.5 Ah LFP cylindrical cells 100% SOC overheat.
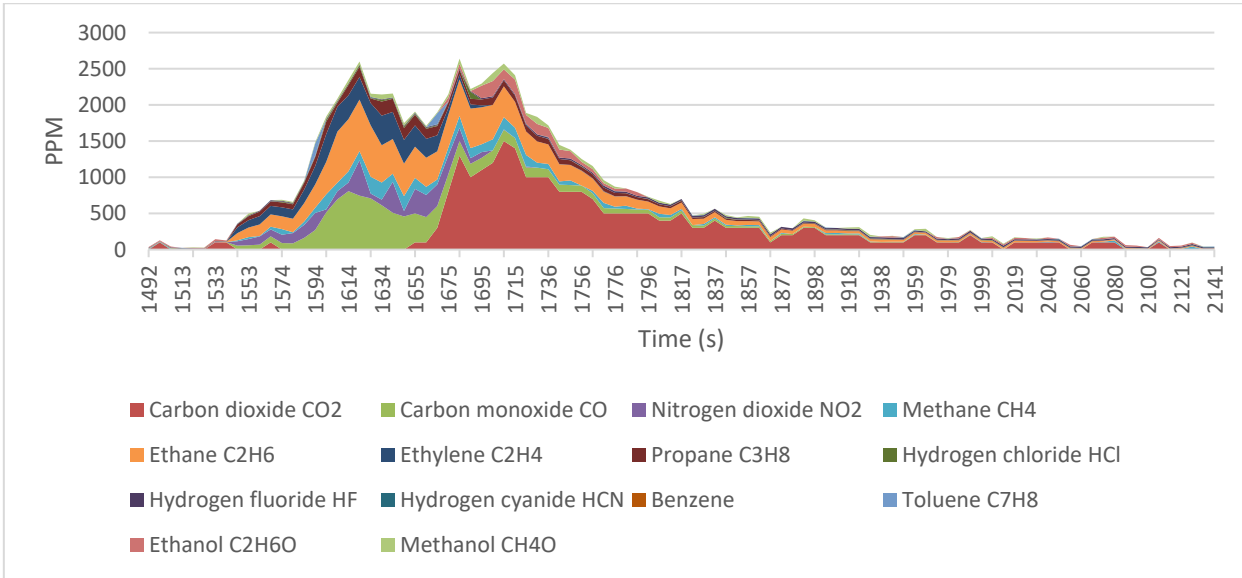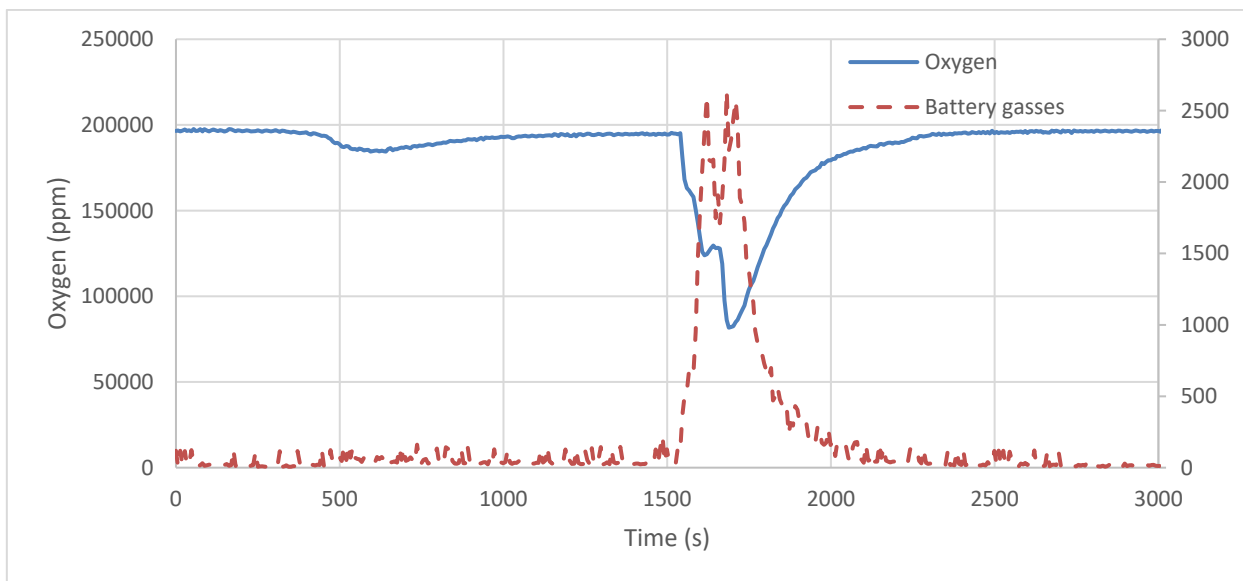
13.2.2 Temperature profiles

13.2.2.1 NMC 63 Ah

Figure 13-25, Figure 13-26, Figure 13-27, Figure 13-28 and Figure 13-29 shows the cell surface temperatures for test JDP2, JDP5, JDP1, JDP3 and JDP7 respectively. These can provide visual indication of the temperature profile when the cell goes into thermal runaway.

In almost all cases, there is a point at which heating of the temperature accelerates, characterized by a point that does visually appear as an inflexion point relative to the rate of temperature increase. Following this, it is common to see a point where the temperature will dip down – this coincides with a preliminary gas release. However, we see that this is still clearly not 'thermal runaway'. The primary points of focus are the sharp spikes in temperature, where we see close to 50°C per second temperature rise, or several hundred in the overcharge case shown here. This will define the onset of the thermal runaway.

Table 13-2 provides a summary of key data points to use for comparison. Max temperature, max temperature increase and temperature at onset is presented.

Since the measurements for the overheat 100% SOC was noisy at the point where the thermal runaway appeared, an estimation of the temperature profile has been done.

Table 13-2 – Characteristics for identification of thermal runaway NMC pouch cells

Test ID	Failure mode	Max Temp (°C)	Max Temp increase rate (°C/second)	Temperature at onset (approximate)
JDP2	Overheat at 50% SOC	417	29.27	250
JDP5	Overheat at 75% SOC	481	24.36	200
JDP1	Overheat at 100% SOC	475	66.07	173
JDP3	Overcharge	602	229	80

| JDP7 | Ext Short Circuit | 177 | 13.6 | 30 |
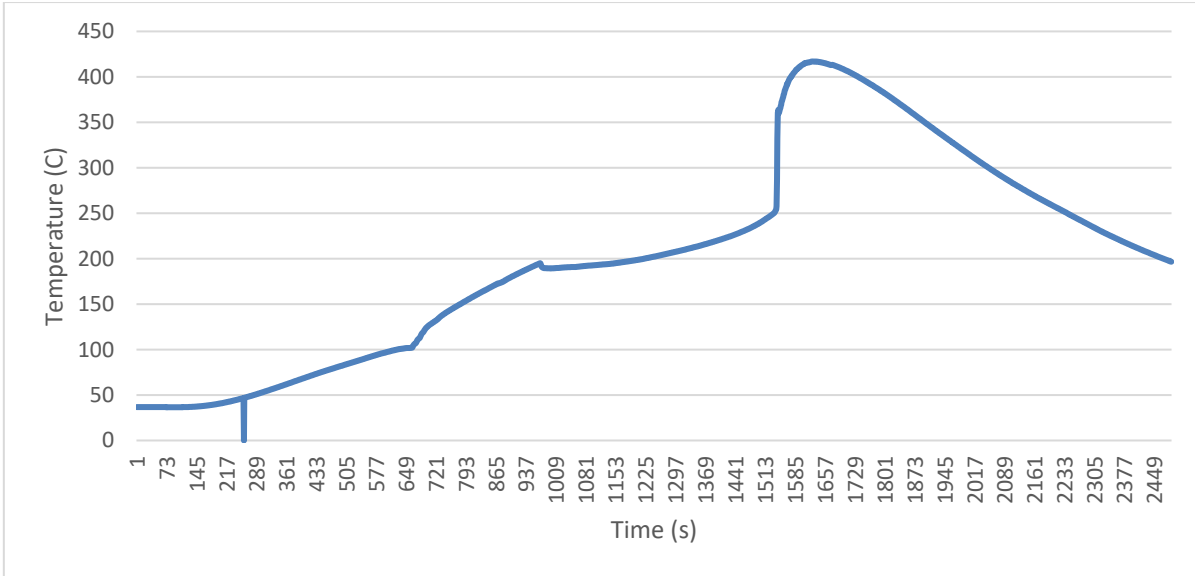
Figure 13-25 – Battery surface temperature for overheating a cell at 50% SOC distinguishes thermal runaway from other points of rising temperature
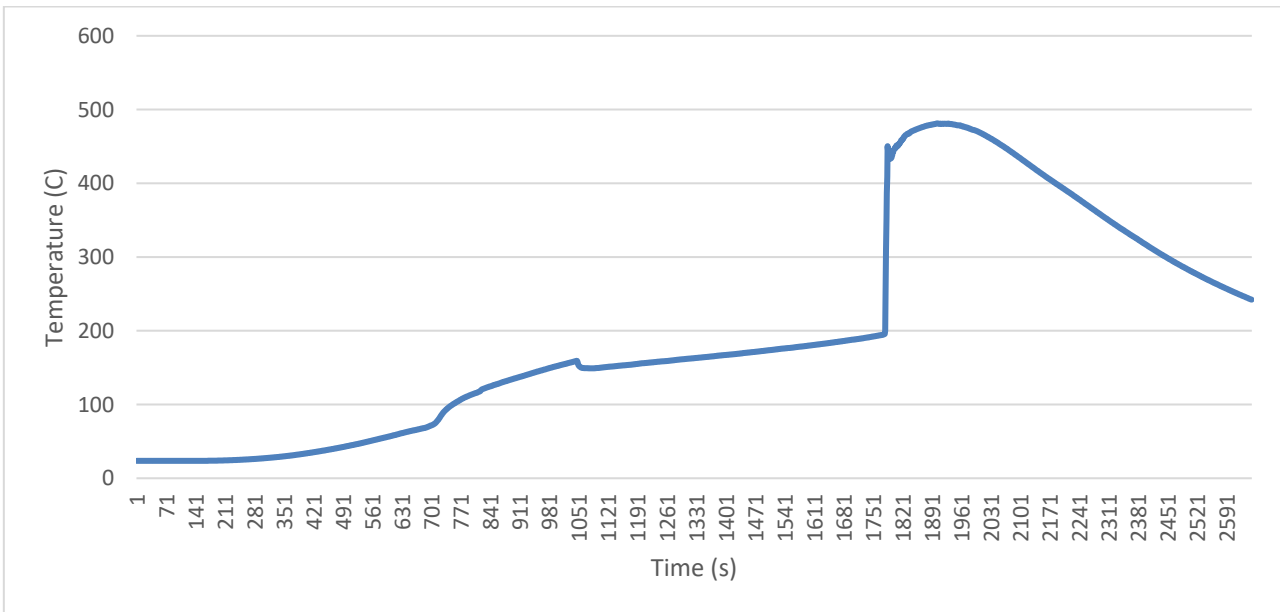
Figure 13-26 – Battery surface temperature for overheating a cell at 75% SOC distinguishes thermal runaway from other points of rising temperature
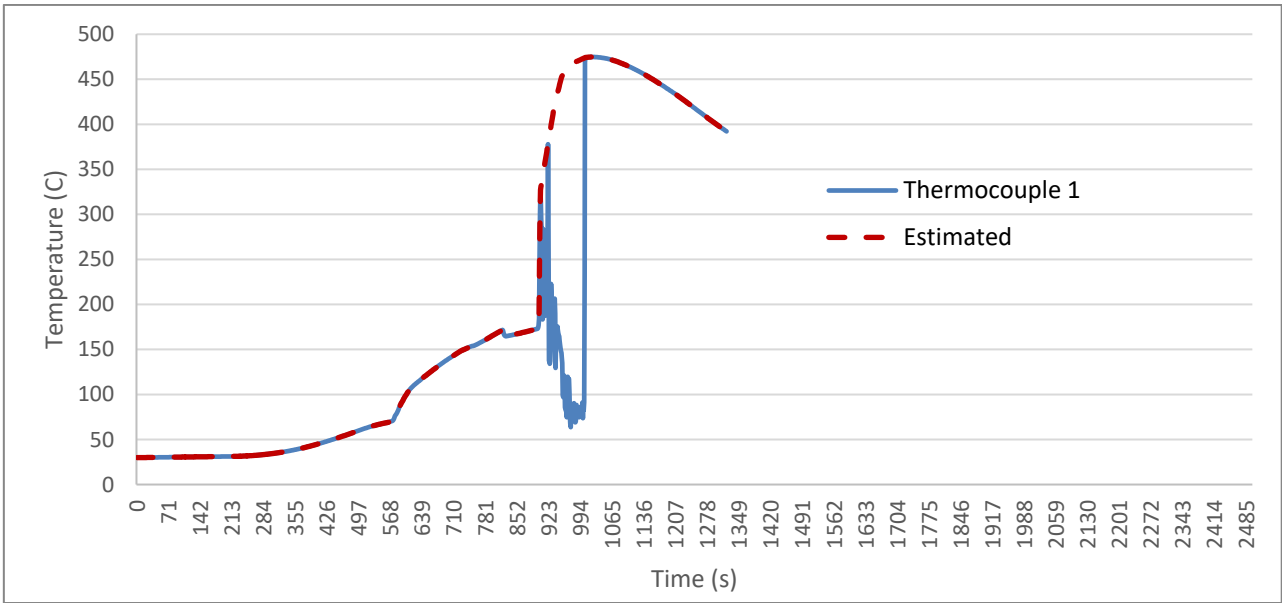
Figure 13-27 – Battery surface temperature for overheating a cell at 100% SOC distinguishes thermal runaway from other points of rising temperature
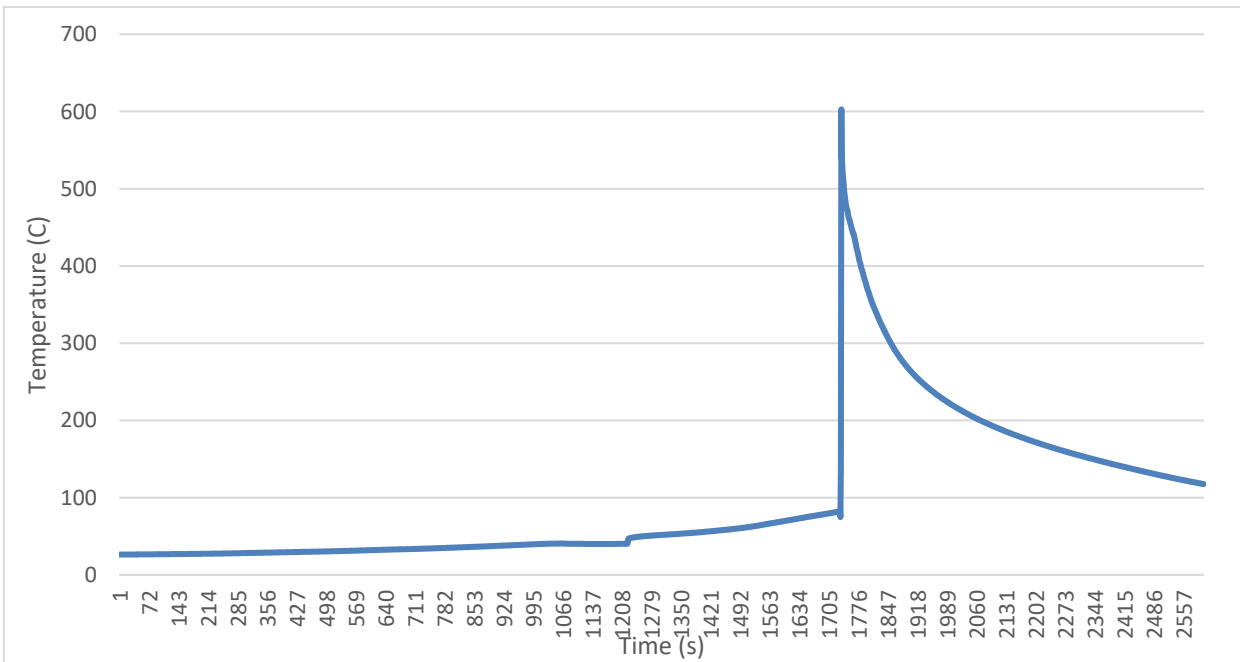
Figure 13-28 – Battery surface temperature for overcharging distinguishes thermal runaway from other points of rising temperature
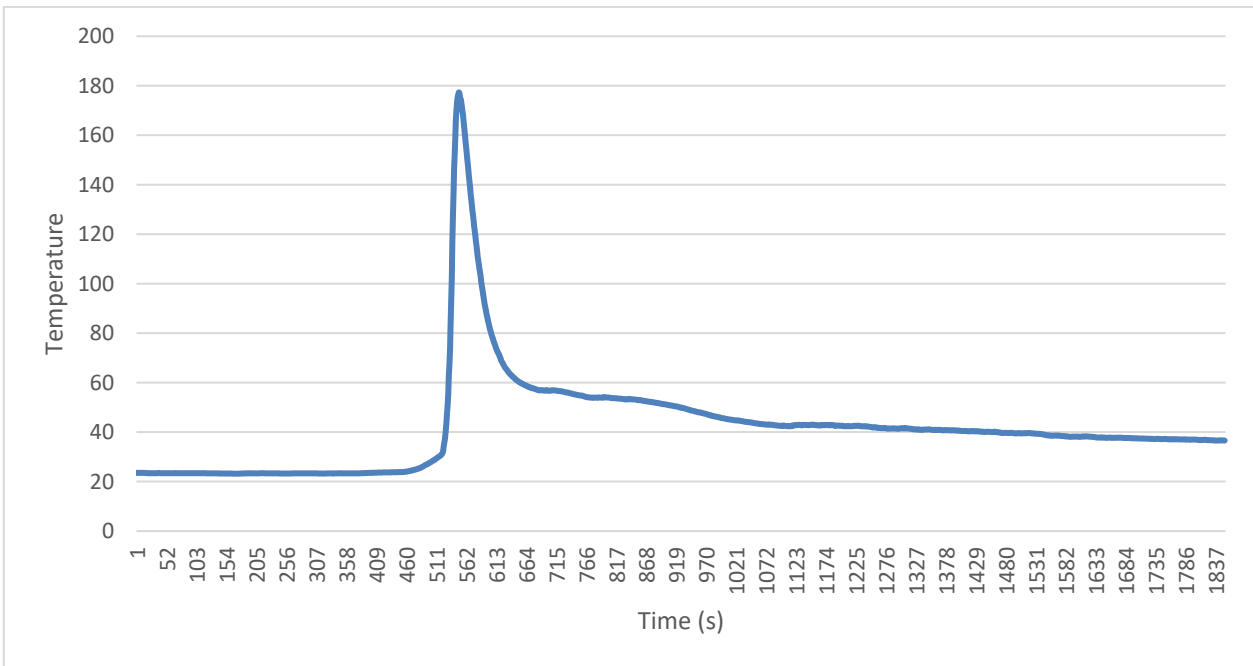
Figure 13-29 – The thermal result of an external short circuit can provide a fast temperature rise, but the rate and maximum value are not similar to other cases or considered to have entered thermal runaway

13.2.2.2 LFP 2.5 Ah

The battery surface temperatures for test A1, A2, A3 and A4 are shown in Figure 13-30 to Figure 13-33. Table 13-3 provides a summary of key data points to use for comparison. Max temperature, max temperature increase and temperature at onset is presented.

As seen from these figures, the temperature characteristics for these cells differs a lot from the NMC pouch cells in terms of max temperature and temperature rise.

For the 2.5 Ah type, the point of thermal runaway cannot be identified based at the measured surface temperature, since it has a steady growth when exposed for external heat. The temperature increase rate is also very low compared to the NMC pouch cell.

**Table 13-3 – Characteristics for identification of thermal runaway LFP 2.5 Ah cylindrical cells**

Test ID	Failure mode	Max Temp (°C)	Max Temp increase rate (°C/second)	Temperature at onset (approximate)
A1	Overheat at 50% SOC	243	0.57	Not able to identify based at temperature
A2	Overheat at 75% SOC	201	0.60	Not able to identify based at temperature
A3	Overheat at 100% SOC	170	0.14	Not able to identify based at temperature
A4	Overcharge	162	0.93	Not able to identify based at temperature
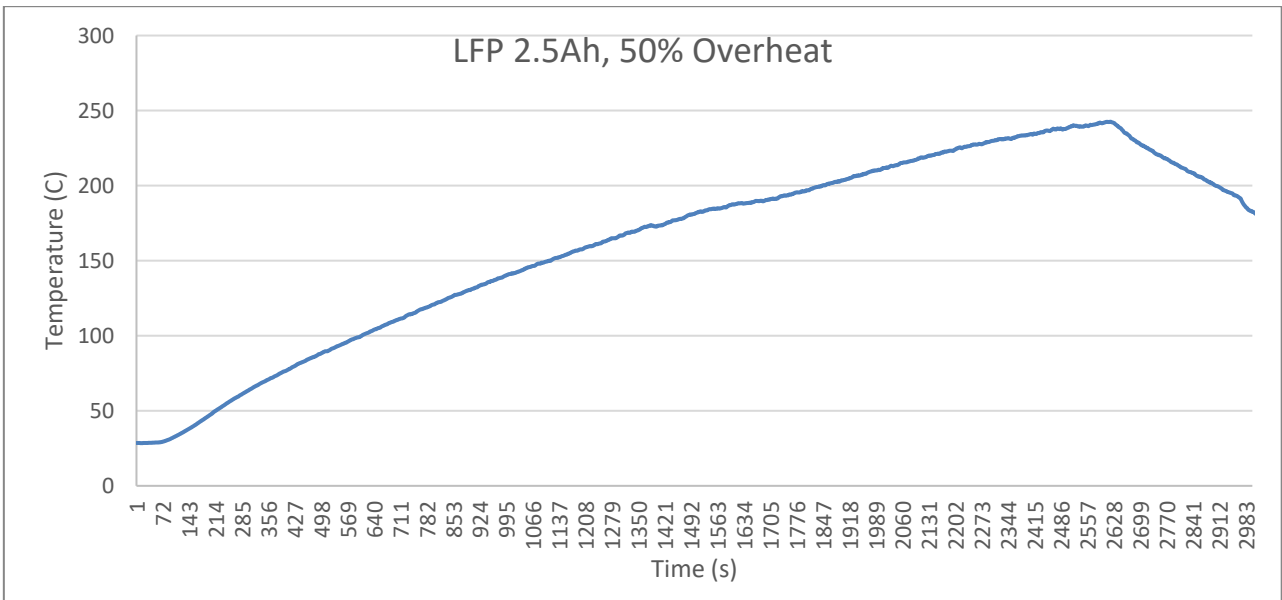
Figure 13-30: Battery surface temperature for 2.5 LFP 50% SOC with overheat
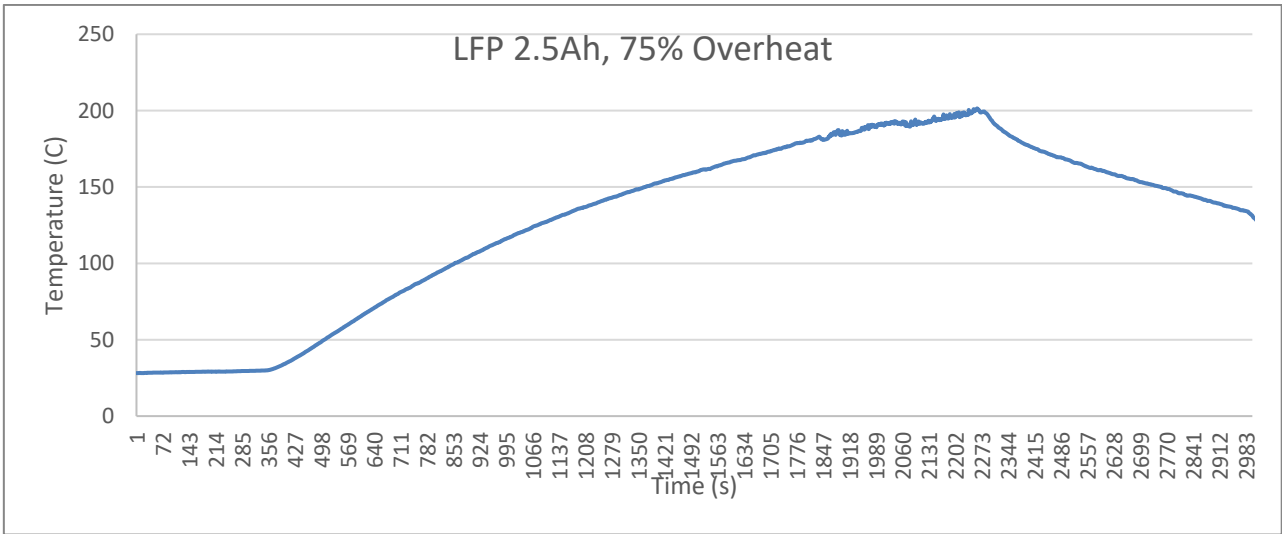
Figure 13-31: Battery surface temperature for 2.5 LFP 75% SOC with overheat
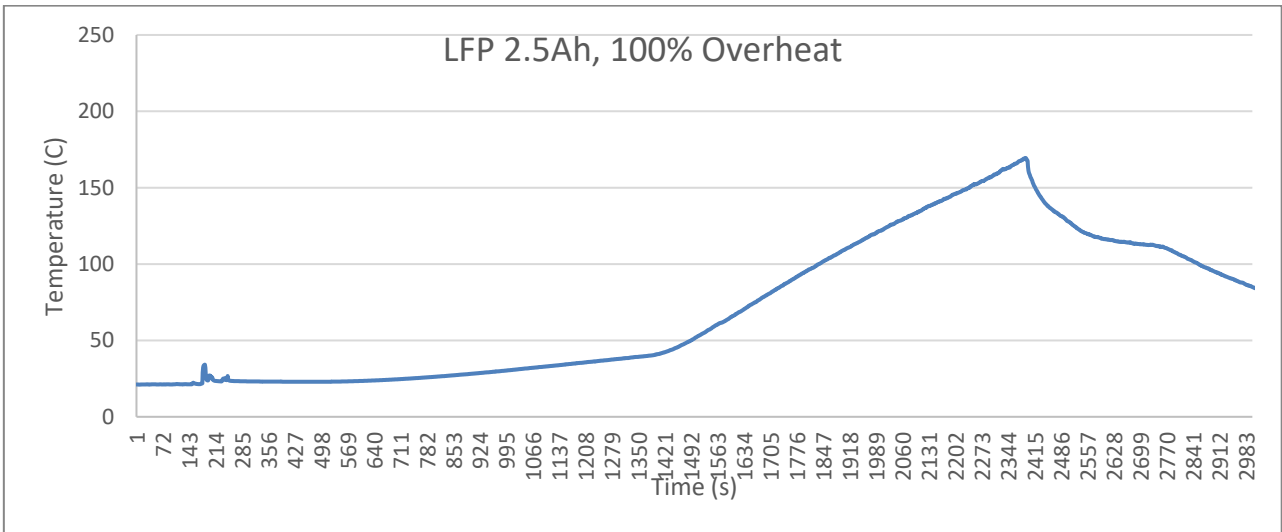
Figure 13-32: Battery surface temperature for 2.5 LFP 100% SOC with overheat
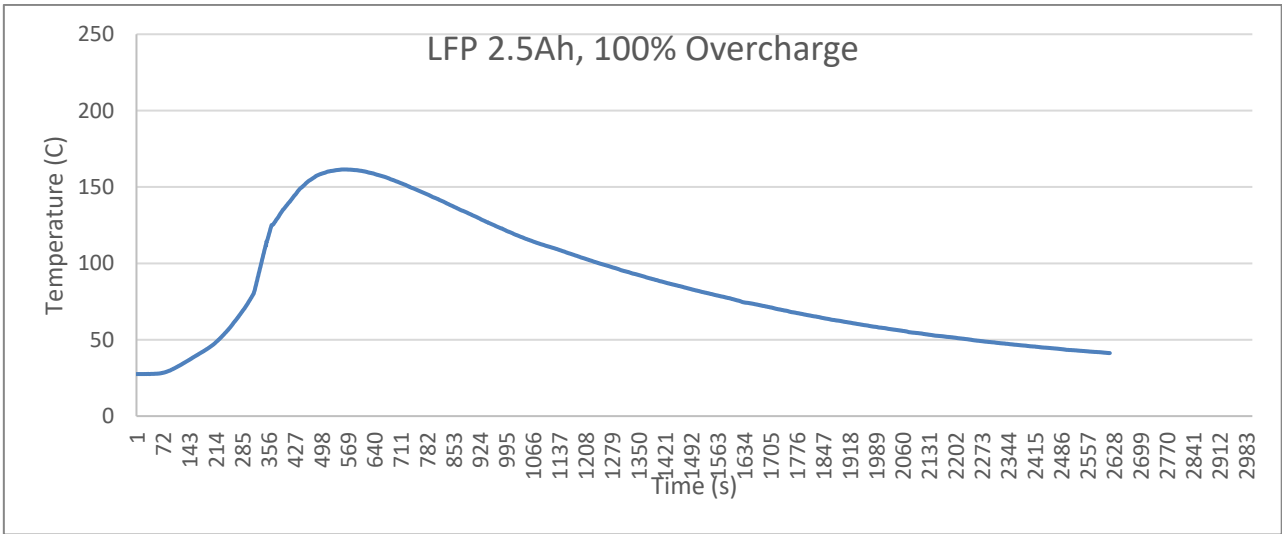
Figure 13-33: Battery surface temperature for 2.5 LFP 100% SOC with overcharge

13.2.2.3 LFP 1.5

The cell surface temperatures for test B1, B2 and B5 are presented in Figure 13-34, Figure 13-35 and Figure 13-36 respectively.

Table 13-4 provides a summary of key data points to use for comparison. Max temperature, max temperature increase and temperature at onset is presented.

Since the measurements for the overheat 100% SOC was noisy at the point where the thermal runaway appeared, an estimation of the temperature profile has been done based at two measurements.

The onset of the thermal runaway was easier to identify for the 1.5 Ah cells. Note however that the temperature increase is very low in all cases compared to the NMC pouch cells.

**Table 13-4 – Characteristics for identification of thermal runaway LFP 1.5 Ah cylindrical cells**

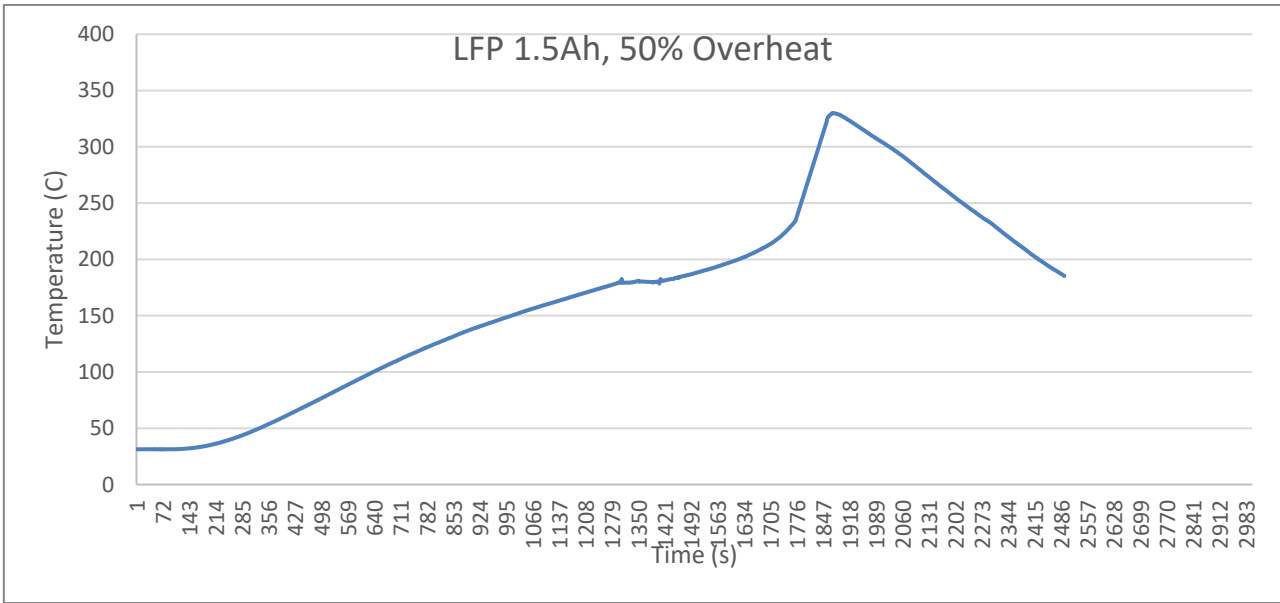| Test ID	Failure mode	Max Temp (°C)	Max Temp increase rate (°C/second)	Temperature at onset (approximate)
B1	Overheat at 50% SOC	330	0.94	220
B2	Overheat at 75% SOC	298	0.45	210
B5	Overheat at 100% SOC	384 (estimated)	5.06	225

Figure 13-34: Battery surface temperature for 1.5 LFP 50% SOC with overheat
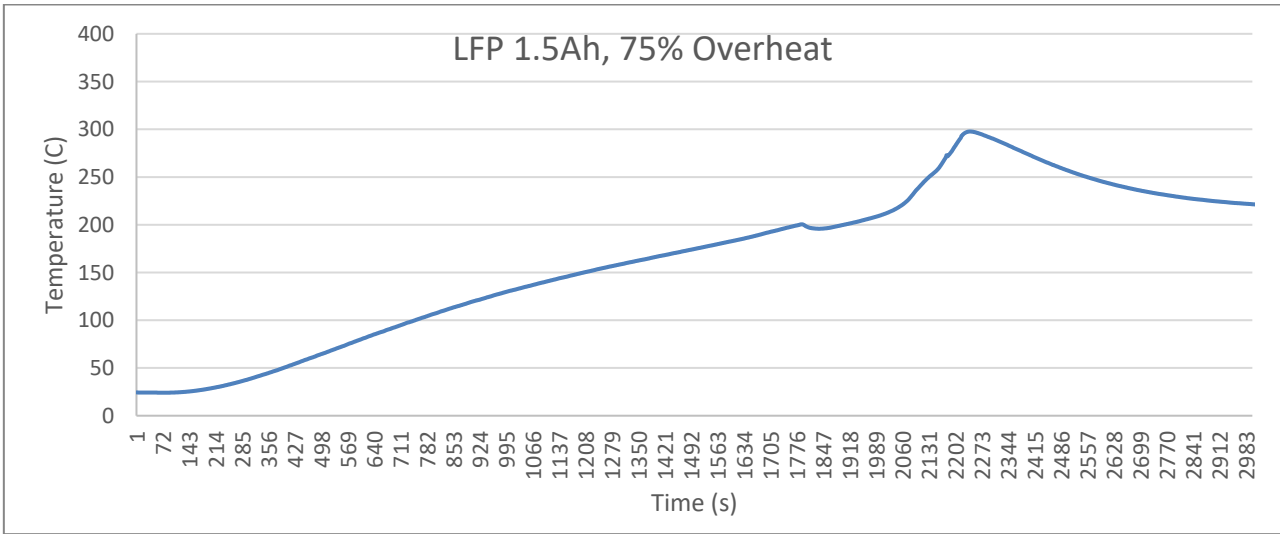
Figure 13-35: Battery surface temperature for 1.5 LFP 75% SOC with overheat
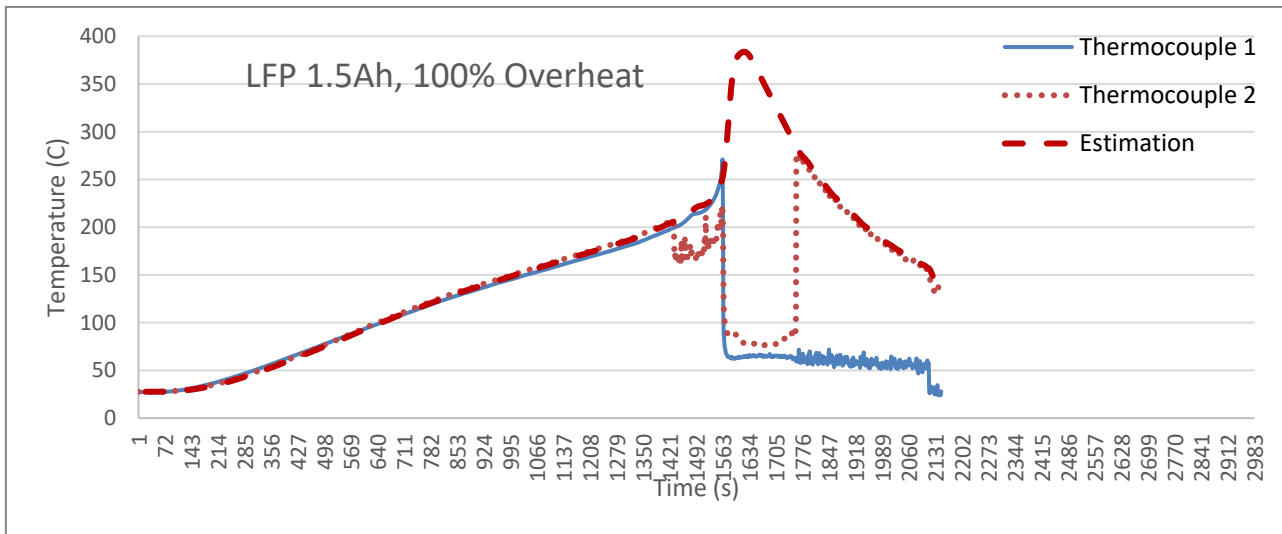
Figure 13-36: Battery surface temperature for 1.5 LFP 100% SOC with overheat

13.2.3 Discussion

13.2.3.1 Gas concentration and volume calculation

The measured gas concentration from the FTIR sensor gives a given concentration at the measurement point at a given time. To quantify the total amount of gases based at these measurements a CFD model of the test chamber has been developed as described in Chapter 13.3. Figure 13-42 show that the concentration in the measurement point and the extraction pipe is the same. To quantify the total amount of the measured gases and their total concentration during the whole off-gas period, the total volume of each gasses extracted in the extraction pipe has been calculated. It is assumed a constant volume flow of 11 L/s. Note that leakage through holes and the test chamber door has not been accounted for. Hence, the numbers presented in Table 13-5 are not exact and should only give an indication of the volume and gas contents and be compared relative to each other. The gas volumes are also normalized to 25 C based at the measured average ambient temperatures.

Table 13-5 – Off-gas values as measured in project testing – from different chemistries, heating at different SOC, overcharge (OC) and external short circuit (SC) when possible.

Value	NMC, 63Ah					LFP1, 2.5Ah				LFP2, 1.5Ah		
SOC	50	75	100	OC	SC	50	75	100	OC	50	75	100
CO2	19,6	25,7	40,3	38,8	65,9	44,3	20,2	63,4	20,9	22,5	23,0	35,1
CO	29,2	38,1	11,4	34,4	19	7,6	15,9	15,1	26,1	12,0	13,9	11,3
NO2	-	-	-	-	-	4,9	9,7	5,9	1,3	4,8	5,6	4,9
CH4 (methane)	12,6	9,4	19,4	12,5	2,7	4,3	5,6	3,0	3,7	5,9	5,9	5,6

C2H6 (ethane)	10,6	10,5	11,7	4,8	7,6	15,6	23,0	7,7	15,4	21,0	23,1	20,0
C2H4 (ethylene)	10,5	4,4	9,6	4,9	1,6	7,3	11,4	1,9	13,7	12,0	8,8	5,8
C3H8 (propane)	-	-	-	-	-	3,9	5,8	0,6	4,2	5,8	3,7	4,5
HCL	9,7	0,8	1,9	0,2	0,2	1,1	0,8	0,2	0,3	2,1	1,9	1,0
HF	0,7	0,3	0,3	0,1	0,1	1,6	1,6	0,4	0,1	1,9	3,7	3,6
HCN	0,0	0,0	0,0	0,0	0,0	0,1	0,1	0,0	0,1	0,4	0,7	0,6
C6H6 (benzene)	4,1	5,2	1,1	4,3	1,9	0,0	0,7	0,0	13,6	0,6	0,0	0,3
C7H8 (toluene)	2,0	4,1	0,3	0,5	0,9	0,0	0,0	0,2	0,0	0,1	0,5	0,7
C2H6O (ethanol)	0,3	0,7	2,9	0,1	0,0	3,7	0,4	0,5	0,0	7,0	4,6	4,0
CH4O (methanol)	0,7	0,8	1,1	0,5	0,2	5,6	4,7	0,9	0,4	3,9	4,6	2,5
Volume [L]	*527*	*182*	*233*	*245*	*180*	*9,4*	*8,4*	*27*	*19,1*	*5,5*	*6,1*	*6,5*
Average ambient temperature during Thermal Runaway [C]	*131*	*166*	*201*	*221*	*57*	*102*	*99*	*81*	*28*	*91*	*82*	*99*
Volume normalized to 25C ambient temperature [L]	*388*	*124*	*146*	*148*	*161*	*7,5*	*6,7*	*23,1*	*18,9*	*4,5*	*5,1*	*5,2*
L/Ah normalized to 25C ambient temperature	*6,2*	*2,0*	*2,3*	*2,3*	*2,6*	*3,0*	*2,7*	*9,2*	*7,6*	*3,0*	*3,4*	*3,5*

Most the tests, both the NMC pouch cells and the cylindrical LFP cells, produced about 2-3 L/Ah.

Test JDP2, where the NMC pouch cell where overheated at 50% SOC produced considerable more amount of gas compared to the other NMC tests. This could be explained by that the cell did not ignite, and visual combustion where not observed. There is for sure an incomplete internal combustion, reflected by the high amount of CO compared to CO2.

For the LFP 2.5 Ah tests, the tests with overheat and overcharge at 100% SOC produced considerable more gas compared to the tests with lower SOC. By inspecting the gas release profile presented in Chapter 13.2.1.2 it seems that this can be explained by the increased amount of CO and CO2.

The LFP tests at 50% and 75% SOC, two gas spikes are observed with some delay in between. The second spike is mainly accelerated by CO2. For higher SOC, these two spikes appear very close to each other.

13.2.3.2 Ignition and combustion

Opposed to the LFP cells, the NMC cells produces its own oxygen when the electrodes are set on fire. Since the NMC batteries show more aggressive temperature profiles and higher maximum temperatures and seems easier to ignite compared to the LFP, it can be concluded that the fire in the NMC cells are more severe and easier to ignite compared to the LFP cells. It also seems from the oxygen measurements that the NMC battery fire consumes the oxygen in the room. The produced oxygen from the NMC cells will probably contribute to CO and CO2 release rather than direct O2 emissions. Hence, the oxygen production makes the cell itself burn easier with higher temperature, but will not have a significant impact at a macro level in a battery room.

It can be seen that CO2 is released at thermal runaway, while a large amount of CO is released before thermal runaway has been released.

For the NMC cells, it is seen that the duration of the gas spike release is between 40-50 sec. For test JDP2, where it was no combustion, the aggressive release had a duration of approximately 150 seconds. The short circuit test had a release duration of 1050 seconds. It seems then that the total combustion produces higher values at shorter duration, while the total amount of gas produced, might be higher for the non-combustion case, since the duration of the gas release is longer.

13.2.3.3 Thermal runaway identification

From the temperature profiles and the key temperature data, it seems that the ability to monitor thermal runaway, will vary based on cell packaging. For cylindrical cells, packaging is often more robust and failures will thus be more delayed and then also more drastically as more temperature and pressure nominally has been built up (for instance a very quick pressure release or pop) after build up, rather than a clear thermal runaway. Further, in cases of fire and distinct thermal runaway, high temperatures are concentrated at the ends where gasses are released, often visually representing specific jet flames.

Hence no general thermal runaway identification method can be found for all the cell types tested based on temperature monitoring.

For NMC pouch cells however, a temperature increase of 10 °C/sek seems to be sufficient to identify thermal runaway for all the tested failure modes, and could be used to identify the onset point.

13.2.3.4 Flammability and explosiveness

The Lower Explosion Limit (LEL) values for each of the identified gases are presented in Table 13-6 /16/ together with the maximum observed concentration for the tests.

Table 13-6: Identified explosive gases and their Lower Explosion Limit /16/

Gas	Max % observed from cell level	LEL (%)	UEL (%)
CO	38.1%	12.5%	74.0%
CH4 (methane)	19,4%	5.0%	15.0%
C2H6 (ethane)	23,1%	3.0%	12.4%
C2H4 (ethylene)	13,7%	2.7%	36.0%
C3H8 (propane)	5,8%	2.1%	9.5%
HCN	0,7%	5.6%	40.0%
C6H6 (benzene)	13,6%	1.3%	7.9%
C7H8 (toluene)	4,1%	1.2%	7.1%
C2H6O (ethanol)	7,0%	3.3%	19.0%
CH4O (methanol)	5,6%	6.7%	36.0%
H2	30%	4.0%	75.0%

To find the LEL and UEL values for a mixture of gases, Le Chatelier's mixing rule (weighted average) is applied at all tests.

$$LFL_{Combustable\ Gas} = \frac{1}{\sum_i \frac{x_i}{LFL_i}}$$

x_i is the volume percentage of the combustible gas component. The amount of hydrogen is assumed to be 30% considering only H2, CO2, CO, CH4, C2H4 and C2H6. When these gases are presented in the literature, the H2 varies between 5-30%. Thus, the hydrogen concentration when considering the additional gases in this study is about 24-28%. The combined LEL and UEL values are presented in Table 13-7.

Table 13-7: Combined Lower Explosion Limit for the combined battery gas for all the tests performed

Test ID	Chemistry	Size (Ah)	Cell type	SOC	Failure mode	LEL combined battery gas	UEL combined battery gas
JDP1	NMC	63	Pouch	100%	Overheat	5.8%	36.4%
JDP2	NMC	63	Pouch	50%	Overheat	5.2%	36.6%
JDP3	NMC	63	Pouch	100%	Overcharging 50A	6.2%	46.9%
JDP5	NMC	63	Pouch	75%	Overheat	5.0%	35.3%
JDP7	NMC	63	Pouch	100%	Short Circuit between battery terminals	8.0%	70,3%
A1	LFP	2.5	26650	50%	Overheat	6.2%	43,6%
A2	LFP	2.5	26650	75%	Overheat	5.0%	32.8%
A3	LFP	2.5	26650	100%	Overheat	8.9%	79.3%
A4	LFP	2.5	26650	100%	Overcharge 50A	3.9%	27.6%
B1	LFP	1.5	18650	50%	Overheat	4.8%	31.4%
B2	LFP	1.5	18650	75%	Overheat	5.2%	33.3%
B5	LFP	1.5	18650	100%	Overheat	5.6%	36.3%

It is seen that the combined LEL and UEL for both all the tests are quite similar, with typical LEL values of 5-6% and UEL of around 35%. Test A4 has a low value of 3.91% due to the large amount of benzene. Hence no differentiation can be made between the cell chemistry regards LEL and UEL of the battery gas.

Note also that a low LEL value do not necessary indicate that the gas composition is better. Compositions with low LEL also gives a low UEL and a smaller window where the gas is explosive.

13.2.3.5 Toxicity

For the most part, lithium-ion batteries are not more significantly toxic than a comparable plastics fire; but there absolutely is the potential for low concentrations of more harmful gasses to be produced, which can depend on the cell being used (particularly the electrolyte formulation; Polyvinylidene Fluoride in particular can directly affect HF levels) /3/.

To give an indication of the toxicity level of the identified gasses, immediately dangerous to life or health (IDLH) values are presented in Table 13-8. These values are defined by the US National Institute for Occupational Safety and Health (NIOSH) as exposure to airborne contaminants that is "likely to cause death or immediate or delayed permanent adverse health effects or prevent escape from such an environment." Above the IDLH, only supplied air respirators should be used; below the IDLH, air purifying respirators may be used, if appropriate. The current definition has no exposure duration associated with it; workers should not be in an IDLH environment for any length of time unless they are equipped and protected to be in that environment /6/. This is used as a reference to the severity of the toxic gases identified in the tests. For general guidance on quantities of the more toxic substances that should be expected to be present, the max observed concentration and the liters of gas per Ah assuming 2.6 L/Ah is also presented.

Table 13-8 – Volumes of primary gasses of concern with regard to toxicity

Gas	Max % observed from cell level	L of specific gas per Ah (assuming 2.6 total L/Ah)	Immediately dangerous to life or health (IDLH) [ppm]
CO	38.1%	0.9906 L/Ah	1200
NO2	9.7%	0.2522 L/Ah	20
HCL	9.7%	0.2522 L/Ah	50
HF	3.7%	0.0962 L/Ah	30
HCN	0.7%	0.0182 L/Ah	50
C6H6 (benzene)	13.6%	0.3536 L/Ah	500
C7H8 (toluene)	4.1%	0.1066 L/Ah	500

Table 13-9 show the normalized IDLH values with respect to the gas concentration for the specific tests.

$$IDLH_{Normalized} = \frac{IDLH_i}{x_i}$$

where x_i is the gas concentration of the specific toxic gas. This reflects the battery gas concentration needed in the room to reach the IDLH value. It is seen that for the NMC cells, CO and HCL is the most dangerous gases, while for the LFP the IDLH value for NO2 is reached first.

Table 13-9: Concentration of battery gas needed to reach the IDLH values for the toxic gases

Cell type	SOC	CO	NO2	HCL	HF	HCN	C6H6 (benzene)	C7H8 (toluene)
NMC 63Ah	50	0,56 %	-	0,07 %	0,58 %	-	1,65 %	3,38 %
	75	0,43 %	-	0,86 %	1,37 %	-	1,32 %	1,67 %
	100	1,46 %	-	0,36 %	1,39 %	-	6,30 %	23,08 %
	OC	0,49 %	-	3,50 %	4,20 %	-	1,63 %	13,99 %
	SC	0,88 %	-	3,49 %	4,19 %	-	3,68 %	7,76 %
LFP 2.5Ah	50	2,12 %	0,05 %	0,61 %	0,25 %	6,70 %	-	-
	75	1,00 %	0,03 %	0,83 %	0,25 %	6,65 %	9,49 %	-
	100	1,10 %	0,05 %	3,45 %	1,03 %	-	-	34,45 %
	OC	0,62 %	0,21 %	2,23 %	4,01 %	6,69 %	0,49 %	-
LFP 1.5Ah	50	1,32 %	0,06 %	0,31 %	0,21 %	1,65 %	11,00 %	66,00 %
	75	1,15 %	0,05 %	0,35 %	0,11 %	0,95 %		13,30 %
	100	1,41 %	0,05 %	0,66 %	0,11 %	1,11 %	22,15 %	9,49 %

Thus, the primary recommendation is that, following a lithium-ion battery fire, there should be no re-entry without sufficient Personal Protective Equipment.

13.2.3.6 Toxicity vs Explosion risk

By comparing the normalized IDLH values and the combined LEL levels of the battery gases for all the tests, it clearly shows that a room will reach the IDLH values before the LEL values.

However, local explosive pockets of gas above LEL may appear in the room that might create lethal explosions before the IDLH values are exceeded in the part of the room where humans normally are located.

13.3 CFD Analysis based at cell level tests

The purpose is to provide greater insight and accuracy to gas data collected. The CFD simulations assisted on calculating the amount of gas coming out from the cell during the event. Further, the temperature of the released gas, and the composition is addressed. The flow behavior in the box is also compared with the video where more details of the flow is visualized from the CFD simulations.

In principle, the experiments provide physical data such as concentration and temperatures at certain given coordinates and times. Whereas the CFD model provides a full 3D understanding of the heat and fluid flow in the test chamber. By combining the results from experiments and CFD, the integrated defining parameters such as total amount of gas from the event is found. This provides a reference for release rates, and gas conditions that can be used in CFD and other models later.

13.3.1 Strategy for CFD investigation

The principle followed is to first build the geometry model with the ventilation setup that is used in the experiment. Then gas/smoke is released from the cell or battery with a best guess for the release rate

and the time development of the release. Since the main parameter to decide is the total release rate, this rate is varied in four different CFD cases while keeping all other parameters constant. When the results are obtained, they are compared with the measurements, and the cases that are closest are used to interpolate the release rate that would give a best fit. Since both the gas concentration and temperature is compared with measurements at certain location, both the total release rate and the release temperature are deduced from this assessment.

The gas composition is obtained from the measurements, although this varies during the experiment, it is found an averaged composition that is recorded during the most violent part of the release.

13.3.2 General release scenario

The event from the onset of the most violent part of the release until it reaches a neglectable amount is modelled. The small initial release that is seen as some smoke coming from the cell is not modelled. The smaller off-gassing that happens prior and after the violent eruption is hence neglected. Measurements also indicate that this amount of gas is relatively small and would not contribute to the risk due to being below ignitable concentrations.

The release can be defined by the following parameters where the ranges of the typical parameter values is also indicated:

- Release profile, release rate (kg/s) given as a function of time, typically a function that rises quickly (over 2-10 s) to a maximum release rate, and then it decays linearly or exponentially to zero. The rupture of the cell poach is a typical event that causes this profile shape.

- Total volume or mass of gasses released during off-gassing scenario. Typically, 2 l/Ah has been a "rule of thumb" in the industry. This amount is varied from 1 to 3 l/Ah in the simulations. Note that it is only the most violent part of the off-gassing scenario that is assumed to create this amount of gas.

- Maximum release rate typically, 0.001 to 0.01 kg/s.

- Duration of simulated, violent part of the release. Release duration as simulated is from 10 to 30 seconds, typically.

- Temperature of the release, assumed typically from 500 C or 800 C for non-combusting to combusting gases. Different temperatures in this range is applied in the simulations.

- Composition of the release is given below based on measurements.

- Typical density of the released gas from 0.3 to 0.5 kg/m3.

13.3.3 Model description

A CFD model is made of the internals of the test box including the fan piping, and the fan. The geometry configuration, dimensions and fan flow rate were modelled as per description in test setup at section 13.1.

Figure 13-37 shows in 3D view the model of the chamber that was built and used for the CFD analysis. Initial circulation of air is established with air flowing out from the 3-inch pipe at the top and air flowing in the chamber from the eight 1" holes in the bottom.
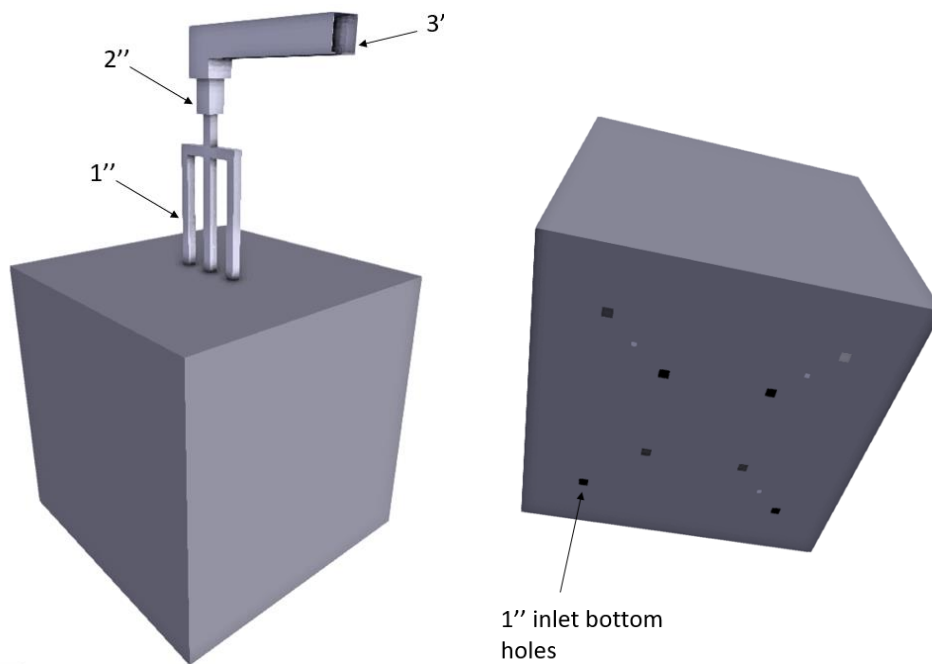
Figure 13-37: Snapshot of the 3D model of the chamber as it was used for the cell CFD simulations.
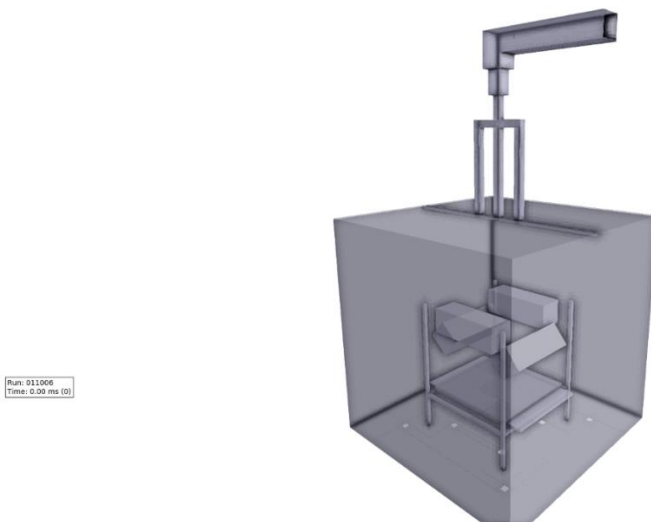
Figure 13-38: Snapshot of the 3D model of the chamber with internal configuration of the cell, support structure and heaters.

13.3.3.1 Domain, grid and gas source

The simulation domain is limited to the interior of the chamber, with constant pressure boundary conditions on all sides. The grid consists of uniform, cubical 1 cm control volumes throughout the entire domain (illustrated in Figure 13-39).
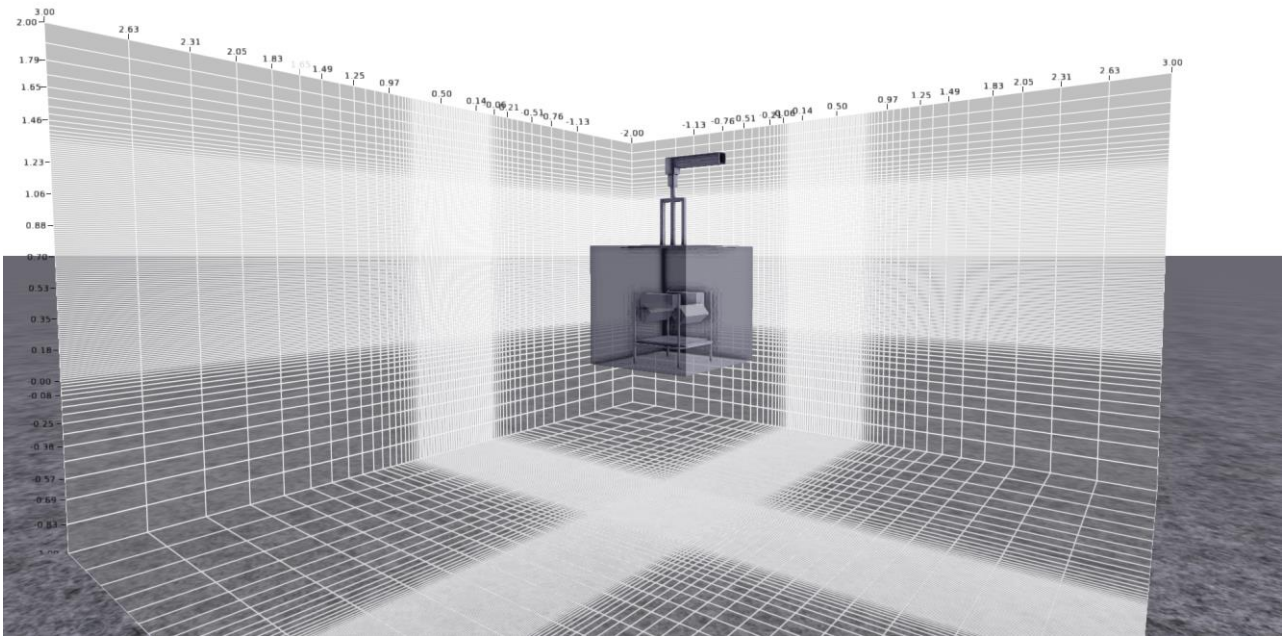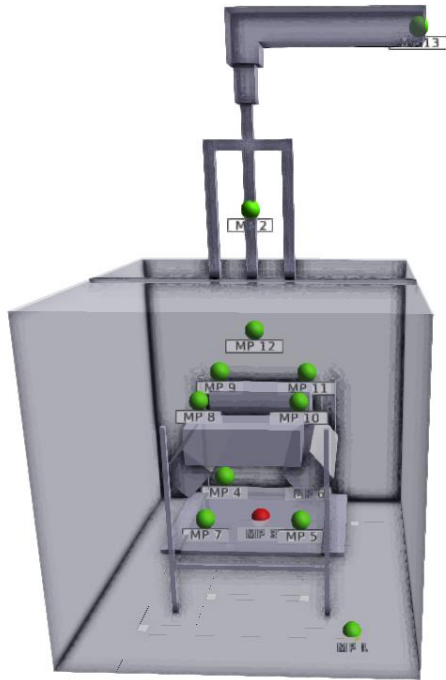
Figure 13-39: Illustration of the monitor points location (top) and the uniform grid domain (bottom).

**Table 13-10   Case definitions CFD cases cell level tests.**

FLACS Case no	Total release during scenario (l/Ah)	Maximum release rate (kg/s)	Release duration (s)	Release temperature HIS	Comment
011007	1	0.0023	30	527	Profile shape Figure 13-40
011017	2	0.0047	30	527	
011027	3	0.007	30	527	
011007	1	0.0023	30	727	
011017	2	0.0047	30	727	
011027	3	0.007	30	727	

13.3.4 Results

### 13.3.4.1 Initial cases result

The first set of cases is run with the best guess release conditions and gas definitions.

Parameters that are varied are release rate and release temperature. The release rate is defined from the total gas release of 1, 2, and 3 l/Ah. The release temperature is 527C and 727C. In total this is 6 cases.
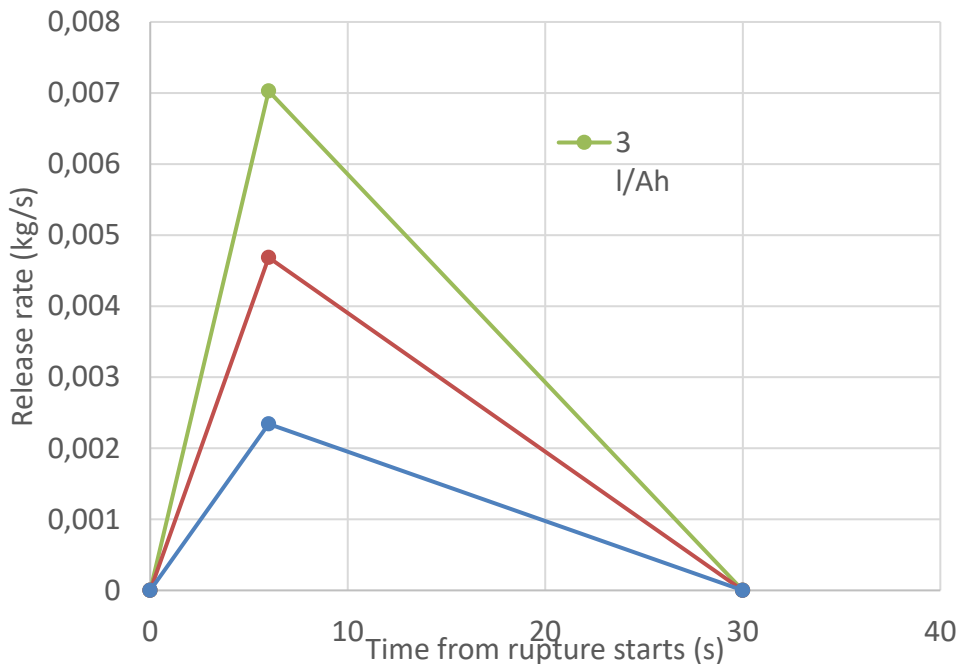
Figure 13-40   Release profiles for the initial release cases.

CFD shows that outlet composition/concentration is nearly identical to mixture at FTIR data collection point (See Figure 13-41).
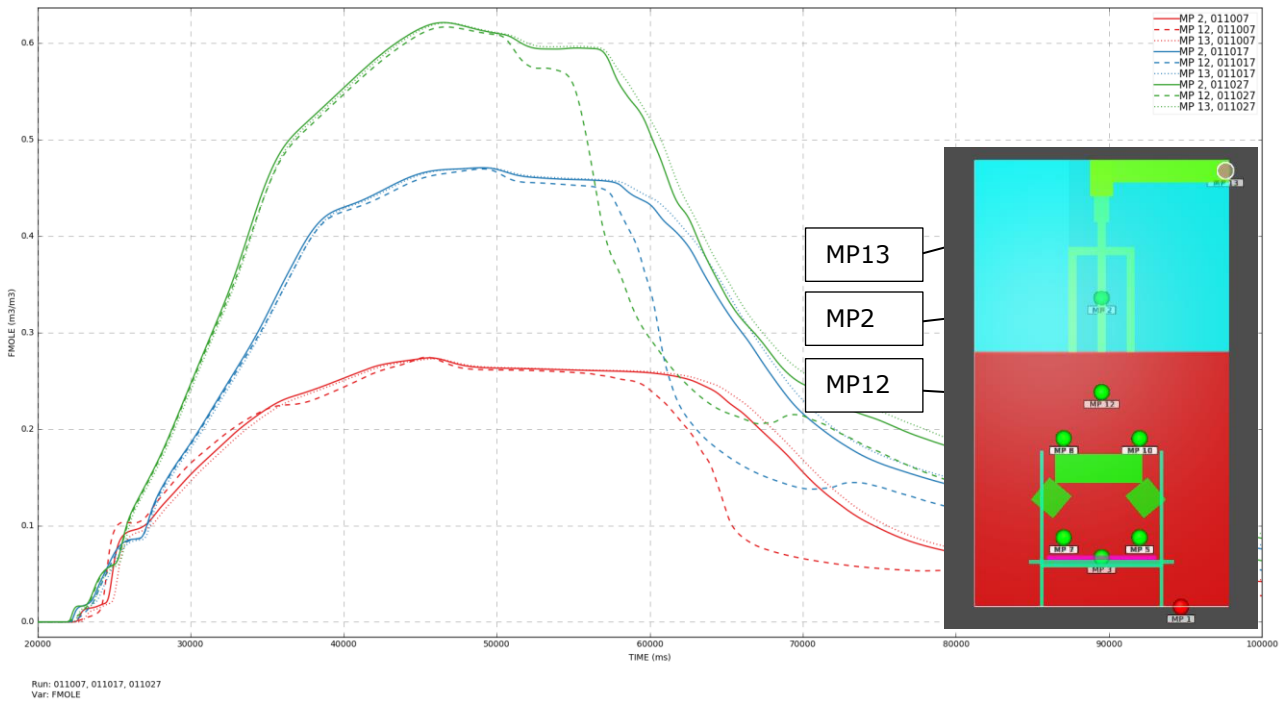

Figure 13-41: Time series of percentage of gas in three different monitor points (MP2, MP12, MP 13) for the three different cases (line type (dashed , solid etc.) defines which monitor point is shown whereas color indicates the three different release rate cases).
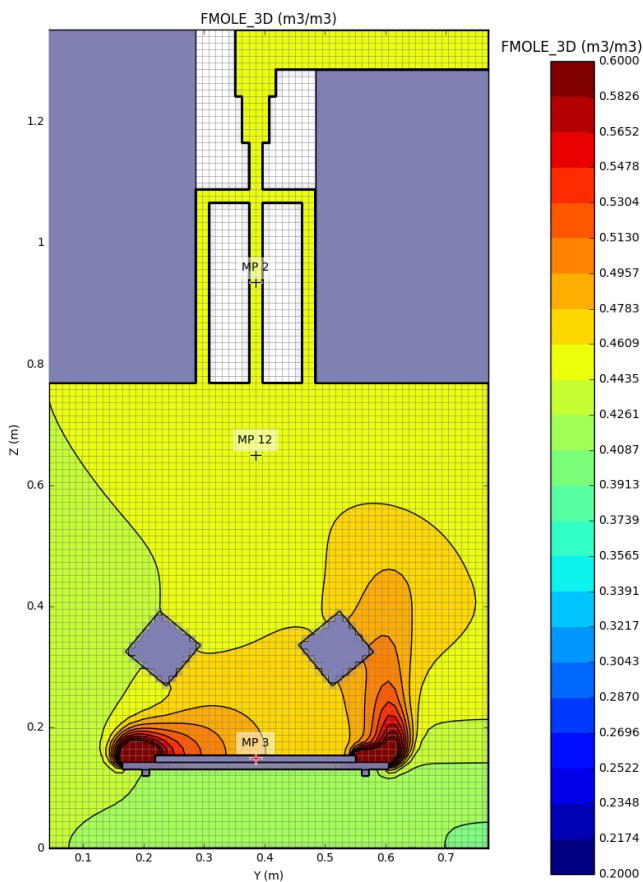
Figure 13-42: 2D contour of concertation in the box and the pipe outlet.

CFD also showed that the temperature in the box and at the outlet is the same for any case that was simulated (Figure 13-43).

Run: 011007, 011017, 011027
Var: T
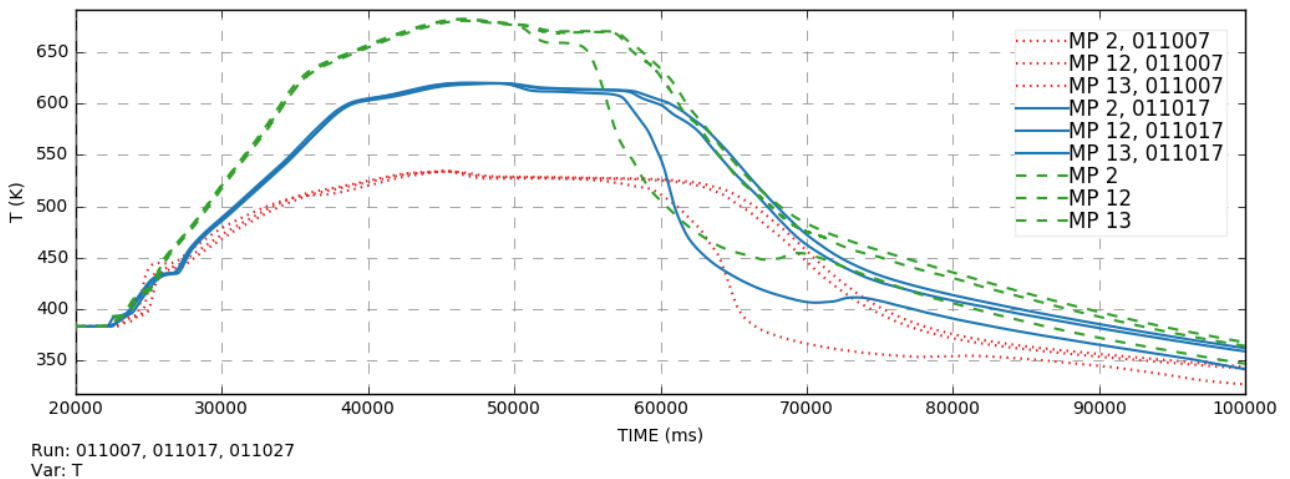
Figure 13-43: Time series of the temperature development in three different monitor points (2 at the middle 1" pipe, 12 at the middle of the box above the cell, 13 at the outlet at the fan)

CFD also shows us the approximate volume flowing out of chamber (calibrated to temperature aka relative air flows confident). However, it also shows that depending on the release profile (1, 2 or 3 l/Ah)

there is gas leaking out from the bottom holes. In this phase of the modelling work and based on the input information from the measurements, the exact amount that leaked is uncertain. The influence that the amount of leaked gas can have on the total amount of gas produced from the battery can be significant. Therefore, one should account for this parameter when similar tests are executed in the future.

When simulations with different release rates are compared and calibrated to temperature measurements, we get good fit, assuming approximately 350 deg C with the 3l/Ah case. Concentrations of gasses can be significantly lower than what is estimated from the measured data. Noting that the measured gas concentration is uncertain due to the unknown amounts of hydrogen from the measurements.

13.4 Results summary

Modelling of the off-gassing phenomenon at cell level in order to reproduce the test executed in the experimental campaign proved to be rather challenging. Several assumptions and simplifications were needed in order to achieve an accurate model.

On the other hand, CFD provided important insight on the likely conditions in the box in areas further than the few monitor points that were used in the experiments. This information was the basis and was proven invaluable in order to estimate the released gas volumes at the outlet from the fan.

In short, CFD showed that:

- It is valid one to assume that the concentration of the gas measured at the Gasmet DX4000 Fourier transform infrared spectroscopy (FTIR) gas analyser is the same as the one at the very end outlet after the fan.

- The temperature is the same at the monitor point in the box and at the outlet.

- Depending on the leak release profile different amount of gas leaks off the bottom holes of the chamber.

14 MODULE LEVEL TEST RESULTS

Evaluation of battery system failure scenarios at the module or rack level introduces a significant number of additional aspects of the battery fire. Full scale failure testing of lithium-ion batteries produces significant and non-linear departures from evaluations at the cell level. These deviations depend on many different aspects of system level design – packaging, sealing, enclosure, cooling, ventilation, volume, thermal mass.

The main objective of module scale testing was to evaluate effects of different fire suppression materials in an arrangement representative of an actual battery installation. Secondarily it was to produce data that could be used to inform and calibrate CFD models with regard to ventilation assessments.

14.1 Test setup

Module scale test setup was built to mimic actual rack installations in a generalized manner. Thus, a rack configuration was constructed similar to many systems, as shown in Figure 14-1. Cells were placed inside each module, totaling approximately 1.3 kWh for all tests as shown in Figure 14-2.

Figure 14-1 – Steel rack and drywall used to simulate battery enclosure spaces and arrangements.

Figure 14-2 – Fully outfitted battery test room within a 20' container.

Resistive AC heaters were placed between cells which were then banded together. Materials were also used to represent a minimal amount of packaging – aluminum in the case of NMC pouch cells shown in Figure 14-3, and some plastics in the case of LFP cylindrical cells shown in Figure 14-4. This approach was intended to be worst case, to maximize likelihood that the cells would propagate and combust all cells in the ion modules were constructed in order to represent a worst-case design.

Figure 14-3 – How (NMC pouch) cells were packaged for testing – aluminum plating and stainless steel bands with resistive heaters placed in-between.

Figure 14-4 – How (LFP cylindrical) cells where packaged for testing.

Modules were mild steel boxes of 0.5 mm thickness, measuring 500 mm x 300 mm x 200 mm; shown in Figure 14-5. Boxes were drilled for a plastic wire pass-through gland. This was the configuration used for 'IP4X' boxes. In addition, boxes were drill with 6 ½" diameter holes on both the front and rear (top and bottom as in picture below), this was the configuration used for 'IP2X' boxes.


Figure 14-5 – Mild steel electrical boxes used to simulate battery module enclosures for testing.

Tests were conducted in a standard 20-foot container as shown in Figure 14-6, with a partition built in the center, such that the effective test volume was 10' x 8' x 8.5'; or 680 ft3 or 19.25 m3.

Figure 14-6 – Large scale test facility located in Piqua, OH and fire service staff.

To monitor the temperature in the failed module, the neighboring dummy modules and the room itself, thermocouples where placed at different locations in the test room as shown in Figure 14-7. The black symbols are thermocouples monitoring the battery module temperatures, and the battery cell surface temperature itself, while the blue symbols are thermocouples used to monitor the thermal gradient temperatures.
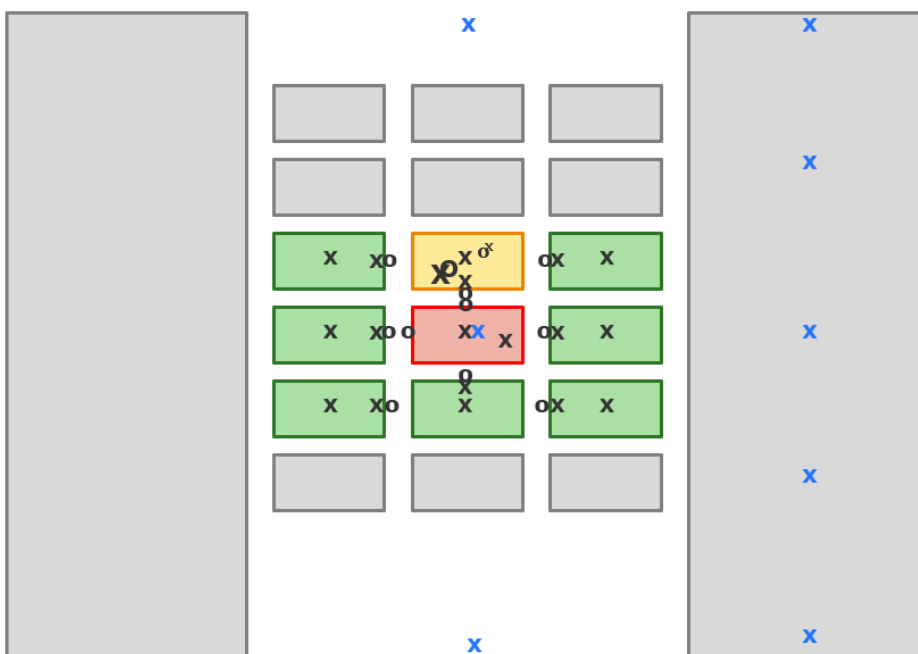
Figure 14-7 – Placement of thermocouples for all module testing – black 'x' internal to modules, black 'o' external to modules, blue 'x' indicating ambient room thermal gradient temperatures.

To measure the amount of gas in the battery room, a LEL sensor is used. This sensor records the LEL% as shown in the formula below.

$$LEL\% = \frac{Gas\ Consentration\ in\ Room\ [vol\%]}{LEL\ for\ Gas\ [vol\%]}$$

In addition, an off-gas specific sensor called the Li-ion Tamer® developed by Nexceris and a smoke detector was installed.

Fans was installed to create 6 ACH (Air Changes per Hour) and 30 ACH.

14.1.1 Test variations

Testing covered combinations of multiple variables. Key variations of test setups:

Module enclosure sealing	Battery cells used	Ventilation	Fire suppression materials
IP4X	NMC pouch cell 63 Ah	0 ACH	None
IP2X	LFP 18650 cell 1.5 Ah	6 ACH	Sprinklers
Open lid		30 ACH	Hi-Fog
			Novec
			FIFI4Marine CAFS
			Water injection (direct to modules)

Testing all the combinations of the listed variations was not practical possible. A critical selection was made prioritized to testing the fire suppression and the ventilation effectiveness. The test performed with the associated variations are listed in

Table 14-1: Module tests performed with the different variations

Test ID	IP Rating of box	Battery	Ventilation	Suppression	Container status	Combustion	Comment
1	44	NMC pouch	No ventilation	n/a	sealed	Yes	-
3	20	NMC pouch	No ventilation	Novec	sealed	Yes	-
4	44	LFP 18650	No ventilation	n/a	sealed	no	-
6	44	LFP 18650	No ventilation	n/a	sealed	Partial	-
7	44	NMC pouch	No ventilation	FiFi4Marine	sealed	Yes	-
8	20	NMC pouch	No ventilation	n/a	sealed	Yes	-
9	20	NMC pouch	No ventilation	Hi-Fog	sealed	Yes	-
10	44	NMC pouch	No ventilation	Hi-Fog	sealed	Yes	-
11	44	NMC pouch	No ventilation	Hi-Fog	vents open	Yes	-
12	44	NMC pouch	No ventilation	Sprinklers	sealed	2 cells vented	-
13	44	NMC pouch	No ventilation	Sprinklers	Sealed	Failed, Delayed	-

14	20	NMC pouch	No ventilation	Sprinklers	Sealed	Insufficient	-
15	Open lid	NMC pouch	No ventilation	Sprinklers	vents open	Yes	-
16	Open lid	NMC pouch	No ventilation	Hi-Fog	vents open	Yes	-
17	44	NMC pouch	No ventilation	Direct Water	sealed	Yes	-
18	20	LFP 18650	6 ACH Positive low side	n/a	high open, low partial closed	Partial, Sufficient	Ventilation ineffective. Ventilation failed to overpower smoke in room, which was escaping even from the low side around the fan due to pressure. Gas Data available
20	Open lid	NMC pouch	6 ACH Negative high side	n/a	low open, high partial w/ fan	Yes	Ventilation ineffective.
21	Open lid	NMC pouch	30 ACH, negative	n/a	low open, high partial w/ fan	Yes	Accidently pointed positive for initial burst. Drastically increased flame intensity until turned.
22	20ish	LFP 18650	30 ACH, negative	n/a	low open, high partial w/ fan	Partial	-

14.2 Module Scale Test Findings

This section presents results and findings of the module scale testing grouped into evaluations that provide indications and reference on key technical questions and comparisons.

14.2.1 Effect of battery module enclosure and sealing

As shown with regard to cell level testing gas data contents and quantities, a lithium-ion battery failure demonstrates significantly different properties based on whether the gas is ignited or not, and particularly whether it continues to combust. Module tests were performed specifically to evaluate this behavior.

Availability of oxygen is a key factor with regard to combustion behaviors. Though many academic studies will reference the fact that lithium ion cathodes of the layered metal oxide variety (NMC, LCO, etc) will produce oxygen as they fail and this produces a potential source. However, as we see in actual tests, a lithium ion battery fire is so fuel rich it will tend to consume every molecule of available oxygen. In many cases, as shown in the testing below and in testing performed by other JDP project partners, the fire consumes all of the oxygen and will thus extinguish itself. This leaves a highly gaseous and dangerous mixture that requires extreme caution and attention with regard to handling, but it is very often that gassing and even propagation can continue once the fire is extinguished. This is highly dependent on heat levels. Ignition of the gasses is a key uncertainty but is directly related to heat, and this can equally apply to re-ignition of gasses – for instance, once gas release tapers off and oxygen is reintroduced.

Characterizing the main differences at the system level – such as gasses in the room and heat in the modules – between combustion compared to non-combustion was a desired outcome from the testing.

Comparison of these two phenomena is enabled by testing with an IP2X module which allows more gas & oxygen flow in and out of the module and a IP4X module which is much more enclosed. The main observations are summarized in Table 14-2 and Table 14-3. The temperature profile and the LEL% value for the IP2X module is shown in Figure 14-8, and Figure 14-10 for the IP4X test.

For additional context, additional tests were conducted with both IP2X and IP4X modules where combustion was not witnessed. In most cases a cell goes into thermal runaway, combusts quickly, nominally consuming all of the oxygen available, and then the fire goes out and the cell continues to off-gas and neighboring cells then fail and off-gas without subsequent combustion.

Table 14-2 – Summary of frequency with which module tests combusted external to module, consuming gasses.

Module Enclosure	IP4X	IP2X	Open Lid
Percentage of Tests with External Combustion	0	60%	80%

NOTE: the IP2X test indicated also consisted of a NOVEC release approximately 30 seconds after the identification of the fire.

Table 14-3 – Summary of key parameters differentiating tests with external combustion vs not.

| Test ID	Cells	Enclosure	External Combustion	Max LEL%	Time to LEL% (s)	Max Internal Temp Module above	Max External Temp Module above
1	NMC Pouch	IP44	No	69%	120	29	92
3	NMC Pouch	IP20	Yes	26%	500	152	252

The results presented in Table 14-3 show that Test 3 with external combustion produced significant less gas compared to Test 1 with no external combustion. The cell level tests presented in chapter 13.2 also supports this observation.

Dealing with battery fires, an evaluation must be made whether the space should be sealed or ventilated. If it is sealed the fire temperature is limited and the explosion risk increases with increased off-gassing. If the ventilation is running, keeping the room atmosphere below the LEL limit, the fire temperature will be higher.

The tests clearly show that limiting the oxygen to the fire will reduce the module heat, while the off-gassing and hence the explosion risk increases. This also indicate that if the ventilation is closed, the

heat will eventually go down when the oxygen is consumed, while the off-gassing will increase. This is an important finding when evaluating the explosion risk of the room.

Fire propagation is extremely unpredictable and variable. Even in the tests performed with identical setups, designed with the intention and maximum probability to propagate, it was inconsistent. For one this speaks to the importance of repeated testing. Secondarily this speaks to the relative difficulty of getting lithium-ion cells to propagate.
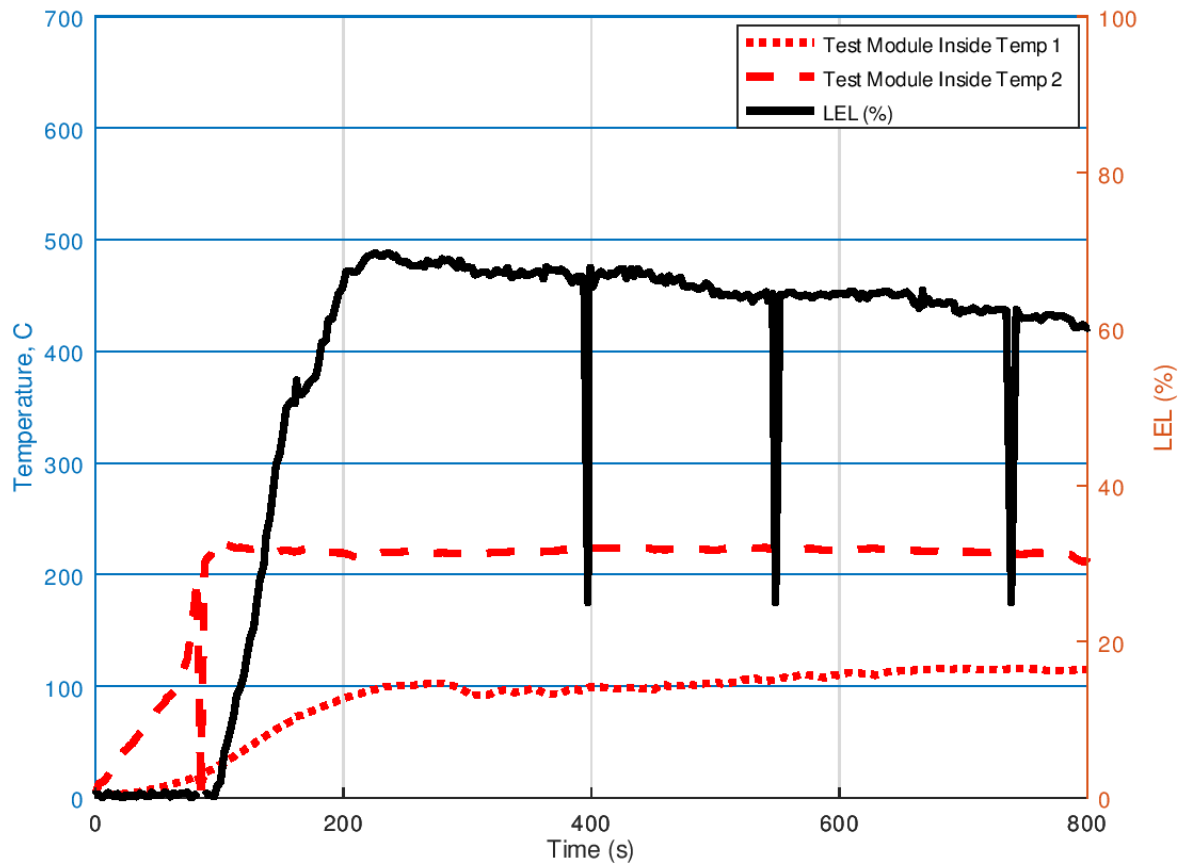
Figure 14-8 – Results showing low internal temperatures and high LEL% accumulation without combustion of gasses for an IP44 module test.

Figure 14-9 – Video illustrates the gasses accumulated without external combustion – 30 seconds after initiation; from test data shown in Figure 14-8.
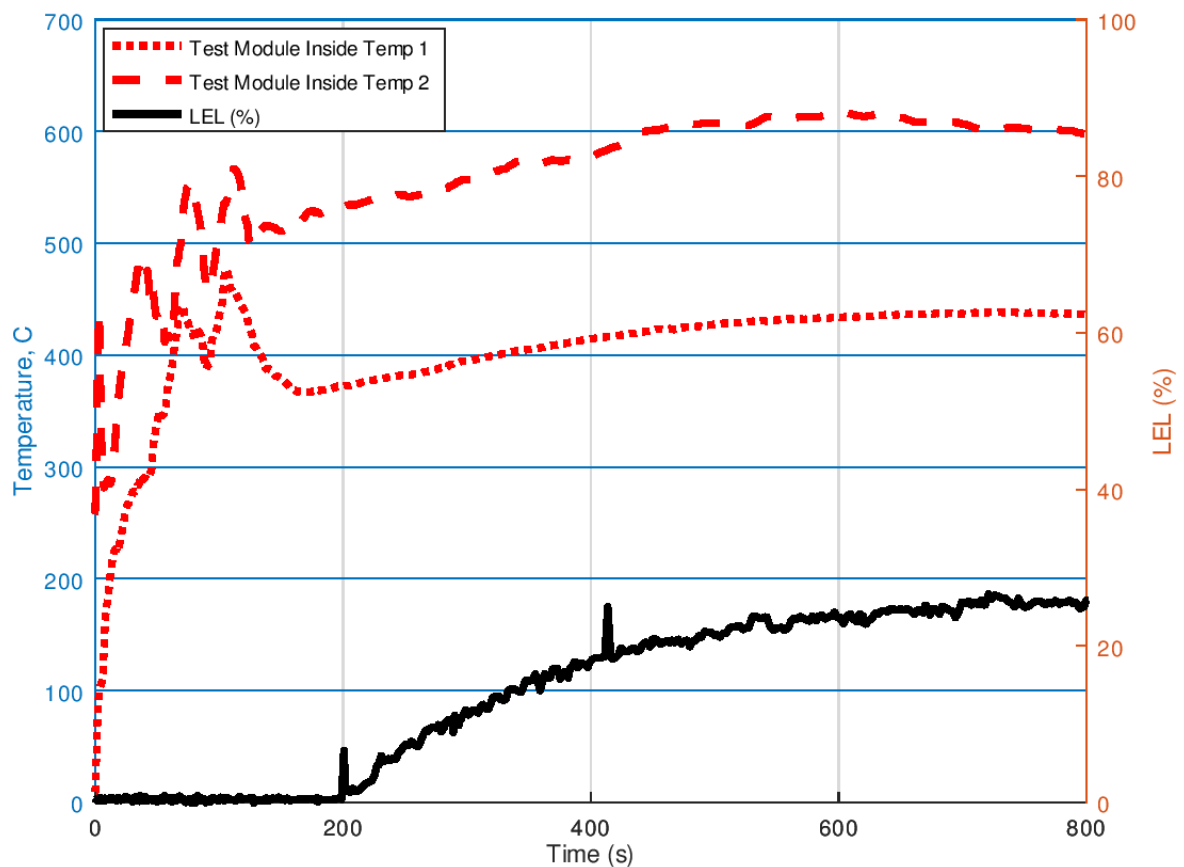
Figure 14-10 – Results showing high internal temps and low LEL% accumulation with combustion of gasses for an IP2X module test.

Figure 14-11 – Video illustrates the lack of gasses accumulated with external combustion – 30 seconds after initiation; from test data shown in Figure 14-10.

14.2.2 Gas detection

The performance of the Li-ion Tamer® gas detector and the smoke detector is shown for Test 1, Test 3, Test 7 and Test 9 in Figure 14-12, Figure 14-13, Figure 14-15 and Figure 14-14 respectively. The temperatures inside the test boxes are also shown, to give an indication when in the thermal runaway process the gas is detected. The key properties of the tests are shown in Table 14-4. The sensors were placed on the module above the device under test for this measurement, thus nominally giving a 'best case' capability evaluation.

Table 14-4: Key properties of gas detector tests

| Test ID	IP Rating of box	Combustion	Visual external Combustion	Time difference between Li-ion Tamer® and Smoke detector	Max temperature inside the test box before detection
1	44	Yes	No	22 sec	16°C
3	20	Yes	Yes	9 sec	290°C
7	44	Yes	No	21 sec	173°C
9	20	Yes	Yes	44 sec	440°C

The tests with IP 44 boxes, without external combustion, produces more gas than the tests with IP 20 boxes with external combustion. It can be seen from the figures that both the smoke detector and Li-ion Tamer® can detect the gas for cases with and without external combustion. The Li-ion Tamer® detects the gas first in all tests, 10-45 seconds faster than the smoke detector.

However, the temperatures inside the boxes exceeded 170°C for three of the four tests before the gas was detected. This indicates that the batteries have entered thermal runaway before the gas is detected. Compared with the cell level tests, where the sensors were placed in the same enclosure as the battery cells, the gas is detected much later when the sensors are placed outside the modules. Hence, for early detection, the placement of the sensor is a key factor for early detection, and the sensor should be placed as near the battery as possible, ideally within the module enclosure.

It can be concluded that both the gas sensors are capable of detecting the battery gas. The placement of the sensor is a key factor for early detection, and the sensor should be placed as near the battery as possible, ideally within the module enclosure.
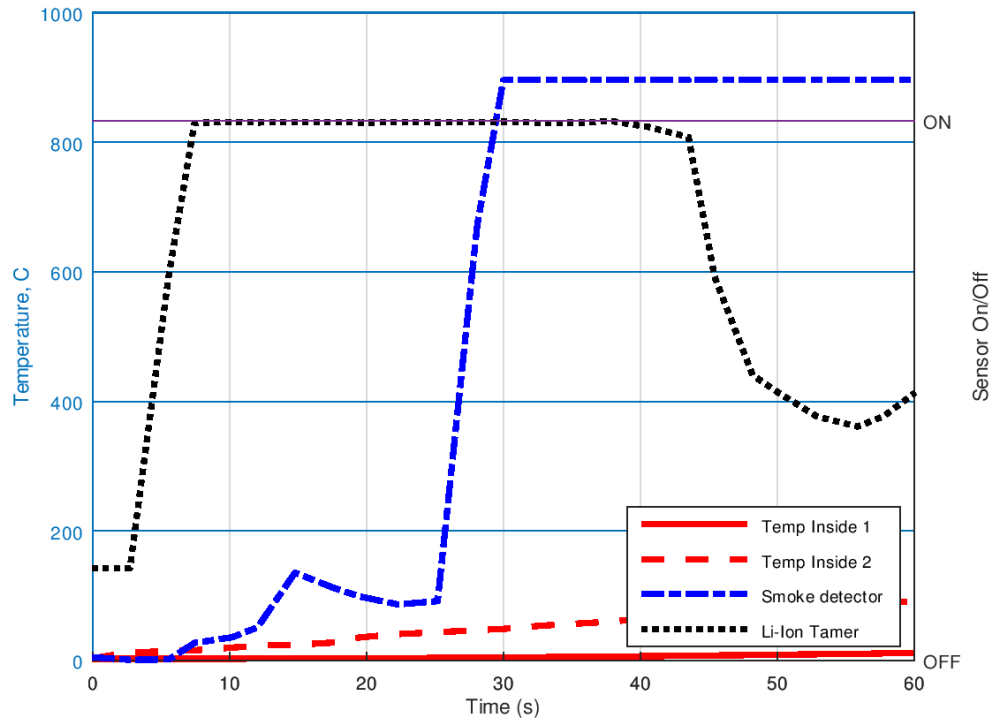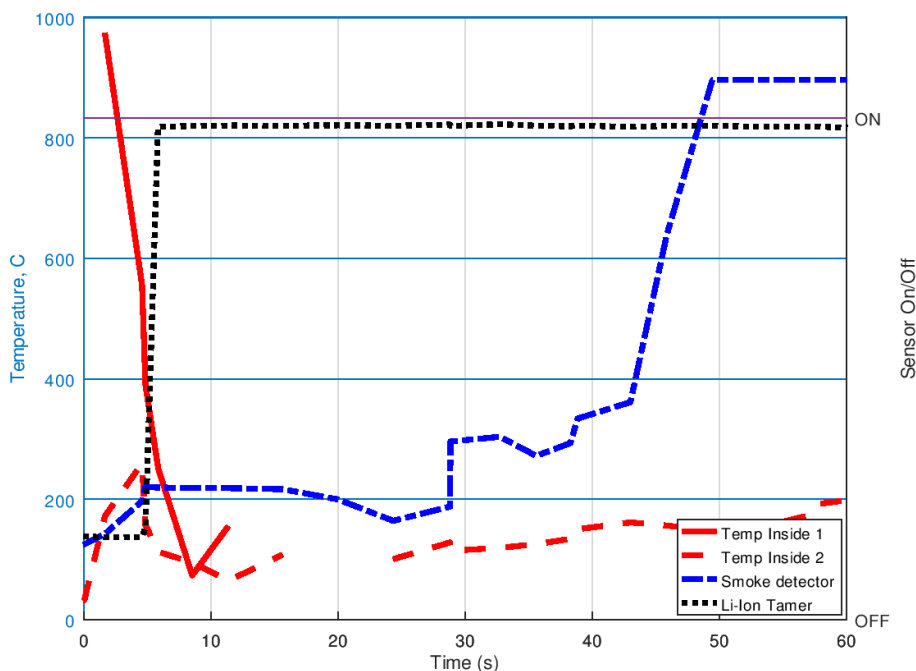

Figure 14-12: Li-ion Tamer® gas detector and Smoke detector performance together with temperatures inside the battery module box for Test 1
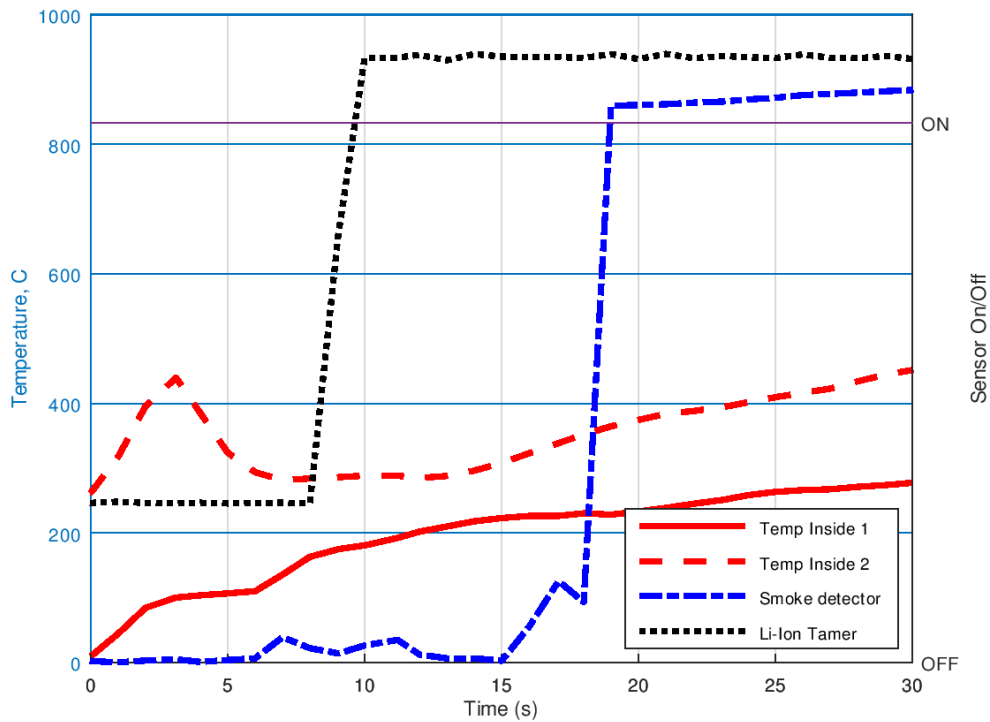
Figure 14-13: Li-ion Tamer® gas detector and Smoke detector performance together with temperatures inside the battery module box for Test 3
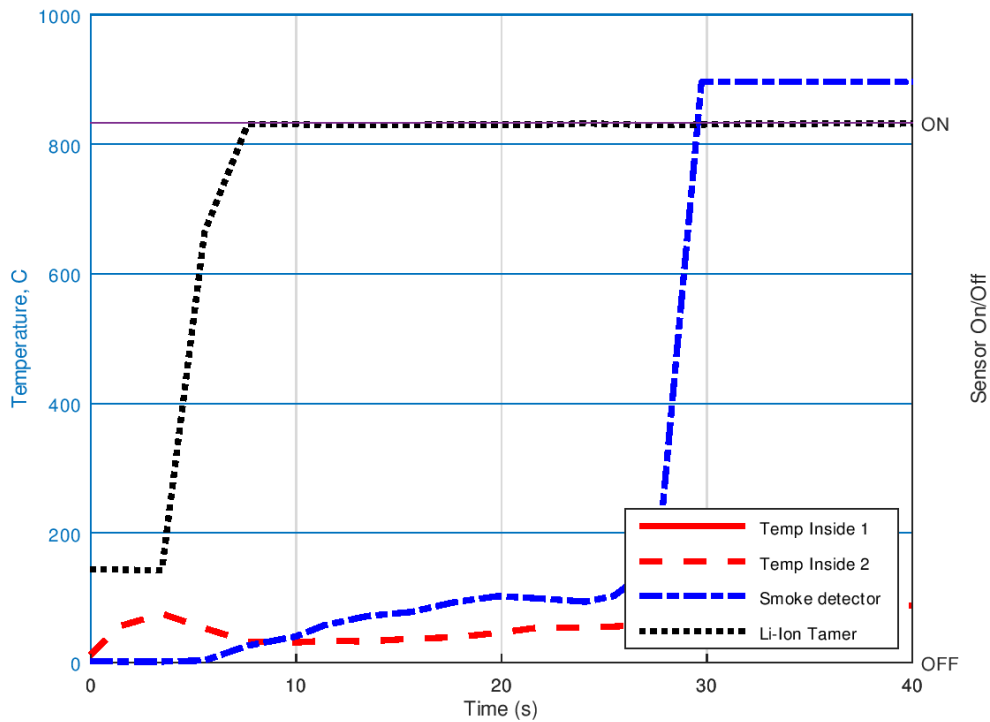
Figure 14-14: Li-ion Tamer® gas detector and Smoke detector performance together with temperatures inside the battery module box for Test 7

Figure 14-15: Li-ion Tamer® gas detector and Smoke detector performance together with temperatures inside the battery module box for Test 9

14.2.3 Suppression systems

The following suppression systems where evaluated in the test setup:

Total flooding systems:

- Sprinklers: Offer a common method for fire extinguishment that is in line with lithium-ion expected requirements – large amounts of volume can be supplied to provide for maximal heat absorption.

- Hi-Fog: Is a high-pressure water mist system that produce a fine mist which increases surface area for heat absorption. A typical water mist system would have capacity for a minimum of 30 min freshwater release, followed by back-up access to seawater from the vessel fire main providing cooling properties over time. However, the time duration of the discharge can be increased based upon required protection time limits defended in the design phase of the system.

- NOVEC 1230: Is an equivalent gas-based fire suppression system. The primary function of NOVEC is to put out flames by physically cooling below the ignition temperature of what is burning and chemically inhibiting the fuel source. The agent does not deplete oxygen levels in the room, where fire itself is the only actually consuming oxygen. Sealing of the space is key for ensuring adequate concentrations of NOVEC 1230.

Direct injection systems:

- Direct injection of water: For the purpose of combating heat generation, direct injection of water is considered as the most efficient alternative. In the industry today this method is generally included as a last resort back-up since the affected module(s) will be considered lost after

deployment. The test setup included a fire hose connection with direct access to the interior of the battery module under testing.

- FIFI4Marine CAFS: is a foam-based system, that can be installed to deploy directly in to the battery modules, their surroundings in the racks or in the room. The concept evaluated in this report is only direct injection into the modules. The FIFI4Marine CAFS system is designed to re-deploy several times during an incident as the foam will degrade over time as it participates in combating the battery fire.

14.2.3.1 Total flooding systems; Sprinklers, Hi-Fog and NOVEC

The key performance data is summarized in Table 14-5. Here it is seen that the LEL% after the release drops significantly with Hi-Fog, but also some with NOVEC, compared to the LEL% with no suppression.

Table 14-5: Key data for Hi-Fog and NOVEC tests

| Suppression System	Test #	Enclosure	Highest Neighbor Box External Temp At Release	Highest Neighbor Box External Temp 200s after Release	Highest Neighbor Box Internal Temp At Release	Highest Neighbor Box Internal Temp 200s after Release	LEL% (after release)
None	1	IP44	435	-	132	-	69%
Hi-Fog	11	IP44	117	116	65	59	10%
NOVEC	3	IP20	120	84	52	50	26%

The temperature measurements from Test 15 where sprinklers were used is shown in Figure 14-16. The temperatures for Test 16 with Hi-Fog is shown in Figure 14-17. These figures show the short-term temperature effects. These tests were both performed with open modules (door off).

Both tests show similar max temperatures on test cells inside the box and both show similar max temperatures on surfaces of neighboring modules of just over 600C. Both suppression systems where able to bring the neighboring module temperatures down under 200C after approx. 100 seconds after release.

Additionally, photos show that Hi-Fog has better capability to suppress flames. Flames where seen outside rear window on the sprinkler case and not for the Hi-Fog test.

The LEL% was not recorded for the sprinkler test. Based upon experience and other tests performed by the project participants, it is concluded that the sprinklers are not capable of reducing the gas concentration. It can actually be argued that it increases the explosion risk, since the water displaces the gas into pockets with higher concentrations.

Due to the flame extinction and the gas absorption capabilities, it can be concluded that the Hi-Fog performed better compared to the sprinkler.
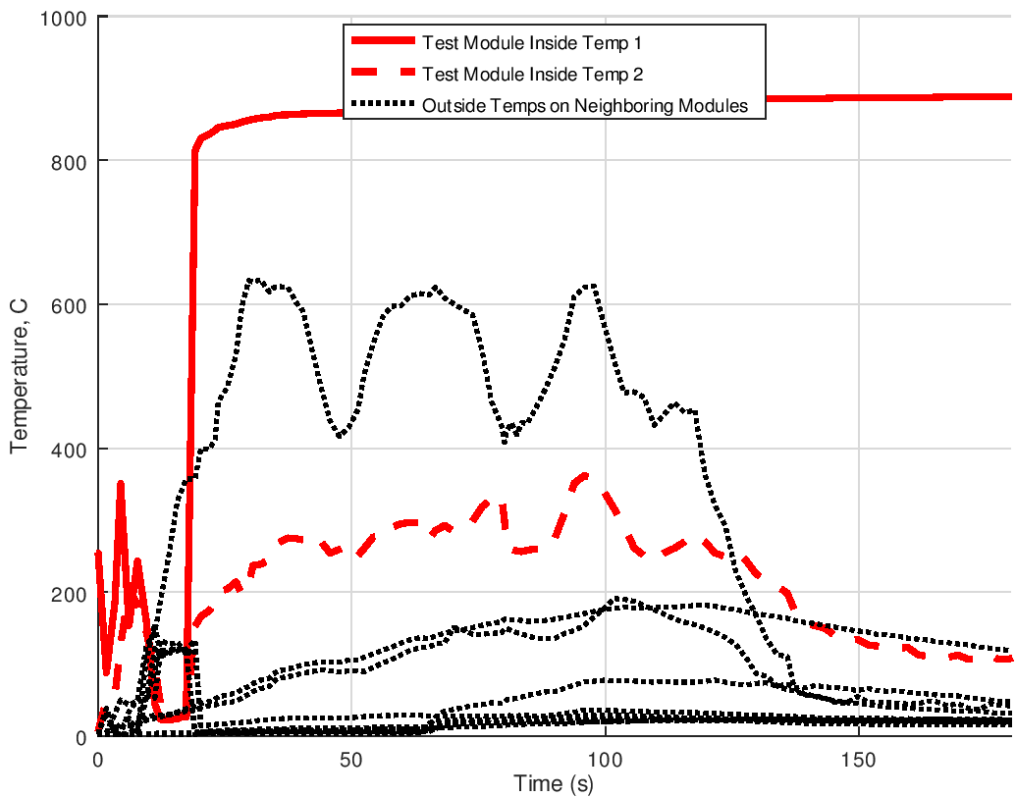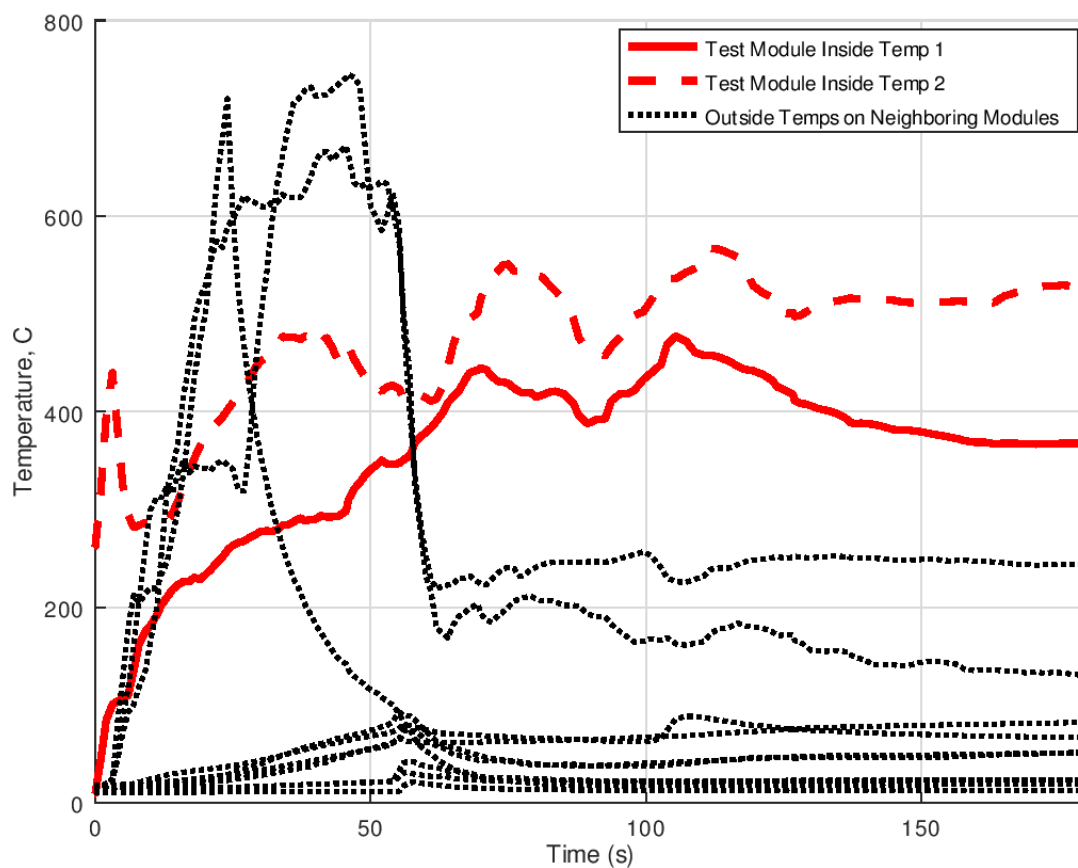
Figure 14-16: Temperatures inside and outside the modules for Test 15 where sprinklers are used as fire suppression.
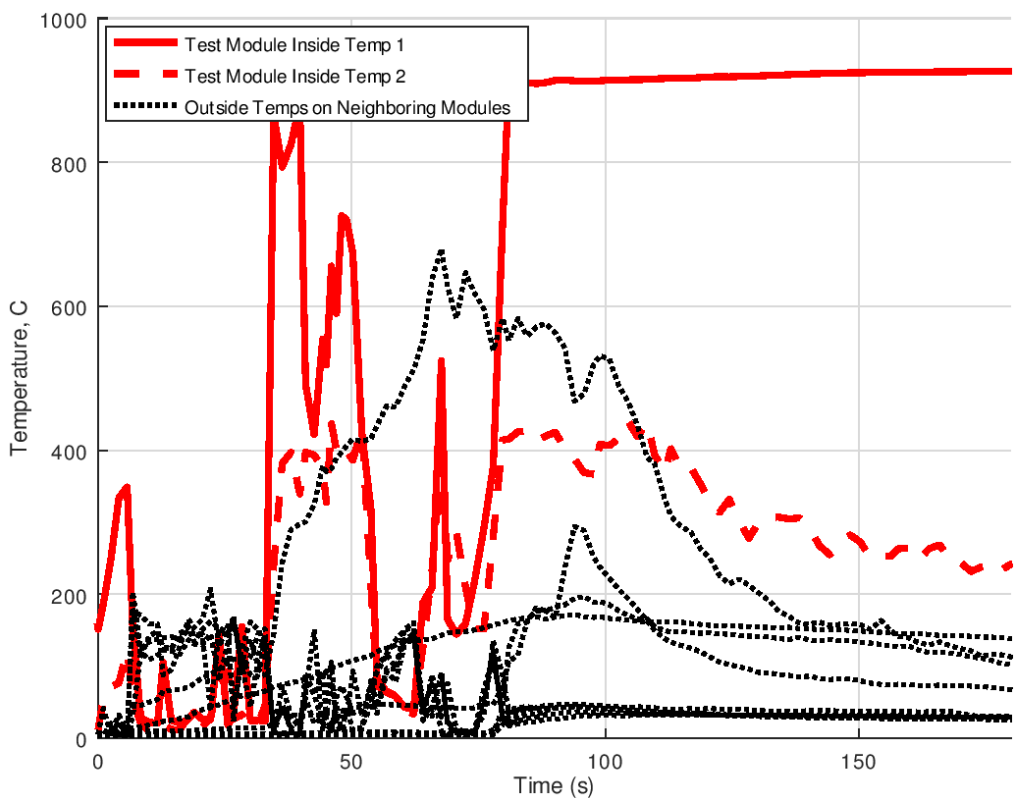
Figure 14-17: Temperatures inside and outside the modules for Test 16 where Hi-Fog is used as fire suppression.

For comparison to NOVEC, Test 3 produced the most relevant results. These are shown in Figure 14-18. However, this test was performed with the module fully enclosed, whereas Test 15 and 16 was with open lid. This would primarily suggest that the media is less able to cool down the internal temperatures of the box. On the other hand, since the lid is on it serves as a shield for the neighboring modules to the open flames. This should make it easier to cool down the neighbor modules since there is a less direct heat source. The internal box temperatures were actually lower compared to Test 15 and 16, but also that temperatures of neighboring were of similar magnitude. This indicates that Novec is less capable of cooling down the neighboring modules compared to sprinkler and High-Fog.

However, we can see that Novec produces more immediate effects, compared to sprinklers and Hi-Fog, as temperatures drop more rapidly.


Figure 14-18: Temperatures inside and outside the modules for Test 3 where Novec is used as fire suppression.

For the long term effects, the sprinklers with open lid is shown in Figure 14-19 and Hi-Fog with open lid is shown in Figure 14-20. Test 11 was performed with Hi-Fog and an IP44 box and is shown in Figure 14-21. In Figure 14-22, the long-term effects of Test 3 with Novec with an IP20 box is presented. It is seen that for both Hi-Fog and the sprinklers, the temperatures of the neighboring modules go down and stays down at a lower temperature compared to the Novec test.

Looking at the respective tests of Hi-Fog under IP20 conditions the same level of combustion and heat generation was not observed, so the results do not provide a good basis for comparison. The suggested

conclusion is that Novec is not able to cool down long term, but this is not heavily substantiated. It is however, in line with theoretical calculations based on mass and absorption rate.
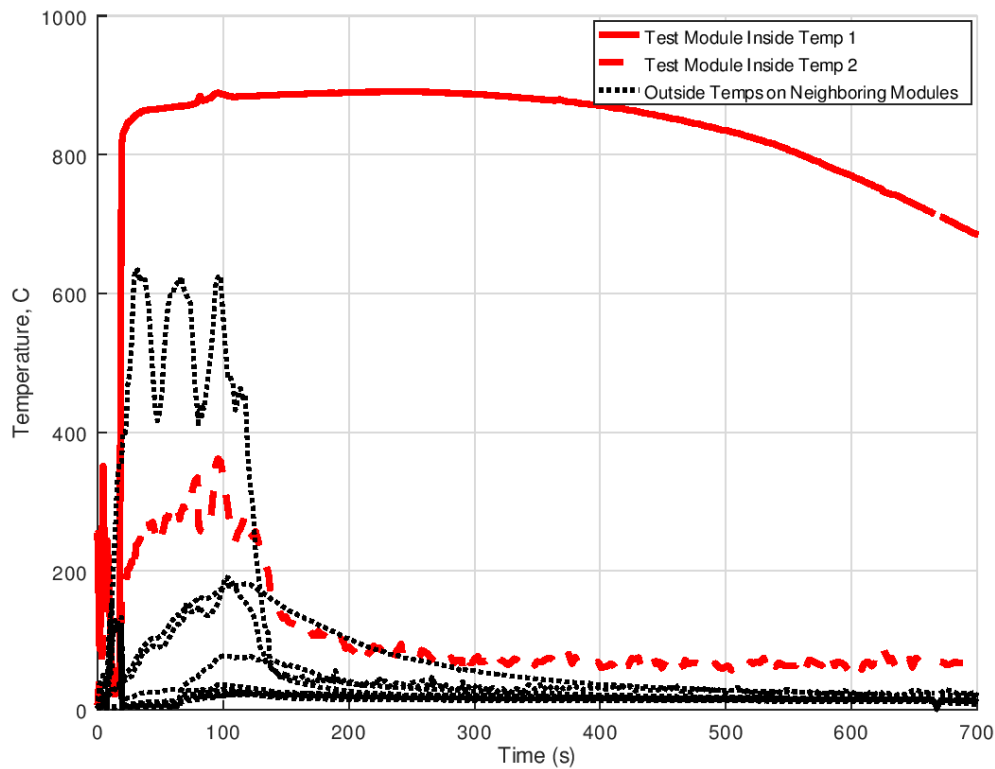
Figure 14-19: Test 15 shows the long-term effect of Sprinkler with open lid
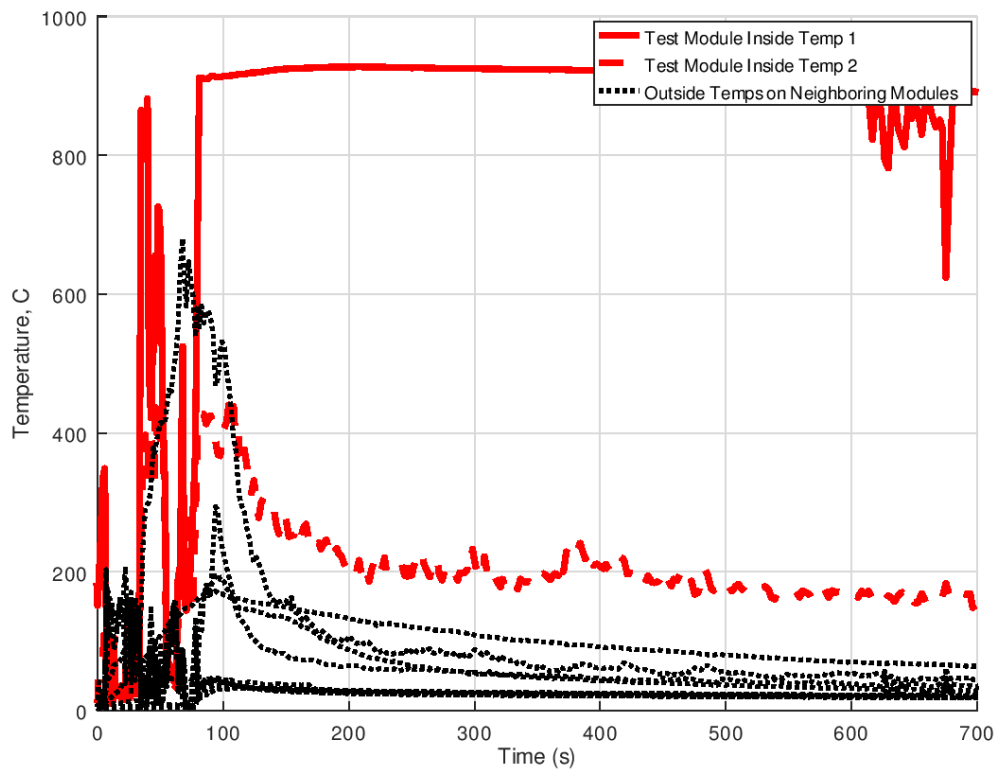
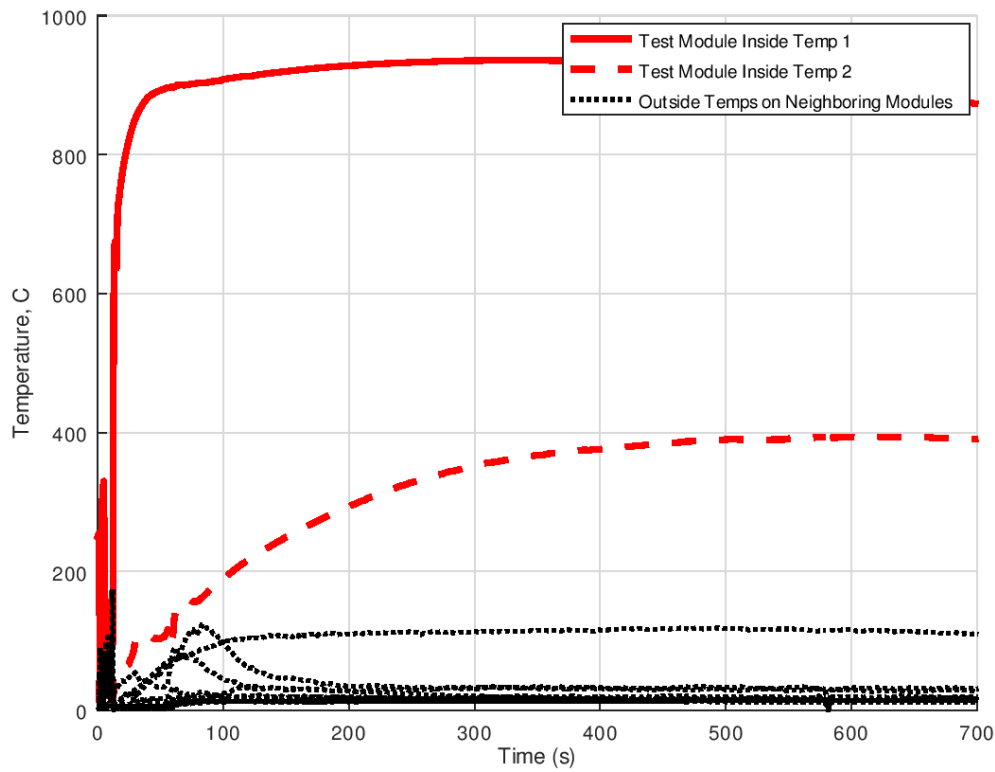**Figure 14-20: Test 16 shows the long-term effect of Hi-Fog with open lid**

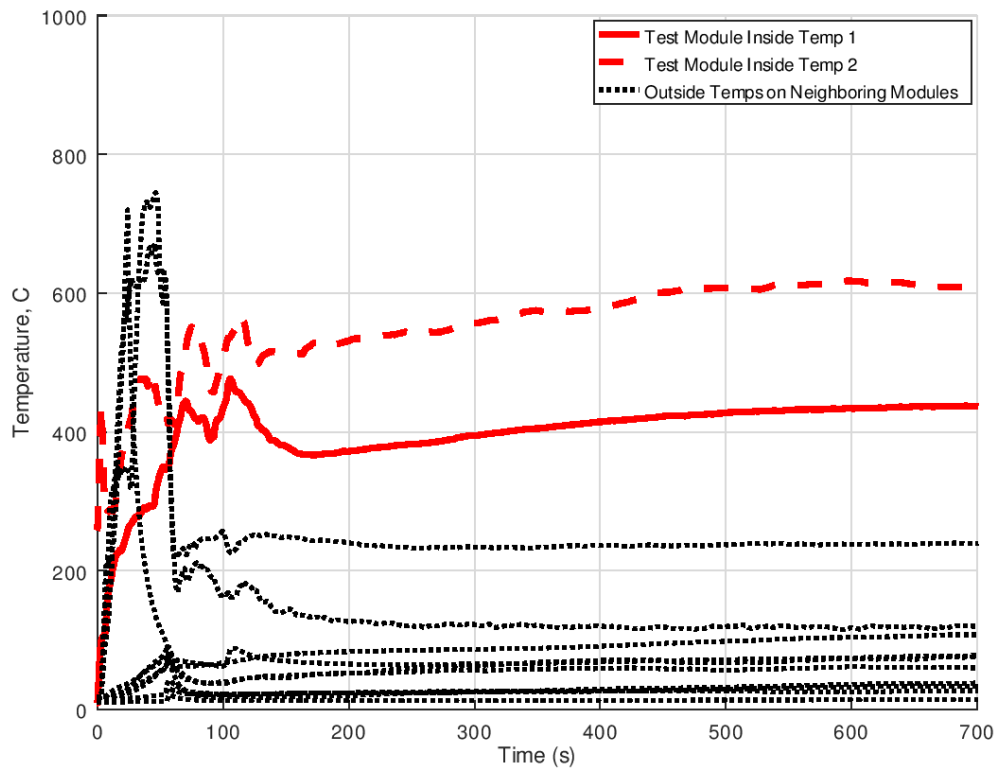**Figure 14-21: Test 11 shows the long-term effect of Hi-Fog with an IP44 box**

Figure 14-22: Test 3 shows the long-term effect of Novec with an IP20 box

To evaluate the gas temperature reduction capabilities in the room, the ambient temperature measurements, indicated by the blue crosses in Figure 14-7 is used. Test 20, shown in Figure 14-23, has been used as a reference since it was performed with open lid. The sprinkler test is shown in Figure 14-24, the two Hi-Fog tests are shown in Figure 14-25 and Figure 14-26 and the NOVEC test is shown in Figure 14-27.

All the suppression media contributes to a lower ambient temperature. Both the sprinkler and Hi-Fog shows equal capabilities and stabilizes at a lower temperature than NOVEC.
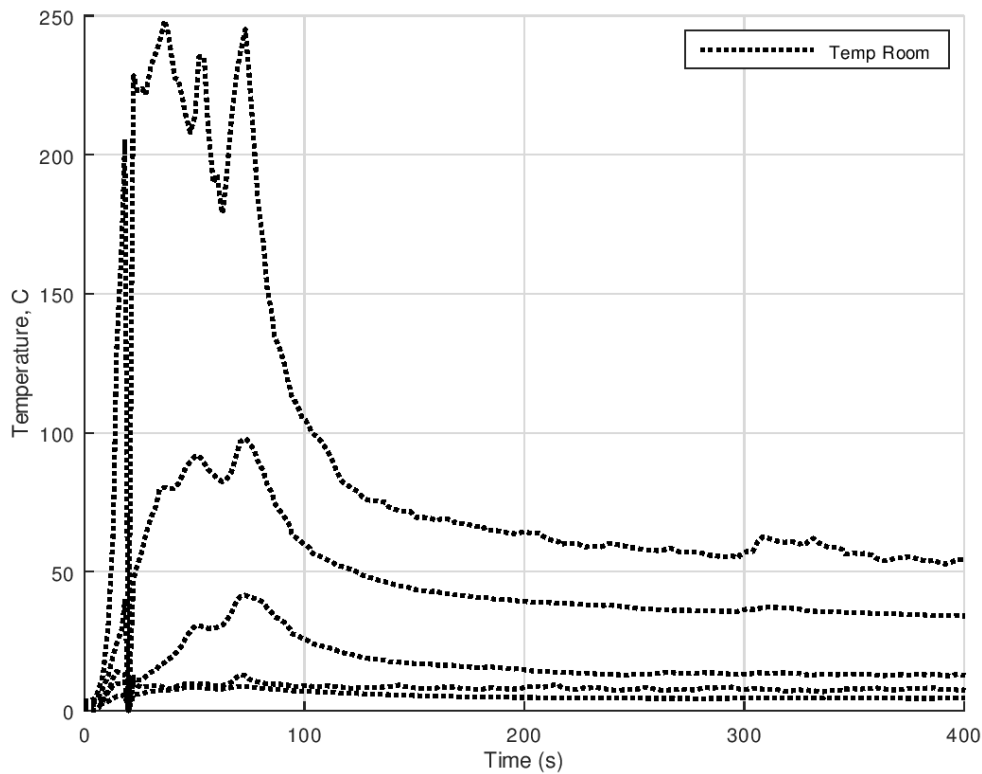
Figure 14-23: Ambient temperature measurements for Test 20 with open lid, no suppression and 6 ACH ventilation.
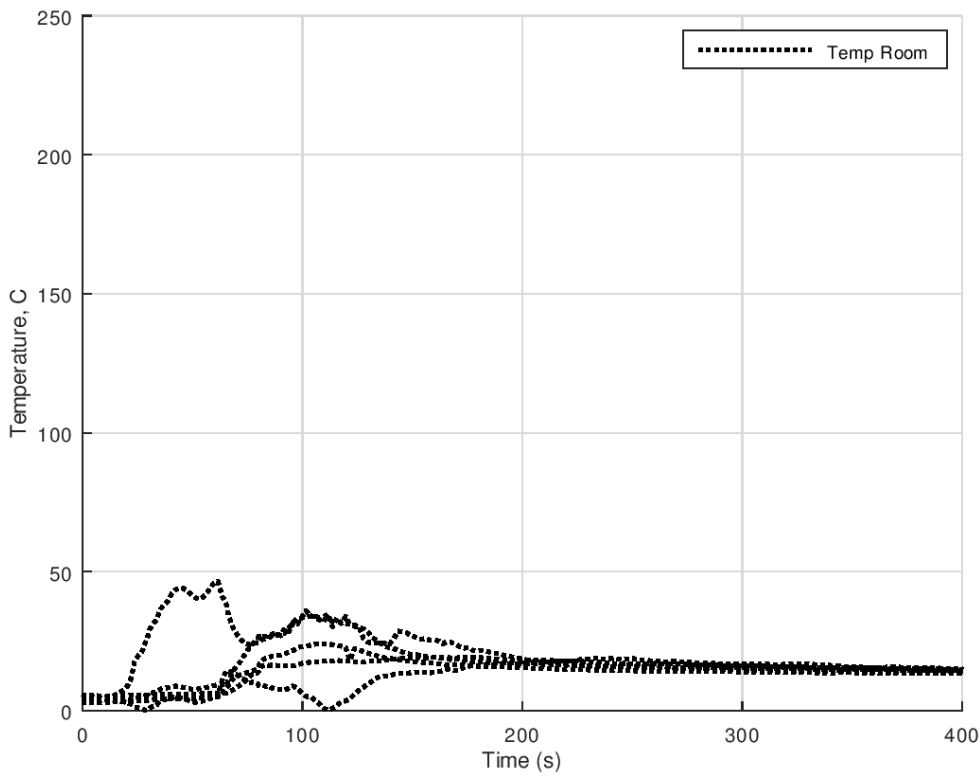
Figure 14-24: Ambient temperature measurements for Test 15 with open lid and sprinklers.
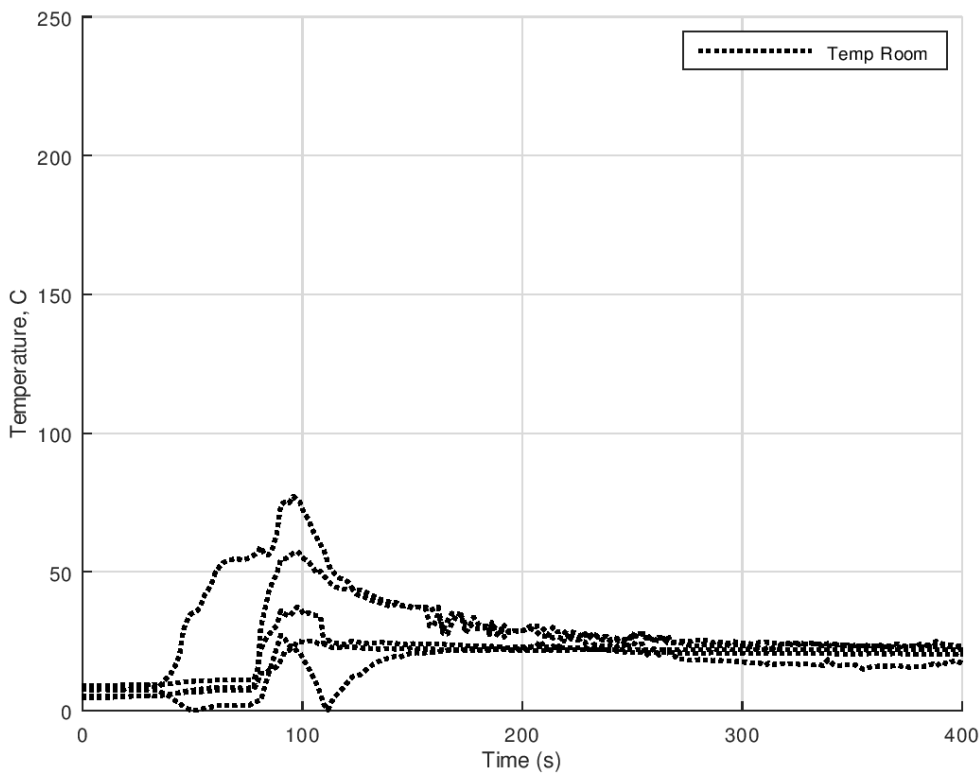
Figure 14-25: Ambient temperature measurements for Test 16 with open lid and Hi-Fog
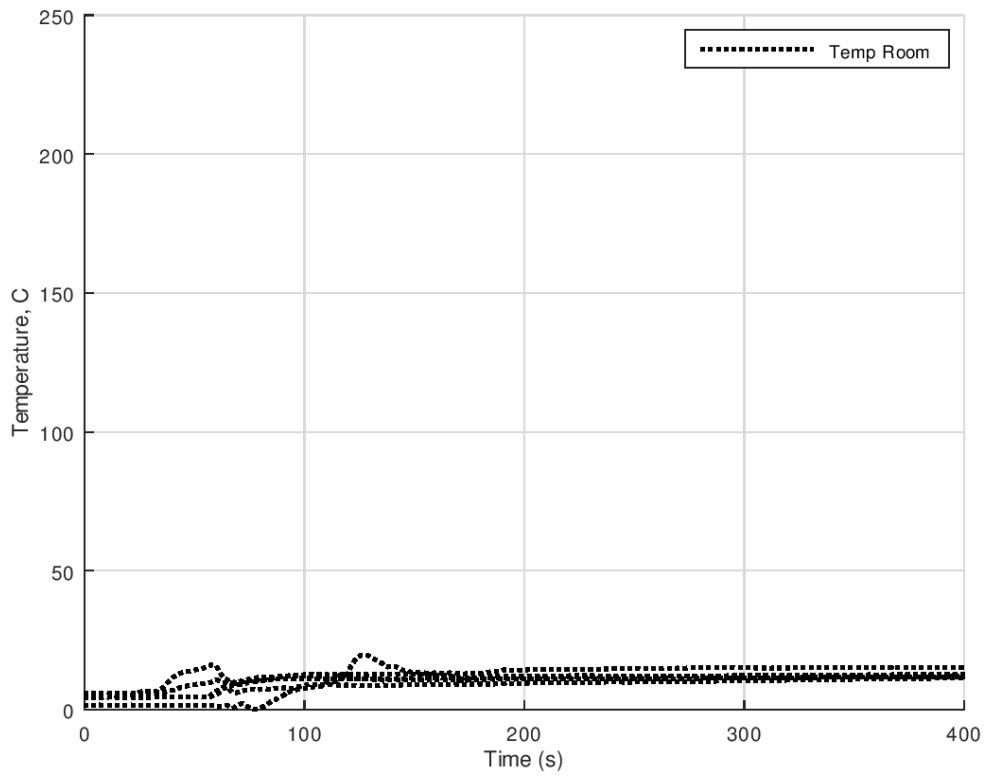
Figure 14-26: Ambient temperature measurements for Test 11 with IP44 and Hi-Fog.

Figure 14-27: Ambient temperature measurements for Test 3 with IP 20 and NOVEC.

14.2.3.2 Direct injection systems; FIFI4Marine CAFS and direct water injection

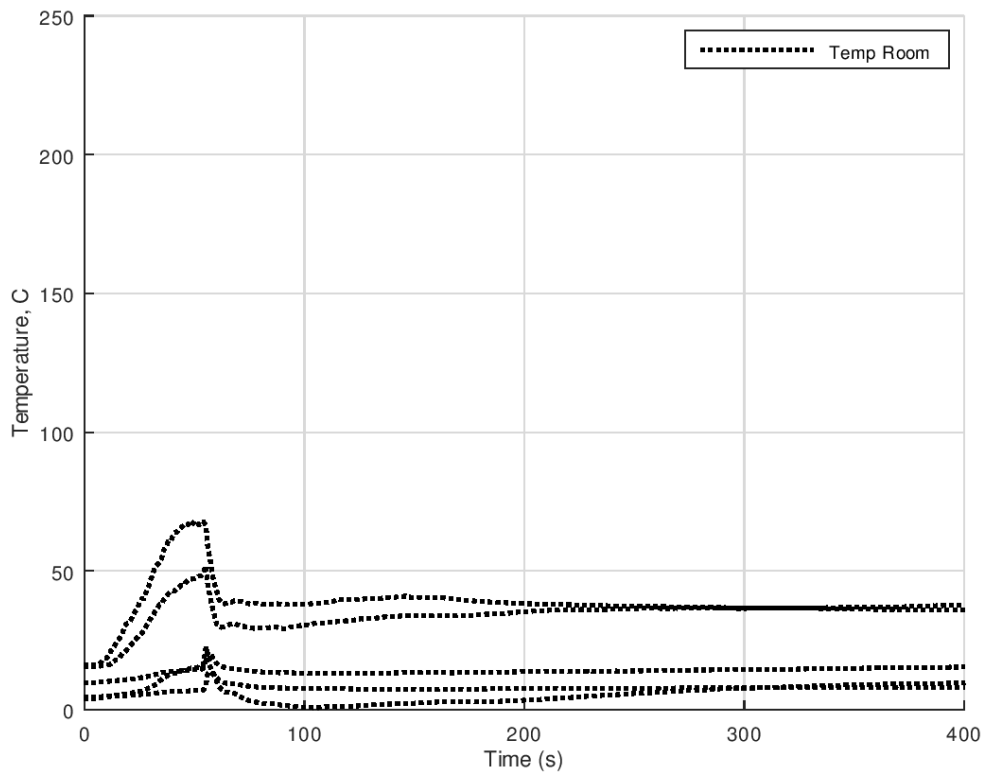A direct comparison between the two direct injection systems are here presented. Both direct water injection and the foam based FIFI4Marine CAFS where tested with IP 44 boxes and NMC cells. Both systems were allowed to burn for approx a minute before suppression initiated. From the standard video, we can see that in both cases the room fills with smoke and gas of sufficient volume to block view of the camera.

Thermal cameras provided additional insight in this case, and actually indicated hotter temperatures at the module box surface in the FIFI4Marine CAFS test compared to direct water injection.

Both the foam-based and the direct water injection reduced the main battery fire temperatures to under 80°C within 600 seconds. This represents a significant improvement over what can be achieved with fire suppression media applied outside of the module – where the main battery fire temperature was unaffected and quite stable at around 900°C. External temperatures on neighboring modules are also significantly reduced from the use of direct water injection – reducing to below 20°C within 150 seconds after release. The direct injection foam-based system had recorded temperatures below 50°C within 700 seconds.

Table 14-6: Key data for direct injection suppression systems

Suppression	Test #	Temperature before mitigating (°C)	Temp after mitigating (°C)	Test box temps at end of test (°C)	Surrounding boxes
Direct Water Injection	17	899	98	< 65	No increase observed
FIFI4Marine CAFS	7	275 *)	100	< 60	Bottom of box above 29°C

*) Only one of the two temperature readings inside the box was functional during this test. The value presented is from Temp 2 sensor plotted in Figure 14-16 to Figure 14-22, Figure 14-28 and Figure 14-29. The value for Temp 1 sensor is expected to be the same range as for Direct Water Injection.
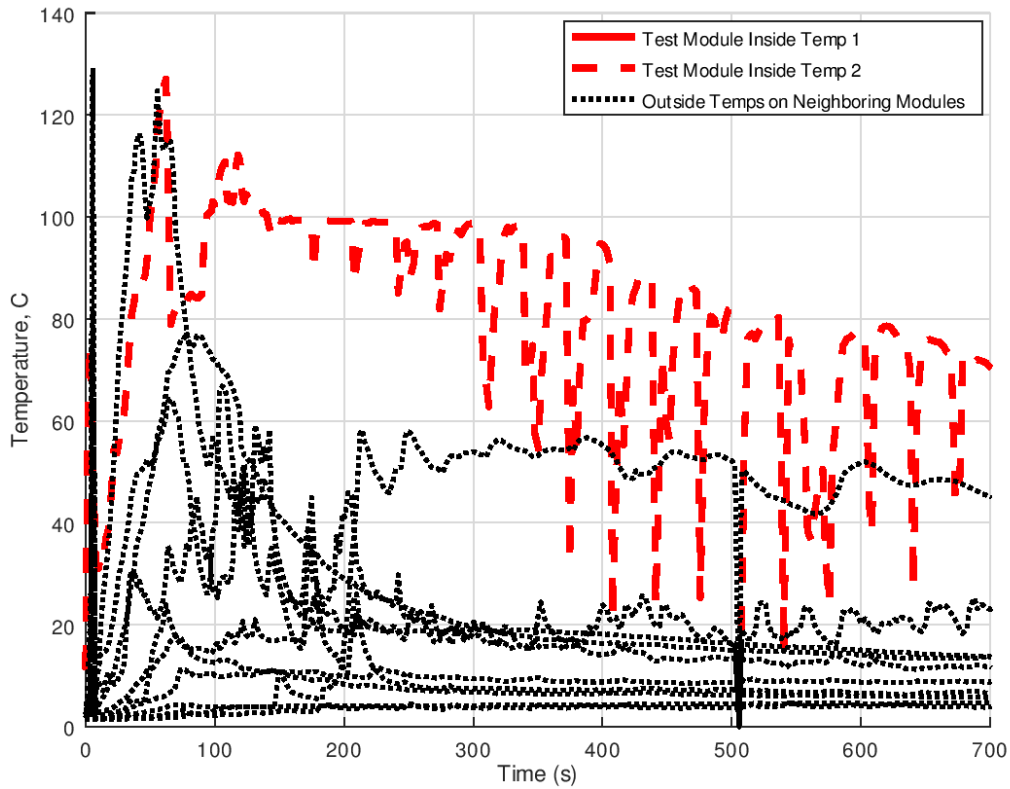
Figure 14-28: Temperatures inside and outside the modules for Test 7 with FIFI4Marine CAFS fire suppression.
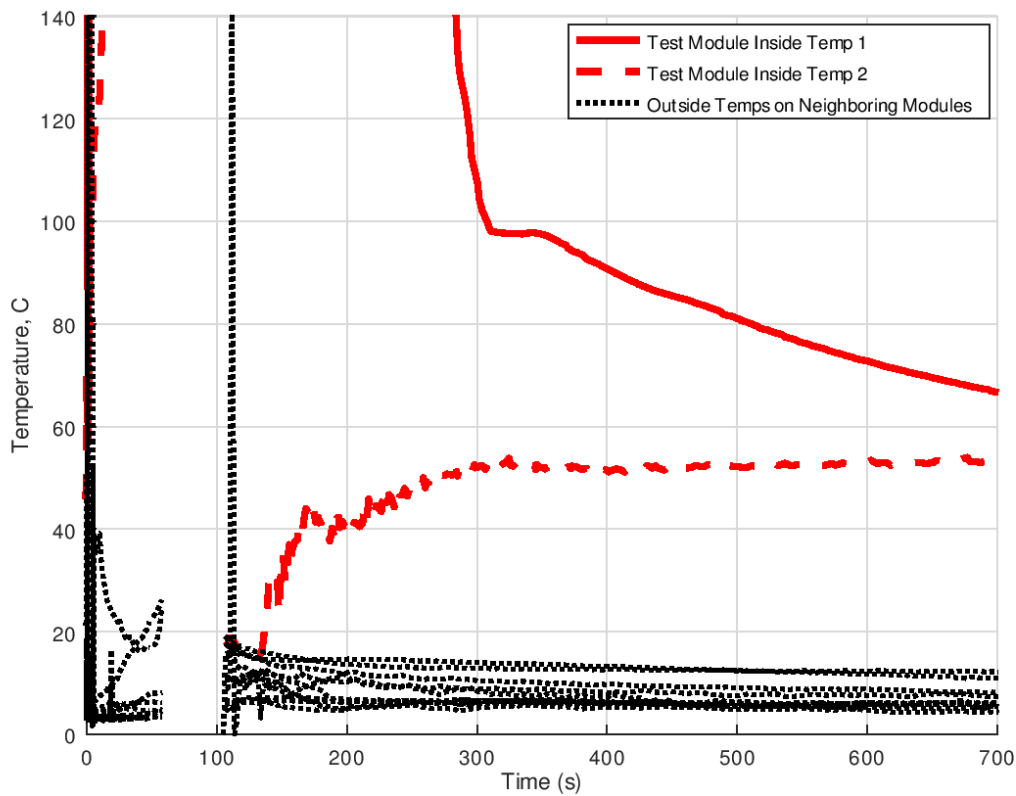
Figure 14-29: Temperatures inside and outside the modules for Test 17 where direct water injection is used as fire suppression.

14.2.3.3 Summary

The table below summarizes the capabilities of the fire suppression systems based at the tests performed.

Table 14-7 – Fire suppression systems' capability matrix

	Primary objective			Secondary objective		Suppression method properties	
	Flame extinction	Long Term Heat Absorption	Short Term Heat Absorption	Reduce Gas Temp in room	Gas Absorption in room	Can be Used with Ventilation	Suppression method
Sprinkler	[Medium]	[Medium]	[Low]	[High]		YES	Total-flooding
Hi-Fog	[High]	[Medium]	[Low]	[High]	[High]	YES	Total-flooding
NOVEC 1230	[High]		[Medium]	[Medium]		NO	Total-flooding
FIFI4Marine	[High]	[High]	[High]	Not evaluated	Not evaluated	YES	Direct injection
Direct Water injection *)	[High]	[High]	[High]	Not evaluated	Not evaluated	YES	Direct injection

*) Not expected or recommended to be used in practice for high voltage applications, due to the risks of short circuit and hydrogen production. The method is presented as a flame extinction and heat absorption capability reference.

- [High capability]
- [Low capability]
- [Medium capability]
- [No or very low capability]

15 EXPLOSION ANALYSIS AND ASSESSMENT

Explosions are primarily prevented by reducing or eliminating the gas release and resulting gas cloud formation. If this cannot be achieved, mitigations for the explosion pressures can be employed such as explosion relief panels. The final strength of the walls in the room may also need to be improved if the risk of explosions is unacceptable.

In the present assessments, it is mainly gas/smoke release and the fire and gas dispersion phenomenon that is investigated both with experiments and with 3D CFD simulations.

Batteries are typically located in enclosures (rooms in a ship, or in a container) where the module racks are packed quite dense. The room size is limited and in an off-gassing event, when enough flammable gases are created, it usually ignites early and cause a violent fire, but no explosion. The heat from the off-gassing event is often above the auto ignition temperature of the gas hence causing an early ignition of the release. In some cases, however, the gases do not ignite early and can then create an explosive atmosphere in the room. If the release is large enough, it can cause a severe explosion. It is also a risk of back fire or a second ignition. This can occur if the first ignition starts a small fire which consumes all the oxygen in the room. Then the gas from the event will continue without burning creating a possible large flammable cloud.

The fine balance between released gas (fuel) and oxygen in the room can cause different scenarios during the event which needs to be considered. The design of protection systems need hence to consider both fires and explosions. The present chapter consider the explosion potential.

15.1 Preliminary CFD ventilation studies

In order to benchmark risk magnitudes and thus provide guidance and direction for the project some preliminary assessments were performed as first stage of the JDP. These were aimed at forming a basis for where key questions and risks lay with regard to scale of failures, particularly with regard to explosion and off-gas formation. This initial work then comprised of performing CFD models of a representative battery room to evaluate the explosion risks of different scales of failures and understand where key risks and attention should be given for project research.

15.1.1 Setup of battery room and scenarios

Models were built aimed at assessing potential volume of flammable gas in maritime battery room from battery off-gassing events, and the resulting potential explosion overpressure. This approach was to use CFD simulations with inputs coming from team experience and available public data. The intention was to perform a range of simulations, with variation of key parameters to show spectrum of outcomes and identify key ranges which would require further assessment.

For the model, shown in Figure 15-1, based on a typical container and notional battery setup, a free volume of 25 m^3 was used. Regarding airflow only external ventilation was taken into account – as opposed to any circulation via air cooling. Ventilation comprised of 4 inlets and 4 outlets.
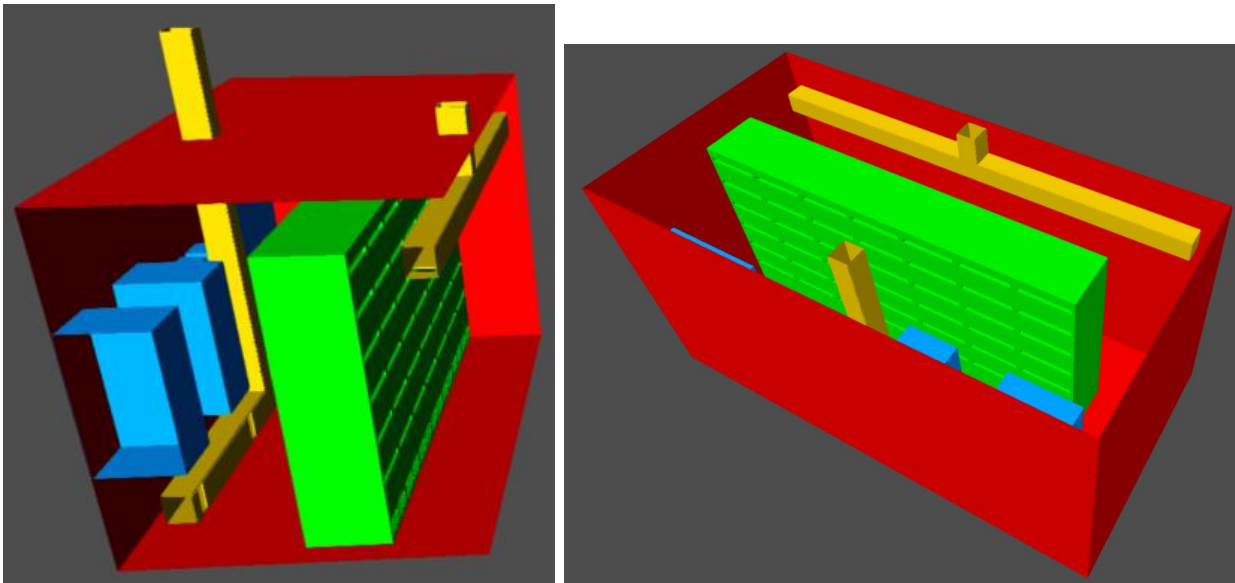
Figure 15-1 – Battery room and components used for initial CFD assessments.

As shown in Table 15-1, concentrations used to construct gas contents were selected to intentionally represent a worst case, nominally slightly more so than would be expected in reality. This is primarily represented in a higher than expected volume of hydrogen. In addition, a key parameter of study was to be release profile, which was thus maintained as a variable as far as shape and rate. Triangle and square profiles of differing durations were used, as shown in Figure 15-2, to encapsulate the full range of potential real world cases. In all cases, it was assumed a total of 140 liters of gas per cell, based on 2.0 l/Ah, which was believed to be a representative worst case, and assuming fairly large 70 Ah cells. For full module evaluations two different cell to cell propagation patterns were studied. One was linear, one additional cell failing at a time, and the second was exponential, where two additional cells failed at a time.

Table 15-1 – Gas concentrations used for preliminary worst-case modelling.

Component	Concentration (volume)
Methane	10 %
Ethane	10 %
CO	30 %
CO2	0 %
H2	50 %
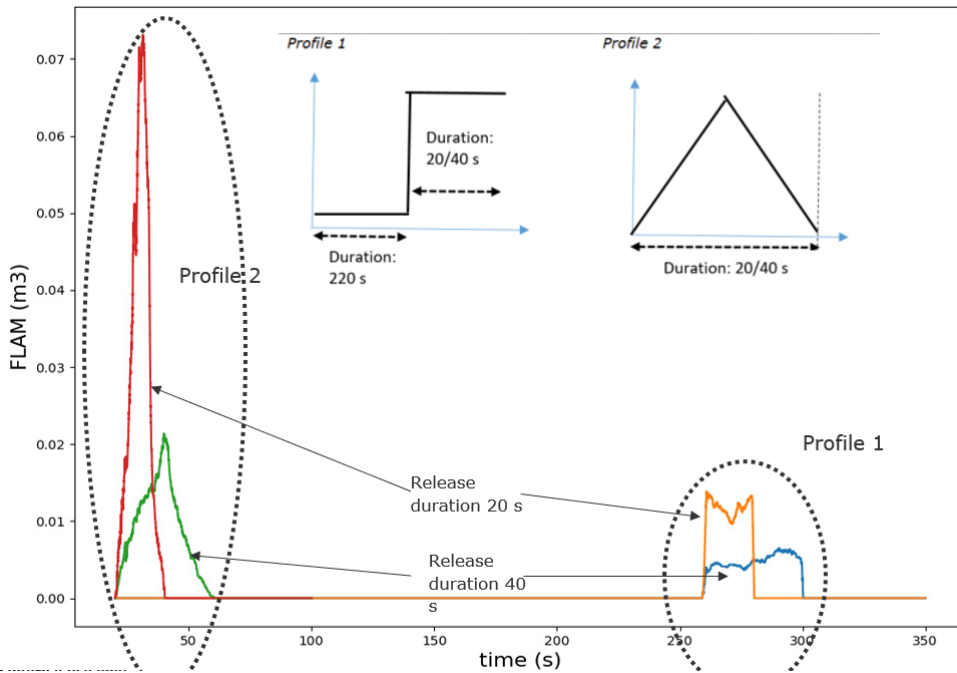
Figure 15-2 – Release profile shapes and release rates used for initial benchmarking studies.

A key motivation for these initial assessments was to evaluate the relative magnitude of explosions and effectiveness of different ventilation rates – specifically studied were 0, 5, 10 and 30 ACH.

Explosions were considered on the basis of flammable gas build up (FLAM) – this is the total volume of gas between LEL and UEL. The magnitude of explosion is thus proportional to the amount of FLAM. The stoichiometric mixture equivalent is what drives calculation for maximum potential magnitude of explosion. This can be calculated explicitly in more specific future studies; but for these initial assessments, expert experience suggests that assumed to be half of the FLAM. Explosion (deflagration) overpressure is linearly proportional to the volume of gas as a percentage of total room volume. Max possible is 8 barg.
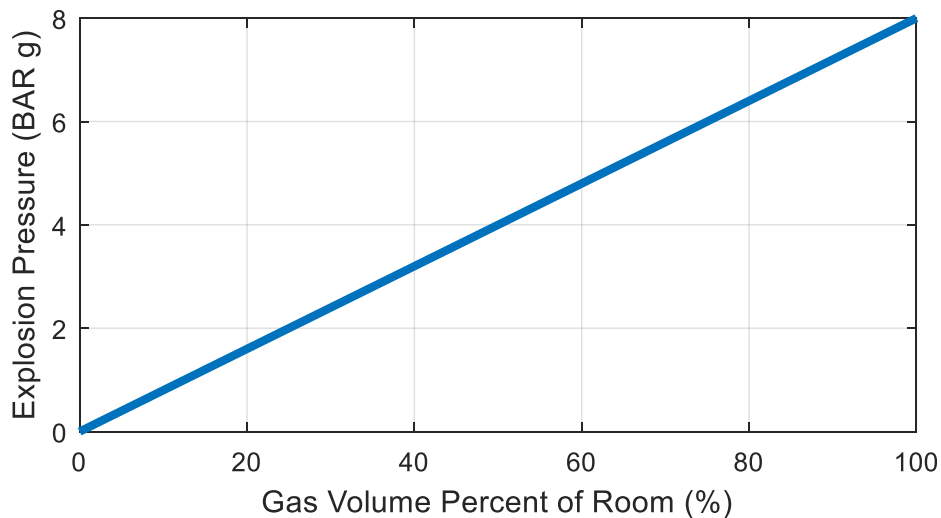
Figure 15-3 – Explosion pressure as a function of filling percent of a stoichiometric gas cloud in the room. Gas expansion effect in a fully enclosed room /4/.

15.1.2 Studies and Findings

When comparing all different variations at the single cell volume release level, it was found that ventilation has near zero effect. This is 10, 5 and 0 ACH respectively. Logically, release profile has significant impact on flammable gas buildup. Based on all iterations, in the worst case, for a single cell FLAM = 0.08 m3. If ignited this results in an explosion of 0.02 BARg. For comparison, this is below the fluctuation in blood pressure between heartbeats. Within the range of being enough to break a glass window. Thus, explosion from gas release of a single cell is not considered a primary threat. However, this does suggest the need to define the limit as far as what can be considered safe as far as size of a cell.
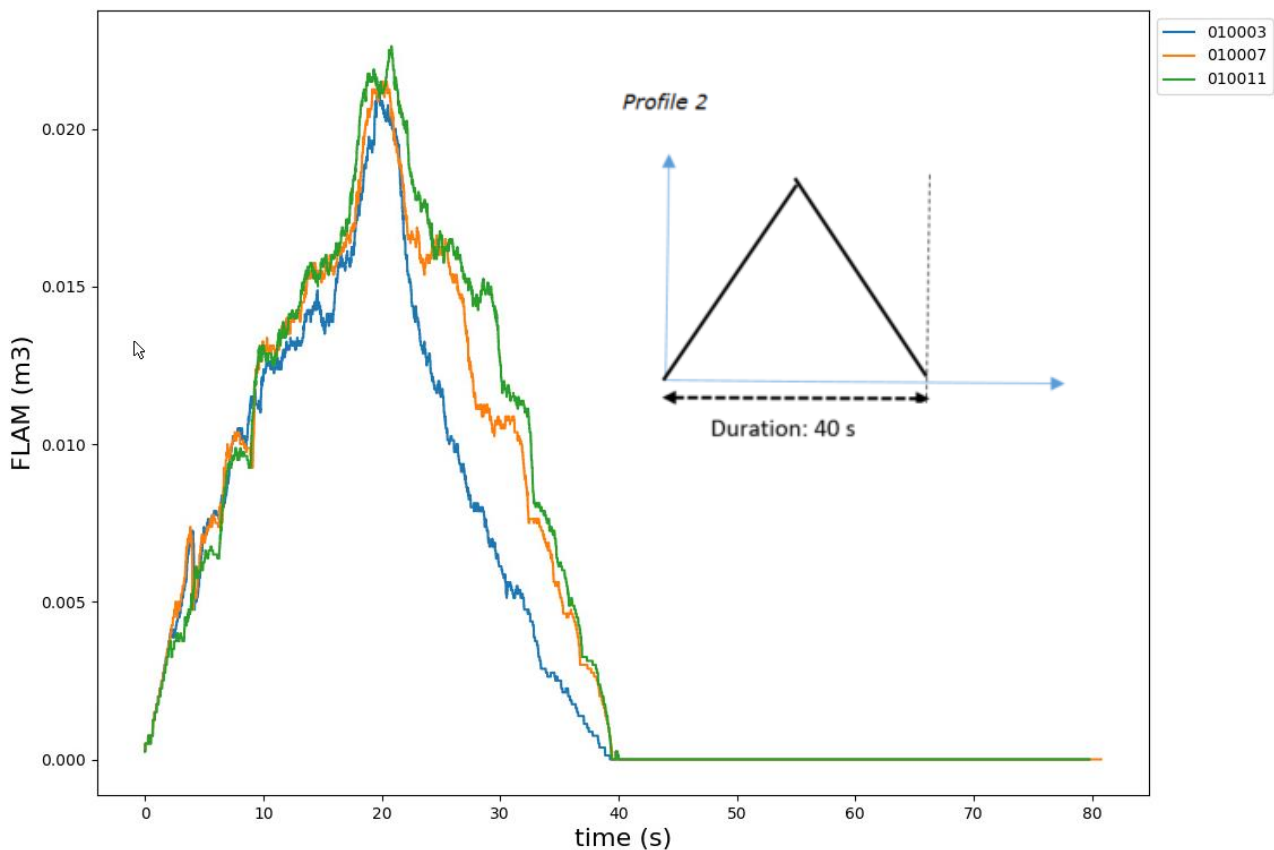
Figure 15-4 – FLAM produced at cell level is not affected by ventilation – 0, 5, 10 ACH shown

At the full module level, gas volumes increase considerably, as expected – but release profile is shown to matter much less. Figure 15-5 shows total FLAM resulting from different cell release profile shapes, at 10 ACH.
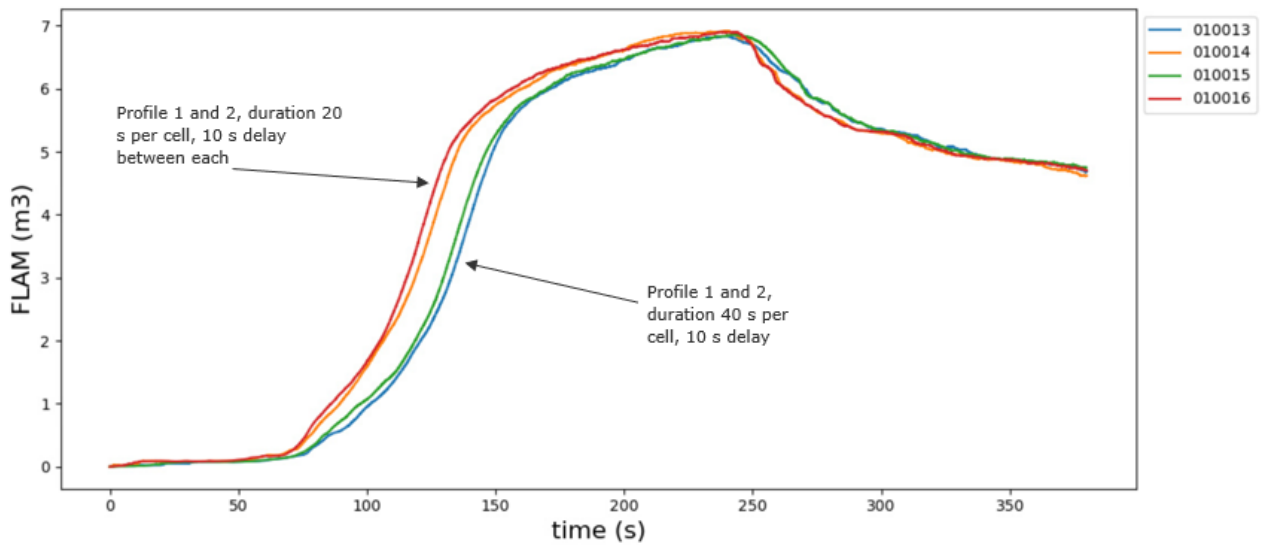
Figure 15-5 – Effect of cell release profile on FLAM from module

Further, ventilation rate does have a significant impact at the module level. Figure 15-6 indicates FLAM for full module with 10, 5, 0 ACH. All modules are assuming 10 seconds between cell offgas releases (Profile 1, 40 seconds duration). Results are almost identical for different shapes and 20 seconds duration.
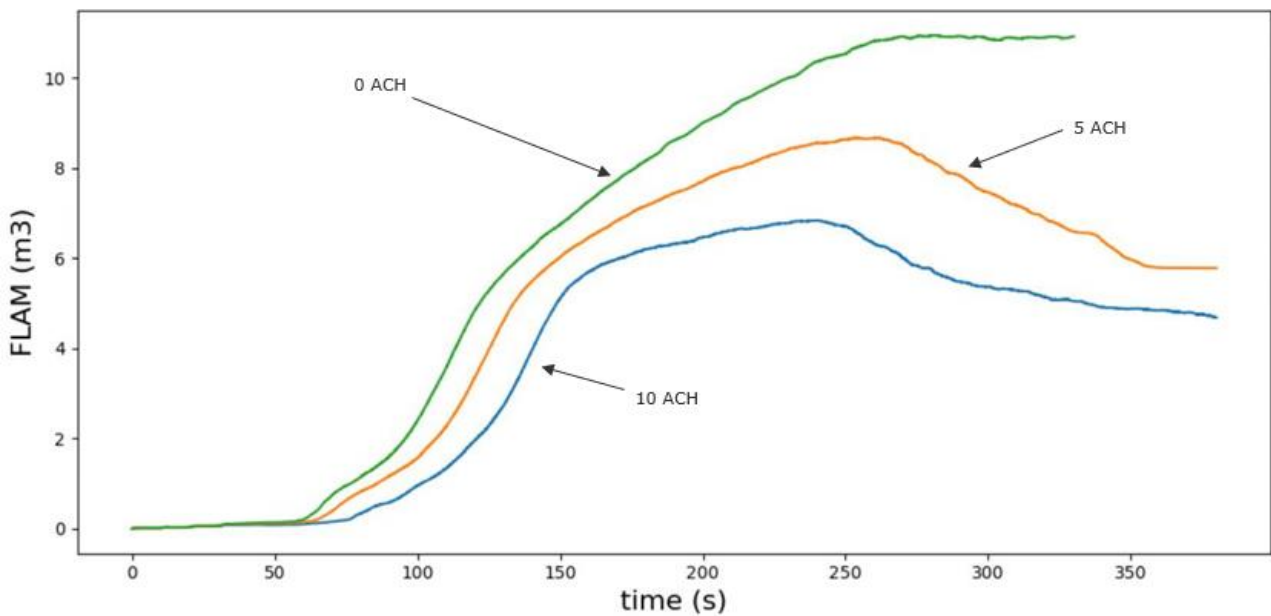
Figure 15-6 – Effect on FLAM of different ventilation rates

Module level FLAM also sees significant difference with regard to how fast propagation occurs between cells. Figure 15-7 shows the total amount of flammable volume for cases with linear propagation between cells, 1 – 2 – 3 – 4 – 5 – etc, compared to exponential propagation, 1 – 2 – 4 – 8 – 9 cells at a time where the number of cells releasing doubles every 10 seconds. Both cases shown in Figure 15-7

use 10 ACH of ventilation, with 10 seconds between each stage of cell release. Logically, as shown in the figure, exponentially fast propagation causes gasses to release faster which does indicate a probability of having a higher flammable volume concentration.
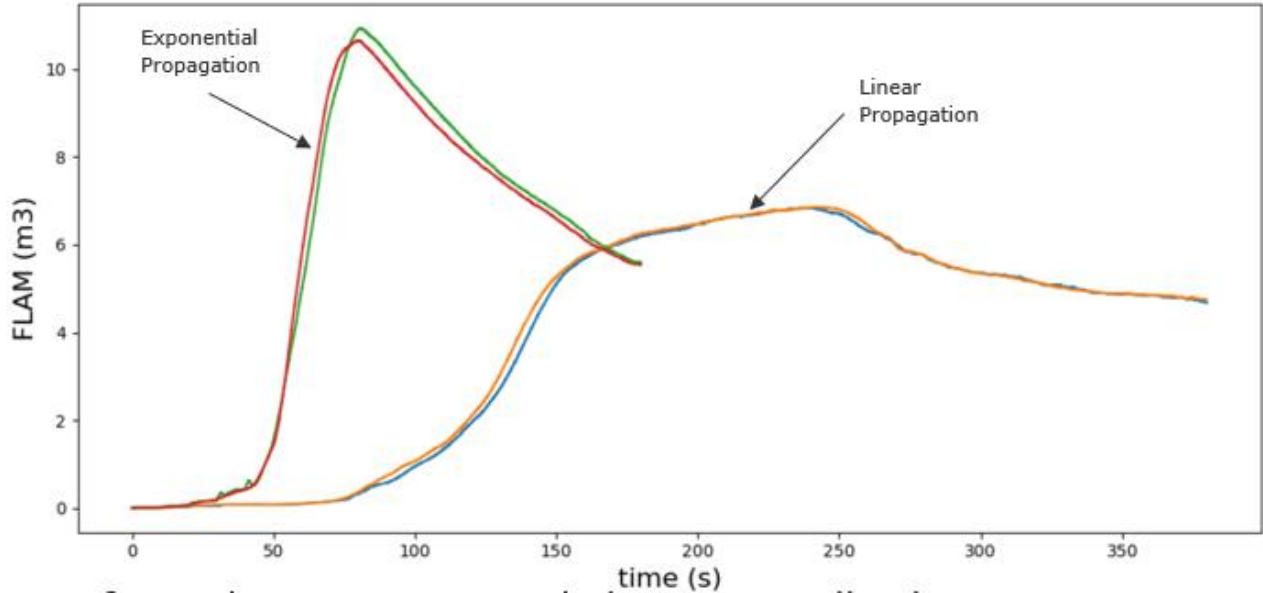
Figure 15-7 – Effect of the rate of cell to cell propagation on FLAM level from module

Figure 15-8 shows the effect of ventilation rates, explicitly 10 ACH and 30 ACH, using the case of exponential propagation as a basis. As can be seen, 30 ACH causes over 20% reduction in peak FLAM.
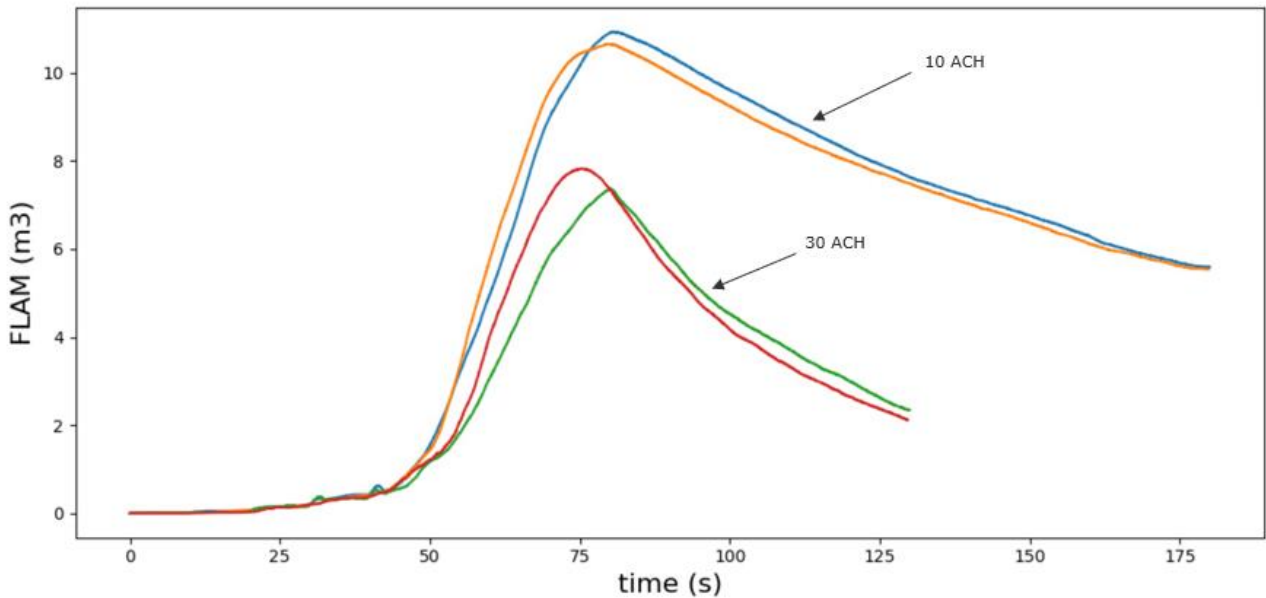
Figure 15-8 - Effect of ventilation for case of exponential propagation.

In addition, as a result of the theoretical and practical evidence of the gas' tendency to rise; it was found that locating the ventilation duct nearest the ceiling of the room produced significant effect. In the case of 10 ACH running, this relocation of the duct produced a 15 – 20 % reduction in the peak FLAM; as

shown in Figure 15-9. Figure 15-10 shows that the effect is significantly exaggerated in the case of a higher ventilation rate – when 30 ACH is running, with a reduction in FLAM of 55 – 75 %.

Figure 15-9 – Effect of higher ventilation duct location with 10 ACH.

Figure 15-10 – Effect of higher ventilation duct location with 30 ACH.

The key metric for assessing the consequence of these failures is the explosion (deflagration) magnitude – calculated as worst case: ignition at the exact time of maximum flammable volume. The approximation used for considering threat level was 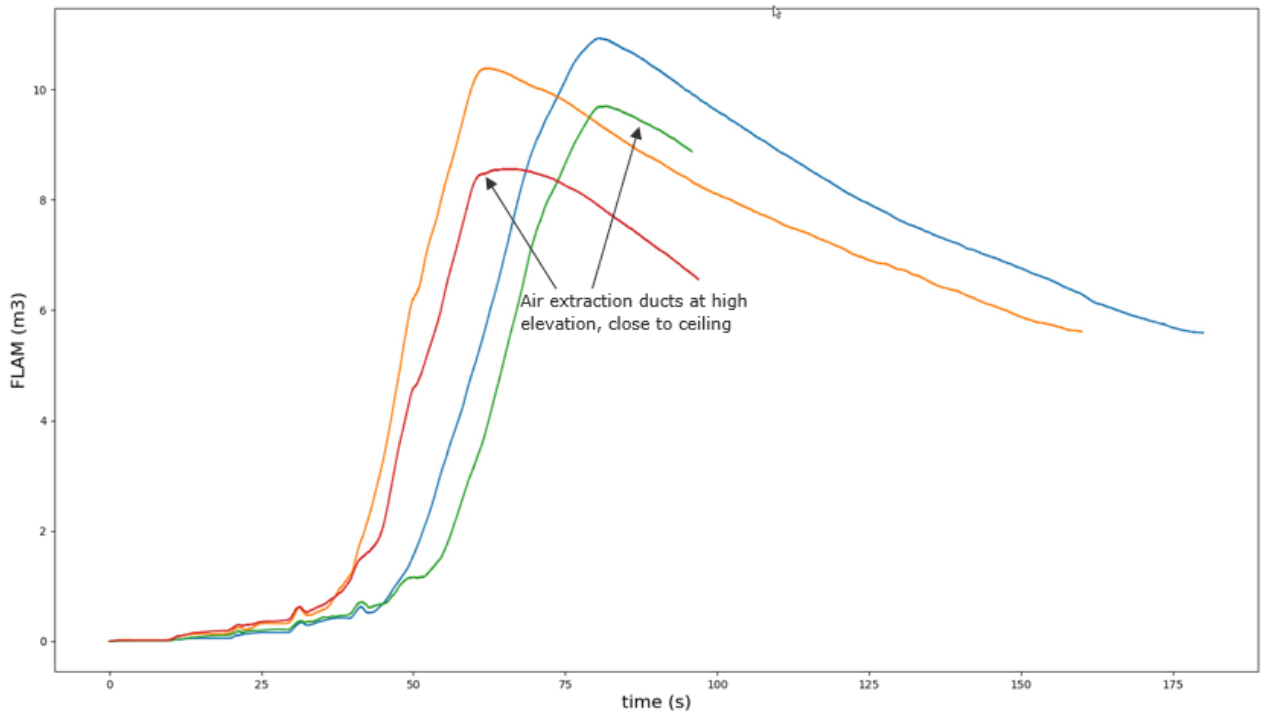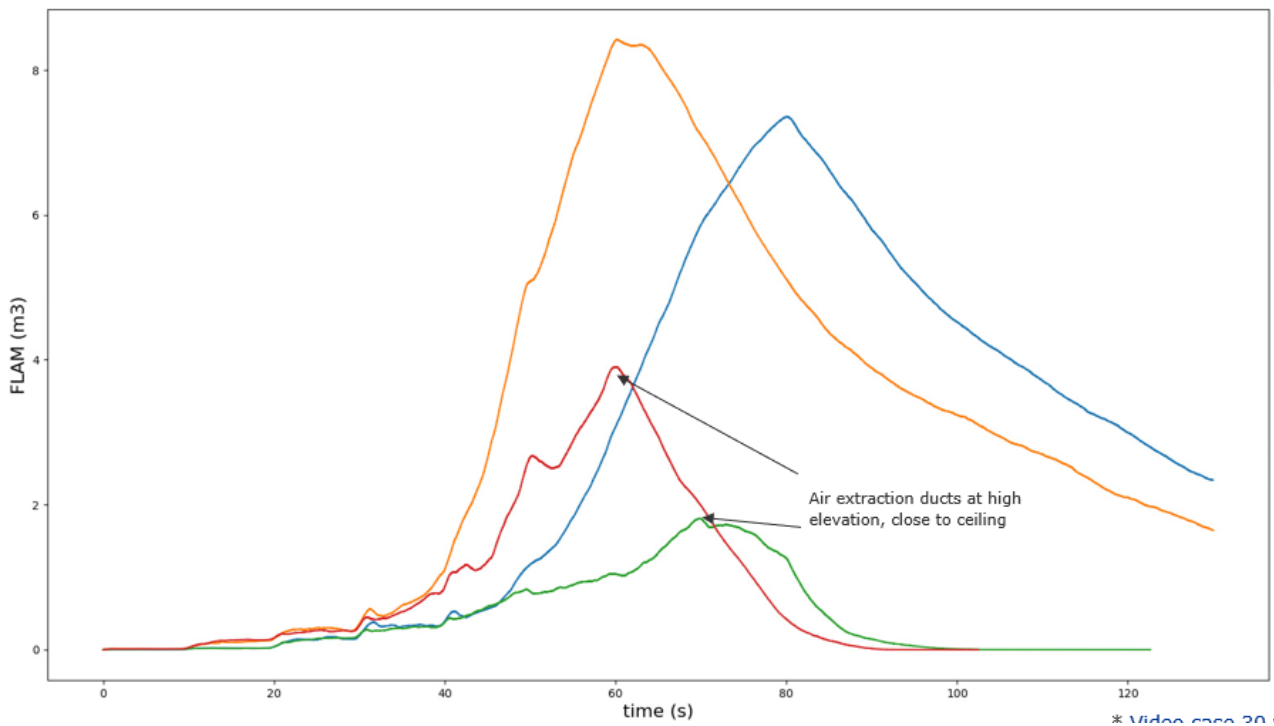structural damage to the room which was considered to result from any explosion over 1 barg. Based on this premise, we can see that several cases at the module level do present significant risk from explosion. This threshold is actually not dependent on the rate of cell propagation within the module, as we see any of these cases can produce flammable volumes with explosion potential over the acceptable limit of 1 barg. And only an ideally placed ventilation system of maximum rate is able to keep this level just barely under the threshold. Otherwise we do see that the single cell case presents a trivial explosion risk, though defining the size of cell is important for this purpose.

Table 15-2 – Summary of preliminary CFD explosion evaluations.

Case	Ventilation (ACH)	Flammable volume (m^3)	Stoichiometric Volume Approximation	Explosion Overpressure (BARg)
Single Cell	Any	< 0.08	< 0.04	< 0.02
Slow module propagation	10	7	5.7	1.8
Fast module Propagation	10	11	8.7	2.7
Fast module propagation	30	8	6.3	2.0
Fast module propagation, improved ventilation location	30	3.9	2.8	0.9

15.2 CFD Analysis based at module level tests

15.2.1 Overview and objective

Similar to the cell-scale CFD analysis described in section 13.3, the purpose of this analysis is to provide more complete information about the dynamics involved in gas release from malfunctioning batteries, where in this analysis, the release is from a full module. This is achieved by reconstructing the physical experiment described in Section 14 as a CFD simulation and utilize experimental data to "calibrate" key parameters of the CFD model against it.

The advantages/benefits tied to this is two-fold; firstly, a coherence between simulation and experiment would strengthen confidence in recorded measurements (which also naturally contain uncertainties and complications). But secondly and perhaps more importantly, a quantification of decisive release parameter is essential when running CFD in future projects; one can investigate the effects of changing

ventilation, geometry and other parameters, and ultimately predict the impact of other battery-related scenarios (e.g., thermal runaway scenarios in battery-rooms in ships).

The module level simulations described in this chapter obtain the size and location of the flammable gas cloud in the container when there is no ventilation, and with two different ventilation rates. This is used to assess the effectiveness of the ventilation, and to aid in the location of gas detectors, etc.

15.2.2 Methodology

Again, as with the cell-scale analysis (Section 13.3), the key unknown parameter to determine using CFD simulations is the release profile (time-varying rate of mass, kg/s) of gas released from the module. This can be achieved by reconstructing the test scenario as a simulation and then compare the resulting gas concentrations and temperatures in the simulation with those measured in the experiment. The model is run iteratively to approach a "best-fit" release profile, hence producing an estimation of the actual amount of gas released, and which temperature. All simulations were performed with the software FLACS /5/.

15.2.2.1 Scenario selection

Among the list of conducted experiments, the following three is considered the most suitable (most reliable measurements, satisfactory combustion level etc). The cases are also selected with one case with no ventilation, and two cases with different forced ventilation. Figure 15-11 indicates the LEL% sensor data for Test 1, peaking at 69%.

Table 15-3 List of "target" cases from experiments to reconstruct using CFD. The LEL% value is measured from the experiments.

Test	Cell	Ventilation ACH	LEL%	Notes
1	LGC	0	69%	Fully enclosed container with no forced ventilation. Cracks modelled with small openings for outflow.
20	LGC	6	30%	Low pane opposite of battery racks replaced with fan, high pane behind racks open
21	LGC	30	0%	Same scenario as Test 20, but with increased ventilation.
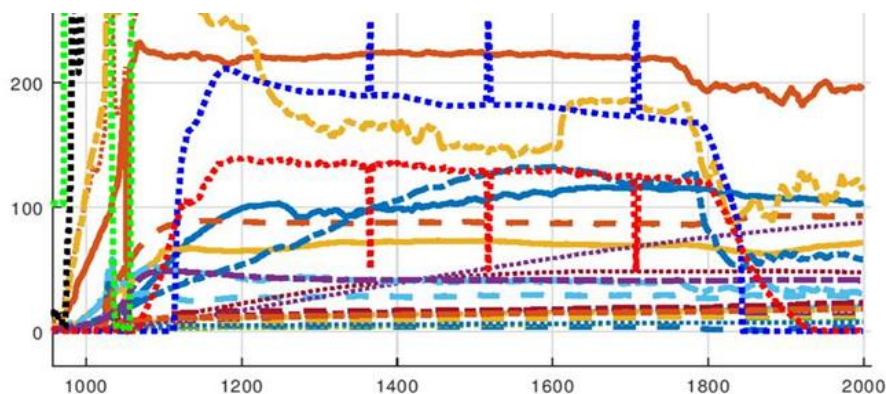
Figure 15-11 Sensor readings from the experiment Test 1. The red stapled line shows LEL*200, peaking at 69 % LEL after approximately 200 s after thermal runaway.

15.2.2.2 Geometry

Figure 15-12 shows a screenshot from the interior of the geometry model, aiming to represent the experiment surroundings (described in test setup, Section 14.1) in sufficient detail to recreate the relevant physics. For *Test 1,* the container is fully enclosed with no openings. However, for numerical stability, and to reflect that it is still not fully air tight, 5% porosity is attributed to the sealed/packed openings in order to let some air or gas slip through. For cases *Test 20* and *Test 21*, virtual fans are employed so that ACH reaches roughly 6 and 30 1/h, respectively.
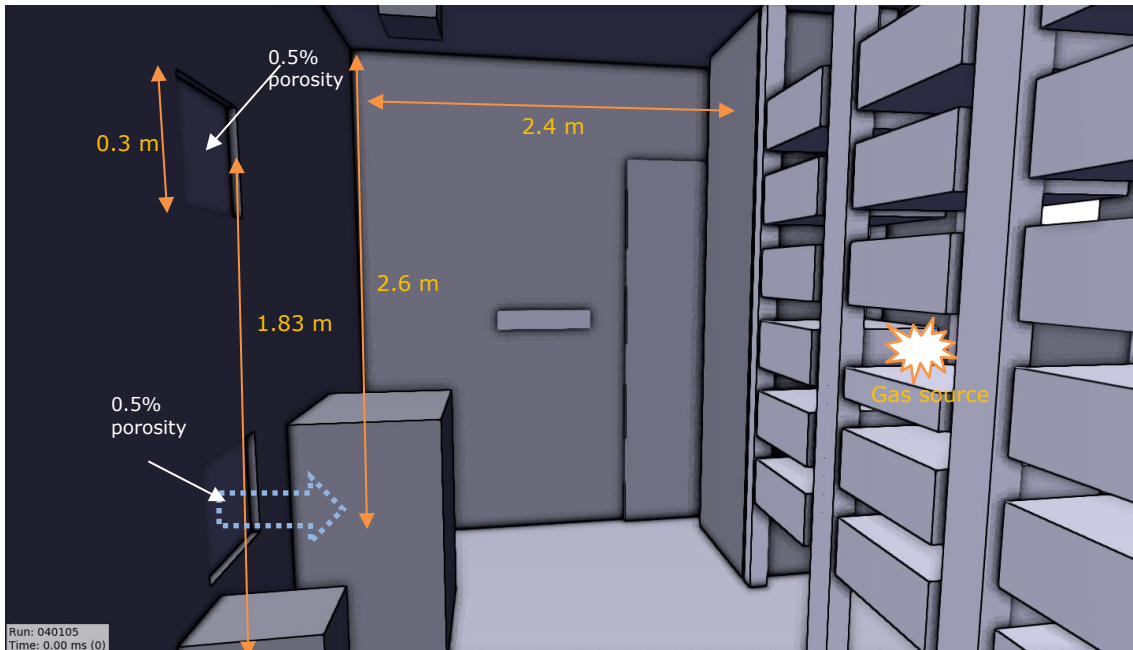
Figure 15-12 Screenshot from the simulation domain interior, indicating location of gas source and room dimensions. Blue dotted arrow shows the virtual fan placement in Test 20 and 21 as well as venting direction. The length of the container is 5 m. The closed openings in Test 1, modelled with 5% porosity, are visible on the wall to the left.

15.2.2.3 Domain, grid and gas source

The simulation domain is limited to the interior of the container, with constant pressure boundary conditions on all sides. The grid consists of uniform, cubical 5 cm control volumes throughout the entire domain (illustrated by light lines in Figure 15-13). The gas emanating from the battery is represented as a diffuse, momentum less gas source situated as indicated on Figure 15-12 and Figure 15-13.

The air temperature in the simulation is set to 2 °C, equal to the temperature the day the test was performed.
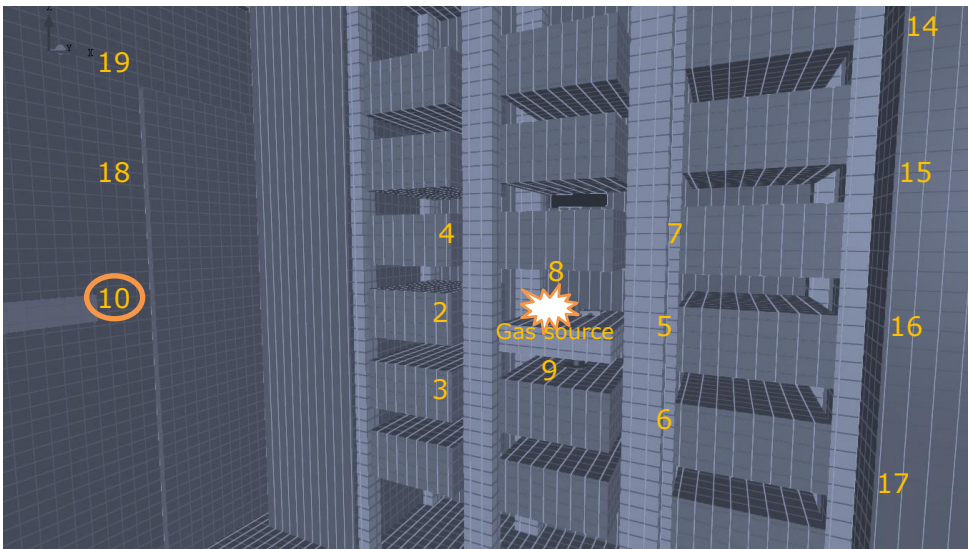
Figure 15-13 Geometry and super-imposed grid indicating size of control volumes (5 cm). Numbers indicate the location of virtual monitor points used in the simulation (most being equivalent to gas meters and thermocouples in the experiment. Monitor point 10 represent the gas LEL% meter used in the experiment.
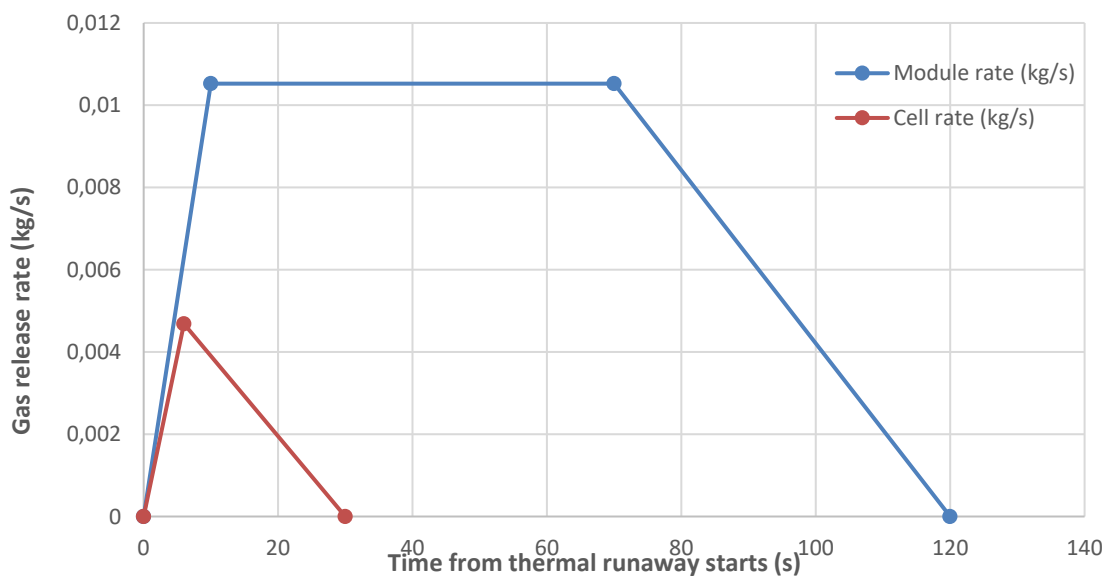
Figure 15-14 Theoretical/principle release profile used in the simulations.

The release profile shown in Figure 15-14 reflects the volatile part of the thermal runaway process with the highest rate of gas release. The cell rate is the same used in the cell level CFD models in Figure 13-40. The small initial release observed in the experiment is not reflected in the model.

The release can be defined by the following parameters:

- Release rate, given as a function of time. For the module release, a relatively quick propagation from cell to cell is applied. It is considered likely that it propagates to two cells in each step. Typically, a function that rises quickly (over 2-10 s) to a maximum release rate, then a constant release rate for a certain period before linearly decaying.

- Total volume or mass of gasses released, typically 2 l/Ah or possibly higher.

- Maximum release rate typically, 0.001 to 0.02 kg/s.

- Experiments indicate that released gas is roughly 450 °K.

- Composition of the release is given below based on measurements.

- Typical density of the released gas from 0.3 to 0.5 kg/m^3.

For the module tests, it was observed open fires producing a lot of smoke. It is likely that the air supply is insufficient to produce incomplete combustion.

The released gas in the simulation represents the gas or smoke that is generated *after the fire*. It is an incomplete combustion and the released gases hence has used some of the O2 that came from the air before it combusted. The released mass of gas in the simulations is therefore a bit larger than the pure released mass of gas from the module.

15.2.3 Simulation Results

Based on the methodology above, the leak profile in Figure 15-15 were estimated based on comparison between test measurements and equivalent data (virtual measurements) from the simulation. The graph indicates a quick rise and a slightly longer tail, encompassing an area (total released gas) exceeding 820 liters. Assuming 6 cells with 63 Ah per cell, this equals approximately 2.2 l/Ah. The blue and green stapled lines represent hypothetical release profiles for larger batteries able to release indicated amount of gas during a thermal runaway. In order to release more than 3000-4000 l, it is expected to require an escalation between modules, as illustrated in Figure 15-22 .
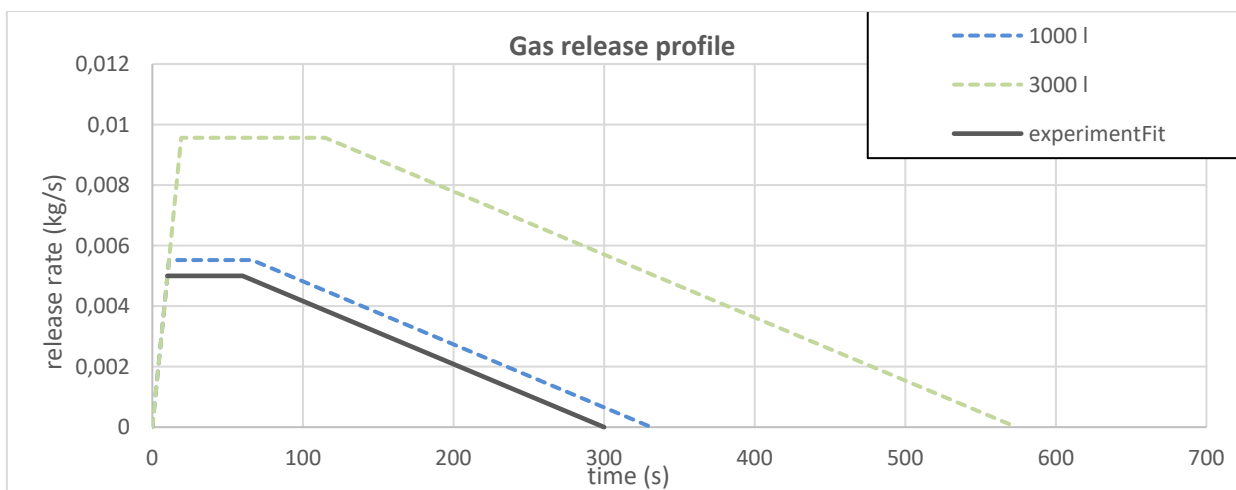
Figure 15-15 Release profile used as basis for the simulations presented above, equivalent to 820 liters of gas (2.2 l/Ah). The dotted lines indicate the same release profile scaled up to 1000 l and 3000 l of gas.

The following simulation results were obtained when employing the release profile in Figure 15-15 for simulated reconstructions of Test cases 1, 20 and 21 (Table 15-3).

Figure 15-16 shows %LFL during simulation of Case 1, as recorded by virtual monitor points at elevations 1.5, 1.7, 2.0, 2.3 m (respectively for monitor points 10, 18, 19, 20 and 21). It is immediately evident that the resulting gas concentration is highly dependent on height, i.e., that there is a strong

vertical gradient due to gas buoyancy. Monitor point 10, placed at a position corresponding the LEL%-meter in the experiment, shows a peak value around 70%, which matches fairly well with the test measurements presented in Table 15-3. The vertical stratification is also evident from virtual thermocouples in Figure 15-17. However, the temperature increases near the ceiling are significantly larger than measured in the experiment. The reason for this may be that the simulation does not incorporate heat transfer between gas and geometry, as would be the case in reality (the cold metal would act at as a heat-sink for the gas temperature inside. There may also be that the (input) gas discharge temperature of 450 °K is overestimated and could in reality be slightly lower.
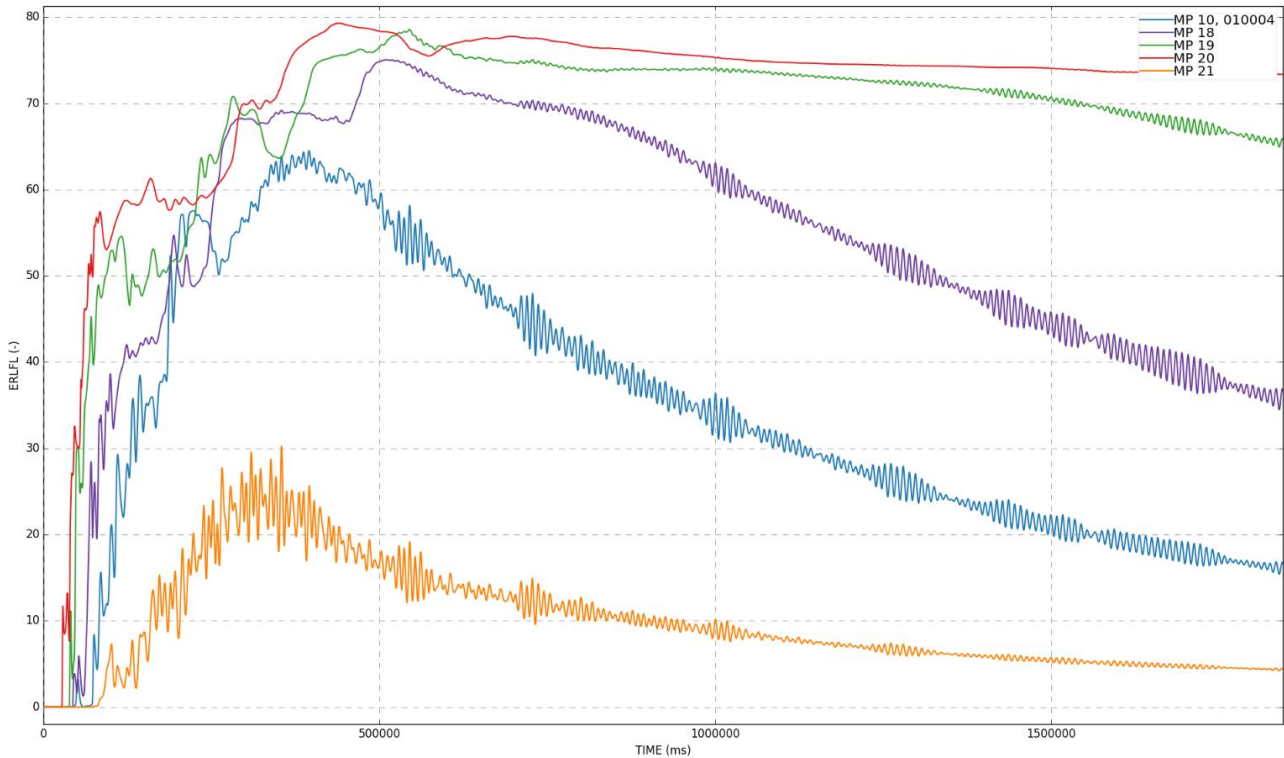
Figure 15-16 Percentage of LFL shown at five different monitor points (see Figure 15-13). Monitor 10 is analogous to the gas meter in the test chamber.
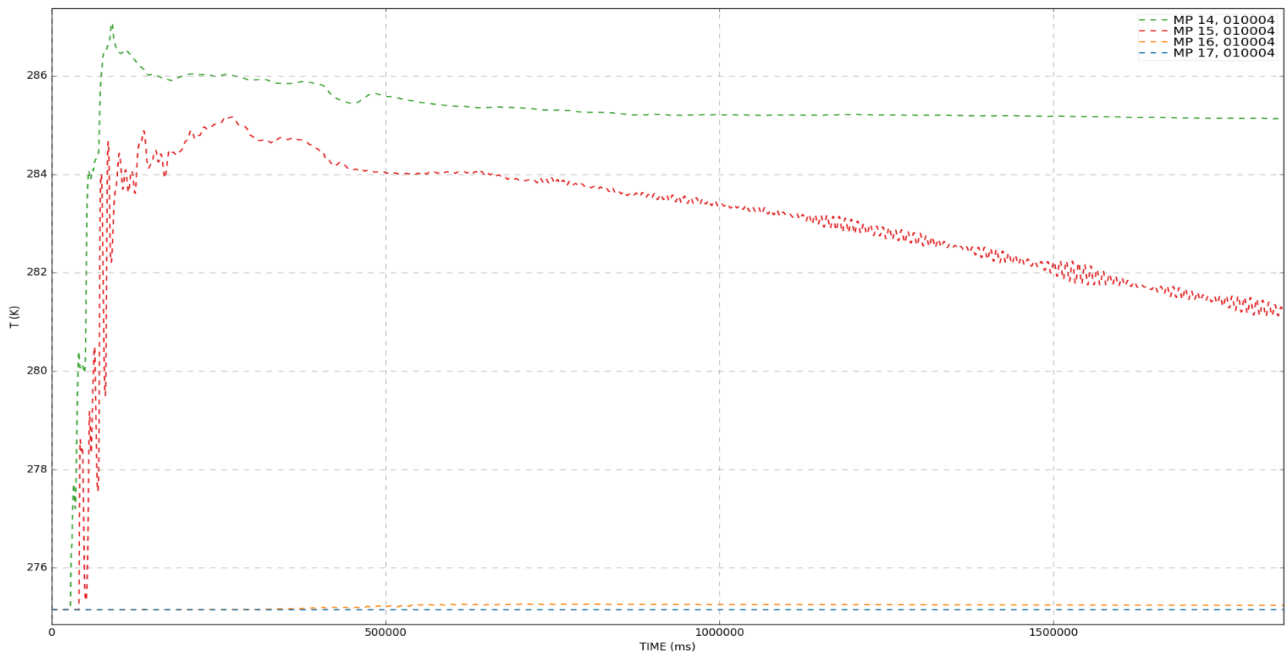
Figure 15-17 Temperature (ºC) at four different monitor points (see Figure 15-13). Monitor 14 to 17 are equivalent to the thermocouples mounted on the drywall, shown in Section 14.1)
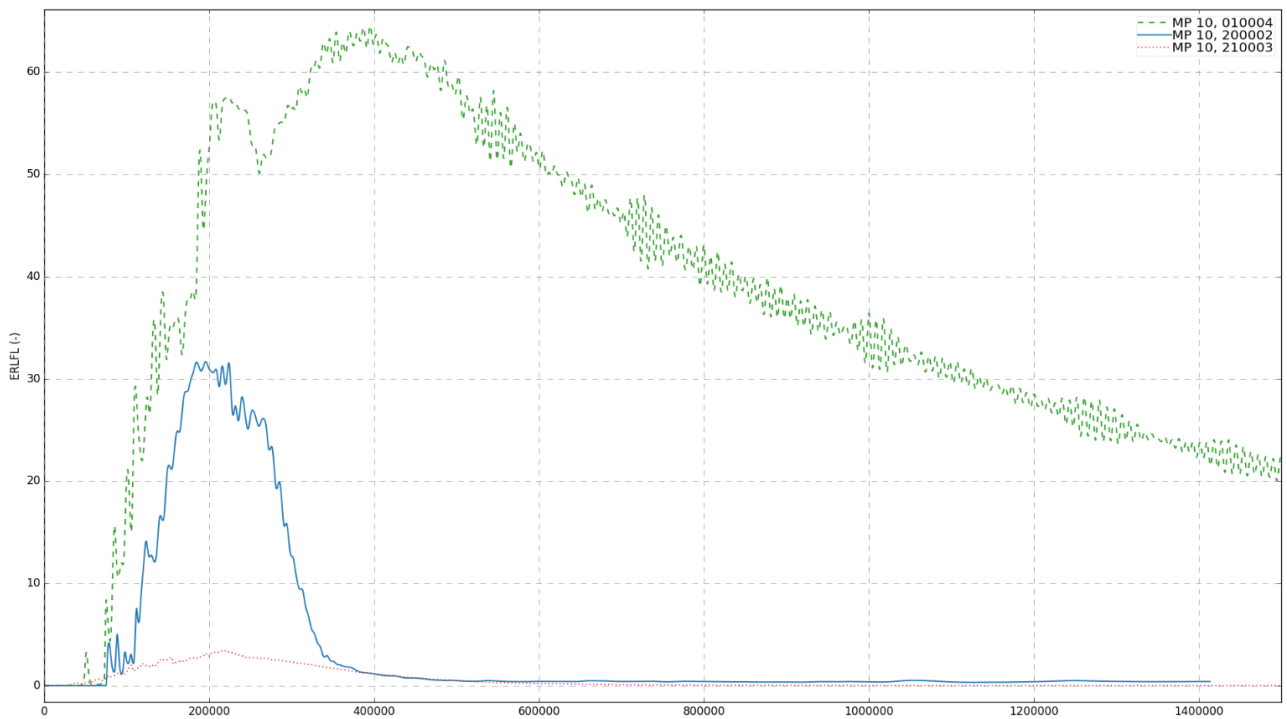
Figure 15-18 Transient %LFL for indicated runs (the two first digits indicate the corresponding test case)

Figure 15-18 shows %LFL values for the three cases (1, 20 and 21) using the same release profile. Peak values are 63, 31 and 4 %LFL, which is comparable to the measured values listed in Table 15-3. While a decent fit, the difference between high and low ventilation is however slightly lower than indicated by the experiments. It should be emphasized that the graphs are highly dependent on elevation of the monitor

point, considering the strong vertical stratification. Because of this, it is found that at least two gas meters at different heights would offer more robust conclusions compared to the single one available in the experiments conducted for this analysis. Figure 15-19 shows the development of flammable cloud size (m^3) during the same three cases. It is evident that moderate ventilation levels, such as 6 ACH, will cut down cloud sizes with roughly 60%. When increasing ventilation in the test chamber to 30 ACH, the reduction of the largest cloud is above 80%.

Figure 15-20 shows the hydrogen concentration throughout the simulations of cases 1, 20 and 21, in terms of volumetric portion (m^3/m^3). The hydrogen concentration for monitor point 10 (again location equivalently to the gas meter in the experiment) is 1.7%. This is only slightly higher than the 1% concentration that was measured in the experiment, but relative terms is constitutes a substantial discrepancy of 70%.

In conclusion, the results from the iterative simulations seem to support an estimation of 2.2 l Ah per module and suggests a release profile of the type presented in Figure 15-15. This observation is used as a basis for generic room volume and ventilation sensitivities in Section 15.3.
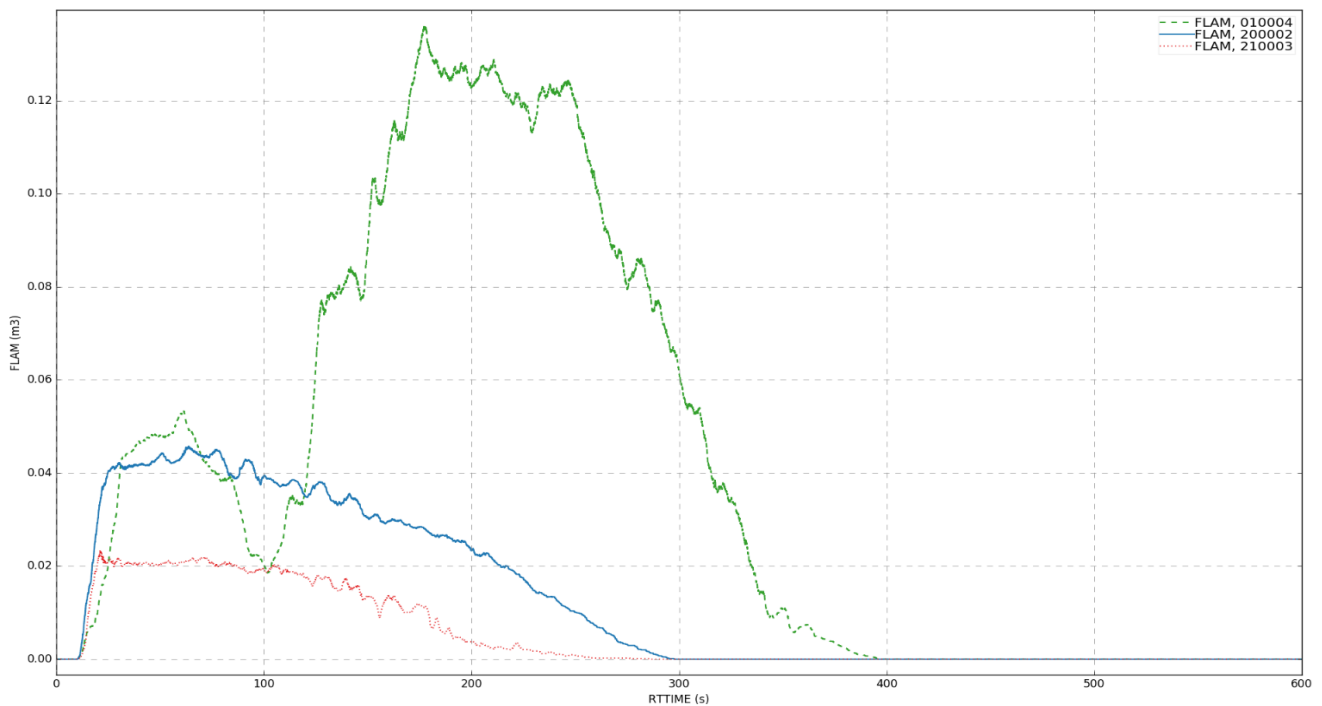
Figure 15-19 Volume [m^3] of flammable clouds vs time. Green line is with 0 ACH, blue is with 6 ACH and the red is with 30 ACH
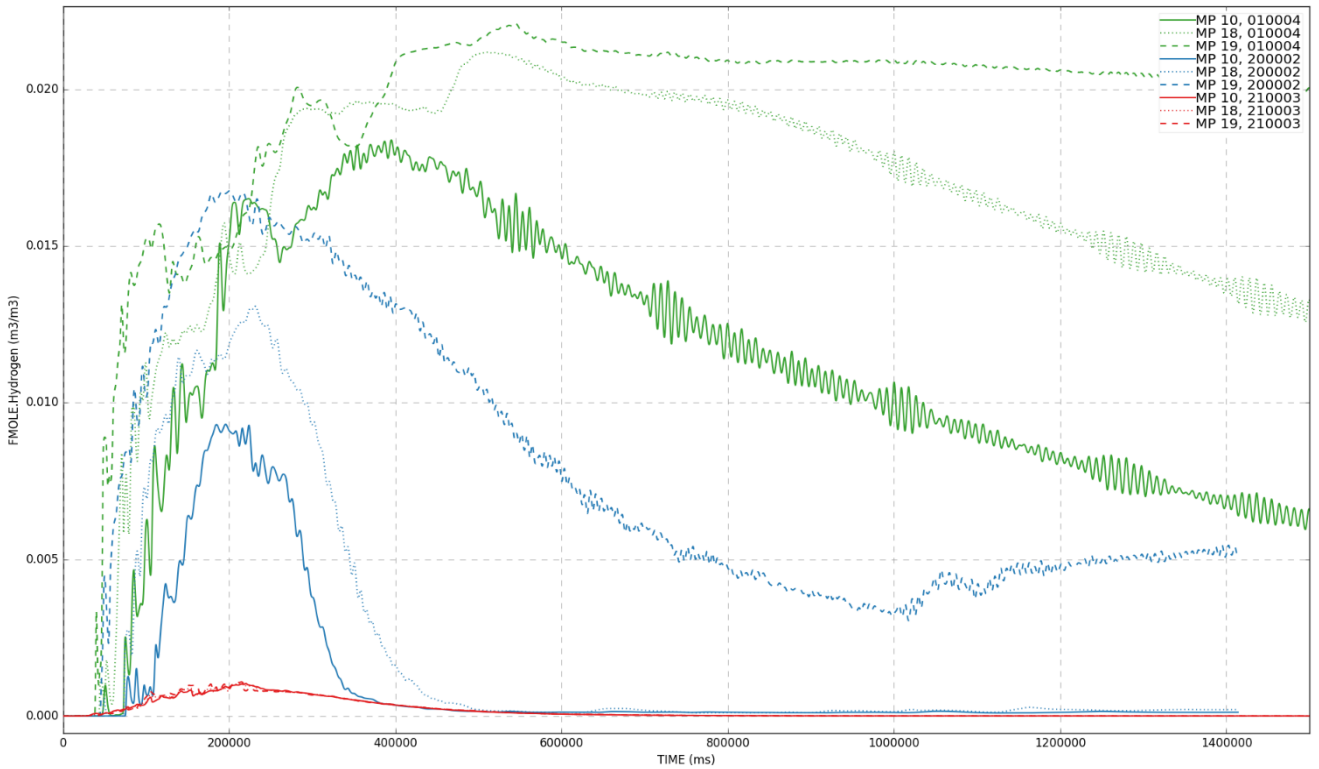
Figure 15-20 Hydrogen fraction throughout the simulations.
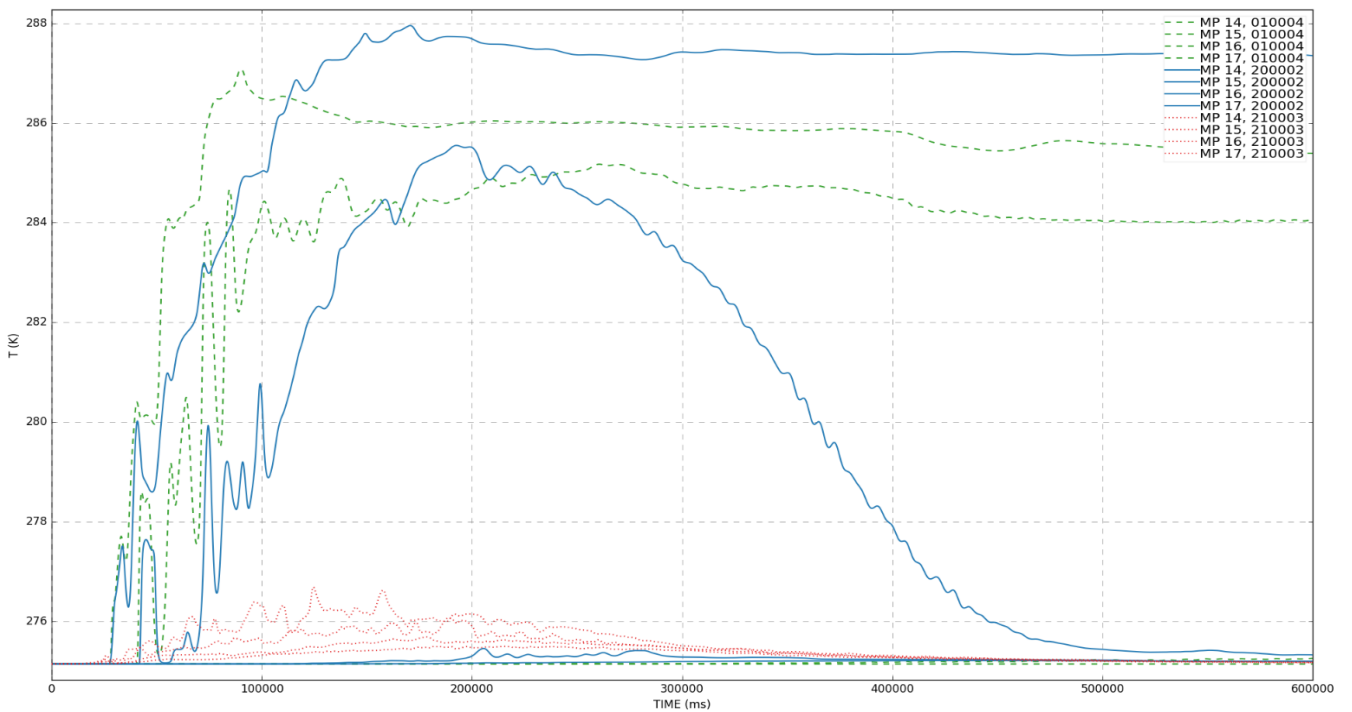
Figure 15-21 Temperature at monitor points 14 through 17 (corresponding to thermocouples mounted at the drywall).

Figure 15-21 shows temperatures at the drywall thermocouples for cases 1, 20 and 21.

15.3 Battery room ventilation requirement assessment

Mitigation of explosion risk due to off-gassing in a battery room can be done by ventilation. The purpose of the ventilation is then to dilute and air out the combustible gasses before they can accumulate and cause an explosion.

The goal of this assessment is to provide requirements for ventilation rates in battery rooms. An approach is developed where designers can find required ventilation rates based on the main battery room design parameters. The main effects and parameters that needs to be available are the room size in free open space (m3), size of the battery that can create off-gas (Ah) or amount of off-gas that can be released from an event (Nm3), strength of walls against an internal explosion pressure build-up in the room (barg).

15.3.1 Basis for modelling

In the present assessments, the minimum air ventilation rate that can prevent an explosive atmosphere is found by running a CFD model of the off-gassing scenario in two different battery rooms.

The following basis is used for this assessment:

- The type of cells and modules that is assumed in the battery room are the ones which will vent the gasses out in the room. If the modules and racks are equipped with closed ventilation systems that can collect the gasses, then the present assessment is less relevant.

- It is assumed that a propagation test of the modules and racks is performed so that the number of cells and modules that can cause off-gassing is known. This number of cells and modules that can create off-gas is used to set the size and duration of the off-gassing scenario.

- The scenarios considered are scenarios that only produces combustible gas and is not ignited during the scenario. In most accidents and tests, the off-gassing event is ignited by the hot runaway cell or module causing a fire instead of an explosion. The scenario considered with no ignition and a late ignition after a large cloud is formed occurs less frequent, however, it is a scenario that can happen, and it should therefore be designed for.

- It is assumed that the ventilation strategy is to have an inlet of fresh air to the room, and an outlet that goes to a safe location. The ventilation system needs to deliver a certain air change rate (ACH) which is the aim of the analysis to find. It is also assumed that the ventilation system is running during the off-gassing event. It can be started as a high emergency ventilation rate when combustible gas is detected provided it starts early during the off-gassing scenario, before the peak bursting of gas is occurring. The ventilation must run with the high ventilation rate until a fire is detected, or until the off-gassing scenario gets too large for the ventilation to handle.

- It is not assumed that there are explosion relief panels in the walls or roof of the battery room. If such panels are installed, a larger gas release and gas cloud can be mitigated. A combination of ventilation and release panels can in some cases also be necessary.

- Two battery rooms are used in the modelling, and if the battery room at hand is very different (e.g. much larger or smaller) then the present assessment may not be valid, and a separate assessment is recommended. Details of the modelled battery rooms are given below.

- It is assumed some specific ventilation arrangements in each of the modelled battery rooms. Details of each ventilation system is provided below. If the ventilation arrangement is very different, a separate assessment is recommended.

- The pressure that the walls of the battery room can withstand is a design parameter that is used to decide the allowed cloud size and ventilation rate.

15.3.1.1 Quantification of release from the off-gassing event

The amount of gas coming from the off-gassing event as a function of time is shown in Figure 15-22. This release rate "profile" is used for both battery rooms.

This release profile is obtained after assessing test results from several tests. The total amount of gas as well as the duration of the event, the initial growth rate, and the flat constant release rate at the top of the curve are all important parameters that influences the gas cloud size. All these parameters are adjusted to cover typical events that are observed, with a conservative approach to set the curve parameters when experiments show some variations. The release profiles should hence be realistic and on the safe side.

For different battery types (cell types, modules and racks), the amounts of off-gas coming from an event is often not known from testing since it is difficult to measure, and it is not required to measure and quantify the amount of off-gas. Therefore, it is developed a typical amount of off-gas related to the size of the battery. The rule of thumb is that 2l per Ah is typically coming from an event. Using this, the battery sizes used in the models are 500, 1 000, 2 000 and 4 000 Ah.

It is further applied that only one module is erupting for the first three cases, i.e. the gas is coming out from only one module. In the last case with 8 000 l, it is assumed that the event is escalating to the above neighboring module above after 3 minutes.

A module in the center of the rack is assumed failing and releasing the gas in the model.

The gas composition with a large amount of hydrogen is applied for both battery rooms, see Table 15-4. This composition has been observed and measured as the worst plausible from various perspectives (Lower flammability level, range of flammability limits, reactivity etc) and is hence a possible and conservative composition. In the future, it is also possible that observations of degassing tests show chemicals with different characteristics or concentrations, that could change the picture. Then, further analysis is necessary.
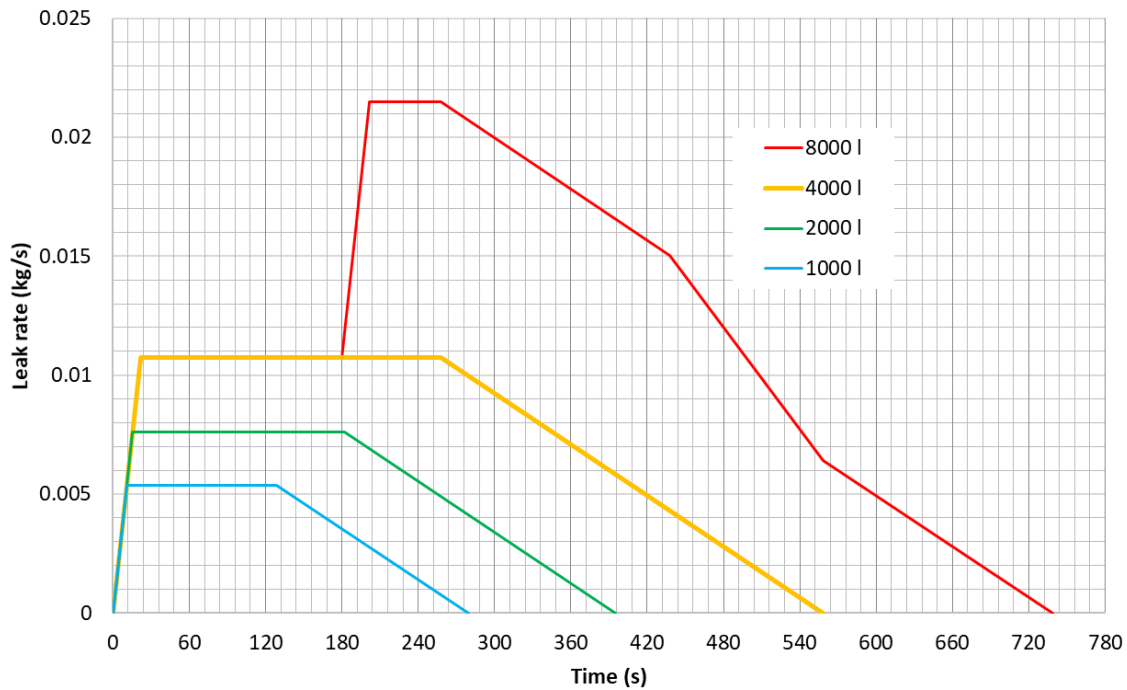
Figure 15-22   Amount of gas as a function of time (release profiles) applied when modelling the off-gassing events for both battery rooms. Up to 4 000 L (liter) is assumed to erupt from one module. The 8 000 L case is from two modules where it is assumed that the second module is escalating after 3 minutes.

Table 15-4   Gas composition used for both battery rooms.

Component	C1, Methane	C2, Ethane	CO	CO2	H2
Mole percent	10	10	30	0	50

15.3.1.2 Geometry and designs of battery rooms

Sizes and plots of the battery rooms are shown in Table 15-5 and Figure 15-23.

Table 15-5   Main volumes of the battery rooms used. The total volume includes all internal solids, whereas for the free volume has the solid volume been subtracted.

	Small room	Large room
Description	Same as in module test, Chapter 15.2	Same as in initial CFD runs, Chapter 15.1
Total volume	22 m^3	31 m^3
Free volume	15 m^3	25 m^3
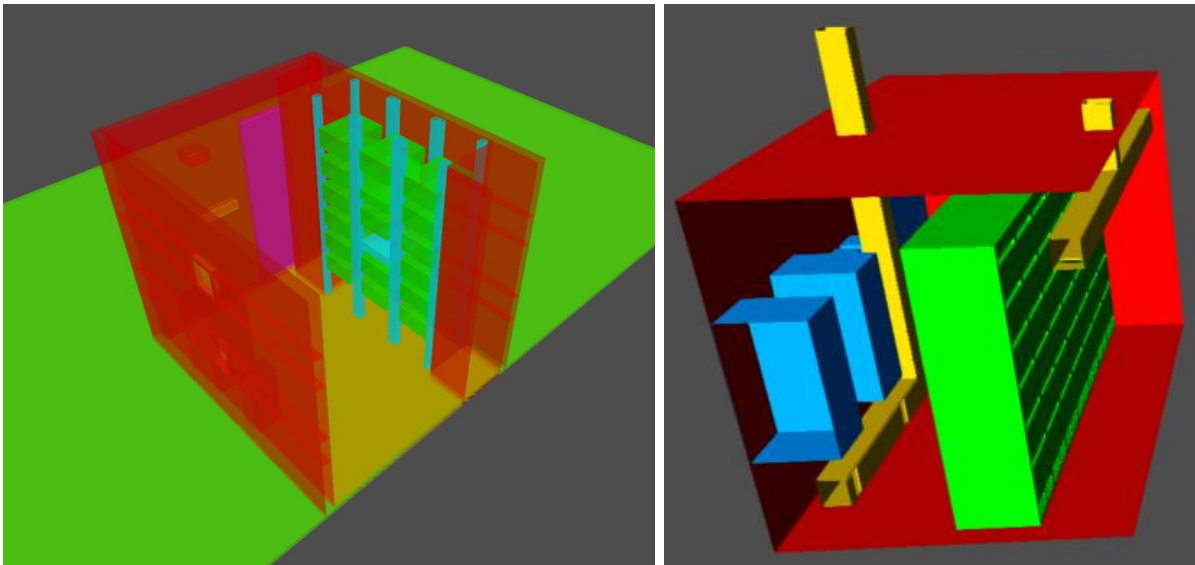
Figure 15-23   Geometries of the two battery rooms, small room to the left and large room to the right.

15.3.1.3 Ventilation arrangements

Testing show that during the most active part of the off-gassing event the gasses are hot and therefore lighter than air. The ventilation arrangement is therefore with inlet air close to the floor, and the outlets close to the ceiling.

Only the room is modelled with air flow in and out, and it is not relevant to specify in the model if the location of the fans is at the inlet (blowing) or at the outlet (sucking). The flow that is modelled can this way be representative for both arrangements. The room is modelled completely air tight except from the inlet and outlet ducts.

For the small battery room, the ventilation inlet is low on the long wall and the outlet is located 0.8 m down from the ceiling on the short wall (see results section).

For the large battery room, the ventilation inlets are along the long wall with four inlets close to the floor, seen with the yellow duct in Figure 15-23 and the outlet is along the opposite wall with four outlets close to the ceiling, 0.4 m down.

Internal ventilation is also modelled to represent air cooling fans on each module. This is running during the scenario.

It is also applied that the air inflow and extraction is already running before the release scenario starts. This could represent a constant ventilation, or a ventilation system that is turned on at a certain detection of a low flammable gas concentration in the room. It can also represent a low ventilation that is running constantly which is ramped up at a detection of a low flammable gas concentration. The off-gassing scenario is typically starting slowly with a small release of flammable gas that can be detected, hence it is assumed that it is possible to start the high extraction ventilation before the most intense part of the off-gassing scenario takes place.

The ventilation philosophy and recommendations are further discussed in the results section.

More details of the effects of the ventilation can be seen in the results section where the velocity vectors show flow directions and strengths.

15.3.1.4 Simulation cases

Simulation cases were first defined with a matrix of different release cases and ventilation rates as illustrated in the matrix below. The orange cells represent the focus area where the threshold cloud sizes are expected to be. E.g. for a larger release volume, it is expected that a higher ventilation rate is needed. After running the first batch of cases, some new simulations were run so that a better resolution could be found around the points where the critical cloud sizes are found.

Table 15-6   Illustrative matrix of cases investigated with variation in the total volume of gas released and the ventilation rate. Keeping the total volume of gas released constant when varying the ventilation rate, the effect of ventilation is found. Yellow is expected to give a small cloud, red is expected to give an unacceptable cloud, and orange is expected to be on the borderline.

Total gas released: / Ventilation rate:	Very Small 120 l	Small 500 l	Small 1000 l	Medium 2000 l	Large 4000 l	Very large 8000 l
0						
low						
medium						
high						

Table 15-7: List of simulation cases executed with input parameters and main results, both for container 1 (Free volume 15 m³) and container 2 (free volume 25 m³).

Case no.	Total Release (L)	Emergency Vent ACH	Results		
			Cloud Size, Q8 [m³]	Fill fraction	Over-Pressure [barg]
Container 1: Total 22m3, Blocked 7, Free 15m3					
010001	1000	0	6.3	0.42	3.35
010002	1000	2	6.1	0.41	3.25
010003	1000	5	5.6	0.37	3.00
010004	1000	10	5.0	0.33	2.65
010005	1000	20	4.0	0.27	2.15
010105	1000	30	3.3	0.22	1.76
010006	1000	50	2.3	0.16	1.25
010107	1000	80	0.0	0.00	0.03
010007	1000	100	0.0	0.00	0.02
020001	2000	2	6.6	0.44	3.51
020002	2000	5	6.4	0.42	3.40
020003	2000	10	6.0	0.40	3.21
020004	2000	20	5.2	0.35	2.76
020005	2000	50	3.4	0.22	1.79
020105	2000	80	2.0	0.14	1.09
020106	2000	90	0.2	0.01	0.11
020006	2000	100	0.1	0.01	0.06
040001	4000	10	6.2	0.41	3.31
040002	4000	20	5.6	0.37	3.00

040003	4000	50	4.3	0.29	2.28
040004	4000	100	0.7	0.05	0.38
040104	4000	110	0.4	0.03	0.20
080001	8000	20	5.6	0.37	2.97
080002	8000	50	4.2	0.28	2.23
080003	8000	100	4.3	0.28	2.27
Container 2: Total 31m3, Blocked 6, Free 25m3					
120001	120	0	0.015	Negl	0
120002	120	2	0.015	Negl	0
120003	120	5	0.015	Negl	0
120004	120	10	0.015	Negl	0
120005	120	20	0.015	Negl	0
500001	500	0	5.2	0.21	1.65
500002	500	2	4.5	0.18	1.43
500003	500	5	3.6	0.14	1.15
500004	500	10	1.6	0.06	0.50
500005	500	20	0.1	0.01	0.04
010001	1000	0	12.3	0.49	3.93
010002	1000	2	9.9	0.40	3.17
010003	1000	3	7.4	0.30	2.38
010004	1000	6	5.3	0.21	1.70
010005	1000	12	3.2	0.13	1.04
010105	1000	30	0.2	0.01	0.07
010006	1000	50	0.09	0.00	0.03
010007	1000	60	0.08	0.00	0.02
020001	2000	2	11.83	0.47	3.79
020002	2000	5	9.90	0.40	3.17
020004	2000	20	5.67	0.23	1.81
020104	2000	30	3.7	0.15	1.17
020005	2000	50	0.3	0.01	0.09
020006	2000	60	0.1	0.00	0.03
040001	4000	10	8.3	0.33	2.66
040002	4000	12	7.6	0.30	2.42
040003	4000	20	6.6	0.27	2.12
040102	4000	30	6.1	0.24	1.96
040103	4000	50	1.2	0.05	0.39
040004	4000	100	0.2	0.01	0.06
080001	8000	20	10.1	0.40	3.22
080003	8000	50	8.0	0.32	2.55

15.3.2 Simulation results

Transient simulation results showing the cloud size as a function of time from all cases is shown in Figure 15-24. The cloud size reaches a maximum during the end of the release when the release rate starts decaying. This maximum cloud size is found for each case (see table with cases) and is used in the further analysis as representative for each scenario. It is hence applied that ignition occurs during the worst time when the cloud is largest.
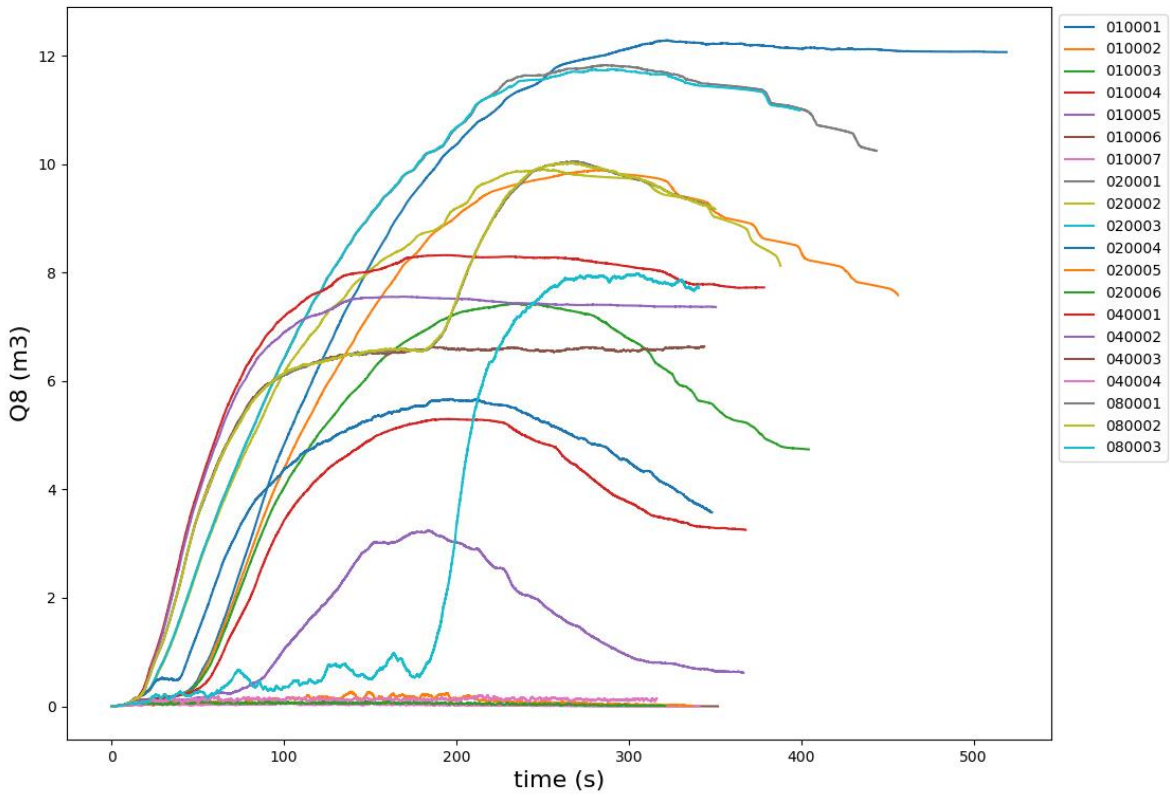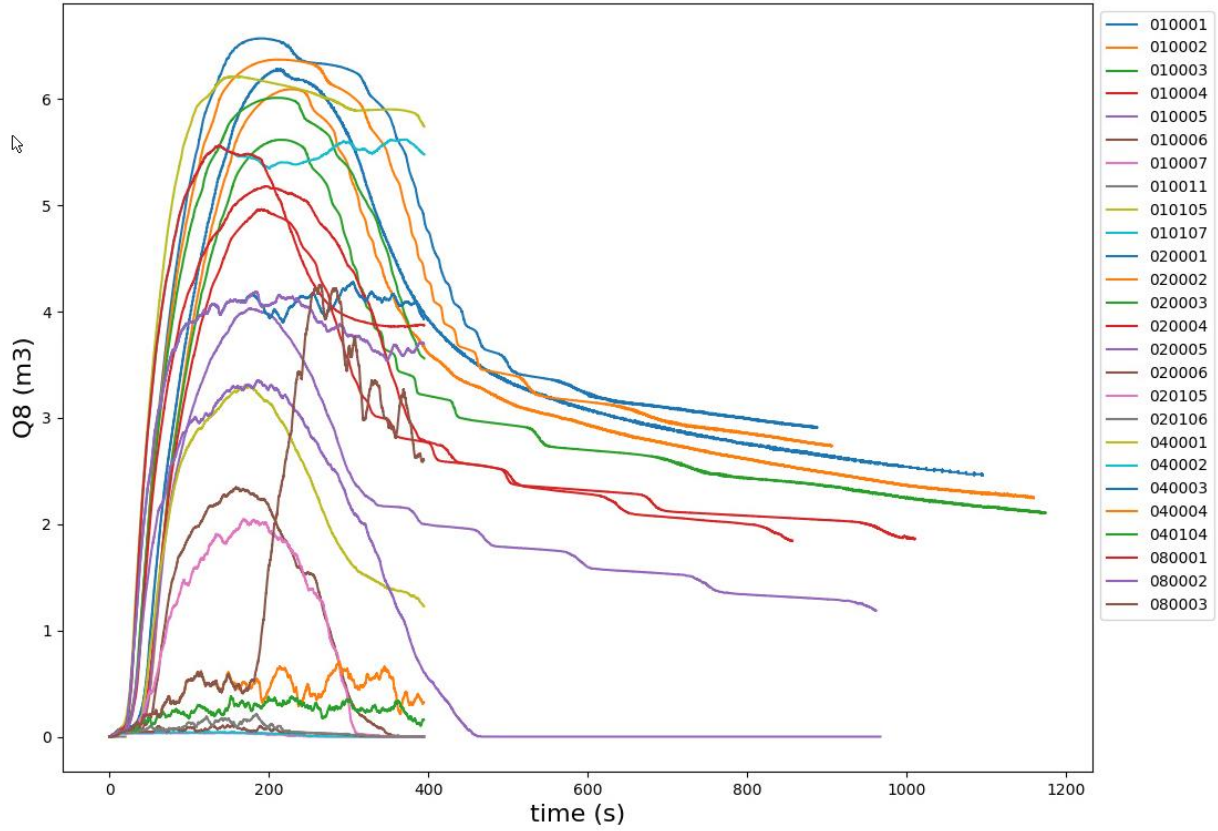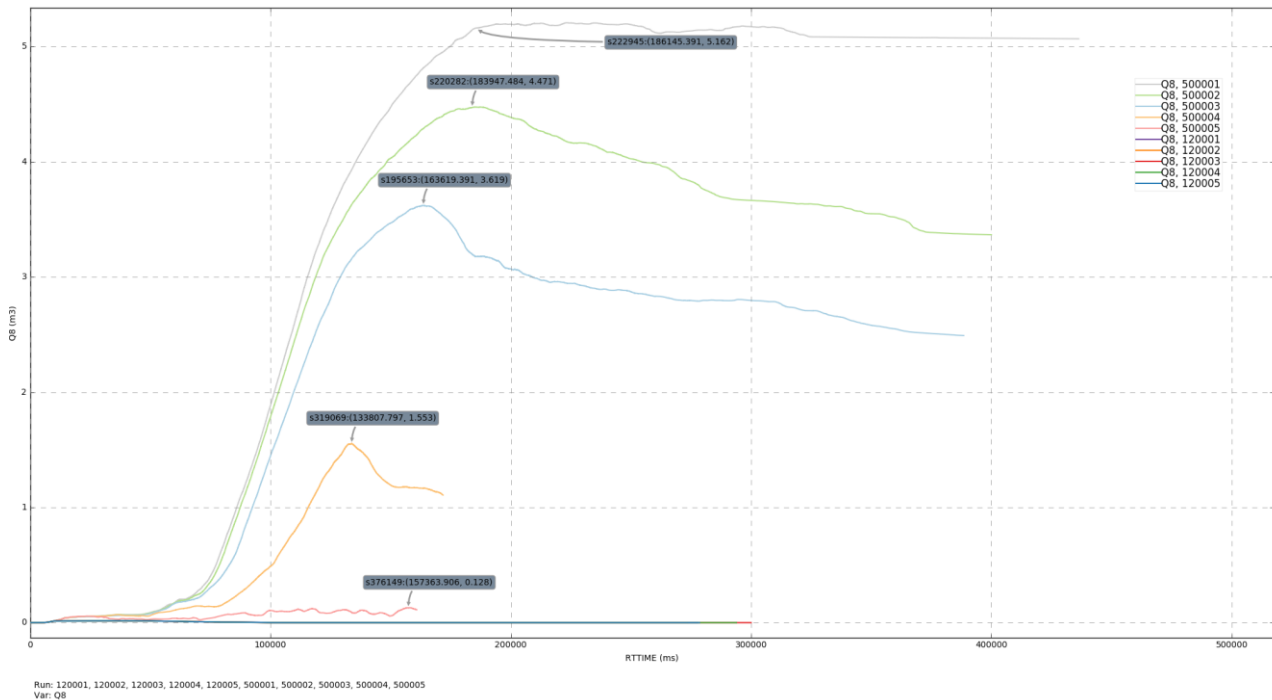
Figure 15-24   time development of the equivalent stoichiometric cloud size Q8 for all cases. Upper plot, small container; lower plots, large container large releases (top) and small releases (bottom).

15.3.3 Analysis of needed ventilation rate

The main results are plotted in Figure 15-25 showing the effect of increased ventilation for different release sizes. The trend that the cloud size goes down when ventilation increases is shown, and the point that causes the cloud size to be a certain threshold is used to set the needed ventilation rates in the rooms. For example, for the case with 1000 l gas release, it can be read that the need ventilation rate is 68 and 22 ACH, for the small and large room, respectively. The green line represents the threshold cloud size that can generate an expansion pressure of 0.5 barg in the room. The needed ventilation rate is hence found where the line for the cloud size is crossing the green line.

Using a design pressure of 0.5 barg, the needed ventilation rates as a function of the release size is plotted in Figure 15-26. Similar needed ventilation rates can be found for different design pressure.

The relation between design pressure and threshold cloud size is simply:

$P_{DAL} = 8\ Q8_T/V,$

where V (m3) is the free volume of the room, $Q8_T$ (m3) is the critical threshold cloud size, and P_{DAL} (barg) is the design value of the walls, see Figure 15-3. Hence, if the design pressure is 0.5 or 1 barg, then the threshold cloud size is V/16 or V/8, respectively.

For example, using the graphs in Figure 15-25 to find the needed ventilation rate with a design pressure going from 0.5 to 1 barg, then the ventilation rate can be reduced from 22 to 11 ACH for the large room and the 1000 l release case.
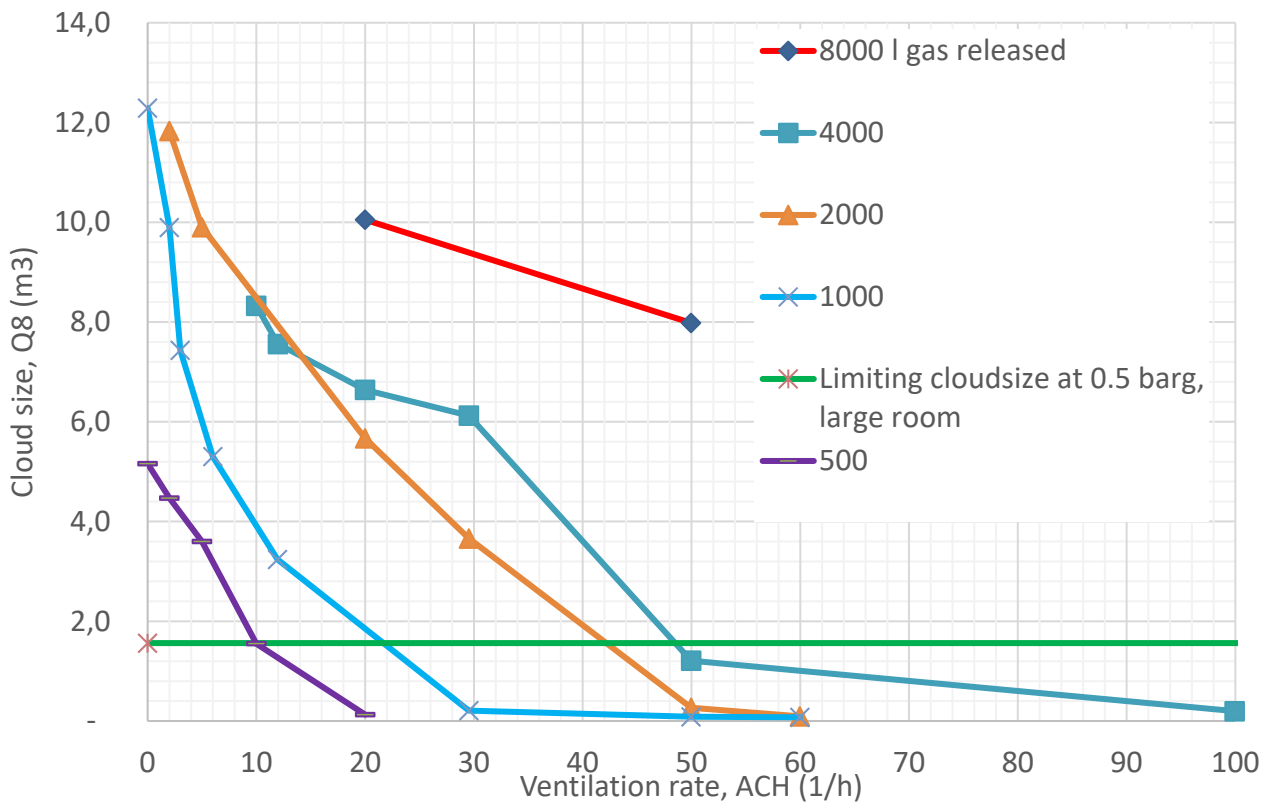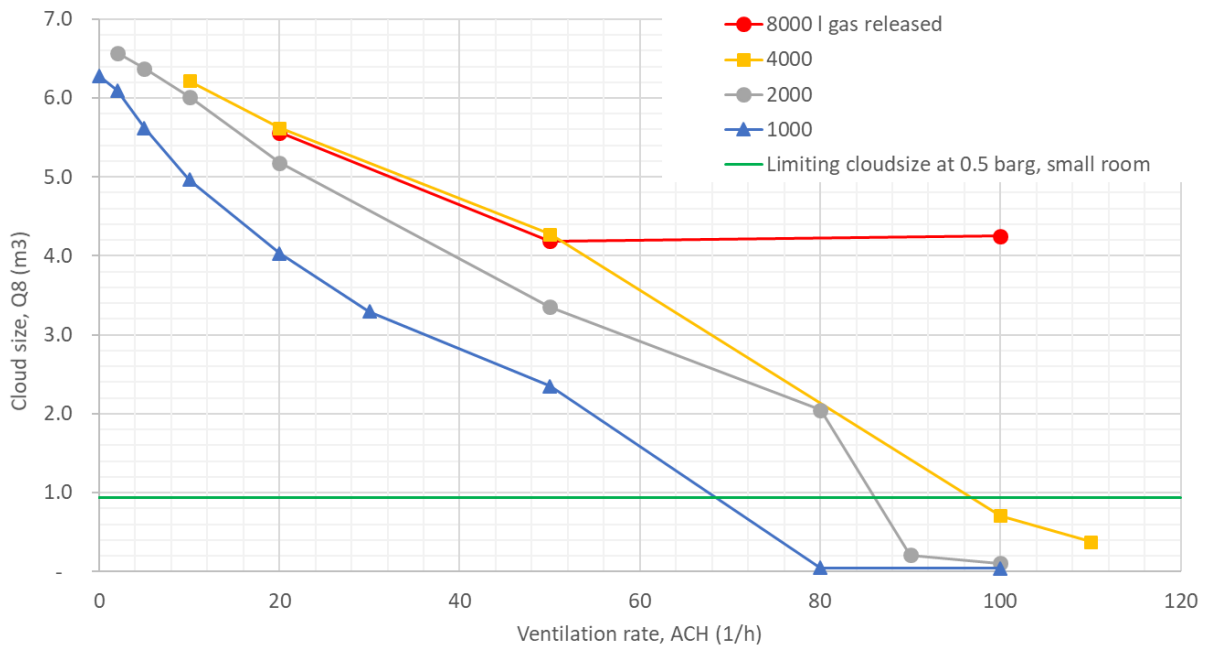
Figure 15-25: Cloud size from the simulations as a function of the ventilation rate for the different release cases: Small room, above; large room, below. The limiting cloud size that gives 0.5 barg on the walls is indicated for both rooms with a green line. The variable Q8 represents the equivalent cloud size that contributes to the expansion explosion in enclosed rooms.
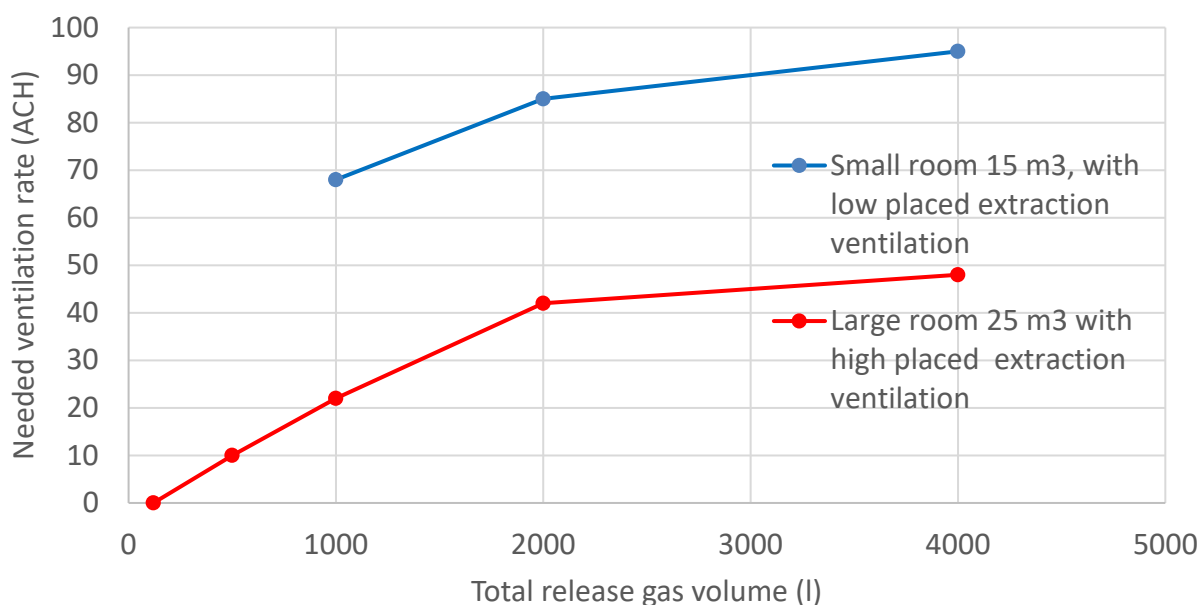
Figure 15-26   Needed ventilation rates as a function of the total volume of gas released from the battery. This ventilation rate will prevent the explosion pressure to go above 0.5 barg.

Table 15-8 – Needed ventilation rates (ACH) from CFD analysis based on gas volumes produced and types of room using a design pressure of 0.5 barg. The battery size in Ah is shown assuming a gas production rate of 2l/Ah. This gas production rate may change between different cells.

Battery size releasing* (Ah)	60	250	500	1000	2000	4000
Total gas released (l)	**120**	**500**	**1000**	**2000**	**4000**	**8000**
Ventilation rate needed in small room 15 m3 (ACH)	N/A	N/A	68	85	95	NA (>100)
Ventilation rate needed in large room 25 m3 (ACH)	0	10	22	42	48	NA (>100)

 * Assuming gas production is 2 l/Ah.

15.3.4 Discussion of results

15.3.4.1 Effect of ventilation

It is can be seen for both rooms in Figure 15-27 to Figure 15-30 that at a certain ventilation rate, the airflow in the room is strong enough to blow away the stratified layer of hot gas in the upper parts of the room. E.g. Figure 15-27 show that with a 1000 l release in the large room, when the ventilation rate goes from 20 to 50 ACH, the flow goes from a stratified layered flow to a total circulation and mixing of the gases in the room. The latter provides a better dilution of the gases in the room and more of the combustible gases are sucked out in the ventilation duct. For the lower ventilation rates, the buoyant effect of the hot gas is strong enough to provide a layering stratified situation where the flammable gas is collecting at the top of the room. The effect of the ventilation air speed is also seen on the plots i.e. for the high and low ventilation cases, the air speed from the jet is around 8 and 2 m/s, respectively. It is also seen from the high ventilation rate plots that the air speed in the room away from the nozzle jet is not more than 3 m/s when the ventilation rate is 50 ACH. When the ventilation rate is increased to 100 ACH, local air speeds outside the jet is up to 6 m/s. This indicates that it is not a very strong air flow in

the room for these ventilation rates. Similar situations are shown for the small room in Figure 15-29 and Figure 15-30, however a higher ventilation rate is needed in the small room due to ventilation extraction duct located lower down from the ceiling. This causes a larger cloud to be collecting above the extraction duct and need for a higher ventilation rate to blow away the upper stratified layer.

Ventilation is hence found to have a good positive effect for the scenarios investigated up to 4000 l gas released. When the gas release volume is 8000 l, the needed ventilation rate is found to be larger than 100 ACH (Figure 15-33), however, more simulations are not run to find the needed ventilation rate for such large release cases. This large ventilation rate is not normally used in maritime rooms, however, it may be considered to apply such high ventilation rate. Note further that the average air speed in the room at 100 ACH is not very high (up to 6 m/s, away from the nozzles) and it is mainly around the air supply nozzles that high air speeds are seen.

It can be recommended to find a cost optimal solution weighing the ventilation rate against the wall strength if the battery can escalate to more modules and release larger amounts of gas than around 4000l. Models like the ones presented here can be used in such investigations to better quantify the effect and find the cost and safety optimal ventilation versus wall strength.
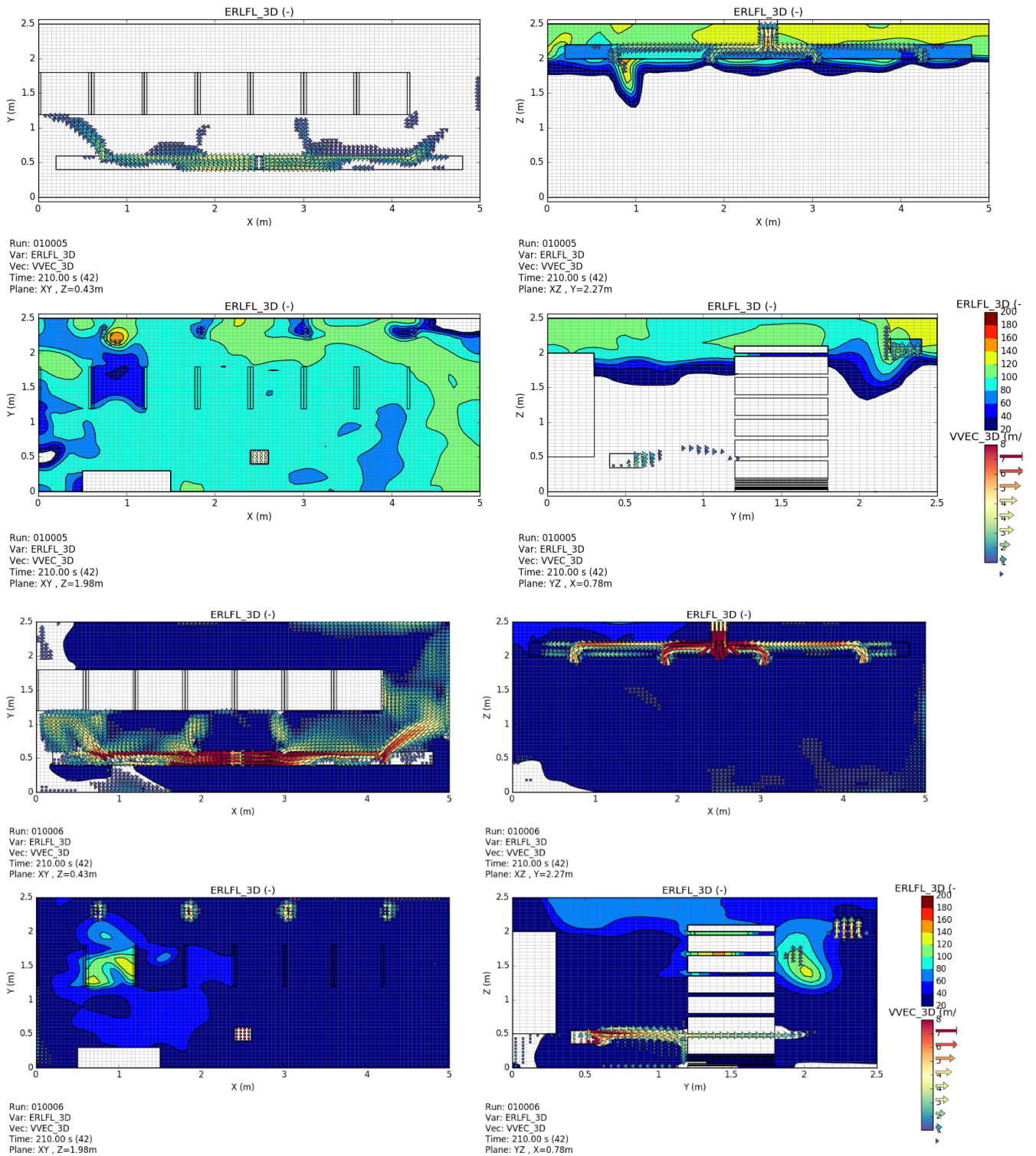
Figure 15-27: Gas concentration contours and velocity vectors in four cuts for two different cases with 1000 l release for the *large* battery room: Upper four plots, 20 ACH; lower four plots, 50 ACH. In the upper plots, the ventilation is not sufficient to dilute the gas in the stratification layers, whereas in the lower plots, the ventilation is strong enough. Cuts and cut plane coordinates are given on each plot
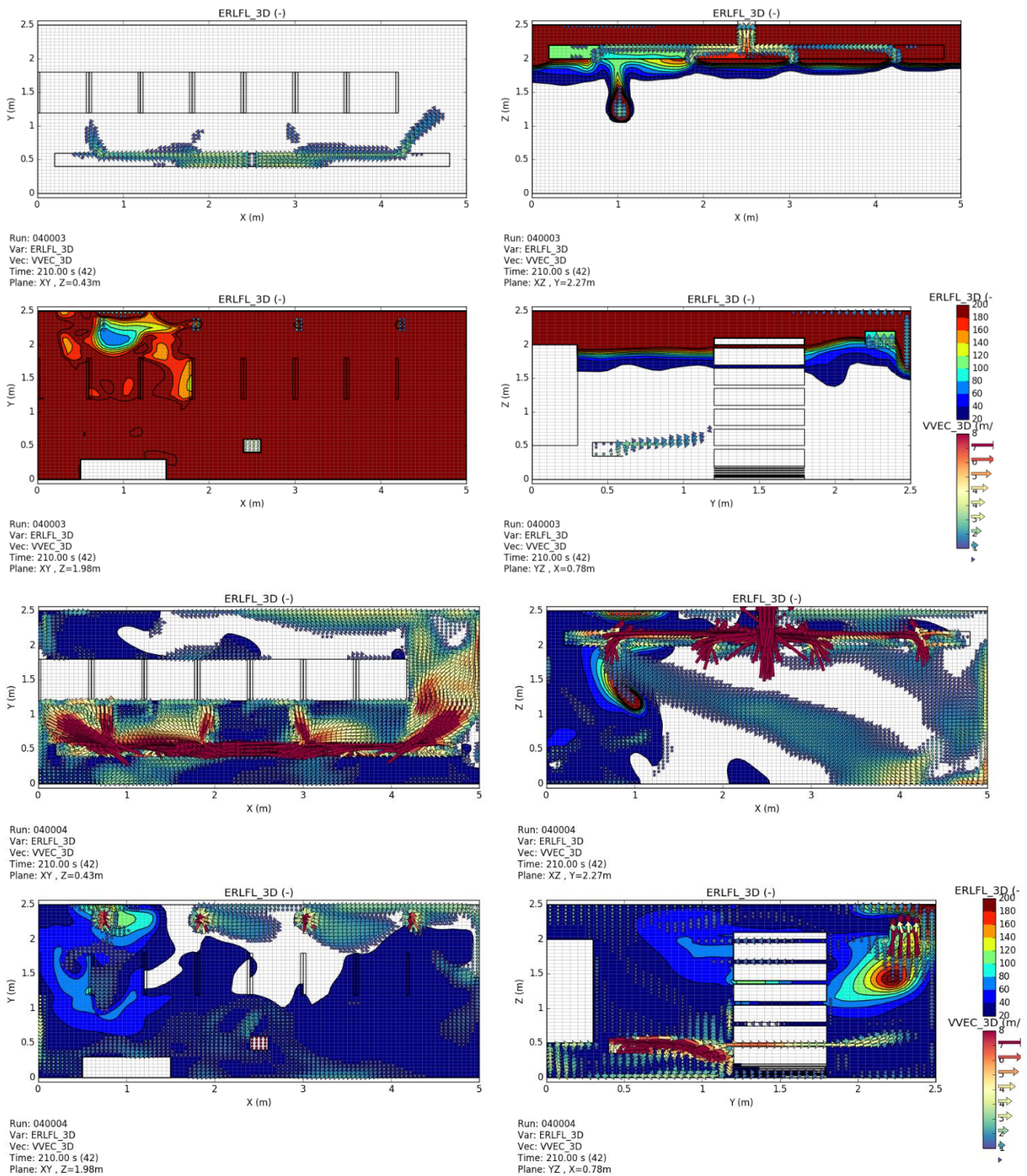
Figure 15-28   Gas concentration contours and velocity vectors in four cuts for two different cases with 4000 l release for the _large_ battery room: Upper four plots, 20 ACH; lower four plots, 100 ACH. In the upper plots, the ventilation is not sufficient to dilute the gas in the stratification layers, whereas in the lower plots, the ventilation is strong enough. Cuts and cut plane coordinates are given on each plot
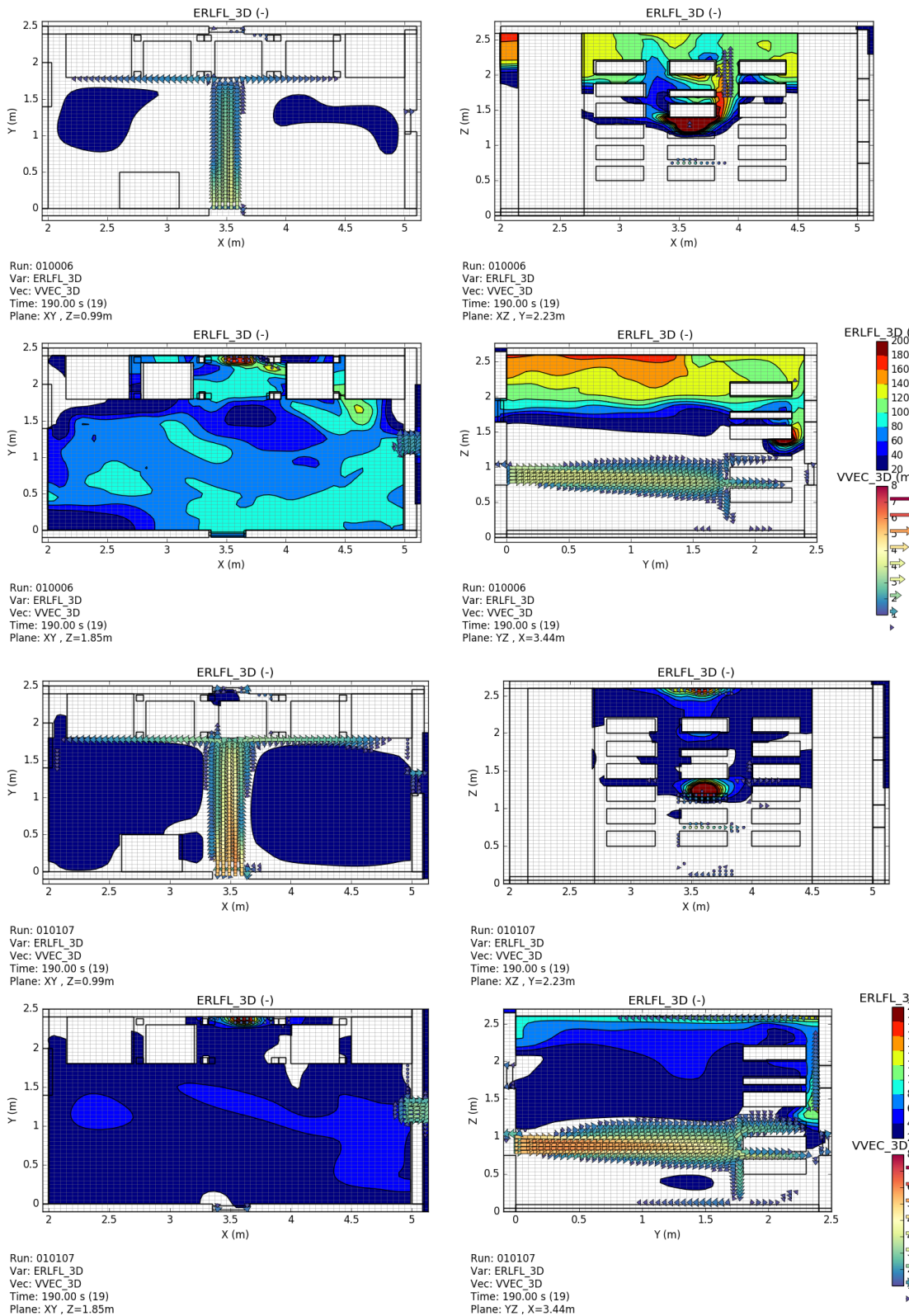
Figure 15-29 Gas concentration contours and velocity vectors in four cuts for two different cases with 1000 l release for the *small* battery room: Upper four plots, 50 ACH; lower four plots, 80 ACH. In the upper plots, the ventilation is not sufficient to dilute the gas in the stratification layers, whereas in the lower plots, the ventilation is strong enough. Cuts and cut plane coordinates are given on each plot

Figure 15-30 Gas concentration contours and velocity vectors in four cuts for two different cases with 2000 l release for the *small* battery room: Upper four plots, 80 ACH; lower four plots, 90 ACH. In the upper plots, the ventilation is not sufficient to dilute the gas in the stratification layers, whereas in the lower plots, the ventilation is strong enough. Cuts and cut plane coordinates are given on each plot

15.3.4.2 Ventilation extraction from the ceiling

In the models applied, the ventilation extraction ducts are located some distance down from the ceiling.

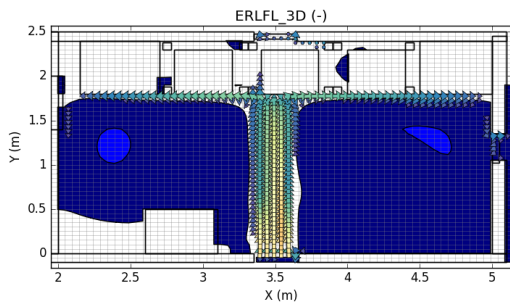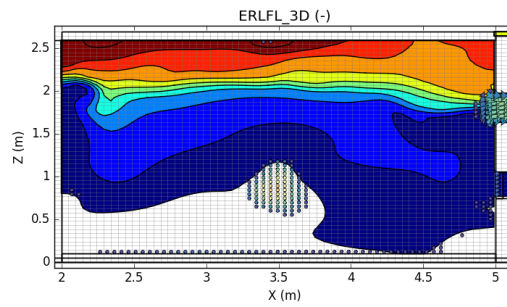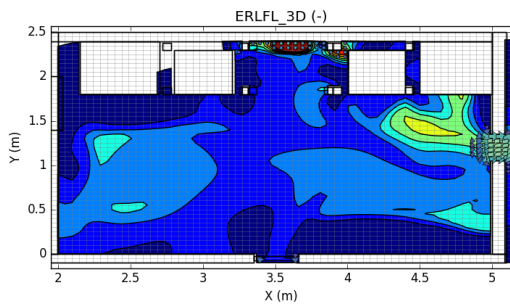A higher ventilation rate is needed for the small room partly because in this room the air extraction duct is located 80 cm down from the ceiling (to the centerline of the duct). In the large room, this extraction duct is located 40 cm down from the ceiling. If the extraction ducts are located higher up, the needed ventilation rate is reduced. If the room has extraction in the ceiling, then the calculated cloud size can be reduced further. From the initial simulation results presented in Figure 15-9 and Figure 15-10 in Section B 15.1, the cloud size at 10 ACH and 30 ACH can be reduced by approximately 20% and 60% respectively. If it is assumed that this trend is general, the results from the large room can be reduced further as shown in Figure 6-2 and Figure 6-3. This is an indication of the benefit from designing ventilation suction from the ceiling.

A duct with extraction from the ceiling can be made by either mounting the duct from the room above and an extraction nozzle flush with the gas tight ceiling plate. Or, if the duct comes in through the wall, the duct can be directed upwards to the ceiling with an extraction nozzle at the end just below the ceiling plate.

A higher ventilation rate is needed for the small room partly because in this room the air extraction duct is located 80 cm down from the ceiling (to the centerline of the duct). In the large room, this extraction duct is located 40 cm down from the ceiling. If the air extraction ducts are located higher up, the needed ventilation rate is reduced. If the room has extraction in the ceiling, then the calculated cloud size is reduced further. From the initial simulation results presented in Figure 15-9 and Figure 15-10 in Section B 15.1, the cloud size at 10 ACH and 30 ACH can be reduced by approximately 20% and 60% respectively. If it is assumed that this trend is general, the results from the large room can be reduced further as shown in Figure 15-31 and Figure 15-32. This is an indication of the benefit from designing ventilation suction from the ceiling.
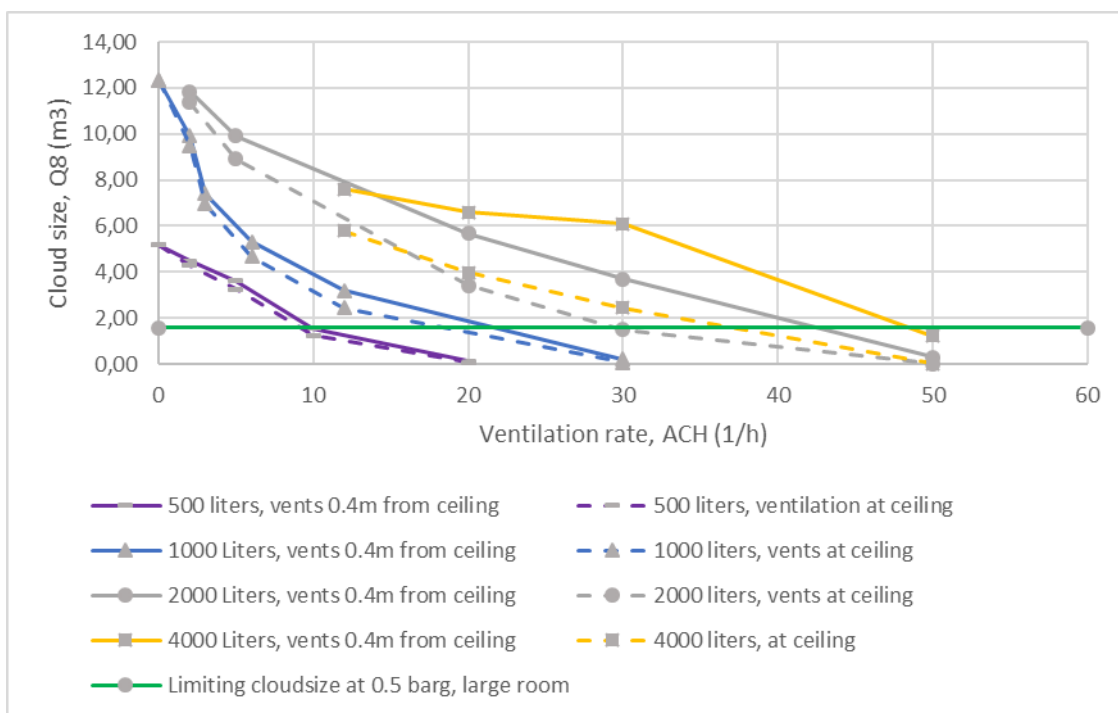
Figure 15-31 – Effect of ventilation located at ceiling for large room at 25m3.
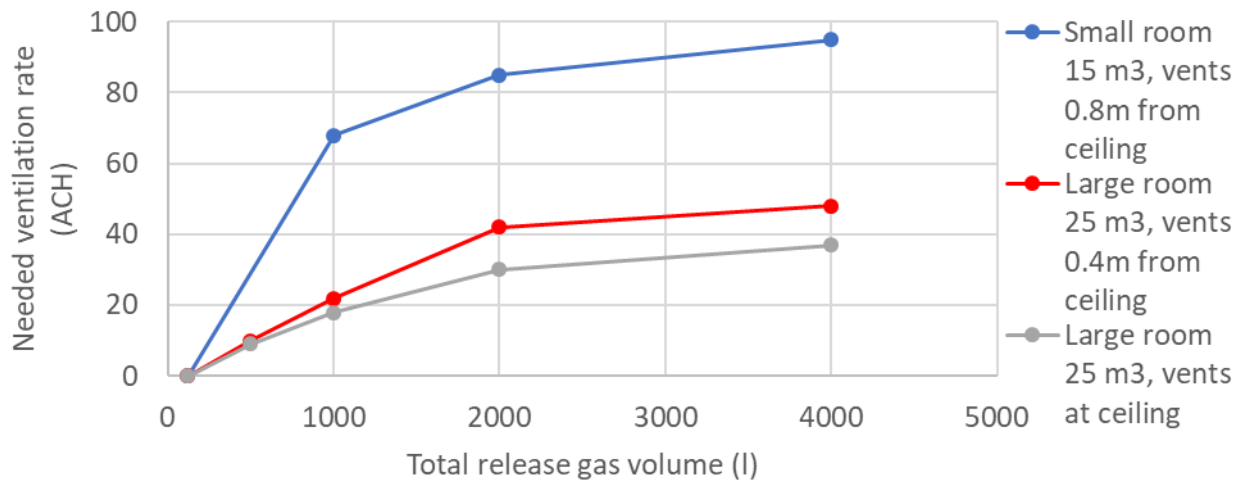
Figure 15-32   Needed ventilation rates as a function of the total volume of gas released from the battery. Note that the biggest contribution is the vent distance from the ceiling, and not the size of the room.

Table 15-9 – Needed ventilation rates (ACH) from CFD analysis based on gas volumes produced and types of room. The battery size in Ah is shown assuming a gas production rate of 2l/Ah. This gas production rate may change between different cells.

Battery size releasing* (Ah)	60	250	500	1000	2000	4000
Total gas released (l)	**120**	**500**	**1000**	**2000**	**4000**	**8000**
Small room 15 m3 ventilation, vents 0.8m from ceiling (ACH)			68	85	95	NA (>100)
Large room 25 m3 ventilation, vents 0.4m from ceiling (ACH)	0	10	22	42	48	NA (>100)
Large room 25 m3 ventilation, vents at ceiling (ACH)	0	9	18	30	37	NA (>100)

 * Assuming gas production is 2 l/Ah.

15.3.4.3 When very large gas volumes are released

Conditions during very large gas releases, e.i. more than a module is illustrated with the 8000 l cases, see Figure 15-33. For these cases a rich cloud is quickly formed in the room, and an increased ventilation rate can in such cases result in larger flammable clouds, and increased explosion risk before the gas is vented out and the risk is reduced. When such scenarios are possible, it can be considered to have a threshold gas concentration where the ventilation system is shutting down. This is unless the ventilation rate can be increased to very high rates, probably above 200 ACH. CFD modelling can be used to find the optimal strategy for such large releases; either use increased ventilation, or no ventilation. The limit to when ventilation should be shut down is hence dependent on the maximum ventilation rate, and the amount of gas released.

The logics for the ventilation should then be to run the ventilation until gas concentration reach above a given upper flammability concentration. When this occurs, the ventilation should shut down. This is similar to the cases when a fire is detected; then the strategy is to shut down the ventilation trying to suffocate the fire.
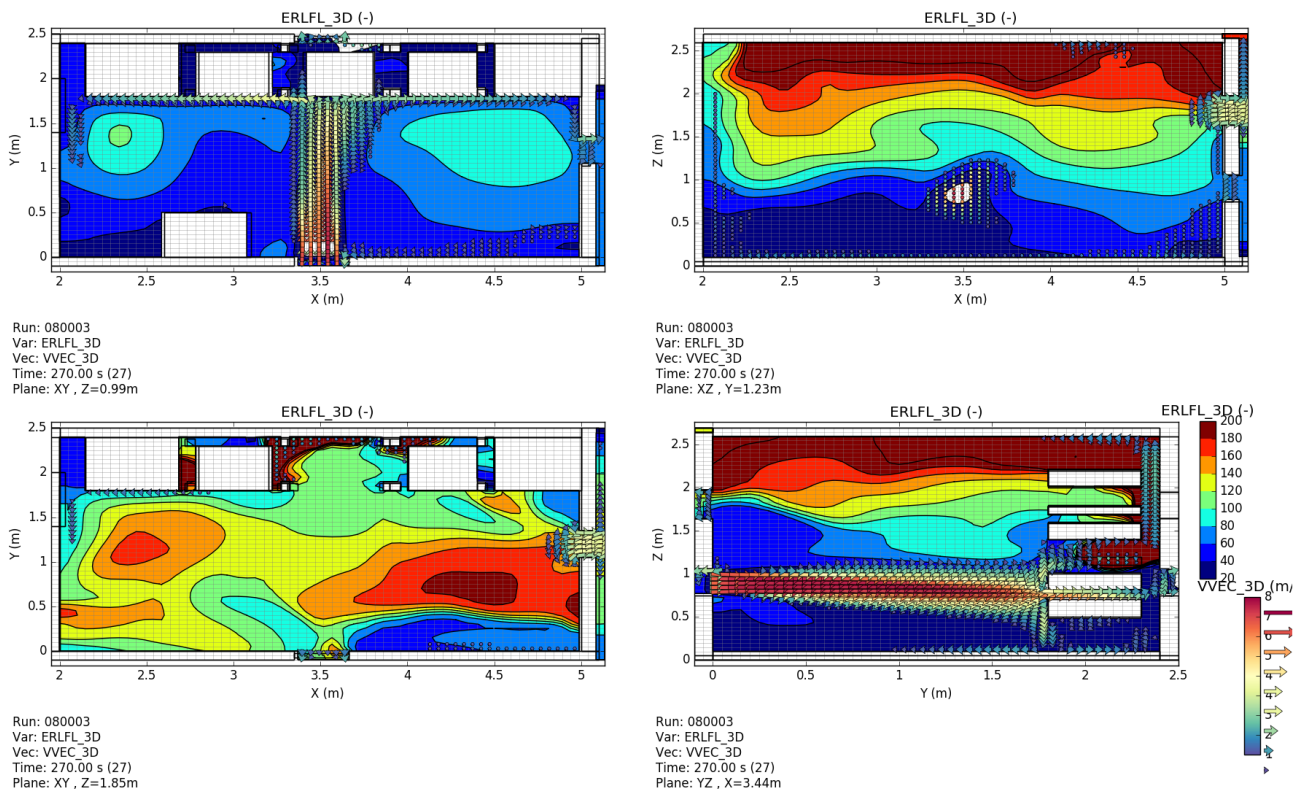
Figure 15-33   Gas concentration contours and velocity vectors in four cuts for case 080003 with 8000 l release and 100 ACH. The jet from the air inlet show airs speeds above 8 m/s locally. Elsewhere in the room, the air speed is below 2 m/s. Cuts and cut plane coordinates are given on each plot.

15.3.4.4 Backfire

With the strategy to turn off air supply at fire or at very high flammable gas concentration, one can get a situation with a very rich gas concentration in the room during and at the end of the scenario. Special procedures need to be in place to vent out and entering the room after the event. It can take several hours before the scenario has died out and during this time, one need to be careful of opening any doors or hatches that could feed fresh air into the room. A backfiring explosion could happen in a similar way that especially fire responders are concerned about of for under-ventilated fires inside buildings. One way to reduce the risk for such scenario is to leave the extraction duct open during the scenario, and only close the inlet of fresh air duct. When the scenario has calmed down, before entering the room, monitoring or a measurement of flammable gasses in the room should be performed. Introduction of inert gas into the room to prevent build-up of a flammable cloud would be the safest solution. Alternatively, at a certain low level of flammable gas, the air supply can be started and ramped up until flammable concentrations are removed before entering the room. Further investigations can be recommended for the specific rooms to develop dedicated routines for the after-incident-actions.

15.3.4.5 Cold gas effects

Simulations are only performed with a relatively hot gas where a gas release temperature of 200 degrees Celsius is used in the simulations for both battery rooms. In a real scenario, the temperature is starting lower than this and may also be so low that the gas become heavier than air and collects on the floor instead of along the ceiling. The room can also be cold with low temperature on the walls caused by winter conditions outside, etc. the cold walls can also cool down the gas and cause it to be heavier than air.

It is also typical that during the most active period of the off-gassing event, then the temperature rises and behaves like a buoyant gas plume. Since simulations are focusing on the active part of the scenario, the gas is modelled with relatively high temperature.

Based on this, it can be recommended to locate gas detectors at a lower level so that the initial phase of the off-gassing event can be detected.

If battery chemistry is changed or other effects causes the gas to be cold and heavy during the event, then the cold gas need to be considered when assessing the location of ventilation nozzles.

15.3.4.6 Other mitigating measures

Other mitigating measures such as explosion relief panels, dedicated extraction ducts on each module, water deluge and other chemical agents, etc. are not considered in the calculations. Such effects should also be considered, especially when the propagation test show that the amount of gas released is high.

15.4 Derivation of ventilation formula based at CFD results

Based at the CFD results, a formula for the ventilation for a typical battery room is here presented. This formula should only be used under the assumptions listed in Section 15.3.1. More specifically,

- Free volume from 10-30m^3.

- Leaking gas volume with less than 4000 liters.

- The extraction duct should be located less than 0.8 meter from the ceiling.

- If the extraction duct is at the bottom only, the formula is not valid.

If the room volume, release profile, ventilation arrangement and the shape of the room is severely different from the simulated cases, a separate CFD analysis should be carried out.

The derivation is solely based at inspecting the curves from the CFD results. The required air changes per hour (ACH) is expressed as shown in the equation below,

$$ACH = A\frac{(1 + Bh)}{v}e\, c^{\frac{(Q8_T + D)}{g}}$$

where $Q8_T$ (m3) is the critical stoichiometric gas cloud size, h (m) is the vent distance from the ceiling, g (liter) is the total liters of gas from the batteries and v (m3) is the room volume.

The variables $Q8_T$ and g can be replaced such that the function considers the design pressure p and the size of the failed batteries Q instead. The relationship between design pressure p, room volume v and threshold cloud size $Q8_T$ are $Q8_T = p\, v/8$, as discussed in Section 15.3.3. The total battery gas released can be expressed as $g = r\, Q$, where r is the gas released per ampere hour and Q is the size of the failed batteries in ampere hours. Hence, the ventilation rate can be expressed as

$$ACH = A\frac{(1 + Bh)}{v}e^{\frac{C}{8}\frac{(vp + 8D)}{rQ}}$$

where p (barg) is the design pressure of the bulkhead, h (m) is the vent distance from the ceiling, Q (Ah) is the size of the failed batteries and v is the room volume. The parameter r is in this chapter assumed to be 2 l/Ah, which is an established rule of thumb. However, the single cell CFD results in this project indicates that this number can be increased up to 3 l/Ah for cases where no external combustion is observed. Cases with no combustion may happen although it is more likely that the gas ignites early without explosion. Since cases with combustion are observed and possible, it is advised that this scenario is accounted for.

To account for model uncertainties and simplifications made in the curve fitting process, a safety factor S should be included, as shown below

$$ACH = SA\frac{(1+Bh)}{v}e^{\frac{C}{8}\frac{(vp+8D)}{rQ}}$$

A proposed value of $S = 1.1$ gives a margin of 10%.

The values for the parameters are listed in Table 15-10. The values for A, B, C and D are found by using *curve_fit* function in the Python optimize package. The "Trust Region Reflective algorithm" is used as the optimization method. Adjusting the parameters to find an optimal fit for the CFD results at 0.5-1.0 barg design pressure has been prioritized. Also, the room with free volume of 25m3 has been given priority over the small room of 15m3. Finally, the release of 500 liters, 1000 liters and 2000 liters have been prioritized over the 4000 liters case.

Table 15-10: Ventilation formula parameters

Parameter	Value
A *)	1282.7
B *)	0.498
C *)	-311.8
D *)	1.579
r **)	2-3 l/Ah
S **)	1.1

*) Parameter found by *curve_fit* in Python

**) Parameter chosen by rule of thumb, and can be changed by the user

The CFD plots for the various simulations are plotted together with the proposed function in Figure 15-34, Figure 15-35 and Figure 15-36. The ventilation rates with a design pressure of 0.5 barg is shown in Figure 15-37.

Table 15-11 provides example values with r = 2 l/Ah and S = 1.1.

Table 15-11: Example values for the formula presented.

Battery size releasing with 2 l/Ah	60	250	500	1000	2000
Small room 15 m3 ventilation, vents 0.8m from ceiling (ACH)	0	27	60	89	108
Large room 25 m3 ventilation, vents 0.4m from ceiling (ACH)	0	10	25	41	53
Large room 25 m3 ventilation, vents at ceiling (ACH)	0	8	21	35	44
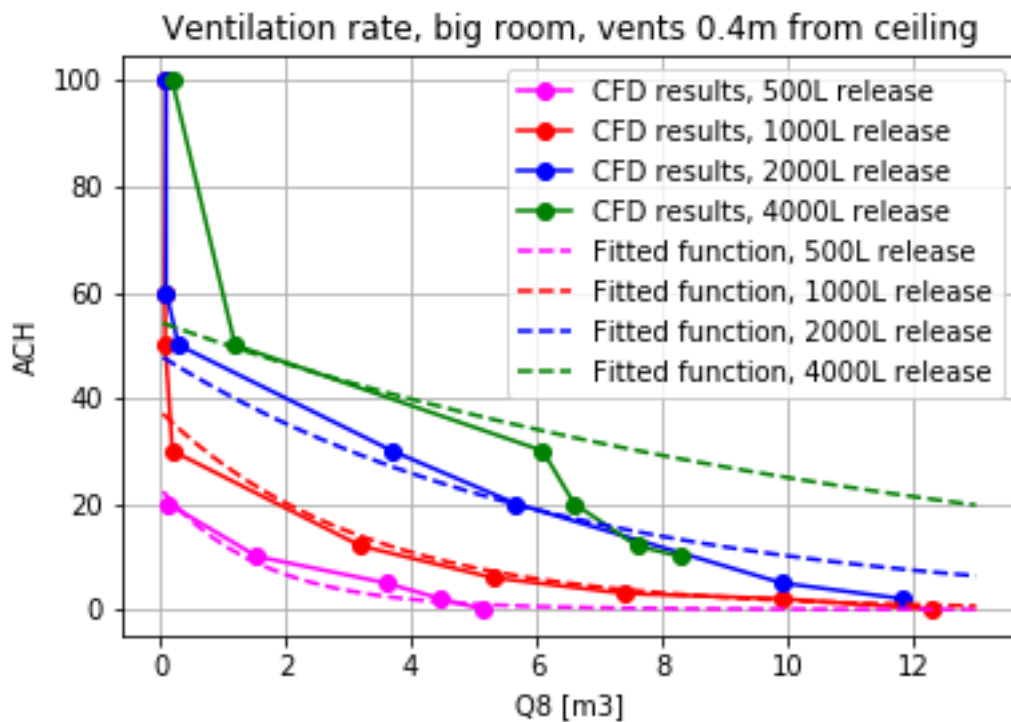
Figure 15-34: Ventilation rates for the big room with vents 0.4m from the ceiling. Both the CFD simulations and the corresponding fitted function is plotted.
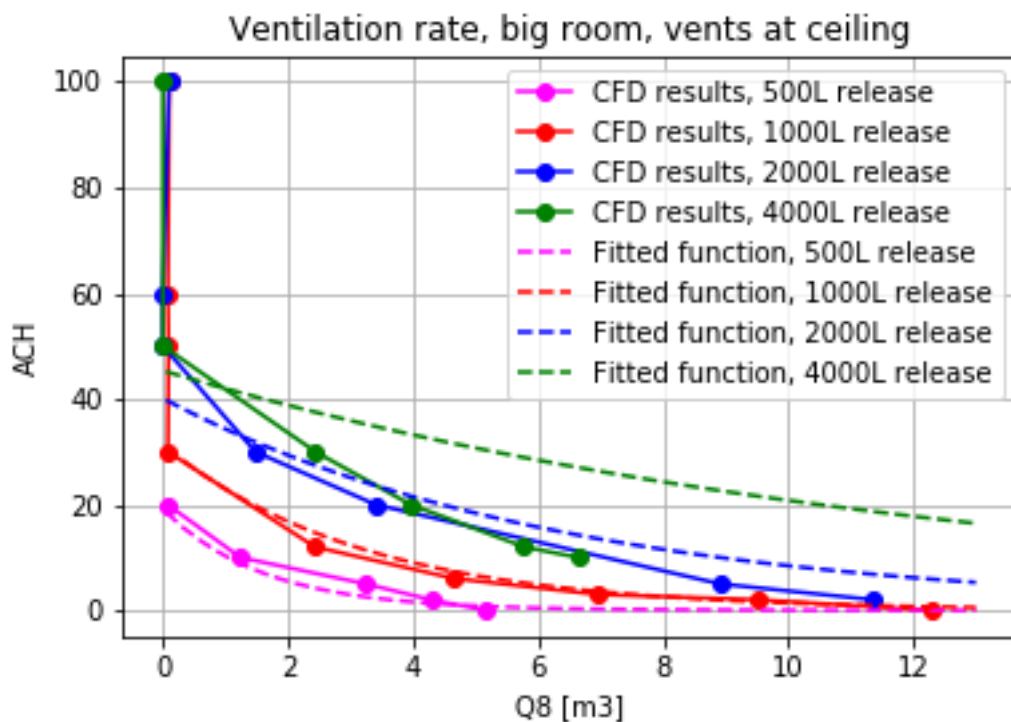
Figure 15-35: Ventilation rates for the big room with vents at the ceiling. Both the CFD simulations and the corresponding fitted function is plotted.
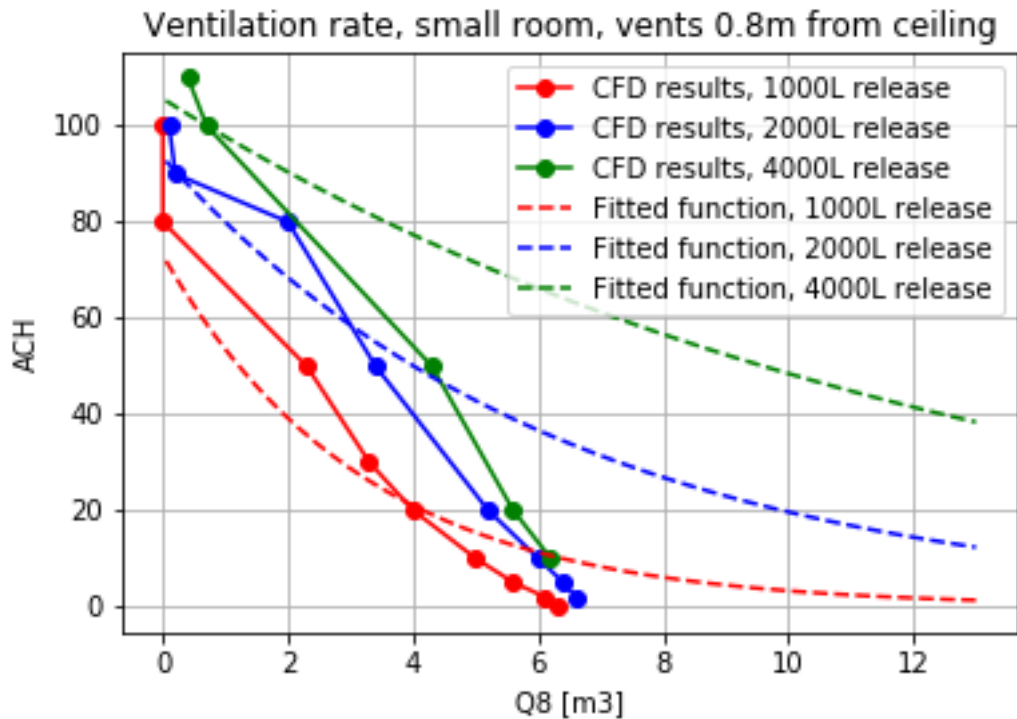
Figure 15-36: Ventilation rates for the small room with vents 0.8m from the ceiling. Both the CFD simulations and the corresponding fitted function is plotted.
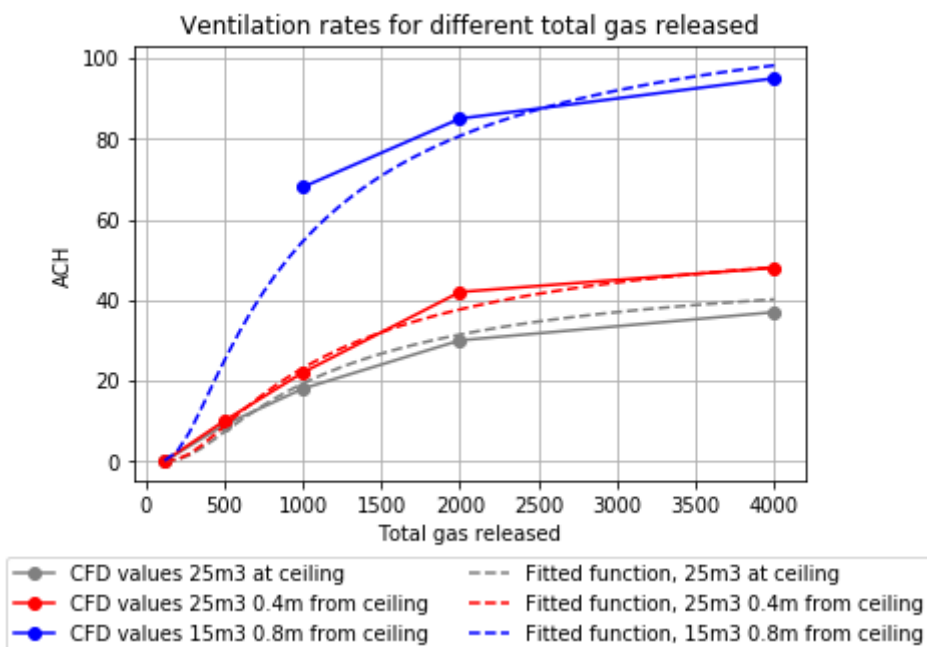
Figure 15-37: Ventilation rates for different gas releases with a design pressure of 0.5barg. CFD results and the corresponding fitting function is shown.

16 QUALITATIVE BATTERY RISK EVALUATION

As discussed earlier in this report, the main risks when the battery system goes into thermal runaway is fire and off-gassing that is both explosive and toxic.

16.1 Heat vs gas generation

Traditionally, the most common mitigating measure of marine firefighting has been to limit the oxygen by closing ventilation and flood the room with some gas. By closing the ventilation, the battery room is sealed together with the explosive and toxic gas. This will increase the toxicity and explosion risk while limiting the heat generation and the probability for the fire to spread to the rest of the battery system, or other items in the room.

The cell level and module level tests in presented in this report provided evidence that visual combustion produced more heat, but less gas compared to tests without visual combustion. As indicated by the figure below, tradeoffs in the risk evaluation needs to be done between extensive heat generation vs extensive explosive and toxic gas generation.
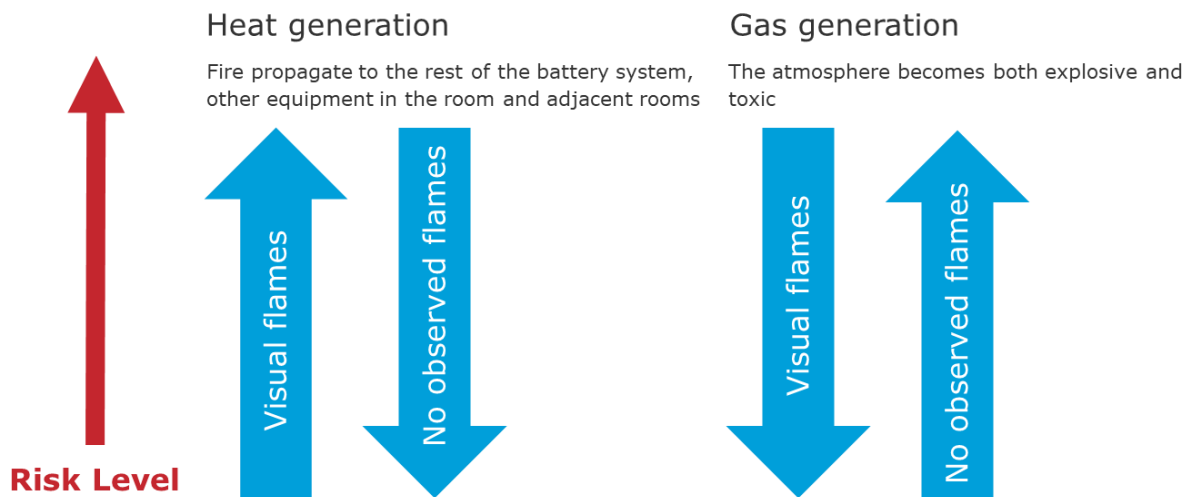
Figure 16-1: Risk tradeoffs between a battery combustion of visible flames compared to a combustion without visible flames.

It also is observed that oxygen is consumed or displaced during a thermal runaway. The produced oxygen will result in more aggressive heat development and increased CO or CO_2 production, depending if the combustion is total or not. It is also seen that limiting the oxygen supply will suppress the battery fire, but not be sufficient to cool down the battery. In these cases, the off-gassing is increased compared to fires where oxygen is fueled to the fire.

These tradeoffs need also to be considered when designing the battery modules and racks itself. If the modules can withstand substantial heat, letting one module burn with visual combustion without propagating to the other modules, it might be considered safer to let it burn. If the modules cannot withstand the heat generation, the fire must be controlled at the expense of increased off-gassing.

Mitigating the explosion and fire risk, is closely related to limit the ignition sources in the room. Installing EX proof equipment is considered important. Note however that the electronics in the battery module itself cannot be EX proof, and with the extensive heat produced during a thermal runaway, the most plausible ignition source is the battery itself.

16.2 Toxicity

When evaluating the toxicity, the main gases the most dangerous gases when normalizing the IDLH values based at the observed concentrations, seems to be CO, NO2 and HCL. Note that NO2 was not recorded for the NMC tests. The NO2 levels where quite consistent for all the LFP tests where no visual combustion was observed. No clear difference can be seen at the CO total concentration between the tests with visual combustion and no visual combustion. Also, the amount of HCL and HF seems to vary between the 50% SOC overheat test and short circuit test, that both did not visually combust.

So, when evaluating the toxicity hazard between visual or no visual combustion, the only parameter is the quantity of the produced gas, which is higher for the cases with no visual combustion. Hence, it can be concluded that the toxicity threat is also increased with no visual combustion.

16.3 Explosion risk

16.3.1 Explosion pressure

FLAM is flammable gas build up – total volume of gas between LEL and UEL. This realistically has a gradient of mixture within it. The stoichiometric mixture equivalent will be calculated for specific final cases (based on final gas constituents and release cases) but for present assessments, this is assumed to be half of the FLAM. Explosion (deflagration) overpressure is linearly proportional to the volume of gas as a percentage of total room volume. Max possible is 8 barg.

The relation between design pressure and threshold cloud size is simply:

$P_{DAL} = 8\ Q8_T/V$,

where V (m3) is the free volume of the room, $Q8_T$ (m3) is the critical threshold cloud size, and P_{DAL} (barg) is the design value of the bulkheads. The relationship is shown in Figure 16-2. In this study P_{DAL} has been set to 0.5barg.
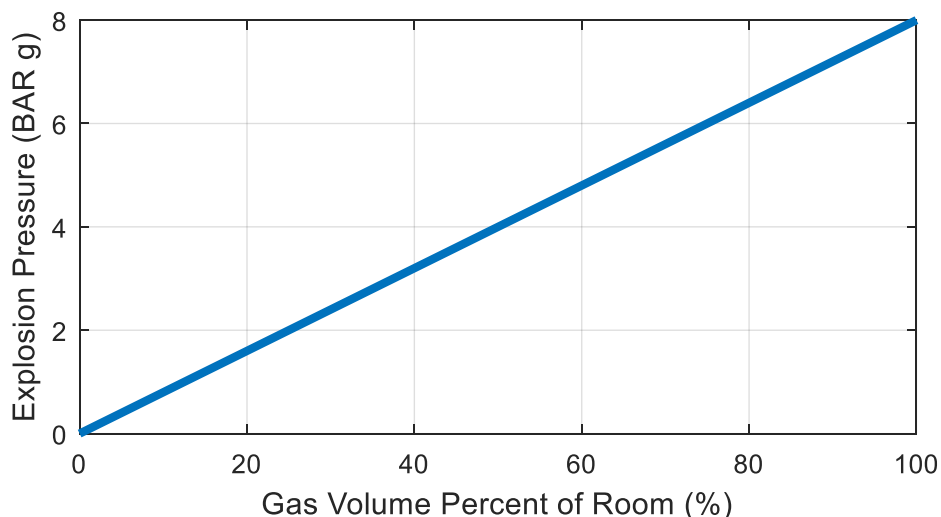
Figure 16-2: Explosion pressure as a function of gas volume percentage of the room

16.3.2 Gas production related to battery size

The established rule of thumb is 2 liters of battery gas per Ah hour. The single cell test results and the CFD results presented in this project gives similar results when external visual combustion is observed. Cases where no visual flames are observed, indicates that this number can be increased up to 3 L/Ah.

For the module tests, it seemed that 2.2 L/Ah matched the test results best.

Hence, a value between 2-3 L/Ah should be used when relating the off-gassing to the battery size.

16.3.3 Ventilation

The typical ventilation requirements for a machinery space at a vessel is 6 ACH. This ventilation rate is assessed to be sufficient for "small" gas releases of 350 liters of gas. This corresponds to a battery of 115-175 Ah. However, it is seen that a room of 25m3 requires 22 ACH when the total release is 1000L to avoid any structural explosion damage. This corresponds to a 500Ah module. If the battery system is designed such that more than 100Ah is involved in a fire, additional ventilation is needed to avoid explosions that damages the bulkhead structures.

In order to realize the most potential of a forced extraction duct, a high extraction point has proven key. This ensures that the required air changes per hour stays low while still providing the necessary dilution of explosive gases in the space.

16.3.4 Gas detection

Off-gas in the early stages of thermal runaway events will be colder than off-gas release in the later stages. The early off-gas can therefore become heavier than the air, collecting at floor level. It should therefore be considered if gas-detection should be applied at both levels, close to the floor and close to the ceiling.

Additionally, tests conducted in this project indicate that solely relying on LEL% sensor(s) and cell voltage levels to detect early stages of a thermal runway event is insufficient. The tests showed that the Li-ion Tamer® sensor and smoke detector, when placed close to or inside the affected module, proved the most reliable means of pre-thermal runaway warning.

17 QUANTITATIVE RISK ASSESSMENT

This section outlines an approach to Quantitative Risk Assessment (QRA) of a battery thermal failure or safety event. This is developed as a framework for assessing the effectiveness and necessity of different barriers under consideration of the overall magnitude of risk. The intention is for development of this tool for guidance of requirements or acceptance criteria definitions, or evaluation of different designs.

Thus, the intention is to evaluate the inputs (See Section 17.1.1) and methodology for appropriateness, refinements or recommendations – as well as suggestions on how it can be used in the project to illuminate various issues and questions.

17.1.1 Reference Data and Failure Rate Statistics

Table 17-1 lists common failure mechanisms that can arise in a battery system, and associated frequencies of occurrence. Publications from Center for Chemical Process Safety (CCPS) /1/ and Institute of Electrical and Electronics Engineers, Inc. (IEEE) /2/ are used as reference for the failure frequencies. For mechanical failure leading to internal short circuit, the frequency is based on the assumption that the six sigma manufacturing/process principle is applied. This implies e.g. that one cell out of one million cells will have a defect due to manufacturing, physical damage due to transport or impact onsite that can lead to internal short circuit during its lifetime. Hence, the frequency for mechanical failure in the battery system will depend on the number of cells. Here only mechanical impact is considered to start at module level, while the rest of the failures are considered to start at the weakest cell.

Table 17-1   Common Failure Mechanisms and Frequency/Probability of Failure

Failure Category	Failure description	Probability of Failure (per year)
Electrical Failure	Overcharge or undercharge based on catastrophic inverter failure	0.01 (IEEE)
Mechanical Failure	Physical damage due to impact onsite (internal short circuit)	0.01 (Six Sigma assumption)
	Physical damage due to impact during transport (internal short circuit)	0.01 (Six Sigma assumption)
	Manufacturing defect (internal short circuit)	0.01 (Six Sigma assumption)
Thermal Failure	Overheating (due to HVAC failure)	0.1 (Process control failure, CCPS)
	Overheating from electrical or mechanical failures referenced in this table	
Human error	Human error during commissioning, installation, repair, or operations activities	0.01
Process Control Failure	Failure of Basic Process Control Systems, such as BMS and EMS/PMS in a battery system.	0.1 (CCPS)

In a battery system, there will be safeguards or barriers that shall prevent the above failures from escalating into severe events. These safeguards have an associated Probability of Failure on Demand (PDF), i.e. the probability that it will fail to perform its function when needed. Typical safeguards are of various types; these are listed in Table 17-2 with the associated PFDs.

Table 17-2: Common Safeguards and Probability of Failure on Demand

Safeguard Type	Safeguards	PFD
Inherent design	UL 1973 Criteria Heating Ventilation and Air Conditioning (Redundant Units)	0.1 (CCPS)
Basic Controls	Active Cooling/Thermal Management Controls HVAC with failure alarm	0.1 (CCPS)
Safety Systems	Battery Management Systems which can isolate battery racks Master Controllers which can isolate battery systems and medium voltage equipment external to the ESS	6.9 – 0.01 (depending on Safety Integrity Level rating) (CCPS)
Electrical protection	Fuses and Circuit Breakers	0.1 (IEEE)
Fire Suppression	Active fire suppression Emergency HVAC	0.1 (CCPS)
Procedures	Remote monitoring 24/7 and isolation	0.1 (CCPS)

17.1.2 Approach

An approach for a quantitative risk assessment setup has been developed as is outlined in the following sections. The object is to identify the safety threats and failure consequences associated with a maritime battery system and quantify the overall safety risk by associating the various consequences with corresponding frequencies.

The approach consists of the following steps:

1. Identify the *threats* (alternatively: *hazards* or *initiating events*). A threat is a failure mode of a system or component and is the initiating event in the event tree potentially leading to unwanted consequences. The threat has a certain frequency of occurring. It is important to identify threats independent from each other, so that no initiating events are overlapping ("counted more than once").

Based on an assessment of a generic battery system, the following threats are identified. Note that the frequencies may differ between specific systems and should be carefully evaluated. A proposed

frequency or approach for determining the frequency is given in Table 17-3. As an example, a frequency of 1E-2 per year means it can be expected once in 100 years for a system.

Table 17-3   List of identified threats

ID	Short name	Description	Proposed frequency
T1	T1-Short-Cell	Internal short circuit in cell, due to manufacturing error or physical damage during transport, maintenance etc.	Following Six Sigma quality principles, it is expected one defect cell per million cells over the battery lifetime, cf. Table 17-1. Assuming a lifetime of 10 years, the frequency then becomes 1E-6 × number of cells / 10 per year
T2	T2-BMSFailure	BMS failure in e.g. controlling current limits, leading to overcharge, discharge or overcurrent	Process controller failure frequency is 0.1 per year, cf. Table 17-1. It is assumed this is equally distributed between T2 and T4, giving 0.05 per year for BMS failure
T3	T3-Converter	Converter failure leading to overcharge, discharge or overcurrent	Catastrophic inverter failure frequency 0.01 per year, cf. Table 17-1
T4	T4-Communication	Incorrect communication between BMS/Converter/PMS leading to overcharge, discharge or overcurrent	Process controller failure frequency is 0.1 per year, cf. Table 17-1. It is assumed this is equally distributed between T2 and T4, giving 0.05 per year for communication failure
T5	T5-HVACFailure	Failure of HVAC system in battery room or module cooling system, leading to battery system operating outside design temperature range, both above (overheating) and below (excessive cold). Overheating will drive degradation and can lead to cell internal temperature to rise, potentially causing thermal event. Excessive cold can lead to lithium plating or formation of dendrites, potentially causing hazardous	0.1 per year, cf. Table 17-1. This is conservative, since it is considered unlikely that the failure of HVAC or cooling system has the potential of increasing cell temperature until runaway temperature.

ID	Short name	Description	Proposed frequency
		condition in cell.	
T6	T6-ExternalShort	Failure on electrical equipment (not battery itself) leading to rapid charge or discharge and potential heating of electrolyte and thermal event	Electrical failure, assuming 0.1 per year, cf. Table 17-1
T7	T7-MechImpact	Physical/mechanical impact to Battery System	Not quantified, for simplicity assumed negligible frequency for developing into a hazardous event. Also, internal cell failure due to damage included in T1.
T8	T8-WaterIngress	Water Ingress in battery room, from pipes, leak etc.	Not quantified, for simplicity assumed negligible frequency for developing into a hazardous event
T9	T9-ExternalFire	Fire in other type fuels, electrical equipment outside of battery space etc., i.e. not caused by battery system, but posing a hazard when exposing the battery system, whose presence may worsen the fire consequences.	Should be assessed specifically for system, assuming 1E-2 per year here for an external fire that threatens the battery space
T10	T10-FullModFail	A full module failing, involving all cells. Could be due to e.g. uncontrolled discharge or arcing.	Uncertain, but considered to be low. Assuming 1E-4 per year

2. Determine the possible consequences. In this analysis, only fire is presently included as consequence. Explosion shall be added in subsequent analysis. However, this requires more knowledge about the likelihood that the gas released is combusting instantly (fire) but undergoes *delayed ignition* (after being mixed with air, implying an explosion). The following fire categories are included as consequence:

- Local Fire: Cell

Limited to only one cell (or a few cells, depending on propagation prevention design) and is mitigated without the thermal event propagating to other cells.

- Local Fire: Module

The thermal event in one cell propagates to the other cells in the module. It could also be the case that an event leads directly to the whole module being involved in the fire, without first being initiated at cell level.

- Global Fire

The thermal event spreads to multiple modules and the fire has the potential of involving the entire battery space and beyond.

3. Barriers (or safeguards) that are in place to prevent or mitigate the consequences following a threat are identified. Each barrier has a probability of failure on demand (PFD), i.e. a probability that it will fail to perform its function when needed. The barriers present in a battery system will be specific for each system. In Table 17-4, a list of possible barriers that can be present is proposed. The various barriers are types as listed in in Table 17-2, i.e. inherent design and procedures, basic controls, safety systems, electrical system and fire suppression. The PFD is set to 0.1 for each barrier, according to the reference data in Table 17-2.

Table 17-4   List of barriers/safeguards typically present in a battery system

ID	Short name	Barrier name	Comment
B1	Breakers	Breakers or other electrical protection	-
B2	CellProp	Cell Fire Propagation Protection	Design to prevent thermal event from propagating from cell to adjacent cells and eventually module.
B3	ConvertProt	Converter Failure protection system	-
B4	CID	Current Interrupt Device	-
B5	Shutdown	Emergency Shutdown/System Disconnect	-
B6	FireDet	Fire and Smoke Detectors	-

ID	Short name	Barrier name	Comment
B7	FireEx	Fire Extinguisher Agent	-
B8	FireWater	Fire Extinguisher Water	-
B9	FireRating	Fire Rating of Battery Room	-
B10	FirePlan	Fire Response Plan & Training	-
B11	Fuses	Fuses	-
B12	GasDet	Gas Detectors	Relevant barrier for explosion
B13	HVAC	HVAC System – Venting of gases	Relevant barrier for explosion
B14	Independent	Independent Voltage or Temperature Shutdown Protections	-
B15	ModCOol	Module cooling system	-
B16	ModProp	Module propagation protection (thermal design)	-
B17	Disconnect	Module/String Disconnect	Redundancy of barrier. Any barrier may have a redundant barrier, acting as a second barrier.
B18	VoltAndCurrentMon	Process control and alarm – Voltage and current (PMS/EMS and BMS)	The BMS here acts as a safeguard, but it should be noted that it can also have failure modes constituting a threat, cf. threat T2 and T4

ID	Short name	Barrier name	Comment
B19	Redundancy	Redundancy of arbitrary barrier	Redundancy of barrier. Any barrier may have a redundant barrier, acting as a second barrier.
B20	TempMon	Temperature Monitoring (PME/EMS and BMS)	-

4. The frequencies of the different consequence categories are calculated for each threat. This is illustrated in Figure 17-1. The initiating frequency is multiplied with the PFDs for all barriers in place to come up with *end frequencies f1$_{threat}$, f2$_{threat}$* and *f3$_{threat}$* for the threat to lead to the three consequence categories respectively. Note that there can be several barriers in place for each consequence; since the barriers are independent, all must fail to lead for the threat to lead to a specific consequence. Therefore, all PFDs are multiplied with each other.
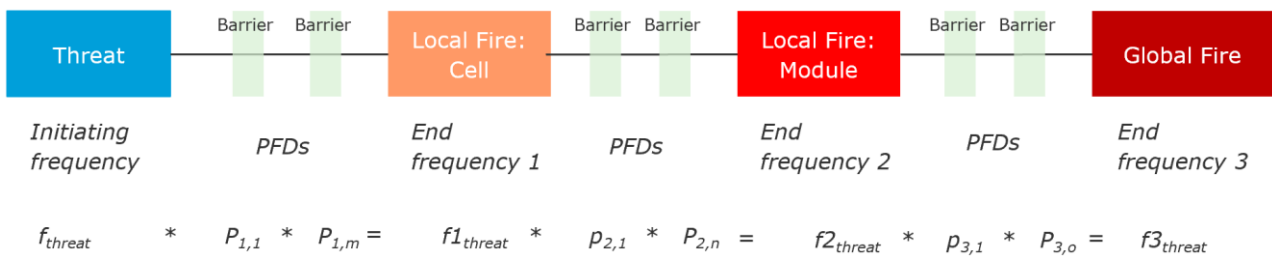
Figure 17-1 – Scheme for calculating frequencies for the different consequence categories caused by a threat

5. All the threats may lead to one or more of the consequences defined. To calculate the final frequencies for each consequence categories, the end frequencies *f1$_{threat}$*, *f2$_{threat}$* and *f3$_{threat}$* for all threats are added together for each consequence category. This is schematically illustrated in Figure 17-2.

$$f1 = \sum_{all\ threats\ x} f1_x$$

$$f2 = \sum_{all\ threats\ x} f2_x$$

$$f3 = \sum_{all\ threats\ x} f3_x$$
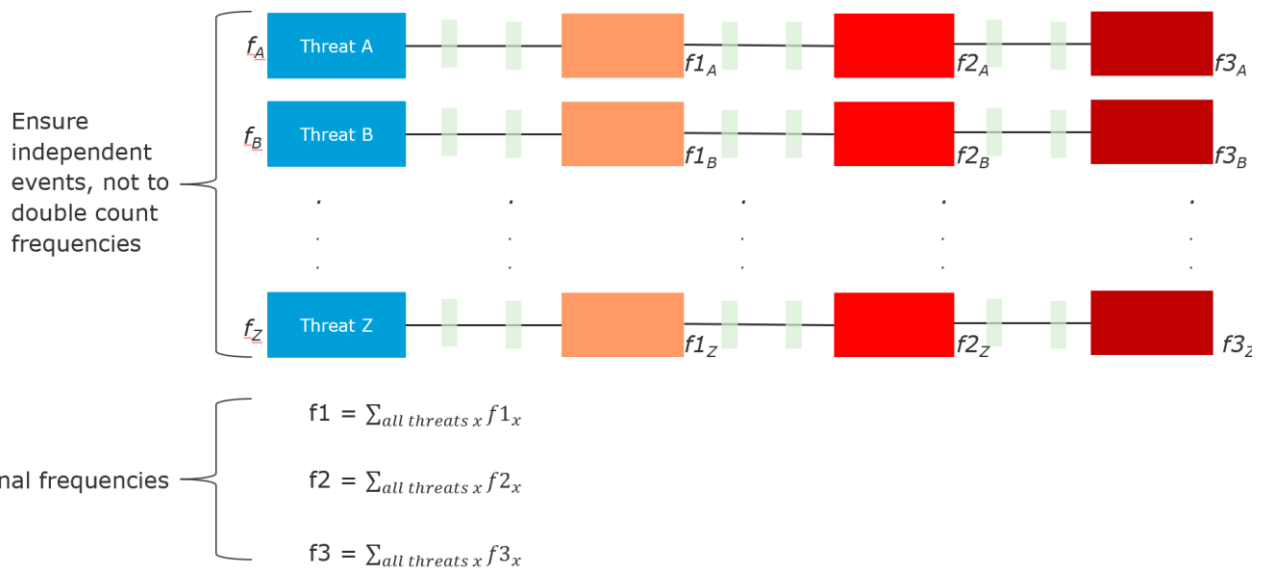
Figure 17-2 – Scheme for calculating final frequencies involving all threats

17.1.3 Analysis

A simple Excel tool is set up to perform the analysis. This includes an assessment where threats are set up with its associated frequencies. For each threat, the barriers for each consequence category are listed, and the PFDs multiplied with the initiating frequency as shown in Figure 17-1. This is summarized for a generic battery system in Table 17-5.

Table 17-5   Assessment of threats and associated barriers for the various consequence categories

Threat	Barriers to Local Fire: Cell		Barriers to Local Fire: Module		Barriers to Global Fire	
T1-Short-Cell	B4	CID	B2	CellProp	B6	FireDet
					B7	FireEx
					B16	ModProp
T2-BMSFailure	B4	CID	B2	CellProp	B6	FireDet
	B5	Shutdown			B7	FireEx
	B14	Independent			B16	ModProp
					B20	TempMon
T3-Converter	B3	ConvertProt	B2	CellProp	B6	FireDet
	B4	CID			B7	FireEx
	B5	Shutdown			B16	ModProp
	B14	Independent			B17	Disconnect
	B18	VoltAndCurrentMon				

Threat	Barriers to Local Fire: Cell		Barriers to Local Fire: Module		Barriers to Global Fire	
T4-Communication	B20	TempMon	B2	CellProp	B6	FireDet
	B4	CID			B7	FireEx
	B5	Shutdown			B16	ModProp
	B14	Independent			B17	Disconnect
	B18	VoltAndCurrentMon				
T5-HVACFailure	B4	CID	B2	CellProp	B6	FireDet
	B5	Shutdown			B7	FireEx
	B20	TempMon			B16	ModProp
	B14	Independent				
T6-ExternalShort	B4	CID	B2	CellProp	B6	FireDet
	B11	Fuses			B7	FireEx
	B1	Breakers			B16	ModProp
					B17	Disconnect
T7-MechImpact		-	B2	CellProp	B6	FireDet
					B7	FireEx
					B16	ModProp
T8-WaterIngress	B4	CID	B2	CellProp	B16	ModProp
	B11	Fuses			B17	Disconnect
	B1	Breakers			B5	Shutdown
					B14	Independent
T9-ExternalFire	B9	FireRating	B2	CellProp	B6	FireDet
	B15	ModCOol			B7	FireEx
					B16	ModProp
T10-FullModFail	-	-	-	-	B6	FireDet
					B7	FireEx
					B16	ModProp

17.1.4 Findings

The generic analysis shown in Table 17-5 results in fire frequencies as listed in Table 17-6. These are considered quite low – a frequency of 1E-4 per year implies an event every 10 000 years of operation for a battery system. It is assumed a battery system of 20 racks each containing 20 modules with 30 cells

each (determining the initiating frequency of T1). As is seen, a global fire has a negligible frequency of around 1E-7 per year.

Table 17-6   Fire frequencies for generic battery system

Consequence Category	Total frequency (per year)
Local Fire: Cell	3.8E-04
Local Fire: Module	1.4E-04
Global Fire	1.3E-07

It should be noted that these are very uncertain numbers for a generic system and could be improved by a more careful walkthrough of threats and barriers for a specific system. Also, the results may change significantly when other initial event frequencies are assumed.

As discussed in section 17.1.1, the analysis should be extended to also consider explosion risk. However, explosions are considered to have the same threats and causes as fires in a battery system and would be a separate branch in the "event tree" (delayed ignition). Because of this, and since many of the same barriers apply to prevent explosion, the explosion frequencies are considered to be of similar or of lower order of magnitude as the fire frequencies.

Figure 17-3 shows how the fire frequencies are distributed between the different threats. The local fire in cell consequence is considered a minor event, whereas a module fire is considered to be a fire of considerable severity. The frequency for module fire is by far governed by threat 10, full module failure, whereas frequencies for module fire is 1E-5 per year or below for the other threats.
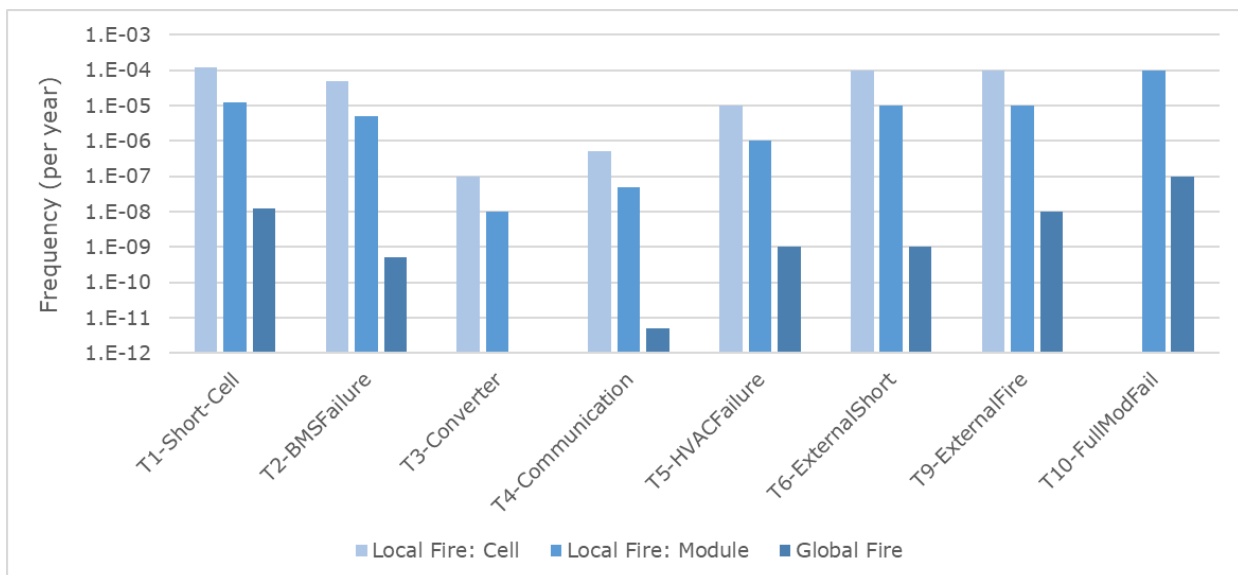
Figure 17-3 – Fire frequencies shown for the various threats (note logarithmic y axis)

17.1.4.1 **Evaluation of effect of presence of selected barriers**

Although the results may be uncertain in terms of absolute values, the analysis can be used to highlight the importance of different barriers, and the relative effect of not having them in place. To illustrate this, the risk resulting from the following system variations is studied:

- No barrier against cell propagation (removing B2)

- Less effective BMS (removing B18 and B20)

- Without independent shutdown (removing B14)

- Without CID (removing B4)

- As a (unrealistic) extreme case, removing all of the above: B2, B4, B14, B18, B20

The results for these cases are shown in Table 17-7 and Table 17-8. This shows that the presence of barriers is crucial for the fire frequencies obtained. CID is very important for reducing the local fire in cell frequency, whereas design preventing propagation from cell to module is important for reducing the module fire frequency.

Table 17-7   Fire frequencies for systems without barriers B2 and B16+B18 compared to base case with all barriers present

Consequence Category	Base case: system with all barriers	Without cell propagation design (B2)		Less effective BMS (B16 and B18)	
		Frequency	Relative to base case	Frequency	Relative to base case
Local Fire: Cell	3.8E-04	3.8E-04	0 %	5.2E-04	37 %
Local Fire: Module	1.4E-04	4.8E-04	248 %	1.5E-04	10 %
Global Fire	1.2E-07	3.5E-07	177 %	1.4E-07	11 %

Table 17-8   Fire frequencies for systems without barriers B20, B4 and extreme case compared to base case with all barriers present

Consequence Category	Without independent shutdown (B20)		Without CID (B4)		Extreme case: Without all (B2, B4, B14, B18, B20)	
	Frequency	Relative to base case	Frequency	Relative to base case	Frequency	Relative to base case
Local Fire: Cell	9.3E-04	143 %	2.9E-03	664 %	2.2E-02	5785 %
Local Fire: Module	1.9E-04	40 %	3.9E-04	183 %	2.3E-02	16197 %
Global Fire	1.4E-07	11 %	2.6E-07	105 %	1.7E-05	13562 %

17.1.4.2 Determining compliance of fire acceptance criteria

Quantifying the risk through an analysis like this can be used to determine how the system compares to acceptance criteria. An acceptance criteria can e.g. be expressed as a tolerable frequency for a

consequence and be compared to the frequency obtained in this analysis. In addition, this methodology can be used to provide guidance towards development of acceptance criteria.

17.1.4.3 Comparison to fire risk of a conventional engine room

The fire risk of a conventional engine room on a ship is difficult to assess but could be evaluated through a proper risk analysis of similar kind as that above. The idea is that this could be compared to the fire frequencies obtained for a battery system, which could be thought of as equivalent to an engine room onboard a conventional ship.

However, in this work a simpler approach is applied to obtain a ballpark frequency of fire to occur in the engine room onboard a ship: All fires registered in the global HIS Fairplay database for the period 1998-2017 and described as originating in the engine room are found from the database. Table 17-9 summarizes the findings – the total engine room fire frequency is found to be 6.8E-4 per ship per year. It is assumed that there is underreporting of events and the numbers presented is assumed conservative.

Table 17-9   Engine room fire statistics from HIS Fairplay database

Ship type	Number of reported fires in engine room	Average number of fires per year (1998-2007)	Approximate number of ships (world fleet with IMO numbers in database, 2016)	Fire frequency (per ship per year)
Wet/dry bulk	300	15	24917	6.0E-04
Cargo/container/RoRo	244	12.2	18396	6.6E-04
Passenger	158	7.9	3254	2.4E-03
Offshore	47	2.35	7248	3.2E-04
Fishing	158	7.9	8142	9.7E-04
Other activities	97	4.85	11774	4.1E-04
Total	1004	50.2	73731	6.8E-04

Based at the numbers presented, it seems that the likelihood of a battery fire is lower compared to a diesel fire. However, engine room fires as registered in the HIS Fairplay database include fires of many different magnitudes not necessarily correlating to the Global fire scenario established in battery system QRA. This means that better data would be necessary to fully evaluate if a battery system is safer than a conventional combustion engine.

18 REFERENCES

/1/ Center for Chemical Process Safety (CCPS). Guidelines for Initiating Events and Independent Protection Layers in Layer of Protection Analysis. Hoboken, NJ, USA: Wiley, Inc., 2015.

/2/ Institute of Electrical and Electronics Engineers, Inc., IEEE Std 493-1990: IEEE Recommended Practice for the Design of Reliable and Commercial Power Systems. 2nd ed. New York: IEEE. 1995. Print.

/3/ DNV GL, Considerations for ESS Fire Safety, Rev.3, Jan 2017

/4/ "Gas Explosion Handbook" Bjerketvedt, Bakke and Wingerden, 2009.

/5/ FLACS Software (HOLD)

/6/ https://response.restoration.noaa.gov/oil-and-chemical-spills/chemical-spills/resources/immediately-dangerous-life-health-limits-idlhs.html

/7/ Quyang, Liu, Chen and Wang; Investigation into the Fire Hazards of Lithium-Ion Batteries under Overcharging, *Appl. Sci.* 2017, *7*, 1314

/8/ Golubkov, Fuchs, Wagner, Wiltsche, Stangl, Fauler, Voitic, Thaler and Hacker, Thermal-runaway experiments on consumer Li-ion batteries with metal-oxide and olivine type cathodes, *RSC Adv.*, 2014, 4, 3633

/9/ Lei, Zhao, Ziebert, Uhlmann, Rohde and Seifert, Experimental Analysis of Thermal Runaway in 18650 Cylindrical Li-Ion Cells Using an Accelerating Rate Calorimeter, Batteries 2017, 3, 14

/10/ IEC 62298 Railway application – Rolling stock – Onboard lithium-ion batteries (2017-12)

/11/ IEC 60050-482 International Electrotechnical Vocabulary – Part 482: Primary and secondary cells and batteries (2004-04)

/12/ IEC 62619 Secondary cells and batteries containing alkaline or other non-acid electrolytes – Safety requirements for secondary lithium cells and batteries, for use in industrial applications (2017-02)

/13/ IEC 62864-1 Railway applications – Rolling stock – Power supply with onboard energy storage system –Part 1: Series hybrid system (2016-06)

/14/ IEC 62933-1 Electrical energy storage (EES) systems – Part 1: Vocabulary (2018-02)

/15/ DNVGL Ship rules Pt.6 Ch.2 Sec.1 Battery Power (2018-01)

/16/ https://www.mathesongas.com/pdfs/products/Lower-(LEL)-&-Upper-(UEL)-Explosive-Limits-.pdf

/17/ https://www.safetyandhealthmagazine.com/articles/consider-toxic-gas-density-when-positioning-a-gas-monitor-2

/18/ http://inchem.org/

/19/ http://www.iceweb.com.au/F&g/positioning%20of%20sensors%20guidelines.pdf

/20/ https://www.internationalgasdetectors.com/placement-gas-detector-guidelines/

APPENDIX A – ABBREVIATIONS AND DEFINITIONS

ABBREVIATIONS

ACH   Air Changes per Hour

CFD   Computational Fluid Dynamics

JDP   Joint Development Project

LEL   Lower Explosion Limit

LEL%   Percentage of the Lower Explosion Limit

LFP   Lithium Iron Phosphate

NMC   Nickel Manganese Cobalt Oxide

DEFINITIONS

Definitions are vital for a common and consistent discussion and assessment of safety. This section will present key definitions as agreed upon from JDP discussions.

For consideration, below are the current range of definitions that are found in different reference and standard documents. See reference /10/,/11/,/12/,/13/,/14/ and/15/.

Item	Abbreviation	Reference	Definition
actual energy capacity	$E_c(t)$	IEC 62933-1	EES system energy capacity at a given time as a result of a degraded state of health and other factors Note 1 to entry: The term "actual energy capacity" is not to be mixed up with the term "capacity" (used for cells, batteries, capacitors, etc.), which is a quantity of electricity (electric charge), usually expressed in coulomb (C) or amperes-hour (Ah). Note 2 to entry: Joule (J) is the base unit, other units may be chosen for convenience as well (kWh, MWh).
Available energy		IEC 62933-1	designed value of the energy content of the EES system in continuous operating conditions, starting from a full state of charge and discharging continuously at rated active power during discharge, measured at the primary POC Note 1 to entry: The term "rated energy

			capacity" is not to be mixed up with the term "capacity" (used for cells, batteries, capacitors etc.), which is a quantity of electricity (electric charge), usually expressed in coulomb (C) or amperes-hour (Ah).
			Note 2 to entry: Joule (J) is the base unit, other units may be chosen for convenience as well (kWh, MWh).
Battery Branch		IEC 62928	group of battery packs/modules connected together either in a series and/or parallel configuration, which has the voltage equal to that of the battery system and is the smallest electrically isolatable subsystem
			Note 1 to entry: Electrical isolation is done by means of disconnecting devices, e.g. contactors, switchgears, circuit breakers, etc.
			Note 2 to entry: A battery branch may be contained in a single enclosure or multiple enclosures.
Battery Cell	-	DNVGL Pt.6 Ch.2 Sec.1	the smallest building block in a battery, a chemical unit
Battery Cell Block	-	DNVGL Pt.6 Ch.2 Sec.1	group of cells connected together in parallel configuration
Battery Converter	-	DNVGL Pt.6 Ch.2 Sec.1	the equipment controlling the charging and discharging of the battery system
Battery Energy		IEC 60050-482	electric energy which a battery delivers under specified conditions
			Note – The SI unit for energy is joule (1 J = 1 W · s), but in practice, battery energy is usually expressed in watthours (Wh) (1 Wh = 3 600 J).
Battery Energy		IEC 60050-482	electric energy which a battery delivers under specified conditions
			Note – The SI unit for energy is joule (1 J = 1 W · s), but in practice, battery energy is usually expressed in watthours (Wh) (1 Wh = 3 600 J).

Battery Management System	BMS	DNVGL Pt.6 Ch.2 Sec.1	a collective terminology comprising control, monitoring and protective functions of the battery system
Battery Management System	BMS	IEC 62619	electronic system associated with a battery which has functions to cut off in case of overcharge, overcurrent, overdischarge, and overheating Note 1 to entry: It monitors and/or manages its state, calculates secondary data, reports that data and/or controls its environment to influence the battery's safety, performance and/or service life. Note 2 to entry: Overdischarge cut off is not mandatory if there is an agreement between the cell manufacturer and the customer. Note 3 to entry: The function of the BMS can be assigned to the battery pack or to equipment that uses the battery. (See Figure 5) Note 4 to entry: The BMS can be divided and it can be found partially in the battery pack and partially on the equipment that uses the battery. (See Figure 5) Note 5 to entry: The BMS is sometimes also referred to as a BMU (battery management unit)
Battery management system	BMS	IEC 62928	system associated with a battery pack which monitors and/or manages its state, disconnects or isolates the battery pack, calculates secondary data, communicates data outside of the battery system and/or controls its environment to influence the battery's safety, performance and/or service life Note 1 to entry: The function of the BMS can be assigned to the battery pack or to equipment that uses the battery pack. Note 2 to entry: Its functions include thermal control.

Battery Module	-	DNVGL Pt.6 Ch.2 Sec.1	assembly of cells including electronic control
Battery Pack	-	DNVGL Pt.6 Ch.2 Sec.1	one or more modules including complete BMS and can be used as a standalone unit
Battery Pack	-	IEC 62619	energy storage device, which is comprised of one or more cells or modules electrically connected

Note 1 to entry: It has a monitoring circuitry which provides information (e.g. cell voltage) to a battery system.

Note 2 to entry: It may incorporate a protective housing and be provided with terminals or other interconnection arrangement. |
Battery Space		DNVGL Pt.6 Ch.2 Sec.1	the space enclosed by structural separation in which the batteries are located
Battery String	-	DNVGL Pt.6 Ch.2 Sec.1	a battery string comprises a number of cells or modules connected in series with the same voltage level as the battery system
Battery System		DNVGL Pt.6 Ch.2 Sec.1	the whole battery installation including battery modules, electrical interconnections, BMS and other safety features
Battery system	battery	IEC 62619	system which comprises one or more cells, modules or battery packs

Note 1 to entry: It has a battery management system to cut off in case of overcharge, overcurrent, overdischarge,

and overheating.

Note 2 to entry: Overdischarge cut off is not mandatory if there is an agreement between the cell manufacturer

and the customer

Note 3 to entry: The battery system may have cooling or heating units. |
| Battery thermal management system | BTMS | IEC 62928 | system associated with a battery pack which monitors and/or manages its |

			thermal behaviour in order to maintain the temperature of the battery pack in the intended range for load profile agreed between the integrator and the battery system manufacturers
C-Rate	C	DNVGL Pt.6 Ch.2 Sec.1	the current (A) used to charge/recharge the battery divided by the rated amperhours (Ah)
CP-Rate	CP	DNVGL Pt.6 Ch.2 Sec.1	the power (W) used to charge/recharge the battery divided by the rated Watt-hours (Wh)
Cell		IEC 60050-482	basic functional unit, consisting of an assembly of electrodes, electrolyte, container, terminals and usually separators, that is a source of electric energy obtained by direct conversion of chemical energy
Cell Block	-	IEC 62619	group of cells connected together in parallel configuration with or without protective devices (e.g. fuse or PTC) and monitoring circuitry Note 1 to entry: It is not ready for use in an application because it is not yet fitted with its final housing, terminal arrangement and electronic control device.
Direct Injection	-	-	Practice of filling battery modules/cabinets with a fire-extinguishing agent, e.g. with water or foam-based systems.
Electrolyte		IEC 60050-482	liquid or solid substance containing mobile ions which render it ionically conductive NOTE The electrolyte may be liquid, solid or a gel.
Energy Management System/Function	EMS	DNVGL Pt.6 Ch.2 Sec.1	a system providing monitoring and control of the energy capacities
Explosion		IEC 62619	failure that occurs when a cell container or battery case opens violently and solid components are forcibly expelled Note 1 to entry: Liquid, gas, and smoke are erupted.
Fire		IEC 62619	emission of flames from a cell, module,

			battery pack, or battery system
Gassing of a cell		IEC 60050-482	evolution of gas resulting from electrolysis of the water in the electrolyte of a cell
Leakage		IEC 62619	visible escape of liquid electrolyte
Lower Explosion Limit	LEL		The minimum concentration of a particular combustible gas or vapor necessary to support its combustion in air.
Module		IEC 62619	group of cells connected together either in a series and/or parallel configuration with or without protective devices (e.g. fuse or PTC) and monitoring circuitry
Overcharge		IEC 60050-482	continued charging of a fully charged secondary cell or battery
Rated capacity		IEC 62619	capacity value of a cell or battery determined under specified conditions and declared by the manufacturer Note 1 to entry: The rated capacity is the quantity of electricity Cn Ah (ampere-hours) declared by the manufacturer which a single cell or battery can deliver during an n-hour period when charging, storing and discharging under the conditions specified in IEC 62620:2014, 6.3.1.
Rated capacity		IEC 62864-1	available capacity measured according to certain "rating" condition as expressed in relevant standard
rated energy capacity	E_{RC}	IEC 62933-1	designed value of the energy content of the EES system in continuous operating conditions, starting from a full state of charge and discharging continuously at rated active power during discharge, measured at the primary POC Note 1 to entry: The term "rated energy capacity" is not to be mixed up with the term "capacity" (used for cells, batteries, capacitors etc.), which is a quantity of electricity (electric charge), usually expressed in coulomb (C) or amperes-hour (Ah). Note 2 to entry: Joule (J) is the base unit, other units may be chosen for convenience

			as well (kWh, MWh).
Rupture		IEC 62619	mechanical failure of a cell container or battery case induced by an internal or external cause, resulting in exposure or spillage but not ejection of materials
Venting		IEC 62619	release of excessive internal pressure from a cell, module, battery pack, or battery system in a manner intended by design to preclude rupture or explosion
Sealed Battery		DNVGL Pt.6 Ch.2 Sec.1	a battery that remains closed and does not release either gas or liquid when operated within the limits specified by the manufacturer
Sealed Cell		IEC 60050-482	cell which remains closed and does not release either gas or liquid when operated within the limits specified by the manufacturer Note – A sealed cell may be equipped with a safety device to prevent a dangerously high internal pressure and is designed to operate during its life in its original sealed state.
State of Charge	SOC	DNVGL Pt.6 Ch.2 Sec.1	the available capacity expressed as percentage of the rated capacity (0-100%)
State of Charge	SOC	IEC 62864-1	remaining capacity to be discharged, normally expressed as a percentage of full capacity as expressed in relevant standards Note 1 to entry: Practical definitions of SOC are dependent upon chosen technologies. SOC is applicable to batteries. See Annex A.
State of Charge	SOC	IEC 62933-1	ratio between the available energy from an EES system and the actual energy capacity, typically expressed as a percentage
State of Energy	SOE	IEC 62864-1	remaining energy to be discharged, normally expressed as a percentage of full energy as expressed in relevant standards

			Note 1 to entry: Practical definitions of SOE are dependent upon chosen technologies. SOE is applicable to both batteries and capacitors. See Annex A.
State of Health	SOH	DNVGL Pt.6 Ch.2 Sec.1	reflects the general condition of a battery and its ability to deliver the specified performance compared with a new battery (0-100%)
State of Health	SOH		general condition of the EES system based on measurements that indicate its actual performance compared with its nominal/rated performances Note 1 to entry: The state of health also includes the temporary degradation due to faults inside the EESS subsystems.
Thermal Runaway		IEC 62619	uncontrolled intensive increase in the temperature of a cell driven by exothermic reaction
Thermal Runaway		IEC 60050-482	unstable condition arising during constant voltage charge in which the rate of heat dissipation capability, causing a continuous temperature increase with resulting further charge current increase, which can lead to the destruction of the battery Note – In lithium batteries thermal runaway may cause melting of lithium.
Total-flooding fire-extinguishing	-	SOLAS II-2/10; IFSS Code	fixed fire-extinguishing system, installed for fire suppression within a full space.

\

About DNV GL

Driven by our purpose of safeguarding life, property and the environment, DNV GL enables organizations to advance the safety and sustainability of their business. We provide classification and technical assurance along with software and independent expert advisory services to the maritime, oil & gas and energy industries. We also provide certification services to customers across a wide range of industries. Operating in more than 100 countries, our professionals are dedicated to helping our customers make the world safer, smarter and greener.